TIIA KOHO

Virus-Like Particles for Vaccine Development

ACADEMIC DISSERTATION
To be presented, with the permission of
the Board of the BioMediTech of the University of Tampere,
for public discussion in the Auditorium of
School of Health Sciences, Medisiinarinkatu 3,
Tampere, on June 5th, 2015, at 12 o'clock.

UNIVERSITY OF TAMPERE

TIIA KOHO

Virus-Like Particles for Vaccine Development

Acta Universitatis Tamperensis 2066
Tampere University Press
Tampere 2015

UNIVERSITY
OF TAMPERE

ACADEMIC DISSERTATION
University of Tampere, BioMediTech
The National Doctoral Programme in Informational and Structural Biology (ISB)
Tampere Graduate Program in Biomedicine and Biotechnology (TGPBB)
Finland

Supervised by
Professor Markku S. Kulomaa
University of Tampere
Finland
Docent Vesa P. Hytönen
University of Tampere
Finland

Reviewed by
Professor Kari Airenne
University of Eastern Finland
Finland
Professor Ilkka Julkunen
University of Turku
Finland

The originality of this thesis has been checked using the Turnitin OriginalityCheck service in accordance with the quality management system of the University of Tampere.

Cover design by
Mikko Reinikka

Distributor:
verkkokauppa@juvenesprint.fi
https://verkkokauppa.juvenes.fi

Acta Universitatis Tamperensis 2066
ISBN 978-951-44-9829-9 (print)
ISSN-L 1455-1616
ISSN 1455-1616

Acta Electronica Universitatis Tamperensis 1559
ISBN 978-951-44-9830-5 (pdf)
ISSN 1456-954X
http://tampub.uta.fi

Suomen Yliopistopaino Oy – Juvenes Print
Tampere 2015

For all things small
with great impact

CONTENTS

LIST OF ORIGINAL COMMUNICATIONS

This thesis is based on the following original communications, which are referred to in the text by their Roman numerals (I-IV). This dissertation also includes unpublished results.

I **Koho T**, Huhti L, Blazevic V, Nurminen K, Butcher SJ, Laurinmäki P, Kalkkinen N, Rönnholm G, Vesikari T, Hytönen VP, Kulomaa MS. Production and characterization of virus-like particles and the P domain protein of GII.4 norovirus. Journal of Virological Methods 2012, 179(1), 1-7.

II **Koho T***, Mäntylä T*, Laurinmäki P, Huhti L, Butcher SJ, Vesikari T, Kulomaa MS, Hytönen VP. Purification of norovirus-like particles (VLPs) by ion exchangechromatography. Journal of Virological Methods 2012, 181(1), 6-11.

III **Koho T**, Koivunen MR, Oikarinen S, Kummola L, Mäkinen S, Mähönen AJ, Sioofy-Khojine A, Marjomäki V, Kazmertsuk A, Junttila I, Kulomaa MS, Hyöty H, Hytönen VP, Laitinen OH. Coxsackievirus B3 VLPs purified by ion exchange chromatography elicit strong immune responses in mice. Antiviral Research 2014, 104, 93-101.

IV **Koho T**, Ihalainen TO, Stark M, Uusi-Kerttula H, Wieneke R, Rahikainen R, Blazevic V, Marjomäki V, Tampé R, Kulomaa MS, Hytönen VP. His-tagged norovirus-like particles: A versatile platform for cellular delivery and surface display. Submitted.

* = equal contribution

ABBREVIATIONS

All-cHis-VLP	fully histidine-tagged virus-like particle
APC	antigen-presenting cell
BEVS	baculovirus expression vector system
CAR	coxsackievirus and adenovirus receptor
cDNA	complementary DNA
cryo-EM	cryo-electron microscopy
CsCl	cesium chloride
CVB3	coxsackievirus B3
Da	Dalton
DAF	decay-accelerating factor
DCM	dilated cardiomyopathy
DLS	dynamic light scattering
dpi	days post infection
ELISA	enzyme-linked immunosorbent assay
FDA	food and drug administration
FCS	fluorescence correlation spectroscopy
GMK	green monkey kidney
HBGA	histo-blood group antigen
HEK	human embryonic kidney
His-tag	polyhistidine tag
IEX	ion exchange chromatography
Ig	immunoglobulin
IRES	internal ribosome entry site
IMAC	immobilized metal ion affinity chromatography
LB	Lysogeny broth
M	molar concentration
MOI	multiplicity of infection
mRNA	messenger RNA
Ni-NTA	nickel-nitrilotriacetic acid
NoV	norovirus

OD_{600}	optical density at 600 nm
ORF	open reading frame
P	protruding
PDI	polydispersity index
PEG	polyethylene glycol
pI	isoelectric point
PTM	post-translational modification
qRT-PCR	quantitative reverse transciption polymerase chain reaction
rpm	revolutions per minute
RT	room temperature
S	shell
SDS-PAGE	sodium dodecyl sulfate polyacrylamide gel electrophoresis
SEM	scanning electron microscopy
Sf	*Spodoptera frugiperda*
ssRNA	single-stranded RNA
$TCID_{50}$	50% tissue culture infective dose
TEM	transmission electron microscopy
UTR	untranslated region
VLP	virus-like particle
VP	viral protein

TIIVISTELMÄ

Rakenteellisesti aitoa virusta muistuttavista, mutta ei-infektiivisistä viruksen kaltaisista partikkeleista (VLP) on viimeisen kolmen vuosikymmenen aikana muodostunut laajasti hyväksytty teknologia erityisesti rokotekehityksessä, mutta myös diagnostisten ja terapeuttisten sovellusten kehittämisessä. Alun perin VLP:itä tuotettiin suoraan niitä vastaavista viruksista ja näitä virusrakenteita on ensisijaisesti hyödynnetty kehitettäessä uusia rokotevaihtoehtoja niiden virusta muistuttavan kokonsa ja rakenteensa vuoksi, jossa viruksen vasta-aineita sitovat epitoopit ovat tehokkaasti esillä oikeassa muodossaan. Sittemmin on kehitetty myös monimutkaisempia kimeerisiä VLP:itä, joissa VLP:n rakennetta hyödynnetään muiden kuin vastaavan viruksen antigeenisten epitooppien esittelyyn tai vaikkapa terapeuttisten molekyylien kuljettamiseen.

Tämän tutkimuksen pääasiallisena tavoitteena oli tuottaa ja karakterisoida tietyistä tärkeistä norovirus- ja enteroviruskannoista johdettuja VLP:itä rokotetutkimusta ja diagnostisten menetelmien kehitystä varten sekä muokata niiden rakennetta edelleen kimeeristen VLP:iden tuottamiseksi. Norovirukset (NoV:t) ovat pääasiallisia akuutin epideemisen maha-suolitulehduksen aiheuttajia ympäri maailmaa, kun taas tässä tutkimuksessa käytetyn enteroviruskannan (CVB3) on arveltu olevan syynä akuuttiin ja krooniseen viruksen aiheuttamaan sydänlihastulehdukseen sekä dilatoivaan kardiomyopatiaan. Kaikkien tässä tutkimuksessa kehitettyjen VLP:iden (alkuperäisten NoV VLP:iden, CVB3 VLP:iden sekä molempien kimeeristen NoV VLP -muotojen) havaittiin muistuttavan läheisesti niitä vastaavia viruksia sekä sitovan tehokkaasti niitä vastaavien virusten indusoimia vasta-aineita. Tästä johtuen niitä voitaisiin hyödyntää rokotekehityksessä sekä diagnostisten menetelmien kehittämisessä. Tavallisten VLP:iden lisäksi tuotettiin kimeerisiä NoV VLP:itä, joissa noroviruksen kapsidiproteiinin pintaan lisättiin käyttökelpoinen C-terminaalinen histidiini-affiniteettijakso, ja osoitettiin, että näin syntyvän kimeerisen NoV VLP:n pintaan pystytään histidiinijakson sekä *tris*-nitrilotriasetaattihappo (*tris*NTA)-adaptorin avulla kiinnittämään ei-kovalenttisesti kokonaisia proteiineja, peptidejä sekä fluoresoivia leimoja. Kimeerisiä VLP:itä voitaisiin hyödyntää esimerkiksi

muokattavina nanometri-mittakaavassa olevina kuljettimina tai monipuolisina rokotealustoina.

Uusien rokotteiden tuottamisessa on useita teknisiä haasteita, joita ovat esimerkiksi rokotekäyttöön sopivan tuottosysteemin valinta sekä tehokkaan ja teollisuusmittakaavaan sopivan puhdistusmenetelmän kehitys. Tässä työssä vastattiin näihin haasteisiin tuottamalla VLP:t tehokkaassa aitotumallisessa bakulovirus-hyönteissolu-tuottosysteemissä sekä kehittämällä puhdistuskapasiteetin nostamiseen sopivat joko ioninvaihtoon tai metalli-ioniaffiniteettiin perustuvat kromatografiset menetelmät niiden puhdistamiseksi. VLP-tuotteiden puhtausasteen havaittiin olevan kromatografisen puhdistuksen jälkeen korkea ja niiden todettiin olevan oikeanlaisesti rakentuneita. Kehitetyt puhdistusmenetelmät ovat lisäksi helposti muokattavissa muiden VLP:iden tuotantoon ja tuotannon laajentamiseen teollisuuskäyttötasolle.

Kokonaisuudessaan tässä työssä tuotettiin useita VLP-teknologiaan perustuvia proteiinikomplekseja, joita voidaan soveltaa rokotekehityksessä ehkäisemään niitä vastaavien virusten aiheuttamia tauteja sekä kehitettäessä diagnostisia menetelmiä. Tämän lisäksi NoV P-partikkelien sekä kimeeristen NoV VLP:iden pinnalle lisätyn monipuoliseen käyttöön soveltuvan histidiinijakson ansiosta, tuotteita voitaisiin hyödyntää esimerkiksi niiden hallitussa kiinnittämisessä mikropartikkelien pintaan tai muille soveltuville affiniteettipinnoille sekä konjugoitaessa vieraita molekyylejä, kuten toisen viruksen antigeenejä, niiden pintaan. Muokatut partikkelit ovat näin hyödynnettävissä monipuolisesti esimerkiksi nanobioteknologian sekä biolääketieteen aloilla. Kehitetyt ja tutkitut VLP:t lisäävät tietoa, jota tarvitaan uusien VLP:iden valmistamisessa ja muokkauksessa.

ABSTRACT

Over the last three decades, non-infective virus-like particles (VLP) that mimic the overall structure of viruses have become a widely accepted technology for developing diagnostic tools and therapy vectors, but especially for the construction of novel vaccines. Initially, VLPs were primarily derived from their corresponding viruses, and they proved to be feasible vaccine candidates due to their virus-like size and effective presentation of viral epitopes in a native conformation. Later, a second generation of complex chimeric VLPs utilizing the VLP structure to present antigenic or therapeutic epitopes on their surface or carry therapeutic molecules in their inner cavities has been developed.

The main aim of this doctoral research was to produce and characterize VLPs that derive from relevant strains of norovirus and enterovirus for vaccine development and diagnostics and to modify their structures to produce chimeric VLPs. Noroviruses (NoVs) are a major cause of acute epidemic gastroenteritis worldwide, and the enterovirus strain used in this study (CVB3) is associated in acute and chronic viral myocarditis and dilated cardiomyopathy. All the VLPs generated during this thesis (native NoV VLPs, CVB3 VLPs and both forms of histidine-tagged NoV VLPs) were found to closely resemble their respective viruses and be highly antigenic, and therefore, applicable as vaccine candidates and for use in the development of diagnostic methods. Furthermore, chimeric NoV VLPs were produced by adding a C-terminal polyhistidine-tag to the capsid protein, which projected out of the NoV surface. By using the affinity between polyhistidine-tag and *tris*-nitrilotriacetic acid (*tris*NTA), fluorescent dye molecules, peptides, and even whole proteins were then displayed on the surface of histidine-tagged NoV VLPs to demonstrate that these chimeric VLPs can be used as easily modifiable nanocarriers or a versatile vaccine platform.

To overcome certain technical difficulties present in the development of new vaccines, an efficient eukaryotic baculovirus-insect cell -based production system and several scalable chromatographic purification methods based on either ion exchange or immobilized metal ion affinity, were developed for the VLPs and the protein products generated during this thesis. The chromatographic purification methods resulted in fully assembled VLPs with high purity and also offer the

possibility of adapting this technology for the production and scale-up of other VLPs.

In conclusion, this work produced several VLP-based products that are applicable as vaccine candidates against their respective virus-related diseases and which can also be used for the development of diagnostic methods. In addition, the histidine-tag of NoV P particles and on chimeric NoV VLPs enables the use of affinity matrices for orienting and immobilizing the particles on the surface of microparticles or other appropriate surfaces as well as conjugating foreign molecules on their surface, therefore providing a robust and versatile tool for the nanobiotechnology applications and biomedical sciences. Moreover, the information gathered during the course of this thesis offers valuable insights for the future production and tailoring of VLPs.

1 INTRODUCTION

Vaccination is the medical practice that, together with clean water, has had the greatest impact on overall human health and on the 30-year increase in average human lifespan achieved during the 20th century. The vaccines developed over the first two hundred years since the first recorded vaccine (Jenner's smallpox inoculation) have eradicated or reduced the incidence of many life-threatening and devastating diseases that were long responsible for much of the morbidity and premature mortality of humans and animals. These include for example smallpox, diphtheria, tetanus, measles, mumps, pertussis, poliomyelitis, hepatitis B, *Haemophilus influenzae*, and rubella (Bárcena & Blanco 2013, Rappuoli 2009).

Pasteur's early approaches to vaccine development, inactivation and attenuation of a live pathogen, are even today the two standards of vaccine technology. Most of the currently licensed vaccines are still produced based on the principle of reducing the pathogen's virulence either by chemical inactivation of the whole organism (inactivated vaccines) or biological attenuation of its virulence, usually by repeated passage of viruses in cell culture or in embryonated eggs (live attenuated vaccines). Upon administration, these classical vaccines generally elicit a range of immune responses, which resembles that induced by the authentic virus, and eventually confers the vaccinated host with a life-long protection against subsequent infection by the pathogen. However, in spite of the long and successful use of these classical vaccines, they present relevant drawbacks regarding their usage safety and manufacture. There is a limited, but existing, risk of incomplete inactivation, reversion to a virulent phenotype *in vivo*, or accidental release of the infectious agent from the vaccine manufacturing facilities, any of which can lead to spreading of the unwanted disease. Examples of these problems have been observed involving classical vaccines against poliovirus and foot-and-mouth disease virus (Bárcena & Blanco 2013, Plotkin 2005).

Alternative approaches are, therefore, needed. Over recent years, advances in recombinant DNA technologies, genetic engineering, and an increased understanding of the immune system have led to the development of subunit vaccines that are considered safer than inactivated or live attenuated vaccines. However, the immunogenicity of individual viral proteins is usually lower than that

of the whole pathogen-based vaccines, consequently requiring co-administration of adjuvants, higher doses of immunogen, booster administrations, or the development of alternative approaches for enhancing their immunogenicity (Kushnir et al. 2012). In this regard, a special type of subunit vaccines called virus-like particles (VLPs) represents a major advancement in vaccine development.

VLPs are formed from viral structural proteins, which when overexpressed recombinantly spontaneously self-assemble into hollow particles that mimic the morphology of the native virion. In contrast to viruses, VLPs are devoid of infectious genetic material and are, therefore, non-replicating and non-infective. Consequently, they do not carry the risk of reversion to a virulent form and thus lack the safety concerns related to inactivation failures. VLPs are appealing as vaccine candidates because of their inherent properties. They are virus-sized, and they display antigenic epitopes in an authentic conformation and in a multimeric, highly organized and repetitive manner, which leads to safe but efficient induction of both humoral (B cells) and cellular (T cells) immune responses. They thereby overcome the common drawback encountered with traditional subunit vaccines (Bárcena & Blanco 2013).

The recombinant Hepatitis B virus surface antigen (HBsAg)-based vaccine Recombivax HB® licensed by Merck in 1986 was the first vaccine produced using modern recombinant DNA technology and also the first human vaccine developed using the VLP approach. It was soon followed by other VLP-based HBV vaccine Engerix®-B (by GlaxoSmithKline, GSK) and then 20 years later by the multivalent human papillomavirus vaccines Gardasil® (by Merck) and Cervarix® (by GSK) (Josefsberg & Buckland 2012). The successes of HBV and HPV VLP vaccines have provided a template strategy for the use of VLPs in prophylaxis against other communicable as well as non-communicable diseases and have led to a renaissance in vaccine development. The development of VLPs as platforms for foreign antigen display and as biological nanocarriers has further broadened their applicability both as prophylactic and therapeutic vaccines (Bárcena & Blanco 2013). Today, vaccination remains the most effective strategy for controlling and preventing communicable diseases, and it is still fundamentally needed to fight against new emerging diseases, including chronic conditions like cardiovascular diseases, obesity, diabetes, and cancer. Thus, better knowledge of the vaccination possibilities is essential when developing new vaccines against both existing and still becoming diseases.

2 REVIEW OF THE LITERATURE

2.1 Vaccines

2.1.1 A short introduction to vaccines

The earliest vaccines were relatively crude and consisted of only partially purified inactivated bacteria (e.g., pertussis) or live attenuated viruses (e.g., smallpox and rabies). In fact, the very first recorded vaccine was cowpox (vaccinia virus) pus inoculation introduced by Edward Jenner in 1796, which was used simply by transferring it from animal to human and was intended to immunize against the more pathogenic human smallpox (Josefsberg & Buckland 2012). Coincidentally, Jenner gave origin to the whole field of vaccinology, literally, since the Latin word *vacca* means "cow", and in his famous Inquiry (Jenner 1798), Jenner spoke of *variolae vaccinae*, the Latin translation of cowpox. Over time, more sophisticated approaches were introduced, such as chemical treatment of a bacterial protein toxin to form a toxoid (e.g., diphtheria and tetanus), development of a purified and inactivated virus (e.g., polio), development of virus-like particles (e.g., hepatitis B and human papillomavirus), and purified polysaccharides (e.g., pneumococcal vaccines) (Josefsberg & Buckland 2012). To date, vaccination still remains the most important and cost-effective way to control and prevent infectious diseases.

Over the last decade, new vaccine development approaches have come to the forefront, stemming largely from a major demand for novel vaccines to be better defined and more effective. For instance, reverse vaccinology (Pizza et al. 2000) is an approach that utilizes whole genome analysis across multiple strains of the pathogen to identify the genes that may indicate antigenicity, such as surface-exposed antigens, signal peptides, and B cell epitopes. Once the candidates are identified, they are produced synthetically and evaluated for their suitability in vaccine formulations (Rappuoli 2000). Systems biology is another approach that integrates mathematical models collected from various fields, such as metabolomics, transcriptomics, and proteomics to elucidate the interactions between different biological systems. This can lead to a more detailed

understanding of how vaccine antigens interact with different components of the immune system (Josefsberg & Buckland 2012). By using these approaches, vaccine development can be directed towards more rationally designed vaccines.

2.1.2 Vaccines against viral diseases

Vaccines can generally be classified as live attenuated (viral or bacterial) vaccines or inactivated vaccines that include inactivated whole organisms, (bacterial) toxoids, protein subunit vaccines and virus-like particles, purified bacterial polysaccharides and their conjugate vaccines, and DNA vaccines (Figure 1). They have been also historically introduced more or less in this order (Plotkin 2005).

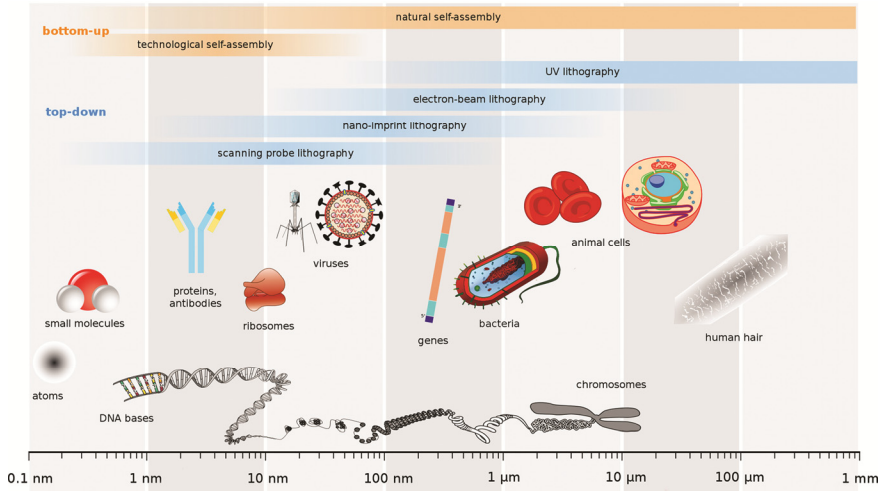

Figure 1. The size scales of various molecules contained in vaccines and other biological assemblies. Adapted with permission from Paumier et al. (2009).

2.1.2.1 Attenuated and inactivated virus vaccines

Human vaccines against viral diseases are historically based on attenuated or inactivated live viruses, and they are still predominantly used today. Among these vaccines are polio vaccines, seasonal and pandemic influenza vaccines, and a rabies vaccine, of which only an inactivated vaccine form is on the market. Live-attenuated vaccines generally induce efficient and prolonged immunity due to their ability to mobilize both humoral (B cells) and cellular (T cells) arms of the adaptive immune system (Figure 2). However, the development of live vaccines can be

especially challenging when the goal is to target multiple viral subtypes or pathogens. There are also potential safety concerns associated with incomplete inactivation of the virus or reversion of an attenuated vaccine strain to a more virulent phenotype that can then lead to the spreading of the disease that the vaccine was originally intended to prevent. For this reason, live-attenuated vaccines are contraindicated for use in newborns, expectant mothers and immunocompromised individuals (Bárcena & Blanco 2013).

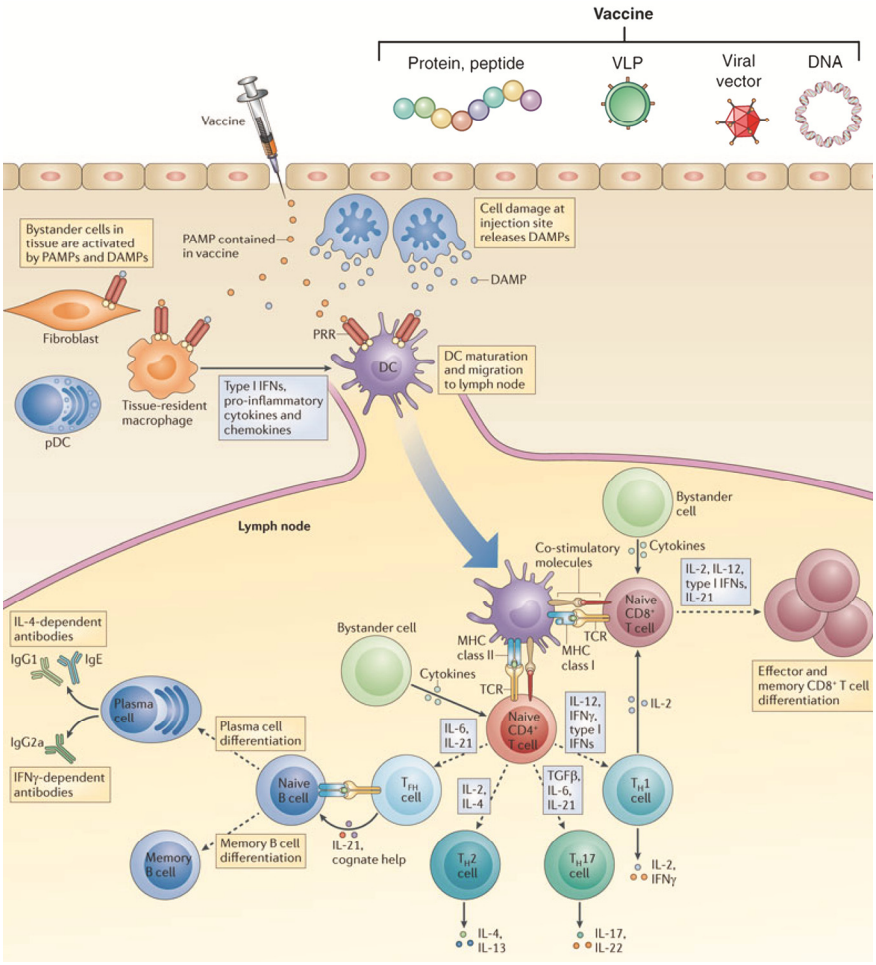

Figure 2. Induction of adaptive immune responses to vaccines through dendritic cell activation. Vaccines may contain pathogen-associated molecular patterns (PAMPs), or they may induce the local release of damage-associated molecular patterns (DAMPs), which are detected directly by pattern-recognition receptors (PRRs) expressed by dendritic cells (DCs), leading to DC activation, maturation and migration to the lymph nodes. Adapted from Desmet & Ishii (2012) and from Liang (2013), copyrights (2012 and 2013) with permission from Macmillan Publishers Ltd (Nature Reviews Immunology and Nature Medicine, respectively).

These safety concerns are particularly important for viruses that have a high degree of genetic exchange and a high mutation rate after inoculation. If a vaccinated individual becomes infected with a virus of a different serotype, recombination or re-assortment of viral genetic material in the vaccinated host can lead to the production of entirely new variants of the virus (Josefsberg & Buckland 2012, Noad & Roy 2003). A well-known example of reversion to a virulent form is the attenuated oral polio vaccine (OPV) also known as the Sabin vaccine. Outbreaks of paralytic poliomyelitis attributable to circulating vaccine-derived poliovirus (VDPV) strains have been reported especially in areas with low coverage of the oral vaccine and poor hygiene (Wringe et al. 2008).

Additionally, some attenuated and inactivated virus vaccines can be associated with other adverse effects, such as teratogenicity of rubella virus in the MMR vaccine during pregnancy (McLean et al. 2013), neurological complications induced by the Japanese encephalitis vaccine (Takahashi et al. 2000) and intussusception in infants following rotavirus vaccination (Murphy et al. 2001). These problems drive the need for the development of new vaccine platforms that are inherently safer to use and offer broader immunogenicity.

2.1.2.2 Protein subunit vaccines

Recombinant subunit vaccines that are based on vaccination with an isolated component of a pathogen, such as a single viral protein or peptide, have offered a safer alternative to attenuated virus vaccines. However, they often have a short half-life *in vivo* and suffer from poor immunogenicity due to incorrect folding and small size (Figure 1) of the target protein or impaired presentation to the immune system. This may lead to a need of frequent administrations and large doses of the immunogen are to elicit the same protective effect as an inactivated or attenuated virus vaccine. This means that many subunit vaccines are significantly more expensive to use for a vaccination program than attenuated vaccines, a fact that undoubtedly has an impact on public health budget outlines (Noad & Roy 2003). Moreover, subunit vaccines typically require formulation with potent immune-stimulating adjuvants, which can cause considerable side effects, including local pain and toxicity, or systemic reactions like fever and autoimmune diseases (Aguilar & Rodríguez 2007). Virus-like particles represent a specific class of subunit vaccines, the features of which are further elaborated later in a dedicated chapter (see section 2.3).

2.1.2.3 DNA vaccines

DNA vaccination is a relatively recent technique, wherein an immune response is elicited by injection of a host with a genetically engineered DNA plasmid containing a gene for a protein-antigen of interest, which is then expressed by the cellular machinery of the vaccinated host. The genes may be introduced into cells via viral vectors (e.g., adenovirus- and alphavirus-based vectors), or through the uptake of naked or complexed plasmid DNA. Especially, the more recent "second-generation" DNA vaccines having improvements in their immunogenicity, made through, for example, antigen optimization and the inclusion of molecular adjuvants within the DNA platform are able to induce both B and T cell-mediated immune responses (Figure 2). They are, therefore, comparable in efficiency to attenuated viral vaccines, but without the risk of reversion.

The safety concerns are associated with the potential for random genomic integration of the DNA and permanent alteration of the host genome, development of anti-DNA immune responses, and generation of immunologic tolerance through the continued expression of the exogenous genes from the introduced plasmid (Ferraro et al. 2011, McCallus et al. 2001). Although only veterinary DNA vaccines have been approved to date (e.g., an equine vaccine against West Nile virus), there are several human DNA vaccines in various stages of clinical trials for such targets as HIV (Kalams et al. 2013, Mulligan et al. 2006, Vasan et al. 2011), many cancers (Eriksson et al. 2013, Tiriveedhi et al. 2013, Yuan et al. 2013), hepatitis B (Godon et al. 2014, Yang et al. 2012), and influenza (Jones et al. 2009, Ledgerwood et al. 2012).

2.1.2.4 Cancer vaccines

In year 2008, it was estimated that of the 12.7 million new cancer cases that occurred that year worldwide, 16.1% could be associated to infectious agents, meaning that around 2 million new cancer cases were attributable to infections (de Martel et al. 2012). The principal carcinogenic agents were the bacterium *Helicobacter pylori*, hepatitis B and C viruses, human papillomaviruses (HPV), the Epstein-Barr virus, and HIV. It follows, therefore, that a large number of cancers could be prevented by protecting the host against these infectious pathogens. Due to this comprehension, cancer vaccines have changed the whole perception of prophylactic vaccine technology. Arguably the first anti-cancer vaccines approved by the U.S. Food and Drug Administration (FDA) in 1986 were Recombivax HB®

and Engerix®-B, which protect against hepatitis B virus infection that as a chronic infection can lead to liver cancer. To date, the FDA has also approved Gardasil® and Cervarix® for protecting against the HPV types that most often cause cervical, vaginal, vulvar and anal cancers and Twinrix®, which protects against hepatitis B and A virus infections (U.S. Food and Drug Administration 2001, U.S. National Cancer Institute 2011).

In April 2010, the FDA also approved the first therapeutic cancer vaccine. This vaccine, sipuleucel-T (Provenge®), was approved for the treatment of metastatic hormone-refractory prostate cancer (Thara et al. 2011). Furthermore, a number of vaccines targeted for cancer prevention or treatment are currently being tested in clinical trials (U.S. National Cancer Institute 2011).

2.2 An overview of noroviruses and enteroviruses

This chapter elaborates on the features of the two virus genera relevant to this doctoral thesis.

2.2.1 Noroviruses

Noroviruses (NoVs) are members of the family *Caliciviridae* and the most common causative agent of nonbacterial acute gastroenteritis worldwide. It has been estimated that in the United States alone, noroviruses cause about 21 million disease episodes and contribute to 71 000 hospitalizations and 800 deaths annually (Gastañaduy et al. 2013). Symptoms appear within 12 – 48 hours after viral infection and are characterized by acute onset of nausea, vomiting, abdominal cramps, and diarrhea. Although norovirus gastroenteritis is generally mild and short (lasting normally 2 to 3 days), severe illness and complications can occur particularly in children, the elderly, and in immunocompromised individuals in healthcare settings. The virus is transmitted through contaminated food or water and via person-to-person contact and infects individuals in all age groups (Donaldson et al. 2010, Herbst-Kralovetz et al. 2010).

Noroviruses possess a high level of genetic and antigenic diversity. Based on the amino acid (aa) sequence of the capsid protein VP1, norovirus genotypes can be classified into five genogroups (GI–GV), which differ by up to 60%. Of these, only the GI, GII, and GIV strains have been detected in humans (Green et al. 2000).

The level of diversity is much higher than that seen for other positive sense, single-stranded RNA viruses (Zheng et al. 2006). Genogroups are further divided into genotypes, of which the GI genotype 1 (GI.1) is the prototypic "Norwalk virus" genotype and the strains of GII.4 are primarily responsible for a majority (80%) of norovirus outbreaks worldwide (Fankhauser et al. 2002, Siebenga et al. 2007).

Following their discovery in the early 1970s (Adler & Zickl 1969, Kapikian et al. 1972), the biological characterization of human noroviruses has been hampered by the lack of an appropriate cell culture system for propagation of the virus. Except for the recently developed gnotobiotic pig model (Cheetham et al. 2006), there was neither a small animal model available for studying the human disease. However, when expressed in a baculovirus or other eukaryotic expression system (Santi et al. 2008, Taube et al. 2005, Xia et al. 2007), the recombinant VP1 capsid proteins self-assemble into empty virus-like particles that are morphologically and antigenically similar to the native virions (Green et al. 1993). Thereafter, norovirus VLPs have been used extensively to study virus structure and stability, host-cell interactions, and as a tool in diagnostic serological assays (Ausar et al. 2006, Patel et al. 2009, Prasad et al. 1999).

The most advanced vaccine candidates against NoV are also VLP-based. The intranasally administered GI.1 VLP developed by LigoCyte contains adjuvants (monophosphoryl lipid A and mucoadherent chitosan). It was shown to induce homologous memory B cell response in clinical studies (El-Kamary et al. 2010, Ramirez et al. 2012) as well as proven to protect against NoV gastroenteritis and infection among vaccinated subjects in challenge studies with homotypic NoV (Atmar et al. 2011). Another VLP-based, bivalent NoV vaccine produced by Takeda Pharmaceutical contains both the GI.1 strain and the GII.4 consensus strain (2002-2006) with adjuvants (monophosphoryl lipid A and alumn). This vaccine was well tolerated and highly immunogenic in phase I volunteer studies (Treanor et al. 2014) and was able to induce cross-protection against severe NoV gastroenteritis, but not protect against NoV infection when challenged with a GII.4 (2002) variant different from the vaccine strain by 19 aa in the hypervariable domain of the NoV capsid (Bernstein et al. 2015).

Noroviruses are small, non-enveloped, round viruses of approximately 38 nm in diameter and possess a single-stranded, positive-sense RNA genome of about 7.6 kilobases (kb) in length. The 5'-terminus is covalently linked to a small virus-encoded protein (VPg) and the 3'-terminus is polyadenylated. The genome contains three open reading frames (ORFs) (Figure 3). The first ORF encodes a polyprotein precursor, which is further processed into non-structural proteins. The

ORF2 encodes the 58-kDa capsid protein VP1 and the ORF3 encodes the minor structural protein, VP2 (Daughenbaugh et al. 2003, Jiang et al. 1993, Prasad et al. 2000).

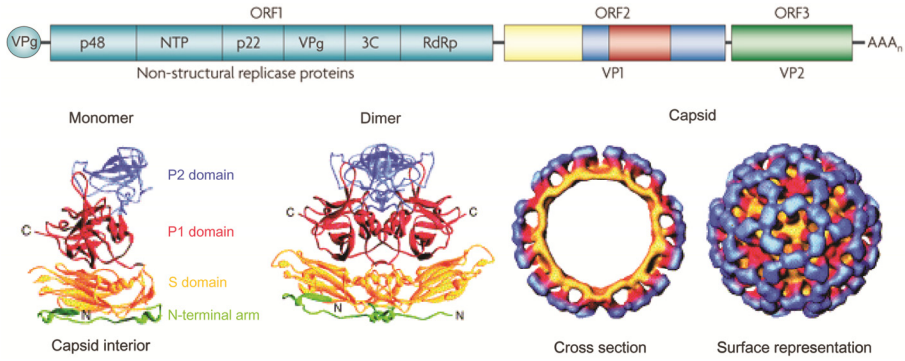

Figure 3. Genome organization and capsid structure of a norovirus. Adapted from Donaldson et al. (2010), copyright (2010) with permission from Macmillan Publishers Ltd (Nature Reviews Microbiology) and from Hutson et al. (2004), copyright (2004) with permission from Elsevier (Trends in Microbiology).

Structural studies of the recombinant norovirus capsid have shown that the viral capsid is composed almost entirely of the 57 kDa VP1 protein encoded by ORF2 and the capsid exhibits a T=3 icosahedral symmetry with 180 molecules of the capsid protein organized into 90 dimeric capsomeres (Figure 3). The capsid protein consists of two domains that are linked by a short hinge region, the shell (S) domain and the protruding (P) domain. The P domain dimers project out from the icosahedral shell. The P domain can be divided further into two subdomains, P1 and P2. Of the two, the highly variable P2 subdomain contains the major antigenic determinants of a host immunological response (Glass et al. 2009, Prasad et al. 1994, Prasad et al. 1999).

Noroviruses bind in a strain-specific manner to histo-blood group antigens (HBGAs), a diverse family of carbohydrates polymorphically expressed on mucosal surfaces. At least eight distinct binding patterns have been described, and all three major histo-blood group antigen families: the ABO, Lewis, and secretor status (i.e., the presence of a functional *FUT2* gene, which encodes for a secretor enzyme α[1,2]fucosyltransferase that adds side chains to a precursor molecule), have been shown to be involved in norovirus recognition. About 20% of people (called "non-secretors") that do not encode a functional FUT2 gene are resistant to genotype GI.1 infection. Epidemic GII.4 strains may predominate because they bind both A, B and O secretors that represent 80% of the population (Debbink et al. 2012,

Lindesmith et al. 2003, Tan & Jiang 2005a). Therefore, because human noroviruses cannot be cultivated *in vitro*, VLP-HBGA binding and blockade assays have been used as a surrogate to evaluate the infectivity of the original virus strain and the potential neutralization response of both monoclonal antibodies and sera (Harrington et al. 2002).

2.2.2 Enteroviruses

Enteroviruses belong to the family *Picornaviridae*, a large and diverse group of small viruses associated with several human and mammalian diseases. Enteroviruses are transmitted by the fecal-oral route, and affect millions of people worldwide each year. Historically, poliomyelitis was the most significant disease caused by an enterovirus (poliovirus) in humans, but also other non-polio enteroviruses may be associated with diseases that range from mild upper-respiratory tract infection (common cold), febrile rash (hand, foot and mouth disease), and acute hemorrhagic conjunctivitis to more severe conditions, such as herpangina, aseptic meningitis, encephalitis, and myocarditis (Pallansch & Roos 2001).

According to the present classification (International Committee on Taxonomy of Viruses 2013) the enterovirus genus is divided into twelve species including Enterovirus A-H and J and Rhinovirus A-B, each comprising numerous serotypes. The human coxsackievirus B3 (CVB3), a member of the species Enterovirus B, regularly causes mild infections (Melnick 1996), but the infection may also lead to more severe diseases affecting the heart, pancreas, or central nervous system. Of the more than 20 common viruses associated with myocarditis in humans (Grist & Reid 1997), CVB3 is considered the most common cause of acute and chronic viral myocarditis. Furthermore, viral myocarditis can lead to dilated cardiomyopathy (DCM) and cardiac failure (Maier et al. 2004, Selinka et al. 2004). In addition, CVB3 is associated with pericarditis (Gaaloul et al. 2014), meningitis (Wong et al. 2011) and inflammatory diseases of the pancreas (Mena et al. 2000), and it is also known to infect stem cells in the neonatal central nervous system (Feuer et al. 2003).

Similar to noroviruses, CVB3, along with other enteroviruses, encompasses a single-stranded, positive-sense RNA genome of about 7.5 kb in length. The viral genome consists of a single open reading frame (ORF) that is translated into a single long polypeptide containing the P1, P2, and P3 regions (Figure 4). The P1 region is further processed by a viral protease to produce the four capsid proteins,

VP0, VP3 and VP1, and VP0 is subsequently cleaved to give VP4 and VP2 during viral maturation. The P2 and P3 regions are processed into seven nonstructural proteins that have roles in polyprotein cleavage, RNA replication, and shut-down of the host cell protein synthesis. The single ORF is flanked by a 5' untranslated region (5'UTR), containing the internal ribosome entry site (IRES) and a small virus-encoded protein (VPg) covalently linked at the 5' end, and by polyadenylated 3'UTR (Esfandiarei & McManus 2008, Klump et al. 1990).

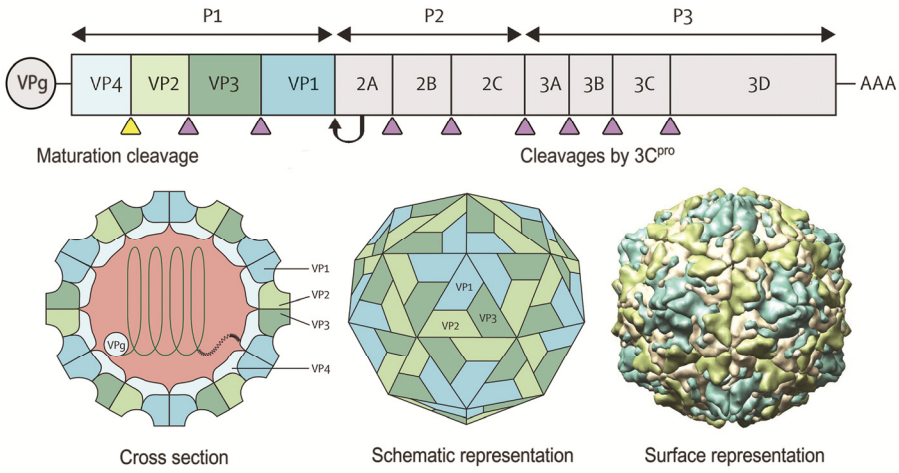

Figure 4. Genome organization and capsid structure of enterovirus. Adapted from Solomon et al. (2010), copyright (2010) with permission from Elsevier (The Lancet Infectious Diseases) and the PDB ID 1COV Muckelbauer et al. (1995) with permission from the RCSB.

The non-enveloped, spherical capsid is about 30 nm in diameter and consists of a densely-packed icosahedral arrangement of 60 protomers with (pseudo) T=3 packing (Figure 4). Each protomer consists of the four capsid proteins VP1-VP4, of which VP1, VP2 and VP3 are exposed at the virion surface, and VP4 is located on the internal side of the capsid (Muckelbauer et al. 1995). The capsid contains canyon-like structures that allow viral attachment through interactions with the host cell proteins coxsackievirus and adenovirus receptor (CAR) and decay-accelerating factor (DAF) (Bergelson et al. 1994, Bergelson et al. 1997, Park et al. 2009). Of the four capsid proteins, VP1 exhibits the highest sequence variability, while VP4 exhibits the lowest (Chehadeh et al. 2005).

The control of CVB3 infection depends on both cell-mediated and humoral immunity (Dotzauer & Kraemer 2012, Kemball et al. 2010). Antibodies play a key role in fighting the CVB3 infection, as reflected by the increased risk of chronic infections in patients with humoral immune deficiencies (Cooper et al. 1983, Hertel

et al. 1989, Misbah et al. 1992). However, B cells may also have a role in virus dissemination because they can carry the infective virus (Mena et al. 1999). The involvement of cell-mediated immunity in coxsackievirus infection and virus-induced myocarditis is less clear and particularly controversial. Increasing evidence suggests that although host T cells help to limit virus production, T cell responses to infection and viral counteractions can increase the pathogenicity of the infection (reviewed in Dotzauer & Kraemer 2012, Huber 2008 and in Kemball et al. 2010). The epitopes that bind neutralizing antibodies are mainly present on VP1 (Haarmann et al. 1994), and potential CVB-specific T cell epitopes have been mapped to both VP1 and VP2 (Huber et al. 1993, Voigt et al. 2010), as well as to the 3A and 3C regions (Weinzierl et al. 2008). Pathogenic determinants have been localized to the 5'UTR of the CVB3 genome (Dunn et al. 2003, Tu et al. 1995) and also to the different parts of the capsid coding region (Knowlton et al. 1996, Park et al. 2009, Stadnick et al. 2004).

2.3 Virus-like particles

VLPs are a distinct class of subunit vaccines that differ from other recombinant antigen subunit vaccines by providing a more potent protective immunogenicity that associate with the VLP structure that mimics the structure of authentic virus particles. Additionally, some VLPs have also proven to be suitable for the fusion or insertion of foreign antigenic sequences, thus allowing the production of chimeric VLPs that expose the foreign antigen on their surface. Other VLPs have also been used as carriers for a variety of foreign molecules or therapeutics (Grgacic & Anderson 2006, Kushnir et al. 2012).

2.3.1 Characteristics of VLPs

The origin of VLPs lies in the basic studies on virus structure and assembly that led to the observation that when expressed by using recombinant expression systems, the viral structural proteins intrinsically self-assemble into hollow particles resembling the parental virus (Burrell et al. 1979, Delchambre et al. 1989, Haynes et al. 1986, Valenzuela et al. 1982) (Figure 5). The first electron microscopy visualization of recombinant hepatitis B VLPs was published in 1982 (Cohen & Richmond 1982). Since then, over three decades of research have led to the

construction and characterization of more than 100 VLPs from 35 different virus families originating from microbial, plant, insect and mammalian viruses (Zeltins 2013), clearly highlighting their versatility and increasing scientific and therapeutic interest.

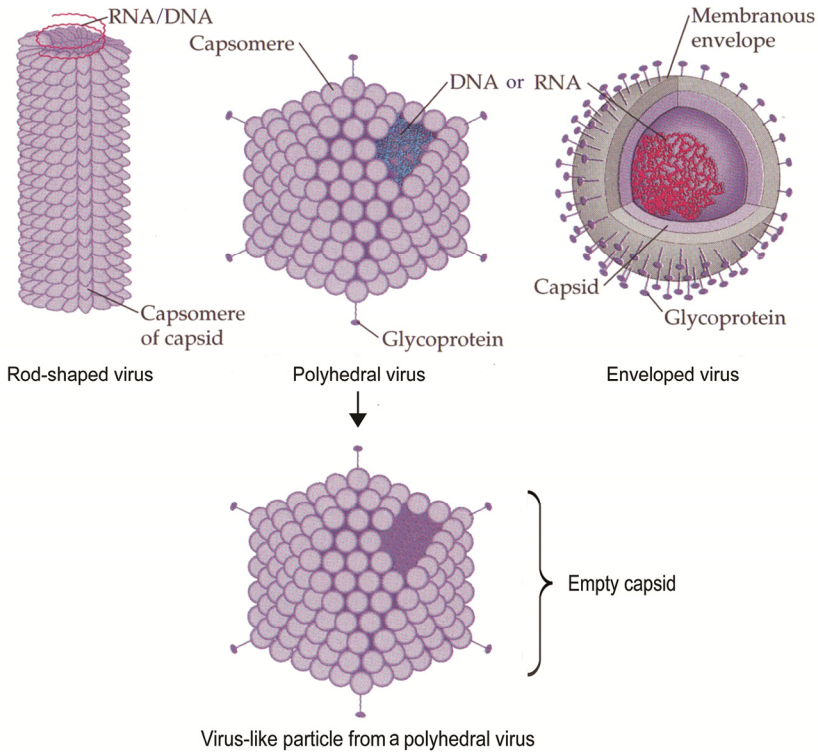

Figure 5. Composition of different viruses and a VLP derived from a polyhedral virus. Adapted from Campbell (1996) with permission from Benjamin/Cummings.

This diverse group includes VLPs that have a single or multiple capsid proteins. Most VLPs are composed of a single layer of viral proteins, while others have a double-layered or even a triple-layered structure. Some VLPs additionally possess a lipid envelope (Figure 5). While a great deal of them were developed for the production of human and animal vaccines, several VLPs have also been generated to promote the fundamental understanding of virus assembly process, the conformational architecture and dynamics of viruses, as well as for diagnostic purposes (Bárcena & Blanco 2013).

Since being originated from a spontaneous assembly of viral structural proteins, VLPs are usually structurally and antigenically indistinguishable from the parental virion. Therefore, they generally retain the ability to present viral epitopes in an

authentic conformation and to bind and penetrate host cells. Consequently, VLPs are highly immunogenic, however, due to the absence of the viral genome, they are unable to replicate and cause a disease (Grgacic & Anderson 2006, Roy & Noad 2008). This means that VLPs have the authentic conformation seen in attenuated virus vaccines without the safety concerns related to possible reversion to a virulent form or to inactivation failures.

VLPs have a well-defined geometry, usually representing either icosahedrons or rod-like structures (Figure 5), and diameters in the range of 20-200 nm (Bachmann & Jennings 2010). The antigenic epitopes are displayed in a correct conformation and in a densely repeated and ordered manner on the surface of the VLPs that leads to a strong antibody response by the crosslinking of B cell immunoglobulin receptors and the activation of B cells (Hinton et al. 2008). Their immunogenicity is further enhanced by the nanometer-scale size of the VLPs, that allows them to be efficiently taken up by professional antigen-presenting cells (APCs), particularly dendritic cells (DCs) (Fifis et al. 2004), which ultimately leads to activation of both the B cells and T cells of the adaptive immune response (Figure 2), even in the absence of adjuvants. This ability to prime long lasting T cell responses in addition to antibody responses makes VLPs generally more immunogenic than traditional subunit vaccines (Grgacic & Anderson 2006).

The generation of VLPs derived from certain viruses has been strongly motivated by the absence of appropriate cell culture systems for the propagation of those viruses, as was the case for hepatitis B and C viruses, HPV, and noroviruses. VLP technology has also enabled the substitution of infective viruses requiring high-level biosafety laboratories for their handling, such as the severe acute respiratory syndrome virus (SARS) or Ebola and Marburg viruses, with VLPs (Bárcena & Blanco 2013).

In some cases, the VLPs are generated from internal structural proteins of the virus particle, such as the HBV core antigen (HBcAg) or the Gag proteins of retroviruses, which are capable of self-assembling into subviral particles. Such VLPs do not mimic the external morphology of the parental virus, and the antibodies elicited against them are not able to protect from infection by the parental virus. Although these VLPs may not be suitable for vaccine development against the viruses from which they were derived *per se*, they can be used as scaffolds for the presentation of epitopes or polyproteins of a completely unrelated virus or pathogen (Bárcena & Blanco 2013).

2.3.2 VLPs as stand-alone antiviral vaccines

The most straightforward use of VLPs is to utilize them for vaccination against the virus from which they were derived. Currently, a handful of prophylactic VLP-based vaccines against human diseases have been commercialized worldwide (Figure 6). These include the first recombinant VLP vaccine, Recombivax HB®, for the prevention of hepatitis B infection, licensed in the U.S. in 1986 by Merck and Co., Inc. and the similar vaccine Engerix®-B (GSK) licensed soon after. Both vaccines consist of 22-nm subviral self-assemblages of the HBV surface antigen (HBsAg), co-assembled with membrane lipids and expressed in genetically engineered yeast (*Saccharomyces cerevisiae*) (Bárcena & Blanco 2013).

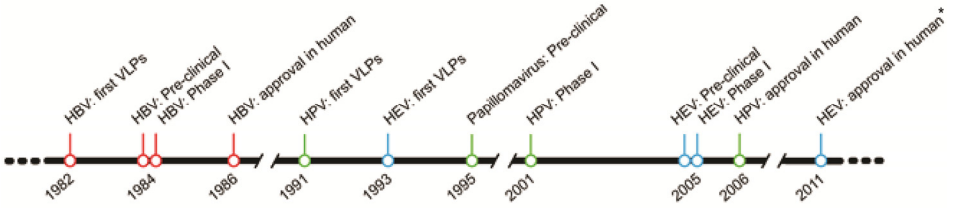

Figure 6. Developmental milestones of the currently approved VLP-based vaccines. *approved by the Chinese Food and Drug Administration. Adapted from Lua et al. (2014), copyright (2010) with permission from John Wiley and Sons (Biotechnology & Bioengineering).

Later on, two VLP-based vaccines against human papillomavirus (HPV) and for the prevention of cervical cancer were approved by the FDA. Gardasil®, which is produced in yeast (*S. cerevisiae*), was licensed by Merck in 2006, whereas Cervarix® (GSK), produced using the baculovirus-insect cell expression system, was licensed in 2009. These vaccines consist of VLPs assembled into 40-nm-sized particles from L1, the major capsid protein of HPV, and contain mixtures of VLPs that are derived from the different HPV serotypes causing genital infections (Bárcena & Blanco 2013). Both vaccines have proven almost completely protective against the HPV serotypes from which each vaccine is derived (Schiller et al. 2008). They both protect against the two HPV serotypes (HPV serotypes 16 and 18) that cause 80% of anal cancers, 70% of cervical cancers, 60% of vaginal cancers, and 40% of vulvar cancers (De Vuyst et al. 2009). Gardasil also protects against HPV serotypes 6 and 11 that provoke genital warts (Lacey et al. 2006). Recently in December 2014, the FDA also approved Gardasil® 9, a nine-valent prophylactic HPV vaccine (HPV6/11/16/18/31/33/45/52/58) (U.S. Food and Drug Administration 2014).

Additionally, a large number of VLP-based vaccine candidates for human diseases are undergoing clinical evaluations. The registry database clinicaltrials.gov, supported by the U.S. National Institutes of Health, lists 99 studies for VLP vaccines, created predominantly against viral infections. Among them, are 37 completed trials for HPV VLP vaccines as well as 21 trials for pandemic and multivalent seasonal influenza VLP vaccines (produced mainly by Novavax and Medicago). Other VLP-based vaccine candidates in advanced stages of clinical trials include those directed against hepatitis E (Hecolin® by Xiamen Innovax Biotech) and B viruses (Sci-B-Vac™ by SciGene Israel), norovirus (Takeda Pharmaceuticals) (Josefsberg & Buckland 2012, Rodríguez-Limas et al. 2013), and the Chikungunya virus (Chang et al. 2014).

2.3.3 VLPs as carriers and foreign antigen display systems

In addition to the straightforward use of VLPs as immunogens, the efficiency with which they stimulate both humoral and cellular immune responses has made them excellent candidates as platforms for a multimeric display of foreign antigens and/or targeting molecules (Figure 7). The display can be achieved through the incorporation of molecules onto or into the VLP either by genetic fusion into subunit proteins of the capsid (chimeric VLPs) or by chemical conjugation to preformed VLPs (conjugated or coupled VLPs). In such cases, the VLPs serve both as a presentation scaffold for extraneous antigens in a suitable repetitive and highly organized context that overcomes the poor immune response of plain soluble antigens and as adjuvants to enhance the immune response (Bárcena & Blanco 2013, Liu & Chen 2005).

Other applications of chimeric VLPs are as carriers of various encapsidated therapeutic or diagnostic agents, such as proteins or nucleic acids, as adjuvants for vaccines or gene therapy, as carriers of small drug molecules to be delivered to specific cells, and in targeting to desired organs, tissues, or cells (Pushko et al. 2013). The ability of VLPs to bind nucleic acids is common for viral structural proteins, and this property can be utilized for the binding and encapsidation of other negatively charged molecules, for instance, oligonucleotides and biological and chemical polymers (Newman et al. 2009, Ng et al. 2011, Storni et al. 2004). However, the packing is limited by the internal volume of the carrier VLP and the availability of positively charges residues in the VLP interior (Zeltins 2013).

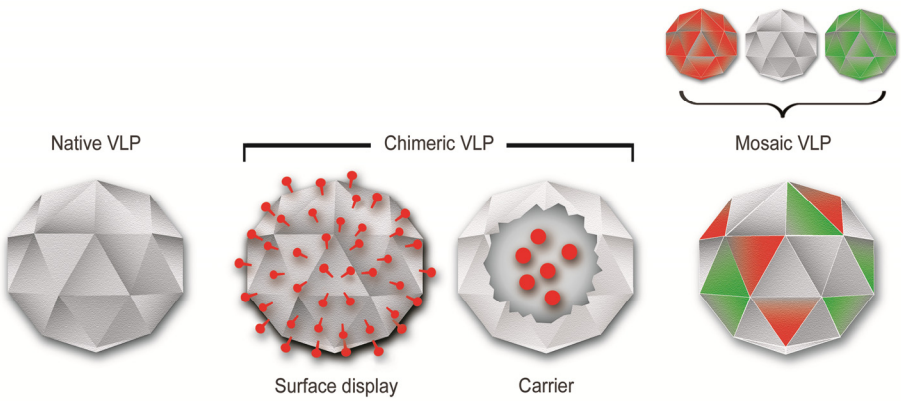

Figure 7. Summary of the different VLP types. In addition to native VLPs, chimeric VLPs can be generated, which represent foreign molecules on their surface or function as carriers of various encapsidated therapeutic or diagnostic agents. Mosaic VLPs contain copies of both the chimeric and native VLP subunit proteins or consist of subunit proteins from different virus strains.

The use of VLPs as carriers of foreign molecules is not limited to those VLPs that originate from economically significant viruses or viruses that relate to the condition to be treated. The VLPs derived from hepatitis B core and surface antigens (HBcAg, HBsAg) and bacterial phage Qβ are the most extensively investigated chimeric carriers of foreign antigens to date (Pushko et al. 2013). For example, the development of the HBsAg-derived RTS,S vaccine against malaria has recently resulted in the first chimeric VLP vaccine to successfully conclude phase III clinical trials (RTS-S Clinical Trials Partnership 2014). Other chimeric vaccines currently undergoing clinical trials include a M2e-HBc-based vaccine against influenza A (Fiers et al. 2009), a CpG-adjuvanted HBsAg-based vaccine against HBV (HEPLISAV™ by Dynavax) (Cooper & Mackie 2011), a HIV vaccine consisting of two chimeric vaccine formulations (Rerks-Ngarm et al. 2009), and a Pfs25-AIMV fusion VLP against malaria (U.S. National Institutes of Health 2014).

2.3.3.1 Genetic insertion

The most common method for displaying foreign epitopes on VLPs is genetic insertion of target sequences into capsid proteins to form chimeric VLPs. Chimeras are produced by cloning the DNA of either linear or conformational epitopes into the genes that encode the self-assembly competent structural proteins of VLPs. Upon assembly of the chimeric subunit proteins, the introduced epitopes

are presented on the VLP surface in a repetitive and ordered fashion, at relatively high density (one copy per subunit), and ideally in the right conformation (Jennings & Bachmann 2008).

The key to this technology is the knowledge of the detailed structure of the VLP in order to identify the suitable insertion sites within the primary sequence of the VLP subunits to incorporate the target epitopes. The correct folding and assembly and, therefore, the structural integrity and immunogenicity of the VLP should not be compromised by the insertion. Naturally, the insertion site differs, depending of the type of displayable foreign epitope. For example, whereas B-cell epitopes should be located at exposed sites and preferably at immunodominant areas on the surface, there are no such requirements for T-cell epitopes which are proteolytically processed by the APCs before being presented to the target cells (Bárcena & Blanco 2013). Often the easiest and least invasive site for the insertion is at the N- or C-terminus of the VLP protein subunit, especially if the three-dimensional structure of the VLP is not available. In such cases, however, the epitope is usually not optimally presented to the immune system.

Still, it is difficult to predict whether the introduced peptides will be compatible with VLP assembly at the intended insertion site or whether the insertions will be immunogenic. For example, minor displacements at the insertion site can cause radical changes in the immunogenicity of the peptide (Rueda et al. 1999). In addition to peptide insertions with high hydrophobicity, a strong positive charge or high β-strand index that are likely to be problematic for VLP assembly (Bárcena & Blanco 2013), the size of the peptide insert is usually restricted to less than 20-30 amino acids. However, there are marked differences among VLPs regarding the size of the tolerated insert, since also relatively large insertions, such as the 238 aa of the whole green fluorescent protein (GFP) inserted onto HBcAg-derived VLPs (Kratz et al. 1999), have been successfully incorporated onto the exposed sites of VLPs.

The assembly of complex VLP chimeras has been facilitated by developing mosaic VLPs (Figure 7). Mosaic VLPs are usually formed by co-expression of a chimeric VLP subunit along with a native VLP subunit. The resulting VLPs contain copies of both chimeric and native VLP subunit proteins, which are incorporated with differing proportions. Alternatively, by using co-expression of VLP subunit proteins that originate from different virus strains, mosaic VLP vaccines that protect against multiple virus serotypes can be generated (Jennings & Bachmann 2008).

2.3.3.2 Chemical conjugation

As stated above, the use of chimeric VLPs has been limited, because the self-assembly of chimeras is often unpredictable, the length of the fused antigen is restricted, non-peptide antigens cannot be inserted and the folding of the introduced antigen is often compromised, which means that conformational epitopes may not be preserved. An alternative approach for displaying antigens on the VLP surface is to use chemical conjugation, in which the native VLP and the target antigen are synthetized separately and then the antigen is conjugated chemically *in vitro,* using either covalent or non-covalent binding to the surface of a preassembled VLP (Jennings & Bachmann 2008). The advantages of this approach are that the size and structure of the antigen to be attached is not limited by the requirements of the correct folding and assembly of the VLP subunits, and that diverse kinds of molecules can be attached. Examples of such molecules are short linear or cyclic peptides, full-length proteins (Bárcena & Blanco 2013), or even non-peptide antigens, such as glycopolysaccharides (Kaltgrad et al. 2008) and small organic molecules, like nicotine, which was attached to the surface of the bacteriophage Qβ-derived VLPs (Cornuz et al. 2008).

Chemical coupling can be addressed basically to any reactive amino acid moiety present on the surface of the VLP, typically to amino groups of lysine, although other residues, such as tyrosine, cysteine, aspartic and glutamic acids can also be chemically targeted. Furthermore, VLPs can be engineered by targeted mutagenesis to contain suitable reactive amino acids on the surface of the particle (Strable & Finn 2009). Surface-exposed lysine residues can also be biotinylated and then used for non-covalent conjugation of antigens to VLPs through the use of streptavidin fusion proteins (Chackerian et al. 2001).

2.3.3.3 VLPs as immune therapy modulators

The technological innovation of VLPs to serve as carriers of B and T cell epitopes has greatly broadened their potential as prophylactic and therapeutic vaccines. Not only can VLPs act as carriers of foreign immunological epitopes and used in immunizations against a variety of pathogens, but they can also be used to present self-antigens to the immune system and overcome B cell unresponsiveness to treat chronic diseases. Towards this end, VLPs have been used to induce autoantibodies to the disease-associated self-molecules involved in chronic diseases, such as hypertension (Ou et al. 2013, Tissot et al. 2008), rheumatoid arthritis (Spohn et al.

2008), Alzheimer's disease (Wiessner et al. 2011, Winblad et al. 2012, Zamora et al. 2006), and certain cancers (Braun et al. 2012, Ding et al. 2009, Dorn et al. 2008, Pejawar-Gaddy et al. 2010). Some of these vaccine candidates have shown efficacy in mouse models, while others have already proceeded to clinical trials.

2.3.4 VLP production systems

There are many expression systems for the production of VLPs, such as various species of yeast that include *Saccharomyces cerevisiae* and *Pichia pastoris*; bacteria, mainly *Escherichia coli* (*E. coli*), the baculovirus expression vector/insect cell system (BEVS/IC), and various mammalian cell lines (Grgacic & Anderson 2006). Some vaccine candidates intended primarily for oral intake (e.g., HPV and NoV) have also been produced in various plants, including tobacco and lettuce leaves and potato (Kong et al. 2001, Mason et al. 1996, Pniewski et al. 2011). The choice of production system depends on the specific target function of the VLP, namely, whether it is significant to retain more consistent original VLP formation and post-translational modifications (PTMs, e.g., glycosylation and phosphorylation). All production systems have their own advantages and drawbacks as discussed briefly below. However, the primary focus within this thesis is on the baculovirus-insect cells system.

Ease of expression, scalability, and low-cost production have made **yeast** a popular choice, and for example, Recombivax HB® and Gardasil® as well as Engerix®-B have been manufactured using this system. However, concerns such as appropriate glycosylation and correct protein folding and assembly may direct choosing towards alternative production systems (Grgacic & Anderson 2006, Kushnir et al. 2012). Although the most widely used expression system for producing recombinant proteins, **bacteria** is not a preferred platform for VLP production due to a number of factors. For instance, they do not generally assemble VLPs of mammalian viruses or post-translationally modify proteins. Therefore, bacterial systems are generally used for the production of bacterial and plant VLPs (Kushnir et al. 2012, Zeltins 2013). **Mammalian** cell culture systems are favored for appropriate modifications and authentic assembly, but they are a more costly and less controllable alternative for production. Retrovirus-based VLPs in particular tend to incorporate unwanted host cell membrane proteins in their envelope during assembly (Grgacic & Anderson 2006). **Plant** expression systems have many advantages compared to mammalian cells. Not only are plant

production platforms cost-effective, highly scalable, and free of mammalian pathogens, but protein folding, assembly and PTMs in plants also resemble those produced in mammalian cells (Kushnir et al. 2012). VLPs can also be created *in vitro* under **cell-free** conditions in solution using translation machinery extracted from cells. The method is particularly useful when production conditions need to be closely controlled or when VLP toxicity prevents production in cells (Carlson et al. 2012, Smith et al. 2012). Although cell-free expression is not yet practical for large-scale protein production, VLPs have been produced in cell-free extracts of *E. coli* (Bundy et al. 2008), yeast (Wang et al. 2008), wheat germs (Takai et al. 2008), rabbit reticulocytes (Jackson & Hunt 1983), and insect cells (Ezure et al. 2010).

2.3.4.1 Versatile baculovirus-insect cell production system

Since first described in 1983 (Smith et al. 1983), the baculovirus-insect cell system has become one of the most extensively utilized systems for VLP production (van Oers et al. 2015). Similar to yeast, **insect** cells (*Spodoptera frugiperda,* Sf9 or Sf21 and *Trichoplusia ni* under the commercial name High Five™) have been the host of several of VLP-based vaccine candidates, as well as, one of the current HPV vaccines, Cervarix®. The baculovirus-insect cell expression system was also used to generate the VLPs within this thesis. A closer look below at the advantages of the insect cell -based production system largely explains its popularity amidst other VLP production systems.

The baculovirus-insect cell -based protein production system possesses many advantages for VLP production. For example, baculovirus expression permits correct protein folding and oligomerization and multiple eukaryotic-type post-translational modifications (e.g., phosphorylation, glycosylation, acylation, disulfide bond formation, proteolytic cleavages etc.). Moreover, insect cells can accommodate a high-level accumulation of foreign proteins, have the capacity for large-scale production, and the possibility to culture without the need of mammalian-derived supplements, which thereby minimizes the risk of co-culturing mammalian pathogens. Furthermore, the system allows the expression of several foreign proteins simultaneously by co-infection with multiple baculoviruses, each expressing a single protein (co-infection), or by a single baculovirus containing a multicistronic expression vector that enables the expression of multiple proteins (co-expression) in the same infected cell and thereby facilitates capsid assembly in each cell (Kost et al. 2005, Liu et al. 2013a, Sokolenko et al. 2012). For example, as much as six different proteins of the herpes virus have been expressed using the

co-infection strategy (Tatman et al. 1994), and the co-expression strategy using tricistronic (Pushko et al. 2005) or even quad-cistronic (Latham & Galarza 2001) baculoviruses has been used for the construction of influenza virus derived VLPs.

The main limitation of the BEVS/IC system is contamination of the target with co-produced, enveloped baculoviruses during infection, which complicates the purification of enveloped VLPs and those VLPs that have sizes within the same order of magnitude as baculoviruses (Grgacic & Anderson 2006, Vicente et al. 2011). Another central disadvantage of this system resides in its pattern of post-translational modifications, which are not necessarily equivalent to those of higher eukaryotes. One of the best examples is that the insect cells perform simpler N-glycosylation than the mammalian cells (Kost et al. 2005). This limitation is particularly troublesome in such clinical applications, where correct glycosylation is essential for the function of the therapeutic protein, such as in vaccines. Within the past decade, extensive efforts have been made to overcome this problem by developing new "humanized" insect cell lines engineered with mammalian genes responsible for the N-glycosylation pathway (Jarvis 2003). More recently, similar improvements have also been developed for yeast cells (Chigira et al. 2008, De Pourcq et al. 2012, Hamilton & Gerngross 2007).

Baculoviruses are now also utilized in biotechnological applications beyond the production of proteins in insect cells. These applications include the development of strategies for displaying foreign proteins and peptides on baculovirus particles and the insertions of mammalian cell-active expression cassettes in baculoviruses to drive the expression of genes in mammalian cells as well (BacMam viruses) (Kost et al. 2005).

2.3.5 Downstream processing of VLPs

Downstream processing of VLP vaccines aims at producing large volumes of concentrated, quality-consistent, and biologically active product, while eliminating contaminants that originate from the host cells and culture media. Additionally, the purification protocol should be robust, cost-effective, scalable and preferably applicable to a wide variety of VLPs (Vicente et al. 2011).

Naturally, the methods that were originally developed for the purification of viruses have been later expanded to the purification of VLPs, although the inability of VLPs to cause disease brings the benefit of needing less stringent biosafety requirements. VLPs, like native viruses, are traditionally purified based on their size

and density using gradient ultracentrifugation techniques through sucrose or cesium chloride (CsCl) (Estes 2004). However, gradient ultracentrifugation-based methods are not practical for large-scale vaccine manufacturing because they are time-consuming, labor-intensive and difficult to scale-up (Rolland et al. 2001). In addition, CsCl is problematic due to its toxicity, induction of deduced infectivity in viruses, and particle deformation (Burova & Ioffe 2005). Due to these limitations, the traditional VLP purification methods are progressively being replaced by more sophisticated techniques, such as tangential flow filtration and chromatography.

2.3.5.1 Chromatography for large-scale purification

The initial clarification of crude lysate by low-speed centrifugation or tangential flow filtration is generally followed by some form of chromatography method (ion exchange, affinity, or size-exclusion) to capture the VLPs (Pattenden et al. 2005). The anion and cation exchange media in **ion exchange chromatography** (IEX) relate to the surface charge of the VLP particle at a given pH, and they can be used to selectively adsorb the VLP particles in the presence of other charged contaminants. For example, a norovirus exhibits negatively charged outer surface at a neutral pH (Goodridge et al. 2004), and therefore, it tends to bind to the positively charged functional groups in the stationary phase of the anion exchange column.

Affinity chromatography is based on specific molecular recognition and reversible binding between two molecules, for example between an antigen and a matrix-bound antibody (Morenweiser 2005). One of the most typically employed forms of affinity chromatography in recombinant protein purification is nitrilotriacetic acid (NTA)-based, immobilized metal ion affinity chromatography (IMAC) (Hochuli et al. 1987, Hochuli et al. 1988), which can be used if the target protein is expressed with a polyhistidine affinity tag (His-tag) that binds to the immobilized metal ions (e.g., Ni, Co, Fe, Cd, or Zn) of the column. Usually, high purity and yield are obtained by affinity chromatography. However, the method is rather expensive at an industrial scale due to the high cost of antibodies and chemicals used. Moreover, the potential immunogenicity of the His-tag sequence and potential allergenic effects of coordination metals, such as nickel, that are used in IMAC pose some safety concerns (Block et al. 2009, Morenweiser 2005).

An additional precipitation step using chemicals, such as ammonium sulfate (Park et al. 2008) or more commonly polyethylene glycol (PEG) to concentrate the VLPs (Guerrero-Rodríguez et al. 2014, Gurramkonda et al. 2013, Tsoka et al.

2000), is often included in the early phase of purification, usually after clarification. Although PEG precipitation significantly decreases the volume of the extract, impurities or polymers often tend to co-precipitate along with the VLPs. Residual PEG may also be disadvantageous in downstream applications (Russell et al. 2007).

Chromatography provides a convenient and practical intermediate step for capturing and concentrating VLPs from cellular and media contaminants. These matrix adsorption-based methods offer several advantages for large-scale VLP purification, including a short processing time and preservation of biological activity, since high flow rates and mild conditions can be used to elute VLPs from the chromatography matrix. In addition, large volumes of cell lysate can be processed, scale-up is relatively easy, and the cost of operation is comparatively low. However, it is worth noting that the traditional chromatographic matrices developed for protein purification are generally poorly suitable for the purification of much larger VLPs (Morenweiser 2005).

Conventional chromatography media that are intended for protein purification consist of resin that typically has a pore diameter of 10-20 nm, or as for perfusive resins, have at least a subset of pores with a wider diameter of order hundreds of nm (Afeyan et al. 1990). VLPs, whose hydrodynamic radius ranges from 20 nm to over 200 nm, are often too large to diffuse into the pores. Therefore, binding of VLPs occurs primarily on the bead surface, and results in sub-optimal usage of such matrices. In addition, VLPs, which diffuse more slowly in solution than much smaller and fast moving proteins and other contaminants, end up competing for the limited number of sites on the bead surface (Morenweiser 2005, Vicente et al. 2011). More recently, new chromatographic matrices especially suited for large particles, such as VLPs, have been developed. These matrices are based on porous membrane layers or monoliths and have increased bead surface areas. Examples of these pore sizes are 0.8 μm for Mustang® membrane adsorbers from Pall, 3 μm for Sartobind® membrane adsorbers from Sartorius Stedim Biotech, and more than 1 μm for CIM® monoliths from BIA Separations. However, concerns have been presented of them being less advantageous for large particles (about >100 nm), which can become entrapped in the unevenly formed pores of these media by the mobile phase flow and then prevent others from entering the pores (Trilisky & Lenhoff 2009, Trilisky et al. 2009).

2.3.5.2 Final polishing and formulation of VLPs

Polishing is a pivotal step if clinical grade material that meets strict regulatory guidelines is desired. For instance, residual host cell proteins and DNA need to be reduced to acceptable threshold values, typically below 100 μg and 10 ng per dose, respectively (European Medicines Agency 2012, U.S. Food and Drug Administration 2010). In addition to being used to capture VLPs from crude lysate, IEX, affinity and **size-exclusion chromatographic** (SEC) and **hydrophobic interaction chromatography** (HIC) processes are also well suited for polishing. While IEX chromatography is a method of choice for removal of residual host cell proteins and DNA from the flowthrough, SEC probably becomes a better alternative if the impurities have the same electrostatic properties and the difference in size is still significant (such as non-assembled proteins or other macrostructures). **Tangential flow filtration** (TFF) can be used at different stages during the purification process from partial purification and initial concentration of crude lysate to removal of low molecular weight impurities and exchange into the final formulation buffer at the final steps of product purification (Morenweiser 2005, Vicente et al. 2011). In practice, different chromatographic purification schemes are often multistep in nature and used together in series. By combining purification steps based on different techniques and optimizing the chromatographic conditions, it is often possible to achieve a high degree of purity, together with high concentrations of the end product.

3 AIMS OF THE STUDY

The main aim of this study was to produce and characterize virus-like particles derived from relevant strains of norovirus and enterovirus for vaccine development and diagnostics as well as to engineer the VLPs.

More specifically, the aims of the study were:

I To produce norovirus- and enterovirus-derived virus-like particles in insect cells and P domain proteins of norovirus in *E. coli* and to develop suitable purification methods for the expressed proteins and VLPs.

II To characterize the produced VLPs and to study the biophysical nature of the VLPs, as well as to study whether a modified RNA can be encapsulated into the VLP.

III To evaluate the antigenicity and receptor binding capabilities of the generated VLPs as well as to study induction of neutralizing antibodies and T-cell responses in mice as markers of immunogenicity and potential as vaccines.

IV To produce chimeric VLPs by introducing a genetic modification to the norovirus VLP structure that would enable non-covalent foreign molecule display on its surface.

4 MATERIALS AND METHODS

4.1 Construction of protein expression vectors (I-IV)

In order to obtain a full-length DNA copy of the VP1 capsid gene (Figure 3) of norovirus genotype GII.4 (GenBank accession number AF080551.1), referred to as NoV VLP (I, II), a cDNA copy of the norovirus genome was obtained from stool-extracted RNA using a reverse transcriptase polymerase chain reaction (RT-PCR). This cDNA was then used as template in a polymerase chain reaction (PCR) to amplify the capsid gene. The amplified PCR product was subcloned into the pFastBac™1 vector (Invitrogen, Carlsbad, CA, USA). The sequence corresponding to the whole P domain protein (I) of the norovirus capsid was amplified by PCR using capsid DNA as a template and primers that contained a C-terminal His-tag. The amplified P domain sequence was subcloned into the pET101/D-TOPO® vector (Invitrogen).

To generate the fully histidine-tagged norovirus-like particle, referred to as All-cHis VLP (IV), the DNA sequence encoding for the norovirus VP1 capsid protein was amplified by PCR using primers that extended the sequence to contain a C-terminal His-tag. The resulting PCR product was cloned into the pFastBac™Dual vector (Invitrogen). For the partially histidine-tagged norovirus-like particle (cHis-VLP, IV), the native norovirus capsid sequence was amplified and cloned into the the pFastBac™Dual vector, together with a fully histidine-tagged capsid sequence.

For CVB3 VLPs (III), a pFastBac™Dual vector containing the DNA copies of the desired genes of enterovirus CVB3 (GenBank accession number M33854.1) was ordered from GENEART AG (Regensburg, Germany). The first insert included the genes encoding the capsid proteins (VP1-VP4) of the CVB3, and the second insert included the whole CVB3 genome apart from the capsid-encoding genes, which were replaced by a mCherry coding sequence (III, Figure 1). All constructs were confirmed by DNA sequencing (ABI PRISM® 3100 Genetic Analyzer, Applied Biosystems Inc., Foster City, CA, USA).

4.2 Expression of recombinant proteins (I-IV)

NoV VLPs (I, II), CVB3 VLPs (III) and both forms of histidine-tagged NoV VLPs (IV) were produced in insect cells using the Bac-to-Bac® Baculovirus expression system (Invitrogen) according to the manufacturer's instructions. The pFastBac1 (I, II) or pFastBacDual (III-IV) expression vector was transformed into DH10Bac™ (Invitrogen) (I, II, IV) or DH10BacΔTn7EGFP (Kärkkäinen et al. 2009) (III) *E. coli* cells to create a recombinant bacmid, which was purified and transfected into *Spodoptera frugiperda* Sf9 insect cells (Table 1). A stock of recombinant baculoviruses was collected from the culture medium and used for a larger scale production of recombinant proteins. Approximately 2×10^9 Sf9 cells were seeded in a volume of 1 liter of HyClone™ SFX-Insect serum-free medium (Thermo Fischer Scientific, Waltham, MA, USA). Recombinant baculoviruses were added at MOI of 2, and the infected cells were cultured at 28°C for 5-6 days. The culture was clarified by centrifugation at 5000 g for 20 min at 4°C. An empty pFastBac Dual was used for the generation of empty baculoviruses (III). Sf9 insect cells infected with these empty baculoviruses were subjected to the same purification process as the CVB3 VLPs, and the product served as the mock vaccine in the mouse immunization studies.

For the expression of NoV P domain protein in bacteria (I), the pET101/D-TOPO expression vector was transformed into BL21 Star™ (DE3) (Invitrogen) *E. coli* cells by heat shock transformation as instructed by the manufacturer. The cells were plated onto Lysogeny broth (LB) plates containing the appropriate antibiotics and incubated overnight at 37°C. Positive colonies were picked and cultured overnight in a seed culture of 5 ml of LB medium including 50 μg/ml ampicillin and 0.1% glucose at 37°C with agitation at 200 rpm (Table 1). Then the bacterial suspension was diluted to a volume of 100 in culture medium, and the cultivation was continued at 26°C until the optical density at 600 nm (OD_{600}) reached about 0.3, after which the protein expression was induced with 0.5 mM IPTG. The cultivation was continued for an additional 16-18 hours, after which the cells were harvested by centrifugation (5000 g, 5 min, 4°C).

Table 1. Summary of protein expression vectors, expression systems and purification methods used in protein production and resulted yields.

Protein (communication)	GenBank accession no.	Expression vector	Expression host	Culture method	Culture medium	Precipitation by PEG	Purification method	Elution buffer	Yield (mg/l culture)
NoV VLP (I)	AF080551.1	pFastBac™1	*E. coli* DH10Bac™, *Spodoptera frugiperda* (Sf9)[a]	Bottle culture, 28°C, 125 rpm	HyClone SFX-Insect serum-free medium	Yes	Sucrose density gradient ultracentrifugation	gradient generated in PBS	100
NoV VLP (II)	AF080551.1	pFastBac™1	*E. coli* DH10Bac™, *Spodoptera frugiperda* (Sf9)[a]	Bottle culture, 28°C, 125 rpm	HyClone SFX-Insect serum-free medium	Yes	CsCl density gradient ultracentrifugation	gradient generated in PBS	35
NoV VLP (II)	AF080551.1	pFastBac™1	*E. coli* DH10Bac™, *Spodoptera frugiperda* (Sf9)[a]	Bottle culture, 28°C, 125 rpm	HyClone SFX-Insect serum-free medium	Yes	Ion exchange chromatography	50 mM sodium phosphate, 1 M NaCl, pH 7.0	10
CVB3 VLP (III)	M33854.1	pFastBac™Dual	*E. coli* DH10BacΔTn7EGFP, *Spodoptera frugiperda* (Sf9)[a]	Bottle culture, 28°C, 125 rpm	HyClone SFX-Insect serum-free medium	Yes	Ion exchange chromatography	20 mM Tris-HCl, 1 M NaCl, 5 mM $MgCl_2$ (pH 7.5)	0.5
cHis-NoV VLP (IV)	AF080551.1	pFastBac™Dual	*E. coli* DH10Bac™, *Spodoptera frugiperda* (Sf9)[a]	Bottle culture, 28°C, 125 rpm	HyClone SFX-Insect serum-free medium	No	Ni-NTA affinity chromatography	20 mM sodium phosphate, 500 mM NaCl, 500 mM imidazole (pH 7.4)	3.0
All-cHis-NoV VLP (IV)	AF080551.1	pFastBac™Dual	*E. coli* DH10Bac™, *Spodoptera frugiperda* (Sf9)[a]	Bottle culture, 28°C, 125 rpm	HyClone SFX-Insect serum-free medium	No	Ni-NTA affinity chromatography	20 mM sodium phosphate, 500 mM NaCl, 500 mM imidazole (pH 7.4)	1.5
P domain of NoV (I)	AF080551.1	pET101/D-TOPO®	*E. coli* BL21 Star™(DE3)	Bottle culture, 26°C, 200 rpm	LB with 50 µg/ml ampicillin, 0.1% glucose	No	Ni-NTA affinity chromatography	50 mM sodium phosphate, 600 mM NaCl, 500 mM imidazole (pH 8.0)	6.0

[a] The *E. coli* strain was used for the generation of a bacmid that was transfected into *Spodoptera frugiperda* (Sf9) cells to generate baculoviruses. MOI of 2 was used for the insect cell infections with baculoviruses.

[b] The protein expression was induced with 0.5 mM IPTG.

4.3 Purification of recombinant proteins (I-IV)

NoV VLPs (I, II) and CVB3 VLPs (III) were concentrated from the clarified insect culture supernatant by precipitation with polyethylene glycol (PEG) as previously described (Abraham & Colonno 1984). The precipitated VLPs were then pelleted by centrifugation (10 000 g, 15 min, 4°C), and the pellet was suspended in the appropriate buffers. The VLPs were further purified using density gradient ultracentrifugation based on sucrose (I) or CsCl (II) or using ion exchange chromatography (IEX) (II, III). A more detailed description of the gradient ultracentrifugation methods is given in the original communications (I, II).

The chromatographic ion exchange purifications of the pretreated VLPs were performed using a column packed with Q Sepharose XL anion exchange resin (5 ml HiTrap® Q XL by GE Healthcare, Uppsala, Sweden) for NoV VLPs and 1 ml monolithic columns based on CIM® technology from BIA Separations (Ljubljana, Slovenia) for CVB3 VLPs, as instructed by the manufacturer. The monolithic columns were chemically functionalized with either quaternary amine (QA, an anion exchanger) or sulfate (SO3, a cation exchanger). Prior to being loaded onto the chromatography column, the VLP-containing supernatants were filtered through a 0.2 μm filter. VLPs were eluted from the columns by using increasing concentrations of NaCl in the respective running buffers (50 mM sodium phosphate, pH 7.0 for NoV VLPs or 20 mM Tris-HCl, 20 mM NaCl and 5 mM $MgCl_2$, pH 7.5 for CVB3 VLPs). The VLP-containing fractions were assessed by SDS-PAGE and stored at -20°C or 4°C until further use. Although CVB3 VLPs were purified by both anion and cation exchange columns, only those VLPs purified by cation exchange chromatography were analyzed to a further extent.

The NoV P domain protein (I) and the engineered NoV VLPs (IV), all containing a His-tag, were purified using Ni-NTA IMAC. For the purification of the P domain protein, the pelleted cells were suspended in binding buffer (50 mM sodium phosphate, 600 mM NaCl, 20 mM imidazole, pH 8.0), lysed using a sonicator, and the cell lysate was clarified by centrifugation (10 000 g, 30 min, 4°C). P domain protein was purified from the supernatant using nickel-charged resin (Ni-NTA Superflow, Qiagen, Hilden, Germany), and the histidine-tagged NoV VLPs were purified from the clarified insect culture supernatant using 5 ml HisTrap™ FF Crude column (GE Healthcare, Uppsala, Sweden) according to the manufacturer's instructions. The P domain protein and histidine-tagged VLPs were

eluted from the column using an increasing concentration of imidazole in the running buffer (50 mM sodium phosphate, 600 mM NaCl, pH 8.0 or 20 mM sodium phosphate, 500 mM NaCl, pH 7.4, respectively). The protein-containing fractions were pooled and stored at 4°C until further use.

The purity of the VLP samples was analyzed by SDS-PAGE. The proteins were denaturated by heating at 95°C for 5 min in SDS-PAGE sample buffer with a reducing agent (β-mercaptoethanol). Proteins were separated by SDS-PAGE in a 10% or 12% gel and subsequently visualized by Coomassie Brilliant Blue, silver staining (PageSilver™ Silver Staining Kit, Fermentas, Burlington, Canada) or Oriole™ Fluorescent Gel Stain (Bio-Rad Laboratories, Hercules, CA). The total protein concentrations were determined by the Bradford method (Bradford 1976) (I, II) or the Pierce® BCA Protein Assay Kit (Thermo Scientific, Rockford, LI, USA) (III, IV). The endotoxin contents of the Nov VLPs and P domain proteins (I) were measured by Limulus Amebocyte Lysate (LAL) assay (Lonza, Walkersville, MD, USA).

4.4 Biophysical analyses (I-IV)

4.4.1 Dynamic light scattering

A dynamic light scattering (DLS) instrument Zetasizer Nano ZS (Malvern Instruments Ltd., Worcestershire, UK) equipped with a HeNe gas laser (λ = 633 nm) was used to determine the hydrodynamic diameter of all VLP preparations (I-IV), as well as the P domain protein of NoV capsid. The samples were measured at 22°C using a scattering angle of 173° and predetermined viscosity and refractive index values. The hydrodynamic diameter was determined from a cumulant analysis of six consecutive measurements, each containing 15 to 17 readings over 10-second intervals and plotted as the mean hydrodynamic diameter of particle population with accompanying standard error. The hydrodynamic diameter of NoV VLPs (II) and CVB3 VLPs (III) was also measured after storage at +4°C and -20°C, respectively. The polydispersity index (PDI) was recorded for each sample. It is calculated from the cumulant analysis of the DLS-measured intensity autocorrelation function, and it describes the width of the assumed Gaussian distribution of the particle sizes. The sample is typically referred as monodisperse if

the PDI value is below 0.1, as values greater than 0.7 indicate a very broad size distribution and, therefore, a very polydisperse sample (Malvern Instruments 2011).

CVB3 VLPs and viruses (III), NoV VLPs and histidine-tagged NoV VLPs (IV) were also subjected to a thermal scanning experiment using DLS. The temperature of the sample in quartz cuvette (Hellma 104-QS, Hellma Analytics, Müllheim, Germany) was gradually increased from 25°C to 90°C at 5°C intervals, and the sample was equilibrated for 5 min at each temperature before the measurement. The hydrodynamic diameter was recorded using three consecutive measurements containing 10×10-s datasets.

4.4.2 Electron microscopy

The cryo-electron microscopy (cryo-EM) analyses of NoV VLPs (I, II) were performed in collaboration with the group of Professor Sarah Butcher (University of Helsinki, Helsinki, Finland). In brief, freshly purified VLP samples were applied onto Quantifoil grids with 2 μm holes (Quantifoil Micro Tools, Jena, Germany) and vitrified by liquid-nitrogen cooled ethane. A Gatan 626 cryoholder was used to observe the sample in a Tecnai F20 (FEI, Hillsboro, OR, USA) field emission gun transmission electron microscope at 200 kV. The images were collected under low-dose conditions (~20e/A^2) at -180°C using an Ultrascan™ 4000 CCD camera (Gatan Inc., Pleasanton, CA, USA) at a nominal magnification of 68 000×, resulting in a final sampling of the images at 0.22 nm/pixel.

The transmission electron microscopy (TEM) and the scanning electron microscopy (SEM) analyses of CVB3 VLPs and the CVB3 virus (III), as well as the TEM analysis of the histidine-tagged NoV VLPs (IV) were performed in collaboration with the group of Docent Varpu Marjomäki from the University of Jyväskylä (Jyväskylä, Finland). Some of the TEM images in the original communication III were acquired by Vironova (Stockholm, Sweden). For the TEM analysis, a small aliquot sample was briefly bound to formvar-coated copper grids that had been glow-discharged just before use. The samples were negatively stained with 1% phosphotungstic acid or 2-3% uranyl acetate. The grid was air-dried before visualization with a JEM-1400 (JEOL, Tokyo, Japan) or a Tecnai 10 (FEI) transmission electron microscope. A more detailed description of the SEM analysis is given in the original communication (III).

4.4.3 Mass spectrometry

Protein identification analysis of NoV VLPs (I) was carried out by peptide mass fingerprinting (PMF) and N-terminal sequencing in collaboration with the group of Dr. Nisse Kalkkinen (University of Helsinki, Helsinki, Finland). For peptide mass fingerprinting (PMF), protein bands were isolated from silver-stained polyacrylamide gel and In-gel digested as described previously (Shevchenko et al. 1996). Proteins were reduced with DTT and alkylated with iodoacetamide before digestion with sequencing grade trypsin (Promega GmbH, Madison, WI, USA). The recovered peptides were desalted using a Millipore® C_{18} ZipTip and subjected to MALDI-TOF mass spectrometric analysis using an Ultraflex TOF/TOF instrument (Bruker-Daltonik GmbH, Bremen, Germany). Protein identification with the generated data was performed using Mascot Peptide Mass Fingerprint software by Matrix Science (London, UK).

For molecular weight determination and Edman degradation, the proteins were first subjected to reversed phase chromatography in a C1 column (TSKgel® TMS-250, TOSOH Corporation, Japan) using a linear gradient of acetonitrile (0–100% in 60 min) in 0.1% (v/v) trifluoroacetic acid. The collected proteins were subjected to molecular mass determination by MALDI-TOF mass spectrometry on the Ultraflex TOF/TOF instrument. Edman degradation was conducted on a Procise 494 HT Sequencer (PE Applied Biosystems, Foster City, CA, USA). The theoretical protein masses and isoelectric points (pI) were calculated using the ExPASy Prot-Param tool by the Swiss Institute of Bioinformatics (SIB).

4.4.4 Amino acid sequence analyses

The protease cleavage sites on a NoV VLP amino acid sequence (I) were predicted using the ExPASy PeptideCutter tool by the Swiss Institute of Bioinformatics (SIB). The similarity alignments and the homology and distance matrixes of NoV VLP capsid and P domain protein sequences (I, Supplementary material) were analyzed by DNAMAN (Lynnon Biosoft, San Ramon, CA, USA).

4.5 Antigenic and immunological analyses (I-IV)

4.5.1 Western blot analyses

For the detection of the expressed proteins by antibodies, the samples were first separated on SDS-PAGE gels and blotted onto a nitrocellulose membrane. The membranes were then incubated in primary antibody, which was norovirus-positive human serum for detection of NoV VLPs and P domain protein (I, II) and mouse anti-enterovirus clone 5-D8/1 (DAKO, Glostrup, Denmark) for detection of CVB3 VLP and virus (III) at a dilution of 1:500 and 1:3000, respectively. Mouse anti-baculovirus gp64 clone AcV5 (Santa Cruz Biotechnology Inc., Heidelberg, Germany) at a dilution of 1:1000 was used to detect baculoviral contamination. The primary antibody was followed by incubation with horseradish peroxidase (HRP)-conjugated goat anti-human IgGs (Invitrogen) diluted 1:10 000 or HRP-conjugated horse anti-mouse IgGs (Vector Laboratories Inc., Burlingame, CA) diluted 1:20 000. The Opti-4CN™ Substrate (Bio-Rad Laboratories) or the Pierce™ ECL Substrate (Thermo Scientific) was used for visualization.

4.5.2 ELISA assays

In order to determine their antigenic potential, NoV VLPs (I), CVB3 VLPs (III) and histidine-tagged NoV VLPs (IV) were subjected to enzyme-linked immunosorbent assay (ELISA). The 96-well plates were coated with 50-150 ng/well of protein antigens, followed by blocking at 22°C for 0.5-1 h with PBST supplemented with 5% (w/v) skimmed milk or 0.1% BSA. The wells were then incubated (37°C, 1 h) with 12 norovirus-positive human sera obtained from patients hospitalized for acute gastroenteritis in Tampere and Kuopio University Hospitals during the years 2006-2008 (I, IV) or six CVB3 VLP or virus-immunized murine sera (III) diluted serially in blocking buffer. HRP-conjugated goat anti-human IgG (Invitrogen) diluted 1:4000 in 1% skimmed milk in PBST or horse anti-mouse IgG (Vector) diluted 1:2300 in 1% BSA in PBST was used as a secondary antibody, and the antibodies were detected using *O*-phenylenediamine dihydrochloride (Sigma-Aldrich, St. Louis, MO, USA) as a substrate. The reaction was stopped with 0.5 M sulfuric acid, and the OD values were measured at 490 nm using a Victor² 1420 Multilabel Counter (PerkinElmer, Waltham, MA, USA). The

statistical significance between the serum titer means (I, III) were determined by the unpaired two-tailed *t*-test for comparison of two population means using GraphPad Prism (GraphPad Software Inc., La Jolla, CA, USA).

4.5.3 HBGA assay

The binding capabilities of the NoV VLPs and P domain proteins (I), as well as the histidine-tagged NoV VLPs (IV) to their putative receptor among ABH and Lewis histo-blood group antigens (HBGAs) were determined as previously described (Rockx et al. 2005). Briefly, purified VLPs or P domain proteins were added to 96-well plates (200 ng/well) and incubated at 22°C for 4 h. After blocking over night at 4°C with 5% skimmed milk in PBS, the plates were incubated (37°C for 1 h) with synthetic biotinylated histo-blood group carbohydrates (Lectinity, Moscow, Russia) diluted in 1% skimmed milk in PBST, washed and incubated again with alkaline phosphatase (AP)-conjugated streptavidin (Sigma-Aldrich) diluted 1:250. Finally, the plates were developed with p-nitrophenyl phosphate substrate (Sigma-Aldrich) and the OD at 405 nm was determined using a Victor² 1420 Multilabel Counter (PerkinElmer).

4.5.4 Immunization of mice

The CVB3 VLP vaccination trial (III) was performed according to the guidelines of the Tampere University Animal Welfare program under the approval number ESAVI/4588/04.10.03/2012 from the Regional State Administrative Agency. Twelve female Balb/c mice at the age of 6-8 weeks were randomly divided into groups of six. The first group was administered 5 μg of CVB3 VLPs, and the second group was given an identical volume of mock vaccine (see section 4.2). In addition, a positive control experiment was performed by administering 5 μg formalin-inactivated CVB3 virus to a group of six mice. All vaccine preparations were mixed with an equal volume of either complete (primary vaccination) or incomplete (booster vaccinations) Freund's adjuvant (Sigma-Aldrich) immediately before administration. The primary vaccination (100 μl) was given subcutaneously, and the two booster vaccinations (200 μl) were given intraperitoneally. Blood samples were collected before vaccination, at days 21 and 42 and by heart puncture at day 63 when the mice were sacrificed. Spleens were also collected from the sacrificed mice.

4.5.5 Neutralization assay

The presence of neutralizing antibodies in CVB3 VLP-immunized mice (III) against the ATCC reference strain Nancy (ATCC number VR-30) was analyzed using a plaque seroneutralization assay as described in detail elsewhere (Roivainen et al. 1998). Sera from mice immunized with the purified and formalin-inactivated CVB3 virus or mock vaccine (see section 4.2) were analyzed as controls. Briefly, monolayers of green monkey kidney (GMK) cells were prepared at 95% confluency and treated with neutralization suspensions, each containing a mixture of serially diluted sera from the immunized mice and an equal volume of virus (approximately 100 plaque forming units, PFUs, of infectious particles). After incubation at 37°C for 30 min, the neutralized virus suspension was removed, and the cells were overlaid with plaque assay medium containing MEM, 1% FCS, 4 IU/ml PS, 20 mM HEPES, 0.23% glucose, 1% L-glutamine, 15 mM $MgCl_2$ and 0.5% carboxymethyl cellulose. The cells were incubated at 37°C with 5% CO_2 for 2 days, after which they were fixed and stained with a 0.8% formalin suspension in PBS containing 0.25% crystal violet for 10 min. The number of viral plaques was identified, and the last dilution of the serum able to reduce the virus infectivity by 80% was reported as the final titer.

4.5.6 Immune cell assay

The analysis of immune cells generated in mice by CVB3 VLP and mock vaccinations (III) was carried out using flow cytometry. In brief, the mouse spleens were disrupted mechanically and prepared into single-cell suspensions as follows: cells were washed with PBS, and red blood cells were lysed using ACK lysing buffer (Lonza). Splenocytes were suspended in 50 ml of 2% FBS, 0.5% penicillin-streptomycin and 1% L-glutamine supplemented RPMI-1640 medium (Lonza) of which two ml per mouse were analyzed. The cells were washed with 0.1% BSA in PBS and stained at 4°C for 20 min with the following fluorescently- labeled antibodies from eBioscience (San Diego, CA, USA) at a dilution of 1:400: CD3-APC (a pan-T cell marker), CD4-PerCP/Cy5.5 (a $CD4^+$ T cell marker), CD8-FITC (a $CD8^+$ T cell marker), CD44-APC/eFluor780 (a differentiated T cell marker), CD62L-PE (a naïve T cell marker) and B220-PE/Cy7 (a B cell marker). The cells were then filtered with cell strainer cap FACS tubes (BD, Franklin Lakes, NJ, USA) and washed with 0.1% BSA in PBS. The FACS analysis was performed using a FACSCanto™II flow cytometer (BD) and the data was analyzed using FlowJo

software (Tree Star, Ashland, OR, USA). A total of 50 000 cells was analyzed for each sample. Live cells were gated, and the number of live cells was confirmed to be similar in each of the sample groups. Of the live cells, the $CD3^+/CD4^+$ and $CD3^+/CD8^+$ T cell populations were gated by plotting $CD3^+$ cells versus $CD4^+$ or $CD8^+$ cells. The effector memory (EM) T cell populations in these two populations were examined by plotting CD62L versus CD44.

4.6 Nucleic acid content determinations and qPCR (III)

The total DNA concentrations of the CVB3 VLP samples (III) were analyzed using Quant-iT™ dsDNA Broad-Range Assay Kit (Invitrogen), and the number of baculovirus genomes was determined using a quantitative PCR (qPCR) kit (BacPAK™ qPCR titration kit, Clontech Laboratories, Mountain View, CA) as instructed by the manufacturer. The qPCR samples were run using the CFX96™ C1000 Real-Time Thermal Cycler by Bio-Rad Laboratories.

To determine if the CVB3 VLPs contained the modified viral genome, a 20-µl aliquot was digested with 25U of RNase If enzyme (New England Biolabs Inc., Ipswich, MA, USA) in 1× NE buffer at 37°C for 2 h. Then the enzyme was inactivated at 70°C for 20 min. Another 40-µl aliquot of VLPs was digested at RT for 20 min with 2.7 Kunitz units of DNase I (Qiagen) in 1× RDD buffer. Both digestions were followed by nucleic acid extraction using a QIAamp® Viral RNA Kit (Qiagen), and the samples were analyzed by enterovirus- and mCherry-specific PCR with and without a preceding reverse transcriptase reaction. The PCR run was performed according to the instructions provided with the Quantitect™ Probe Kit (Qiagen) using Taqman chemistry.

4.7 Molecular display on VLP (IV)

4.7.1 Conjugation of streptavidin

The synthesis of all *tris*-nitrilotriacetic acid (*tris*NTA) conjugates used in this thesis (*tris*NTA-biotin, *tris*NTA-Alexa488, *tris*NTA-SGGG-VSV-G) were carried out in collaboration of with the group of Professor Robert Tampé (Goethe-University

Frankfurt, Frankfurt am Main, Germany) as described in detail in the original communication IV.

Streptavidin (SA) was attached on the surface of the engineered NoV VLPs (IV) using the *tris*NTA-biotin conjugate that binds to a polyhistidine tag. SA was first attached to the *tris*NTA-biotin conjugate by a simple equimolar (one *tris*NTA-biotin per tetramer) mixing of SA (tetramer concentration of 16 μM) and *tris*NTA-biotin with $NiSO_3$ (10 mM) in PBS buffer. After 3 h incubation using a roller mixer, the excess $NiSO_3$ was removed by dialysis against 20 mM NaH_2PO_4, 500 mM NaCl (pH 7.4). A 50-fold molar excess of *tris*NTA-biotin-SA conjugate relative to histidine-tagged VLP was used. The resulting increase in the hydrodynamic diameter of the VLP-SA complexes was detected at 22°C using DLS. Histidine-tagged VLPs alone and SA alone with histidine-tagged VLPs were used as controls.

4.7.2 Conjugation of fluorescent dye

To analyze the binding capacity of histidine-tagged VLPs, 0.4 μM of *tris*NTA-Alexa488 was incubated with 0.2 μM of VLPs in 20 mM NaH_2PO_4, 500 mM NaCl (pH 7.4) at room temperature for 2 h. The excess of dye-conjugate was removed by ultrafiltration using the Amicon® Ultra-0.5mL centrifugal device (MWCO 30K, MerckMillipore, Darmstadt, Germany). The labeling rations per VLP were determined using a UV/Vis spectrophotometer (NanoDrop 1000, Thermo Scientific).

Fluorescence correlation spectroscopy (FCS) was conducted using a Zeiss LSM 780 confocal fluorescence microscope equipped with a Plan Apochromat 63x/1.2 water immersion objective. The argon laser intensity was adjusted to 1.5% of the maximum of the 488-nm laser line. The pinhole was set to 1 Airy-unit. The samples were diluted in 50 mM NaH_2PO_4, 1 M NaCl (pH 7.2) and studied using a Lab-Tek II™ 8-well chamber coverglass (Nunc™, Roskilde, Denmark). The FCS data was collected in 10×10-s or 100×1-s datasets using the following parameters: geometric correction 1, structural parameter 5, and triplet state relaxation time 2 μs. To determine diffusion time for the first component, *tris*NTA-Alexa488 conjugate alone was measured at a concentration of 8 nM. Diffusion time for the VLP particle (second component) was determined from a solution containing *tris*NTA-Alexa488-conjugated All-His-VLPs prepared as described above. A titration experiment was performed using a solution of 8 nM *tris*NTA-Alexa488, where

VLPs were added gradually, and the amount of the second component was determined after each addition of the VLP. Imidazole displacement experiments were performed by mixing 5 mM or 20 mM imidazole into a solution containing different VLPs (subunit concentration of 135 nM) conjugated to *tris*NTA-Alexa488 (8 nM).

4.8 Cell culture studies (III, IV)

4.8.1 Transduction of CVB3 VLPs into GMK cells

The CVB3 VLP transduction study was performed by plating 20 000 GMK cells per well on Lab-Tek™ 8-chamber slide (Nunc™) in minimum essential media (MEM) containing 2% FBS and 0.1% penicillin-streptomycin. After 3.5 h, the cells were treated with 100 µl medium containing a different concentration of VLPs (1.3 nM, 2.6 nM, and 13 nM) and fixed with 4% paraformaldehyde in PBS after 70 h incubation in 37°C and 5% CO_2. The cells were stained with antibodies and mounted using Vectashield mounting medium with DAPI (Vector Laboratories). Rabbit polyclonal anti-RFP (MBL, Naka-ku Nagoya, Japan) diluted 500-fold was used as a primary antibody and FITC-conjugated goat anti-rabbit by Jackson ImmunoResearch (Suffolk, UK) in 200-fold dilution was used as a secondary antibody. The cells were examined by a Nikon Eclipse-Ti inverted microscope with an Andor spinning disk confocal (Yokogawa CSU10 scanner). Buffer-treated cells and cells transfected with a plasmid containing mCherry and EGFP expression sequences were used as controls. Two parallel samples or controls were prepared.

4.8.2 Transduction of cells with surface-decorated NoV VLPs

Transduction of human embryonic kidney (HEK293T) cells with VLPs consisting of surface-displayed *tris*NTA-Alexa488 and *tris*NTA-SGGG-VSV-G-peptide conjugates was performed by plating 50 000 HEK293T cells per well overnight on 35 mm glass bottom Petri dishes (MatTek Corporation, Ashland, MA). The next day, the culture medium was changed and supplemented with 112 nM VLPs displaying *tris*NTA-Alexa488 and *tris*NTA-SGGG-VSV-G-peptide conjugates (conjugated using 2× and 5× molar excess over a capsid protein, respectively, after which the excess of the dyes were filter-removed before the assay). Cells treated

with only PBS and VLPs displaying only *tris*NTA-Alexa488 conjugate were used as controls. The cells were exposed to samples or controls for 3 h, after which the cells were washed three times with PBS and fixed with 4% PFA. The actin filaments in the cell cytoskeleton were stained with AlexaFluor®568 Phalloidin stain (LifeTechnologies, Eugene, OR). The samples were imaged by a Zeiss LSM 780 confocal fluorescence microscope using a Plan Apochromat 63x/1.4 oil immersion objective (Carl Zeiss, Jena, Germany). The experiment was performed two times with two parallel samples.

The average cell intensities in images acquired with a 488-nm excitation laser were analyzed using ImageJ version 1.49m. Briefly, the raw 3D image stack in .CZI format were imported as 8-bit grayscale images and projected into 2D images by using maximum intensity projections of each image. The average fluorescence intensities of the cells were then measured by selecting each cell with the freehand tool and using the "Multi measure" command for analyzing the selected areas. A total of 11-21 cells were analyzed per sample. The average background intensities of the images were measured from a 30x30 μm square outside the cell areas and subtracted from the average intensity values of the analyzed cells. Statistical significance was determined by the unpaired two-tailed t-test.

4.9 Production and purification of CVB3 viruses (III)

To serve as a positive control in the CVB3 VLP mouse studies (III), a Moldova strain variant of CVB3 virus (GenBank accession number AY896763.1), was propagated in GMK cells cultured at 37°C with 5% CO_2 for 2 days in HyClone™ SFM4MegaVir™ protein-free medium (Thermo Fisher Scientific) containing 2 mM L-glutamine and 0.1% penicillin-streptomycin. A MOI of 0.5 PFU/cell was used for the infections. The viruses were harvested by repeated freeze-thaw cycles and centrifugation (9600 g, 20 min, 4°C) and then precipitated with PEG as described earlier (see section 4.3) The precipitated viruses were further purified by ultracentrifugation with a 20-5% (w/v) discontinuous sucrose gradient (103 864 g, 4 h, 4°C) or by ion exchange chromatography using a QA column from BIA Separations described in more detail in the original communication (III). The virus-containing fractions were pooled, pelleted and resuspended in appropriate buffers. The virus titers ($TCID_{50}$) were determined based on the cytopathic effect (CPE) in infected GMK cells. The total protein concentrations and purity of the virus preparations were analyzed using methods described earlier (see section 4.3).

5 SUMMARY OF THE RESULTS

5.1 Production of VLPs (I-IV)

5.1.1 VLPs are successfully produced in insect cells

The expression of the GII.4 norovirus (I, II), CVB3 enterovirus (III) and histidine-tagged GII.4 norovirus (IV) capsid sequences in Sf9 insect cells resulted in the successful production of VLPs. The production of the NoV VP1 capsid protein and subsequent purification by discontinuous sucrose gradient resulted in a high yield of over 100 mg of protein per one liter of insect cell culture (Table 1 and I). The yields were to some extent lower when the same protein was purified by ion exchange chromatography or CsCl gradient ultracentrifugation, being approximately 10 mg/l culture and 35 mg/l culture, respectively (Table 1 and II). The production and purification of the CVB3 VLPs by ion exchange chromatography resulted in a yield of approximately 0.5 mg/l culture (Table 1 and III). All the above VLPs (Table 1 and I-III) were concentrated from the cell culture supernatant by PEG precipitation. Fully and partially histidine-tagged GII.4 NoV VLPs were expressed in insect cells and purified using Ni-NTA metal ion affinity chromatography with a yield of approximately 1.5 mg/l culture and 3 mg/l culture, respectively (Table 1 and IV), whereas the polyhistidine-tagged P domain proteins of GII.4 NoV were produced in *E. coli* and purified using a Ni-NTA column at a yield of 6 mg/l culture (Table 1 and I).

5.1.2 All VLP preparations show high purity after purification

When the total protein content of VLPs and P domain protein preparations were evaluated after purification by SDS-PAGE, the preparation were found to be essentially free from contaminating proteins (Figures 1A, 1A-B, 2B, and 3A in the original communications I-IV, respectively). Regardless of the method of purification, the SDS-PAGE analysis of norovirus VLPs (Figure 9F and I, Figure

1A; II, Figures 2A-B; IV, Figure 3A) showed the presence of a protein approximately 58 kDa with a double band pattern. The NoV P domain proteins showed a single major protein band of about 35 kDa, corresponding to the P protein monomer (I, Figure 1A). The SDS-PAGE analysis of purified CVB3 virus showed the presence of four proteins of approximately 34 kDa, 30 kDa, 26 kDa, and 8 kDa in size (Figure 8C, lane 4 and III, Figure 3B, lanes 4 and 5), which corresponded well with the estimated molecular weights of the four capsid proteins, VP1, VP2, VP3, and VP4, respectively, of CVB3 (Cunningham et al. 1992). The purified CVB3 VLP sample contained only three protein bands in the SDS-PAGE gel (Figure 8C, lane 3 and III, Figure 2B, lane 4) that correlated with the molecular weights of the capsid proteins VP0, VP1, and VP3. VP0 appeared not to undergo cleavage to yield the VP4 and VP2 proteins in insect cells.

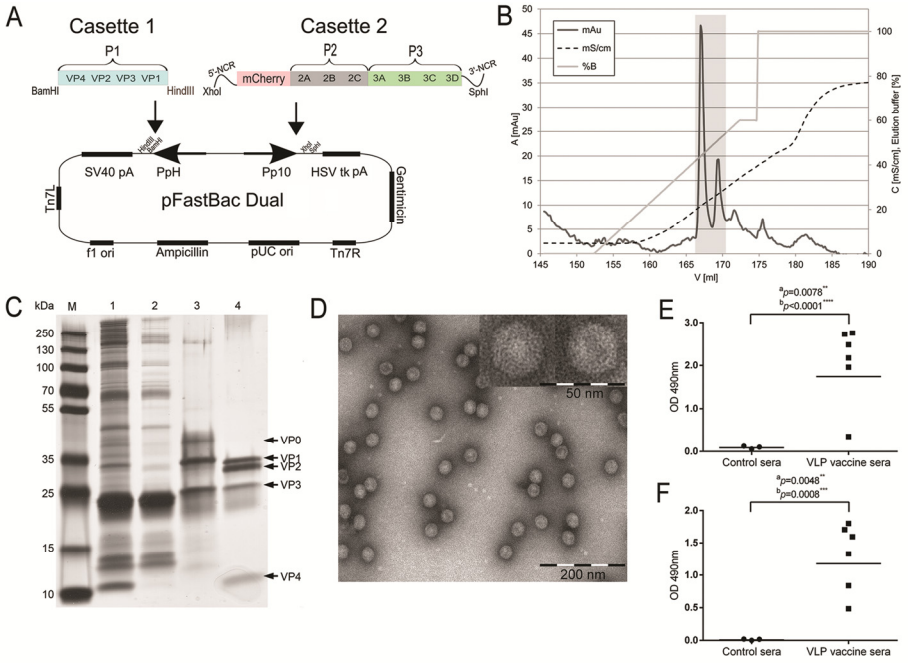

Figure 8. The design and analysis of the CVB3 VLP. **A**) The design of the baculoviral transfer vector containing the CVB3 VLP expression cassettes. **B**) The elution chromatogram of the cation exchange chromatography. **C**) An SDS-PAGE analysis of the CVB3 VLPs. The VLPs in the chromatography input sample (1) bound efficiently to the column (2: flow-through sample) and were purified and concentrated during the chromatography purification process (3). Sample 4: purified CVB3 virus control. **D**) TEM image of CVB3 VLPs. Scale bars 200 nm and 50 nm (close-up). **E-F**) Antibody responses elicited in mice by CVB3 VLP immunization. Binding activity of mice antisera at a 1:8192-dilution to a CVB3 VLP antigen (E) and to a CVB3 virus antigen (F). The line indicates the geometric mean of the group. [a] the one non-responsive mouse included or [b] omitted from the calculation. Adapted with permission from III.

The purity level of all the purified material analyzed by SDS-PAGE was estimated to be very high (for example, over 95% for the chromatography-purified VLPs). In addition, when chromatography-purified NoV VLPs or CVB3 VLPs were analyzed by Western blot, no residual baculovirus-related impurities were detected in the purified material by antibodies against baculovirus gp64 (II, Figure 4 and III, Supplementary Figure S5). The bacterial endotoxin content, determined only for the NoV VLPs purified by discontinuous sucrose gradient and Ni-NTA IMAC-purified P domain proteins (I), was 0.16 EU/10 μg of protein and 100 EU/10 μg of protein, respectively. Therefore, the endotoxin content of NoV VLPs was well below the international standard of ≤30 EU/20 μg of protein (Makidon et al. 2008).

5.2 Biophysical characterization of VLPs (I-IV)

5.2.1 The purified VLPs show correct size and morphology

Dynamic light scattering (DLS) was used to determine the size of the purified VLPs and homogeneity of the particle population in the different VLP preparations. The particle size analysis of the sucrose gradient-purified NoV VLPs (I) revealed the presence of particles with an average hydrodynamic diameter of 37±1 nm, reported by intensity distribution. However, the mean polydispersity index (PDI) value between the measurements was 0.56, which indicated that the sample contained more than one particle populations. Examination under a cryo-EM confirmed the presence of intact and fairly uniform particles (Figure 9E and I, Figure 3). DLS analysis after the NoV VLPs were purified by CsCl gradient (II, Table 1) showed a mean particle size of approximately 33 nm (expressed as volume distribution with a peak distribution varying from 98.5% to 100%) with a similar increase in PDI (mean PDI was below 0.3). The hydrodynamic diameter of the P domain protein (measured by volume distribution, peak 100%) was about 16±1 with PDI of 0.11 (data not shown).

The hydrodynamic diameter measured for the IEX-purified NoV VLPs (II), calculated from the volume distribution (peak 100%), was approximately 45 nm. The PDI was below 0.05, which suggests that the samples contained highly monodisperse and pure VLPs. When the IEX-purified NoV VLPs were analyzed

by DLS again in original communication IV, a mean hydrodynamic diameter (by volume distribution) of 44±1 nm and PDI of 0.06 was observed. The assembly of IEX-purified NoV VP1 protein into monodisperse virus-like particles of about 40 nm in diameter was confirmed by cryo-EM and TEM. Although slight clustering of the VLPs was observed in cryo-EM analysis, no deformation of the VLPs was detected. However, minor deformation was visible in the TEM analysis.

The DLS analysis of CVB3 VLPs purified using IEX (III) showed that the particles had an average hydrodynamic diameter of 31±1 nm (determined by volume distribution, peak 98%), and the sample was relatively monodisperse with a PDI of 0.32. Similar size of 28±1 nm was observed for the IEX-purified CVB3 virus with a PDI of 0.17 (peak 100%). Examination of the CVB3 VLP and virus samples by both TEM and SEM (Figure 8D and III, Figures 5 and 6) showed the presence of intact and uniform particles with the correct size (approximately 30 nm in diameter) and morphology, although in the SEM images, the VLPs appeared somewhat smaller in size than the virus particles.

The mean hydrodynamic diameter in nm of both partially and fully histidine-tagged NoV VLPs (IV) purified using Ni-NTA chromatography was 42±1 (determined by volume distribution, peak 100%) (Figure 9G) with respective mean PDI values of 0.1 and 0.03. TEM analysis revealed that the engineered VLPs were monodisperse, uniform in size (ranging from about 40 nm of partially histidine-tagged to about 50 nm of fully histidine-tagged NoV VLPs) and morphologically indistinguishable from native IEX-purified NoV VLPs (Figure 9D and IV, Figure 2A).

5.2.2 The VLPs withstand long periods of storage and elevated temperatures

When the particle size of NoV VLPs purified by ion exchange chromatography was re-analyzed by DLS after 4 months of storage at 4°C in the absence of preservative agents (II, Table 1), no change in the average particle size or PDI of the VLP sample with a higher initial particle concentration was detected. Similarly, when CVB3 VLP samples were re-analyzed after year-long storage at -20°C, no changes in the particle population size and distribution were observed.

DLS was also utilized to analyze the aggregation temperature of the different VLP preparations. Gradual heating of both the CVB3 VLPs and the virus (III, Figure 4) from 25°C to 90°C led eventually to aggregation of the sample. There

was, however, a difference in the aggregation temperature. The VLPs showed signs of aggregation at already 50°C and were completely aggregated at 55°C, whereas the virus sample showed the first signs of aggregation at 60°C and was completely aggregated at 75°C. Therefore, the aggregation of the CVB3 virus occurred at 10-15°C higher temperature than the corresponding VLP, and the thermally induced events occurred over a much broader temperature range. When histidine-tagged NoV VLPs and native NoV VLPs (IV, Figure 2C) were subjected to gradual heating from 25°C to 90°C, no differences in aggregation temperature (60°C) were observed.

5.2.3 Recombinant NoV VLP proteins are partially truncated at N-terminus

The identity of the dual band patterning of the produced NoV capsid proteins, seen in SDS-PAGE analyses throughout the NoV VLP publications of this thesis, was analyzed by peptide mass fingerprinting, mass spectrometric analysis, and N-terminal sequencing (I). From similar peptide mass fingerprints, both bands were identified as GII.4 norovirus capsid protein. Reversed phase chromatography resulted in one peak, and subsequent MALDI-TOF mass spectrometric analysis of the collected fraction revealed that the fraction contained both protein forms with masses of 55.3 and 58.8 kDa corresponding to the two bands in SDS-PAGE (I, Supplementary Figure S1). N-terminal sequence analysis by Edman degradation of the fraction revealed one sequence that began with a sequence AAIAAPVAGQ, which can be found from the amino acid 35 onwards in the primary sequence of the GII.4 capsid protein. For unknown reasons, the N-terminal sequence of the putative full-length protein could not be determined. Together with calculations of the theoretical average masses of the larger protein starting with MKMASND (58.9 kDa) and the smaller product starting with the amino acid sequence of AAIAAPV (55.4 kDa), it was concluded that the bigger band of about 60 kDa observed in the SDS-PAGE analysis corresponds to the full-length capsid protein, and the 55 kDa band represents a product that has been truncated by 34 aa from its N-terminal end. Potential cleavage sites for only broad-spectrum proteases thermolysin and protease K were found in this position.

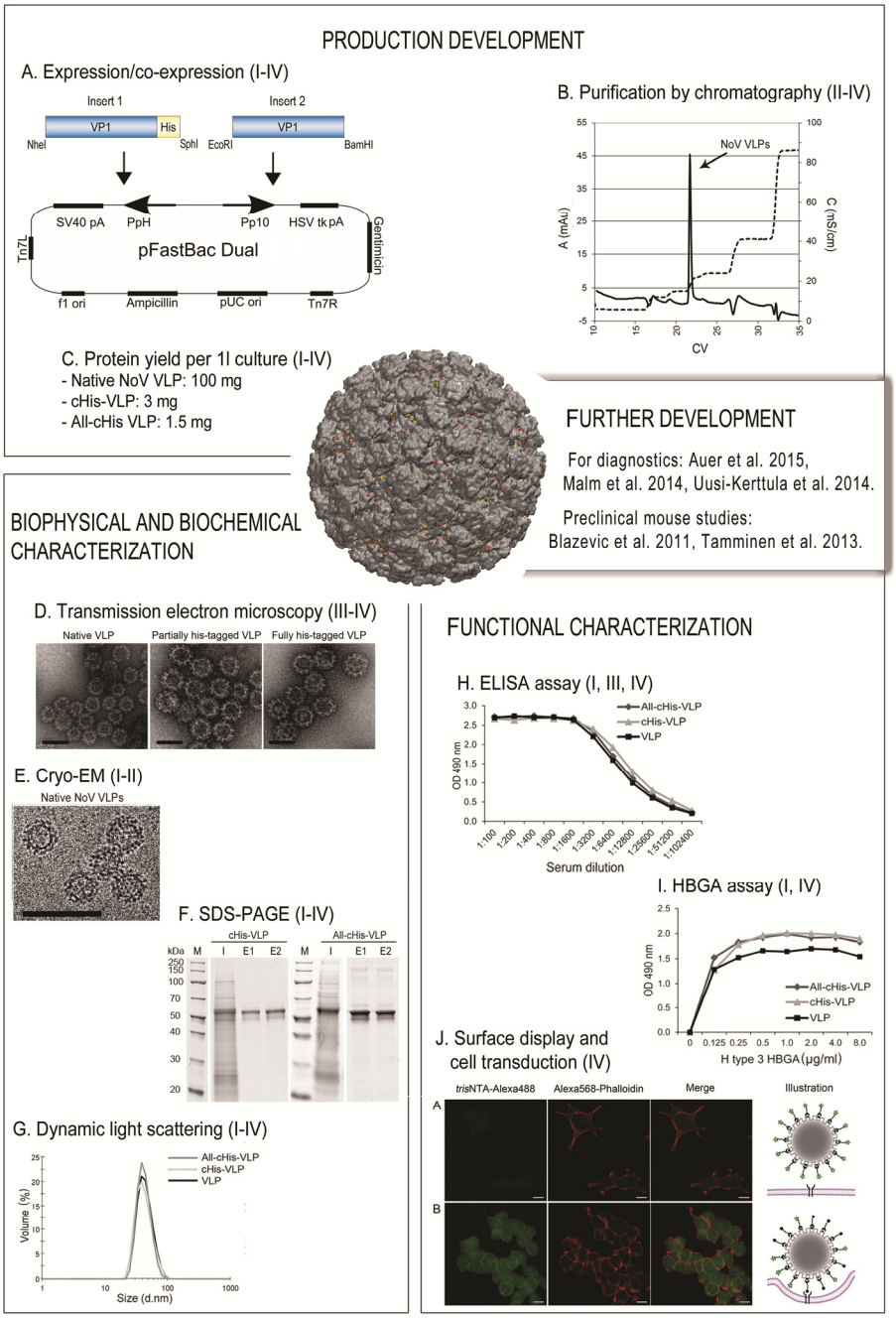

Figure 9. Examples of the overlapping production and analysis methods used throughout this thesis for analyzing the VLPs (**A-J**). Methods are illustrated with example result images from the analyses with different NoV VLP forms. Method usage in the original communications is indicated in parenthesis. F) I: chromatography input sample, E: elution sample. Adapted with permission from I and II.

5.3 Antigenicity of the VLPs is preserved (I-IV)

5.3.1 NoV VLPs are recognized by human norovirus-specific antibodies and bind to their putative HBGA receptor

To compare the antigenic properties of the recombinant NoV VLPs and the P domain protein, equal amounts of the proteins were loaded onto a SDS-PAGE gel for a Western blot analysis (I, Figure IB). Immunostaining using norovirus-specific human serum revealed signal intensities similar to each other. However, further assessment in an ELISA assay (I, Figure 4) suggested that the IgGs of both moderately and strongly norovirus-positive sera had somewhat better recognition for the recombinant NoV VLPs than for the P domain protein. When the geometric mean of the end-point positive titer was determined, the VLPs were recognized about five-fold more strongly compared to the P domain protein by both moderately and strongly positive sera. However, the difference was not statistically significant ($p=0.065$, unpaired two-tailed *t*-test). Similarly, although both the NoV VLP and P domain protein bound with a similar binding pattern to H type 3 HBGA antigen (I, Figure 5), which is one of the putative receptors of GII.4 noroviruses (Harrington et al. 2004), the binding affinity of the P domain protein to the putative receptor was weaker than that of the VLP.

The effect of NoV VLP surface engineering on VLP antigenicity and putative receptor-binding capability was analyzed using ELISA and HBGA assays, respectively. As a result, the engineered VLPs were found to retain their antigenic ability despite the additional surface-expressed histidine tags, proven by the fact that antigen recognition of both histidine-tagged VLPs by human norovirus-positive sera was high and comparable to the native VLP that was used as a control (Figure 9H and IV, Figure 3B). Binding activity of the engineered VLPs to their putative receptors and host susceptibility factors was also unaltered, as demonstrated by comparing their binding activities to synthetic oligosaccharides representing H type 1 and H type 3 HBGA antigens (Figure 9I and IV, Figure 3C).

5.3.2 CVB3 VLPs are recognized by antibodies against enterovirus and elicit antibodies in mice

When their antigenicity was initially analyzed by Western blot, both the purified CVB3 VLPs and the viruses were recognized by mouse antibodies against enterovirus VP1 (III, Figures 2C and 3C). When the antigenic capacity of the antibodies generated by CVB3 VLPs in immunized mice was further assessed using an ELISA assay (III, Figure 7), the sera of the CVB3 VLP-vaccinated mice reacted strongly to both inactivated CVB3 viruses (ATCC, Nancy strain) and the CVB3 VLPs that were used as antigens. High IgG titers were elicited in all but one mouse (mouse no. 11, Figure 8E and Supplementary Figure S8 in the original communication III), and the mean titers were slightly higher when the VLPs were used as antigens than when the CVB3 virus particles were used. As expected, the mock vaccine did not elicit any reactivity against either antigen.

The antibodies generated in the mice that were immunized with CVB3 VLPs or the mock vaccine were then evaluated for their ability to neutralize the infective ATCC reference CVB3 virus strain, which had 100% aa sequence similarity to the strain used for the preparation of the VLP (III, Table 2). When the end-point neutralizing titers (up to 1:4096) were determined for sera collected at the end of the trial (on day 63), high neutralizing antibody titers were induced in the mice immunized with CVB3 VLPs, whereas the mock vaccine failed to elicit any neutralization against CVB3 even at the lowest dilution tested. The mean neutralizing titer in the VLP-vaccinated group on day 63 was over 1:1000, however, considerable variations were observed between individual mice. For example, one mouse (mouse no. 11) failed to generate any antibodies after vaccination. The mean neutralizing titer of the sera from the mice infected with the purified formaldehyde-inactivated CVB3 virus, which was used as a positive control, was 1:2200 at day 63.

5.3.3 CVB3 VLPs induce memory T cells in mice

The spleen cells of CVB3 VLP- and mock-vaccinated mice were analyzed for markers of immune activation (III, Supplementary Table 1). Initially, when the total numbers of B cells, $CD4^+$ T cells, and $CD8^+$ T cells were determined, there was no statistically significant expansion of the effector B or T cells or differences between the study groups. However, upon activation by virus infection, effector memory T cells expand in number and modulate their expression of cell surface

molecules, such as CD62L and CD44, which are down-regulated and up-regulated, respectively, upon effector memory generation (Sprent 1997). Thus, when the numbers of the memory cell populations of CD3 and CD4/CD8 double-positive cells were measured based on the expression of cell surface molecules CD44 and CD62L, numbers of $CD62L^{low}$ $CD44^{high}$ cells in both the $CD4^+$ and $CD8^+$ T cell populations were found to be consistently higher in the VLP-vaccinated mice than in the control-vaccinated mice 9 weeks after the initial immunization. For CD4 cells, the induction was from around 500 to 700 cells, and for CD8 cells, the induction was from around 30 to 45 cells.

5.4 Artificial genome is not encapsidated in the CVB3 VLPs (III)

To determine whether baculovirus-transcribed, modified viral mRNA or DNA from the baculoviral CVB3 construct was packaged into the CVB3 VLPs, RNase If or DNase I digestion experiments were performed for the purified VLP aliquots (III). Nucleases digest RNA or DNA in the supernatant, but not inside the VLP. Digestion was followed by nucleic acid extraction and enteroviral-specific PCR with and without a reverse transcriptase (RT-) step to control whether the PCR signal originated from RNA or DNA. Accordingly, this treatment would release possible nucleic acids also from inside the VLP. The supernatant DNase I -digested samples were negative in the PCR and in the RT-PCR, indicating that the supernatant was free of viral mRNA, and that the VLP particles did not contain RNA or DNA, both of which would have given signals in the RT-PCR and/or in the PCR if they were positive. Naturally, the possible DNA in the supernatant was digested in this setup, and accordingly, did not give any signal. The VLP supernatants digested with RNase If were positive with and without the RT-step, which demonstrated that the signal originated from baculovirus-derived CVB3 DNA that resided outside the VLP (digested in the first setup). The signal could not have originated from the RNA/DNA inside of the particle, since it was already demonstrated in the first setup that the VLPs did not contain any enterovirus-specific nucleic acids. However, the total DNA content of the purified CVB3 VLPs was very low (0.82±0.38 ng/μl), which indicated that the contamination was only minimal. The baculovirus genome content of the samples was 0.02±0.02 ng/μl, measured from four independent purifications.

CVB3 VLPs failed to induce a fluorescence signal in GMK cells from mCherry introduced into the CVB3 artificial genome (data not shown). This may have been

either because of an overall absence of the artificial genome inside the VLPs or a failure of the VLPs to enter the cells.

5.5 His-tagged NoV VLPs are suitable for non-covalent display of foreign molecules (IV)

As demonstrated by the results from TEM and DLS analyses in section 5.2.1 (and in original communication IV), adding of the C-terminal histidine tag on the norovirus capsid protein to produce All-cHis-VLP and cHis-VLP forms did not interfere with protein folding or VLP assembly. Moreover, the integrated His-tags were most likely projecting out of the VLP surface, or otherwise, VLPs could not have been purified and concentrated by IMAC chromatography.

When a streptavidin (SA) was non-covalently attached on the surface of the histidine-tagged NoV VLPs by using *tris*NTA-biotin adaptors that bind strongly to polyhistidine tags via coordinating metal ion (Lata et al. 2005), an increase in the DLS-measured hydrodynamic diameter of the VLP-biotin-SA complexes was detected (IV, Figure 4). Compared to the hydrodynamic diameters measured for histidine-tagged VLPs alone or for control (histidine-tagged VLP with unconjugated SA), an increase in size of approximately 5-10 nm was observed due to a complexation with trisNTA-biotin-SA.

In order to estimate the number of available binding sites for *tris*NTA-conjugated molecules on the VLPs, the particles were labeled using Alexa488 fluorescent dye-conjugated *tris*NTA. When the labeled particles were studied by UV/Vis spectroscopy, a labeling efficiency of 68 and 74 dyes per VLP for cHis-VLP and All-cHis-VLP, respectively, was determined. The respective labeling efficiencies studied by FCS, were 86 dyes per VLP cHis-VLP and 162 dyes per VLP for All-cHis-VLP. An identical diffusion time of around 2 ms was observed for both VLP types in FCS, and high intensity peaks were observed with only a small amount of background signal (IV, Figures 5A-D). By fitting a 2-component model with predefined diffusion times (77.8 μs for the dye and 1974.8 μs for the VLPs) to the obtained data, the amount of fluorescence associated with the VLPs as a function of VLP concentration could be determined (IV, Figure 5E). A strong binding of a high number of fluorescent dyes was observed for All-cHis-VLP, while cHis-VLP showed somewhat lower binding. Minor accumulation of the fluorescent dye was observed also for native VLP, which was completely abolished by the addition of 5 mM imidazole (IV, Figure 5F). In contrast, only moderate

decrease in particle-dye complexation was observed for both types of histidine-tagged VLPs due to 5 mM imidazole (Figures 5E and F in IV). The fluorescent dye was completely released from all the VLP forms by 20 mM imidazole (data not shown).

To demonstrate the effectiveness of engineered VLPs in delivering foreign molecules into cells, HEK293T cells was exposed for 3 h to All-cHis-VLPs that were non-covalently decorated with *tris*NTA-Alexa488 fluorescence dyes and with *tris*NTA-VSV-G peptides to enable NoV VLP transduction into the cells (Figure 9J and IV, Figures 1B and 6). The VSV-G peptide is an ectodomain protein fragment derived from the viral glycoprotein of the vesicular stomatitis virus that is responsible for the receptor recognition and fusion with the cell membrane (Roche et al. 2007). The delivery of Alexa488 into HEK293T cells was seen when the cells were exposed to VLPs displaying both Alexa488 and VSV-G conjugates. By contrast, no detectable fluorescence signal was observed in the cells exposed to VLPs displaying Alexa488 conjugate in the absence of VSV-G conjugate, nor was there any signal in the untreated control cells. When the fluorescence intensities from 11-21 cells per sample were analyzed as maximum intensity projections of the cell area, the cells treated with Alexa488- and VSV-G-displaying VLPs had an average intensity of 8.3±1.2 while clearly a lower intensity of 2.3±0.2 was observed for the control sample (Alexa488-VLP). The difference was statistically significant ($p<0.001$, unpaired two-tailed *t*-test) and the same trend was seen when the experiment was repeated.

6 DISCUSSION

6.1 Feasibility of the produced VLPs as vaccine candidates and diagnostic tools

The properties of the VLPs and protein products developed in this study and their feasibility as vaccine candidates and diagnostic tools are discussed in the following sections.

6.1.1 NoV VLPs are antigenic (I-II, IV)

In the first original communication of this thesis (I), recombinant norovirus capsid proteins of genotype GII.4 and the corresponding P domain protein were produced and extensively characterized. Additionally, the same recombinant NoV capsid proteins were later surface modified by polyhistidine tag to produce chimeric VLPs and characterized in the original communication four (IV). The production of capsid proteins in insect cells resulted in the formation of VLPs that were morphologically similar to the native viruses. Examination of the purified VLPs by cryo-EM and TEM revealed the presence of capsid structures with an average diameter of 40 nm and spike-like structures on their surface, as reported previously (Prasad et al. 1994, Prasad et al. 1999). The correct size of the VLPs and the monodispersity of the samples were confirmed by DLS. The addition of the surface-displayed histidine-tags on the surface of VLPs appeared to increase the diameter to some extent, but did not interfere with protein folding and VLP assembly. Moreover, no differences in aggregation temperature (60°C) were observed between the native and histidine-tagged VLPs, when they were heated from 25°C to 90°C.

The results obtained from the peptide mass fingerprinting followed by mass spectrometric analysis and N-terminal sequencing of the native NoV VLPs (I) showed that the doublet pattern seen in the SDS-PAGE analysis of the original communication I and later in the original communication IV, was comprised of the full-length and a N-terminally truncated forms of the recombinant GII.4 NoV

capsid protein. The two protein forms had also been observed previously by others (Bertolotti-Ciarlet et al. 2003, Jiang et al. 1992, Tan et al. 2004, White et al. 1997). The ratio between the two bands remained unchanged with and without protease inhibitors and showed hardly any noticeable change following 12 months of storage at 4°C. In accordance with the previous results by White et al. (1997), it was concluded that the smaller protein was likely a cleavage product of the capsid protein within Sf9 cells that do not affect VLP assembly and that the N-terminally truncated capsid proteins are embedded in the VLPs. This hypothesis was supported by the fact that the N-terminus is located on the interior side of the particle (Prasad et al. 1999) and is, therefore, presumably protected from proteases once the particle has formed. Furthermore, the position in question, between the amino acid residues G34 and A35, was found not to contain any special protease cleavage sites (I).

Both the native VLPs and the histidine-tagged VLPs were recognized equally and efficiently by norovirus-specific antibodies from patient sera in ELISA, and they bound equally well to their host susceptibility factors in HBGA assay (I, IV). These results demonstrate that like the native NoV VLPs generated during this thesis (I, II), which have already been tested in preclinical trials by our collaborators (Blazevic et al. 2011, Tamminen et al. 2013), both of these histidine-tagged NoV VLP forms are applicable as vaccine candidates against norovirus. The advantage of these engineered VLPs is that the surface-displayed polyhistidine tag allows both direct manipulation of the VLP surface and utilizing an easy and scalable IMAC-based purification protocol that does not include PEG precipitation. While masking the particle's surface, PEG may be problematic in downstream applications, interfere with ligand binding, and suppress the desired immune responses (Scott & Murad 1998).

Native NoV VLPs showed a somewhat superior binding of antibodies to P domain proteins in ELISA as well as host susceptibility factors in HBGA assay (I). The P domain protein was also later shown to be less immunogenic in mice than the VLPs (Tamminen et al. 2012). Although it was speculated in the original communication I that the decreased affinity of P domain proteins to both norovirus-specific antibodies and the putative receptor may at least partially result from the supposed absence of P particle formation, the produced P domain protein was later shown by TEM (Tamminen et al. 2012) and by DLS (result not shown) to form particles of about 16 nm in diameter, thereby corresponding to a 12-mer small P particle (Tan & Jiang 2012a). The P particle formation has been previously shown to occur to recombinantly expressed P domain proteins and

reported also to increase its antigenicity to show VLP-like or even higher receptor-binding activity (Tan & Jiang 2005b, Tan et al. 2008). Still, the difference in antibody binding to VLPs and P particles could be associated with proposed inefficient P particle formation, which was not, according to Tan & Jiang (2012b), adequately assessed, or with difference in the conformation of epitopes or their presentation on the two particles. In other words, the antibodies in the ELISA assay may bind to specific conformational epitopes present on VLPs (and in the antibody-eliciting viruses), but lacking in the somewhat artificial structure of the P domain particle. Hence, the linear epitopes may account for the similar recognition of the proteins in Western blot (see original communication I, Fig. 1B), as the proteins are in their denaturated state, but only VLPs would display correct structural epitopes associated with the virus-like assembly of proteins.

The analyzed GII.4 genotype is relevant, as this genotype has been predominant since the mid-1990s in the United States, Europe, and Oceania, being responsible for 70–80% of all NoV outbreaks (Bok et al. 2009, Siebenga et al. 2009). However, the level of sequence diversity, even among a single genotype of noroviruses is great, and the rate of evolutionary changes within GII.4 genotype in particular is high. Over the past 20 years, GII.4 NoV has evolved a series of novel variants via recombination events and mutations in the P2 domain, some of which have persisted and replaced the previously circulating variants causing worldwide epidemics every 2-3 years (Siebenga et al. 2009, Tu et al. 2008). The specific GII.4 strain used in the original communications I-II and IV (AF080551) belongs to a Grimsby cluster of five major evolutionary clusters associated with and named according to the outbreak strains (Lindesmith et al. 2008). The Grimsby cluster is part of a larger subset of GII.4 strains named US95/96, which were responsible for causing first worldwide epidemics of NoV infection starting in the United States during 1995-1996 and later spreading to at least 7 countries on 5 continents (Noel et al. 1999, Tu et al. 2008).

The strain relevancy was assessed to some degree in the first original communication (I, Supplementary material), where GII.4 genotype diversity was evaluated by comparing the used strain to five more recently isolated epidemic strains of GII.4. The strains were found to be 94.4–95.9% identical to each other in terms of the primary amino acid sequence of the VP1 capsid. However, slightly lower sequence homology between the strains was observed, when only the hypervariable P2 subdomain of the VP1 capsid was compared (90.9–93.6%). Although there were still a considerable amount of similarity, the mutations were located at the key surface-exposed residues in sites that drive antigenic change

(Debbink et al. 2012). The NoV VLPs produced during this thesis work (I, IV), were recognized efficiently by the 12 norovirus-positive human sera collected during years 2006-2008, indicating that the strains of Grimsby/US95/96 were still involved in cases of gastroenteritis in Finland at that time, as they also were at least in Australia (Tu et al. 2008), or that the antibodies raised against the more recent strains were cross-reactive towards the epitopes of the older strain.

Nevertheless, this exemplifies how the development of a NoV vaccine faces considerable difficulties due to strain heterogeneity and fast evolution rates. Consequently, it is likely to drive vaccine development towards multivalent and/or consensus formulations capable of inducing broad cross-reactive antibodies. This approach is demonstrated in the novel human bivalent VLP-based norovirus vaccine by Takeda Pharmaceuticals currently being evaluated in clinical efficacy trials. The vaccine contains both genotype GI.1 and GII.4 components, of which the GII.4 component is a consensus sequence derived from three GII.4 outbreak strains that circulated widely in 2002 and 2006 (Debbink et al. 2014, Parra et al. 2012). Moreover, following the common practice with current influenza vaccines, the NoV vaccines will also likely require reformulation every few years as updated NoV epidemiological data through outbreak surveillance networks like the CaliciNet in the United States and international NoroNet allow identification of the most prevalent strains.

Taken together, the developed NoV VLPs (I-II and IV) are feasible to be used for the development of norovirus diagnostic methods, as has been demonstrated already by us and our collaborators (Auer et al. 2015, Malm et al. 2014, Uusi-Kerttula et al. 2014), and as preliminary tools for vaccine development. In addition, the C-terminal histidine-tag enables the use of affinity matrices for orienting or immobilizing the P particle or VLP on the surface of microparticles or other appropriate surfaces as well as conjugating foreign molecules on their surface using *tris*NTA adaptors (Lata et al. 2005), a feature that is assessed in the original communication IV.

6.1.2 CVB3 VLPs induce strong antibody response in mice (III)

Since the launch of polio vaccines in 1950s, no other enterovirus vaccines have been developed and registered for human use. One reason for this void is that it has been difficult to identify causal serotype-disease relationships among the over 100 different and rapidly evolving enterovirus serotypes that circulate worldwide.

There are, however, certain virus-disease associations that are well established, making the development of novel vaccines worth considering. Among such enteroviruses are EV71 and CVB3, both of which commonly cause severe infections that can be fatal (Maier et al. 2004, McMinn 2012). The recent progress in the development of an EV71 vaccine has been encouraging, as several vaccine candidates have been studied in animal models, and human clinical trials have yielded promising results (Liang et al. 2013). Although vaccination against CVB3 could significantly reduce the incidence of serious or fatal viral myocarditis and other diseases associated with CVB3 infection, breakthroughs in the development of a CVB3 vaccine have not been made. There have been, however, several attempts to demonstrate the potential of vaccination against CVB3, including a subunit vaccine (Fohlman et al. 1990), several DNA vaccines (Henke et al. 1998, Kim et al. 2005, Xu et al. 2004), and numerous attenuated or inactivated virus vaccines (Dan & Chantler 2005, Kim & Nam 2011, Park et al. 2009, See & Tilles 1994, Zhang et al. 1997). However, such vaccines may have safety concerns, or they may not stimulate an ideal immune response (Goldman & Lambert 2004). As an effort to overcome these drawbacks, a promising vaccine candidate against CVB3 based on VLP-technology was developed during this thesis (III). These promising features are discussed next.

The produced CVB3 VLPs resembled in many ways the wild type viruses (III). The VLPs and virus particles were virtually undistinguishable by TEM (see original communication III, Figure 5). The same structural authenticity was also evidenced by DLS, which showed that the purified VLPs and the viruses were very similar in size (diameter, approximately 30 nm) and that the preparations were homogenous. When the heat stability of the particles was analyzed by DLS, the VLPs were found to be resistant to aggregation up to 50°C. They were only slightly more prone to elevated temperatures than the viruses, as VLPs aggregated at temperatures approximately 10-15°C lower than the viruses did (III, Figures 4B and D). The somewhat poorer heat stability of the VLPs was speculated to be because of the lack of the viral genome, which inside a wild type virus may make its structure more stable against heat treatment. Another explanation for the difference in heat stability was thought to be in the capsid structure. Unlike in mature genuine virions, the VP0 capsid protein in enteroviral VLPs is not cleaved into VP4 and VP2 capsid proteins (III, Figure 2B, lane 4 and 5) (Chung et al. 2006, Liu et al. 2012a, Liu et al. 2013b, Zhang et al. 2012), which may have affected the stability of the VLP. Both explanations are supported by the data of Curry et al. (1997), who

reported that empty picornaviral capsids were often lacking VP0 cleavage and were also more thermolabile than genome-containing viruses.

Most importantly, the generated VLPs were highly immunogenic, as shown by the vaccination experiments in mice (III). The anti-VLP sera raised in mice by CVB3 VLP vaccination exhibited a strong neutralizing capacity against the homologous CVB3 strain (III, Table 2) and elicited a strong serum IgG antibody response that reacted with both VLPs and virus antigens within the same genogroup (III, Figure 7). Our results were thus in line with the previous studies showing the efficacy of different enteroviral VLPs as immunogens (Lin et al. 2012, Liu et al. 2012a, Zhang et al. 2012), but especially the work performed by Zhang et al. (2012) with CVB3 VLPs showed similar results. However, compared to the results by Zhang et al., the CVB3 VLPs generated by us were able to generate higher neutralizing titers with smaller doses, which highlights the purity and high immunogenicity of our chromatography-purified VLPs.

The analysis of the B cell, $CD8^+$, and $CD4^+$ T cell responses induced by CVB3 VLPs in mice revealed a limited degree of activation. However, the effector-memory T cell populations were consistently increased by CVB3 VLPs, indicating that an immunological response to the VLPs was obtained. However, without a tetrameric fluorochrome against the MHC receptor-peptide-complex (Klenerman et al. 2002), we were not able to determine that the small increase in $CD8^+$ and $CD4^+$ memory T cell populations was induced specifically by the VLPs. The limited degree of immune cell activation was consistent with similar studies carried out with a CVB3 virus (Kemball et al. 2008, Slifka et al. 2001) and may be connected to the capacity of CVB3 to inhibit antigen presentation through MHC molecules (Kemball et al. 2010).

Taken together, the generated CVB3 VLPs represent a promising vaccine candidate that offers an equally efficient, but safer, protection than inactivated or live-attenuated viral vaccines. The VLPs are also feasible for enteroviral diagnostics, as they are significantly safer to handle than a corresponding virus. The produced VLPs were of high quality in regard to purity and indistinguishable from the native virus in size, composition, and appearance. The VLPs were also highly immunogenic, as shown by the vaccination experiments in mice, and they withstood prolonged storage at -20°C maintaining their intact icosahedral structure.

6.2 Feasibility of the developed production and purification methods

For the development of vaccines today, efficient and technically feasible production and purification methods are essential. In addition, for vaccines intent on protecting from fast-evolving viruses like noroviruses and enteroviruses, quick production times are required.

The baculovirus-insect cell protein expression system is currently the most widely used eukaryotic protein production system, and it has been verified to be effective for the production of different VLPs, including particles of noroviral and enteroviral origin (Roy & Noad 2008). Already, one baculovirally produced human VLP vaccine has gone through the international regulation and validation pipelines and been accepted as a safe product, Cervarix (Harper et al. 2006). Furthermore, other baculovirus-produced VLP vaccines are in the late phases of clinical trials or have already completed them (Roldão et al. 2010, Vicente et al. 2011). These facts, together with the intrinsic safety of the baculovirus-insect cell expression system, i.e., the absence of animal-based reagents during culturing and inability of baculoviruses to replicate in mammalian cells (Gröner 1986, Lapointe et al. 2012), encouraged us to adapt this system for the production of the VLPs in this thesis (I-IV).

Although expression of foreign proteins by the baculovirus expression system has been proven to be an excellent technique for producing large quantities of biologically active proteins, sometimes a simpler and less time-consuming system for the production and purification of an antigen can be valuable for vaccine development and especially for diagnostic purposes. With this in mind, a cost-effective and simple method for production of the P domain of norovirus, which is responsible for immune recognition and host cell attachment of the virus (Tan et al. 2008), in *E. coli* was also developed (I).

In research settings, VLPs like native viruses are typically purified by gradient ultracentrifugation techniques. Although meticulously performed ultracentrifugation does generate high-quality virus material, the procedure is cumbersome and non-scalable, and the yields are modest considering the laborious nature of the method. In addition, there tends to be more variation between purification batches in gradient-based purifications, a tendency that was also observed when the particle size distributions of NoV VLPs after CsCl purifications were compared to those observed after IEX chromatography (II, Table 1). Others have also shown that CsCl is disadvantageous due to its toxicity, induction of

reduced infectivity in viruses, and particle deformation in storage (Burova & Ioffe 2005). On the industrial scale, therefore, other methods, such as chromatography-based purification, are more feasible (Morenweiser 2005). In response to this demand, easily scalable ion exchange chromatography-based purification systems for the NoV and CVB3 VLPs (II, III), as well as metal ion affinity chromatography purification methods for the NoV P domain protein and histidine-tagged NoV VLPs (I, IV) were developed during this thesis. These single-step chromatography procedures yielded highly pure and stable VLPs, and the developed methodologies are also easily scalable for industrial-scale vaccine production.

Chromatographic purification seemed to be efficient in concentrating the VLP capsid proteins, as could be seen for the capsid proteins of NoV VLPs (II, Figure 2) and CVB3 VLPs (III, Figure 2B) that were purified using ion exchange chromatography, as well as for the histidine-tagged NoV VLPs (IV, Figure 3A) purified by metal ion affinity chromatography. They all were significantly concentrated during their respective chromatographic purifications compared to the sample applied to the chromatography column. Both the NoV VLPs and the CVB3 VLPs (I-III) were isolated from the production cells using PEG, because it efficiently decreases the initial sample volume. PEG precipitation alone, however, is not sufficient for the isolation of VLPs from various source materials, as PEG-precipitated VLP samples may contain co-precipitated impurities or aggregated VLPs (see original communication II, Figure 6). A high concentration of PEG can also potentially lead to VLP instability (Huhti et al. 2010), and PEG itself may be a problematic contaminant in downstream applications (Russell et al. 2007). The use of VLPs as vaccines requires highly pure material, and therefore, additional purification steps are necessary. Although of high quality, the total yields of some VLPs were modest (see section 5.1.1 and Table 1) as the production was carried out under non-optimized research laboratory conditions. However, the yield of different VLPs could be significantly improved by further optimization of several process parameters during both production and purification steps, as reviewed by Vicente et al. (2011) and demonstrated by Chung et al. for EV71 VLPs (2010).

Taken together, all the chromatographic purification methods developed during this thesis resulted in fully assembled VLPs with high purity (>95%). The purification protocols can be easily performed within a single working day and offer the possibility to scale up the production of these VLPs and also to adapt this technology to the production of other VLPs.

6.3 Engineering of the VLPs

The observations encountered during the engineering of the VLPs are discussed in the following sections.

6.3.1 Encapsidation of the artificial genomes into the CVB3 VLPs (III)

Although the measured stability characteristics are adequate to maintain the CVB3 VLP vaccine candidate in a stable form at low or ambient temperatures, it was envisioned that the VLPs could be further stabilized by providing *in trans* a modified genome, in which the capsid region was replaced by the mCherry fluorescent protein sequence, that could be packaged into the VLPs (Figure 8A, and original communication III, Figure 1, cassette 2). Concurrently, we aimed to demonstrate, whether these VLPs could serve as carriers of artificial gene sequences into culture cells. However, as suspected after the unsuccessful GMK cell transduction experiment (see section 5.4) and verified by the RT-PCR results, no genomes were packed inside the CVB3 VLPs.

In referential studies done previously with poliovirus and CVB3, a modified genome could be encapsidated into particles (Meyer et al. 2004, Porter et al. 1995, Porter et al. 1998). However, the VLPs used in these studies were produced in mammalian cells, in contrast to the insect cells used by us. Moreover, the capsid proteins were introduced into mammalian cells as infective replicons, and these replicons used T7 RNA polymerase for transciption, which, for example, does not add a 5'cap in the nascent transcript (Kochetkov et al. 1998). By contrast, in our setup the expression of the viral transgenome was regulated by the host's own transcription system. These profound differences in the experimental setups may explain the different outcomes. Also interestingly, Porter et al. (1998) only succeeded in packaging experiments with poliovirus, whereas packaging of enterovirus 70, coxsackievirus A21 and B3 genomes were unsuccessful. Nevertheless, it is evident that the 3CD protease from cassette 2 in our construct, which is responsible for the cleavage of the capsid polyprotein into the VP0, VP3 and VP1 (Liu et al. 2012a) from cassette 1 (Figure 8A and III, Figure 1), was transcribed into functional mRNA and expressed (by insect cells). Otherwise the formation of VLPs would not have been observed.

It is known that during picornavirus assembly, the three cleavage products of P1 (VP0, VP3, and VP1) spontaneously assemble into empty icosahedral

procapsids $[(VP0, VP3, VP1)_5]_{12}$, and the subsequent packaging of the RNA genome will form a provirion. The cleavage of VP0 to form VP4 and VP2 then occurs during provirion maturation by an autocatalytic mechanism that may be RNA-dependent (Hellen & Wimmer 1992, Racaniello 2007). It can be hypothesized, therefore, that the lack of the RNA genome is also the reason, why the VP0 cleavage did not take place in our recombinant VLPs. This hypothesis is also supported by a study by Curry et al. (1997), where the empty picornaviral capsids were often found to be lacking the VP0 cleavage.

There are several reasons why the RNA packaging was unsuccessful in our VLP construct. It is possible that the modified genome, which was produced as an mRNA from the baculoviral DNA copy, was never processed into a negative strand and thus was not replicated and encapsidated accordingly. For example, the 5'cap added at the 5'end of the mRNA during the eukaryotic transcription could disrupt the function or attachment of the viral VPg protein or the many other host and viral proteins and RNA structures needed in the picornaviral replication complex (Lin et al. 2009, Liu et al. 2010). Alternatively, the possibility of the mRNA itself serving as the viral genome would require, at least, that the mRNA is copied in sufficient amounts and localized correctly to associate with the replication-encapsidation complex. Moreover, because the encapsidation of non-progeny nucleic acids is wasteful for the virus and is, therefore, highly specifically restricted to VPg-containing positive-sense RNA genomes (Semler & Wimmer 2002), it is likely that the mRNA would be excluded from encapsidation.

6.3.2 Surface display on NoV VLPs (IV)

VLP vaccines can be further developed by producing chimeric VLPs, where one or multiple antigens are produced as a genetic fusion to viral structural proteins or conjugated chemically to the VLP (Kushnir et al. 2012). In addition to vaccines, VLPs also exhibit great potential in a number of other applications. For example, by modulating VLP packaging, display, and/or targeting, promising VLP-based tools have been developed for gene delivery and immune therapy (reviewed extensively for example in Garcea & Gissmann 2004, Jennings & Bachmann 2009, Kushnir et al. 2012, Ma et al. 2012, and Xiang et al. 2008) and even as new biological nanomaterials (Lee et al. 2009, Liu et al. 2012b, Mao et al. 2004, Wang et al. 2002). As nanocarriers, VLPs offer the advantages of morphological uniformity,

biocompatibility, the capacity to potentiate immune response, and functionalization of both their inner cavities and outer surfaces (Kushnir et al. 2012, Zeltins 2013).

Although the biomedical applicability of several icosahedral VLPs tailored with genetic and chemical conjugation has been studied in detail (reviewed recently in Pushko et al. 2013), such modification procedures have not been established for norovirus VLPs before the present study. However, presentation of foreign antigens attached to surface loops of capsid-derived subviral P particles that consist only of protruding domains of NoV have been reported (Tan et al. 2011). In the original communication IV, we described a nanocarrier platform based on genetically modified NoV VLPs and non-covalent chemical conjugation. The VLPs were modified by adding a C-terminal polyhistidine tag projecting out of the VLP surface (IV, Figure 1A). The added tag was first utilized in VLP purification and later used to demonstrate molecule display on VLPs by attaching a vesicular stomatitis virus G peptide (VSV-G) and a fluorescent dye (Alexa 488), as well as, streptavidin (SA) non-covalently on the VLP surface via *tris*-nitrilotriacetic acid (*tris*NTA) adaptors. *tris*NTA binds polyhistidine tags via coordinating metal ions with high affinity and stability (Lata et al. 2005).

The attachment of *tris*NTA-biotin-streptavidin complexes to histidine-tagged VLPs was detected as an increase in the hydrodynamic diameter of VLP-SA complexes, as measured by DLS (IV, Figure 4). The increase in the diameter of the VLP forms correlated well with the diameter of the streptavidin tetramer (around 5 nm) accompanied by the *tris*NTA adaptor and thus demonstrated that full-length proteins can be attached to the VLP surface without causing disturbance to the VLP structure. By using Alexa488 fluorescent dye-conjugated *tris*NTA adaptors, we could estimate the number of available binding sites for the *tris*NTA-conjugated molecules on the VLPs and study the binding properties more thoroughly. Labeling efficiencies of 86 dyes per VLP for cHis-VLP and 162 dyes for All-cHis-VLP were calculated from the measurements by FCS. Additionally, high intensity peaks with only a small amount of background signal as well as a nearly identical diffusion time of approximately 2 ms was observed for both VLP forms, which indicated that the solutions were monodisperse after conjugation.

When the interaction between the histidine-tagged VLPs and Ni-coordinated *tris*NTA-Alexa488 were studied by adding cHis-VLPs or All-cHis-VLPs to a solution containing the fluorescent conjugate, the fluorescence intensity fluctuation increased significantly from the stable signal generated by the dye alone (IV, Figures 5A-E), indicating the accumulation of the fluorescent conjugate on the particles. Reflecting the relative amount of available binding sites on the two VLP

forms, strong binding of a high number of *tris*NTA-Alexa488 was observed for All-cHis-VLP, whereas cHis-VLP showed a slightly lower level of binding. The fluorescent dye was completely released from the VLPs with 20 mM imidazole.

To demonstrate the effectiveness of the engineered NoV VLPs in delivering foreign molecules into cells, HEK293T cells were exposed to All-cHis-VLPs non-covalently decorated with *tris*NTA-Alexa488 fluorescence dye (IV, Figure 1B). Because noroviruses are inherently incapable of infecting cultured cells, VSV-G cell transduction peptides were attached to the VLP surface using *tris*NTA adaptors to enable them enter into cells. As a result, the delivery of Alexa488 into the HEK293T cells was only observed when the cells were exposed to VLPs displaying both Alexa488 and VSV-G conjugates (Figure 9J and IV, Figure 6). In contrast, there was no detectable fluorescence signal observed in the cells exposed to VLPs displaying only Alexa488 conjugate in the absence of VSV-G conjugate, nor was there any signal in the untreated control. Moreover, the difference in maximum fluorescence intensities of the cell area between the samples and controls was statistically significant ($p<0.001$, unpaired two-tailed *t*-test). To conclude, due to the surface-conjugated VSV-G peptides, NoV VLPs were able to transduce the cells and carry the surface-conjugated Alexa488 dye along. This experiment also demonstrated that these NoV VLPs could be functionalized to versatile nanocarriers by a simple non-covalent conjugation of different molecules.

Taken together, we provided here a systematic analysis of the functional effects of introducing artificial modulatory sites onto a NoV VLP. The study also demonstrated a proof of principle for a fast "click-and-exchange" technology for modulating the VLP surface simply by replacing the non-covalently conjugated molecule that binds to the polyhistidine tags on the VLP surface. The surface display was thus achieved without a laborious genetic fusion of the displayable molecule and capsid gene or a permanent chemical coupling to a preformed VLP. If needed, the displayable molecule can be disintegrated from the VLP with a mild treatment with imidazole. The concept is applicable to a variety of molecules. The NoV VLP could be decorated, for example, with therapeutic peptides that enhance or modulate the immune system or with epitopes, small proteins, DNA, targeting molecules, or reporter tags for tracing vaccine delivery. Moreover, the two histidine-tagged VLP forms, differing by the number of conjugation sites they bear, allow the accommodation of larger complexes and modulation of the number of conjugates on the surface. In conclusion, histidine-tagged norovirus VLPs described in the original communication IV provide a robust and versatile tool for the needs of nanobiotechnology and biomedical sciences.

7 SUMMARY AND CONCLUSIONS

The main goal of this doctoral thesis was to produce and characterize virus-like particles (VLPs) derived from relevant strains of norovirus and enterovirus for vaccine development and diagnostics, and to see whether their structures could be modified. Noroviruses are a major cause of acute epidemic gastroenteritis worldwide, and enterovirus CVB3 is associated with acute and chronic viral myocarditis and dilated cardiomyopathy.

The native norovirus VLP representing a common GII.4 strain (NoV VLP) and the corresponding histidine-tagged P domain of the NoV capsid protein, which was studied as a diagnostic tool for evaluation of norovirus infection, were produced in insect cells and in *E. coli*, respectively. Additionally, the recombinant NoV capsid proteins were later surface modified by C-terminal polyhistidine tags to produce chimeric VLPs (histidine-tagged NoV VLPs) in insect cells. All NoV VLP forms were found to resemble wild type noroviruses in their size and morphology. However, mass spectrometric analyses revealed that some of the recombinantly expressed NoV capsid proteins were missing a 34 residue fragment from their N-terminus located on the interior side of the particles. The truncated proteins were embedded in the NoV VLPs along with the full-length capsid proteins. All NoV VLP forms were recognized equally and efficiently by norovirus-elicited antibodies from patient sera in ELISA, and they bound equally well to their host susceptibility factors in HBGA assay. However, the VLPs showed somewhat superior binding to P domain proteins in both assays.

The insect cell -produced CVB3 VLPs resembled the genuine wild type viruses in many ways. The VLPs and virus particles were morphologically undistinguishable by TEM and DLS, although the VLPs were found to be slightly more prone to elevated temperatures. VLPs aggregated at around 50°C, which was at a 10-15 degree lower temperature than the viruses. CVB3 VLPs were also devoid of the modified genome provided *in trans*, and they lacked the viral maturation cleavage of capsid protein VP0 into VP4 and VP2. These characteristics were thought to be connected to the observed thermolability. The anti-VLP sera raised in mice by CVB3 VLP vaccination exhibited a strong neutralizing capacity against

the homologous CVB3 strain and elicited a strong serum IgG antibody response that reacted to both VLP and virus antigens within the same genogroup.

The GII.4 NoV VLPs were further modified by adding a C-terminal polyhistidine tag projecting out of the VLP surface. The resulting chimeric NoV VLP forms (cHis-VLP and All-cHis VLP) differed by the amount of histidine tags on their surface. By using the affinity between histidine-tag and *tris*NTA, fluorescent dye molecules (Alexa488) and streptavidin-biotin conjugated to *tris*NTA adaptors were displayed on the VLPs to model the use of these engineered VLPs as easily modifiable nanocarriers or a flexible vaccine platform. By using the *tris*NTA adaptors, the engineered VLPs were also able to enter and deliver surface-displayed fluorescent dyes into HEK293T cells via surface-attached cell internalization peptide (VSV-G).

The underlying aim during this thesis was also to proceed from laborious gradient-based purification protocols to more sophisticated and scalable chromatography-based purification methods to answer the needs of industrial-scale vaccine development. Therefore, chromatographic purification methods based on either ion exchange or immobilized metal ion affinity were developed for all the VLPs and protein products generated during this thesis. The developed chromatographic purification methods resulted in fully assembled VLPs with high purity, and further, they can be easily performed within one working day. Moreover, they offer the possibility of upscaling the production of these VLPs and adapting this technology for production of other VLPs as well.

In conclusion, this thesis work led to a production of several VLP-based products using overlapping technologies (Figure 9). The NoV and CVB3 VLPs developed during this thesis are applicable as vaccine candidates against their respective virus-related diseases and as diagnostic antigens. In addition, the C-terminal histidine-tag of NoV P particles and on engineered NoV VLPs enables the use of affinity matrices for orienting or immobilizing the particles on the surface of microparticles or other appropriate surfaces and also conjugating foreign molecules on their surface. Hence, these inventions provide robust and versatile tools for nanobiotechnology and biomedical sciences. Moreover, the information gathered during the course of this thesis gives valuable insights for the future production and tailoring of VLPs.

ACKNOWLEDGEMENTS

I owe my deepest gratitude to my supervisors Vesa Hytönen and Markku Kulomaa. I thank Vesa for his excellent guidance and support on how to do scientific research. Your endless optimism and enthusiasm towards science have been inspiring and have played an important role during this work. I warmly thank you Markku for giving me the opportunity to perform my doctoral studies in your research group, for your kind guidance in research and life in general, and for providing a warm and supporting working environment.

I wish to thank my closest colleagues and friends Juha Määttä, Jenita Pärssinen, and Tiina Riihimäki for all the diverse discussions and moments of laughter we have shared during these years. It has been a pleasure both working and spending free time with you. I also thank the best possible roommates Jenni Leppiniemi and Soili Lehtonen for bearing with me and creating an enjoyable atmosphere in our office. The roommate next door Rolle Rahikainen is thanked for always challenging my wits.

I am thankful to Ulla Kiiskinen, Niklas Kähkönen, Outi Väätäinen, Tanja Rämö, and Laura Kananen for your excellent technical assistance and help with anything and everything. Special thanks go to you Outi and Tanja for your endurance dealing with the endless Western blots and insect cell cultures I asked you to do as well as for the much-cherished off-work discussions we shared over a ~~glass~~bottle of red. I would also like to thank other former and present long-time members of the Molecular Biotechnology and Protein Dynamics groups: Barbara Taskinen, Sampo Kukkurainen, Sanna Auer, Magdaléna von Essen, Latifeh Azizi, Ville Hynninen, and Anssi Nurminen, for creating a pleasant working environment. During the years, I had the pleasure of supervising a Master's Thesis and summer students who have contributed to this thesis, and for that I warmly thank Selina Mäkinen, Rosa Mattila, and Niila Saarinen.

I am grateful to my thesis committee members Pasi Kallio and Olli Laitinen for their invaluable guidance during my thesis project. I also wish to thank all my co-authors of the original articles not already otherwise mentioned: Leena Huhti, Tuomas Mäntylä, Minni Koivunen, Kirsi Tamminen, Vesna Blazevic, Timo Vesikari, Sami Oikarinen, Heikki Hyöty, Anssi Mähönen, Sarah Butcher, Pasi

Laurinmäki, Nisse Kalkkinen, Gunilla Rönnholm, Laura Kummola, Amirbabak Sioofy-Khojine, Varpu Marjomäki, Artur Kazmertsuk, Ilkka Junttila, Teemu Ihalainen, Marie Stark, Hanni Uusi-Kerttula, Ralph Wieneke, and Robert Tampé. Without your significant help and contribution, this thesis would not have been completed. I further express my gratitude to the reviewers of my thesis, Kari Airenne and Ilkka Julkunen for their valuable comments and perceptive feedback to help me finalize my thesis.

Finally I want to thank my friends and family for all the trust and encouragement during these years and for regularly reminding me of life outside work. I am especially grateful to my mom, brother Tomi, and Tommi for your help and invested time with the always ongoing "remppa"-project/s and for babysitting my dogs whenever I needed time to concentrate on research. I also want to remember my late dad for encouraging me to begin this ambitious mission.

This research has been financially supported by the National Doctoral Programme in Informational and Structural Biology (ISB), the Academy of Finland via project funding, the Pirkanmaa Hospital District, and the Finnish Cultural Foundation.

Tampere, April 2015

Tiia Koho

REFERENCES

Abraham, G. & Colonno, R.J. (1984). Many rhinovirus serotypes share the same cellular receptor. *Journal of Virology,* 51(2), pp. 340-345.

Adler, J.L. & Zickl, R. (1969). Winter vomiting disease. *The Journal of Infectious Diseases,* 119(6), pp. 668-673.

Afeyan, N.B., Fulton, S.P., Gordon, N.F., Mazsaroff, I., Várady, L. & Regnier, F.E. (1990). Perfusion Chromatography: An Approach to Purifying Biomolecules. *Nature Biotechnology,* 8(3), pp. 203-206.

Aguilar, J.C. & Rodríguez, E.G. (2007). Vaccine adjuvants revisited. *Vaccine,* 25(19), pp. 3752-3762.

Atmar, R.L., Bernstein, D.I., Harro, C.D., Al-Ibrahim, M., Chen, W.H., Ferreira, J., Estes, M.K., Graham, D.Y., Opekun, A.R., Richardson, C. & Mendelman, P.M. (2011). Norovirus Vaccine against Experimental Human Norwalk Virus Illness. *N Engl J Med,* 365(23), pp. 2178-2187.

Auer, S., Koho, T., Uusi-Kerttula, H., Vesikari, T., Blazevic, V. & Hytönen, V.P. (2015). Rapid and sensitive detection of norovirus antibodies from human serum using biolayer interferometry biosensor. *Submitted.*

Ausar, S.F., Foubert, T.R., Hudson, M.H., Vedvick, T.S. & Middaugh, C.R. (2006). Conformational stability and disassembly of Norwalk virus-like particles. Effect of pH and temperature. *The Journal of Biological Chemistry,* 281(28), pp. 19478-19488.

Bachmann, M.F. & Jennings, G.T. (2010). Vaccine delivery: a matter of size, geometry, kinetics and molecular patterns. *Nature Reviews. Immunology,* 10(11), pp. 787-796.

Bárcena, J. & Blanco, E. (2013). Design of novel vaccines based on virus-like particles or chimeric virions. *In Structure and Physics of Viruses. An intergrated textbook. Subcellular Biochemistry 68*. Mateu, M.G. (Ed.), pp. 631-665. Springer, Netherlands.

Bergelson, J.M., Chan, M., Solomon, K.R., St John, N.F., Lin, H. & Finberg, R.W. (1994). Decay-accelerating factor (CD55), a glycosylphosphatidylinositol-anchored complement regulatory protein, is a receptor for several echoviruses. *Proceedings of the National Academy of Sciences of the United States of America,* 91(13), pp. 6245-6248.

Bergelson, J.M., Cunningham, J.A., Droguett, G., Kurt-Jones, E.A., Krithivas, A., Hong, J.S., Horwitz, M.S., Crowell, R.L. & Finberg, R.W. (1997). Isolation of a common receptor for Coxsackie B viruses and adenoviruses 2 and 5. *Science,* 275(5304), pp. 1320-1323.

Bernstein, D.I., Atmar, R.L., Lyon, G.M., Treanor, J.J., Chen, W.H., Jiang, X., Vinjé, J., Gregoricus, N., Frenck, R.W.,Jr, Moe, C.L., Al-Ibrahim, M.S., Barrett, J., Ferreira, J., Estes, M.K., Graham, D.Y., Goodwin, R., Borkowski, A., Clemens, R. & Mendelman, P.M. (2015). Norovirus vaccine against experimental human GII.4 virus illness: a challenge study in healthy adults. *The Journal of Infectious Diseases,* 211(6), pp. 870-878.

Bertolotti-Ciarlet, A., Crawford, S.E., Hutson, A.M. & Estes, M.K. (2003). The 3' end of Norwalk virus mRNA contains determinants that regulate the expression and stability

of the viral capsid protein VP1: a novel function for the VP2 protein. *Journal of Virology,* 77(21), pp. 11603-11615.

Blazevic, V., Lappalainen, S., Nurminen, K., Huhti, L. & Vesikari, T. (2011). Norovirus VLPs and rotavirus VP6 protein as combined vaccine for childhood gastroenteritis. *Vaccine,* 29(45), pp. 8126-8133.

Block, H., Maertens, B., Spriestersbach, A., Brinker, N., Kubicek, J., Fabis, R., Labahn, J. & Schäfer, F. (2009). Immobilized-metal affinity chromatography (IMAC): a review. *Methods in Enzymology,* 463, pp. 439-473.

Bok, K., Abente, E.J., Realpe-Quintero, M., Mitra, T., Sosnovtsev, S.V., Kapikian, A.Z. & Green, K.Y. (2009). Evolutionary dynamics of GII.4 noroviruses over a 34-year period. *Journal of Virology,* 83(22), pp. 11890-11901.

Bradford, M.M. (1976). A rapid and sensitive method for the quantitation of microgram quantities of protein utilizing the principle of protein-dye binding. *Analytical Biochemistry,* 72, pp. 248-254.

Braun, M., Jandus, C., Maurer, P., Hammann-Haenni, A., Schwarz, K., Bachmann, M.F., Speiser, D.E. & Romero, P. (2012). Virus-like particles induce robust human T-helper cell responses. *European Journal of Immunology,* 42(2), pp. 330-340.

Bundy, B.C., Franciszkowicz, M.J. & Swartz, J.R. (2008). Escherichia coli-based cell-free synthesis of virus-like particles. *Biotechnology and Bioengineering,* 100(1), pp. 28-37.

Burova, E. & Ioffe, E. (2005). Chromatographic purification of recombinant adenoviral and adeno-associated viral vectors: methods and implications. *Gene Therapy,* 12 Suppl 1, pp. S5-17.

Burrell, C.J., Mackay, P., Greenaway, P.J., Hofschneider, P.H. & Murray, K. (1979). Expression in Escherichia coli of hepatitis B virus DNA sequences cloned in plasmid pBR322. *Nature,* 279(5708), pp. 43-47.

Campbell, N.A. (1996). Microbial models: The genetics of viruses and bacteria. *In Biology.* 4th edition, The Benjamin/Cummings Publishing Company, Inc., Menlo Park, CA, USA.

Carlson, E.D., Gan, R., Hodgman, C.E. & Jewett, M.C. (2012). Cell-free protein synthesis: Applications come of age. *Biotechnology Advances,* 30(5), pp. 1185-1194.

Chackerian, B., Lowy, D.R. & Schiller, J.T. (2001). Conjugation of a self-antigen to papillomavirus-like particles allows for efficient induction of protective autoantibodies. *Journal of Clinical Investigation,* 108(3), pp. 415-423.

Chang, L., Dowd, K.A., Mendoza, F.H., Saunders, J.G., Sitar, S., Plummer, S.H., Yamshchikov, G., Sarwar, U.N., Hu, Z., Enama, M.E., Bailer, R.T., Koup, R.A., Schwartz, R.M., Akahata, W., Nabel, G.J., Mascola, J.R., Pierson, T.C., Graham, B.S. & Ledgerwood, J.E. (2014). Safety and tolerability of chikungunya virus-like particle vaccine in healthy adults: a phase 1 dose-escalation trial. *The Lancet,* 384(9959), pp. 2046-2052.

Cheetham, S., Souza, M., Meulia, T., Grimes, S., Han, M.G. & Saif, L.J. (2006). Pathogenesis of a genogroup II human norovirus in gnotobiotic pigs. *Journal of Virology,* 80(21), pp. 10372-10381.

Chehadeh, W., Lobert, P.E., Sauter, P., Goffard, A., Lucas, B., Weill, J., Vantyghem, M.C., Alm, G., Pigny, P. & Hober, D. (2005). Viral protein VP4 is a target of human antibodies enhancing coxsackievirus B4- and B3-induced synthesis of alpha interferon. *Journal of Virology,* 79(22), pp. 13882-13891.

Chigira, Y., Oka, T., Okajima, T. & Jigami, Y. (2008). Engineering of a mammalian O-glycosylation pathway in the yeast Saccharomyces cerevisiae: production of O-fucosylated epidermal growth factor domains. *Glycobiology,* 18(4), pp. 303-314.

Chung, C.Y., Chen, C.Y., Lin, S.Y., Chung, Y.C., Chiu, H.Y., Chi, W.K., Lin, Y.L., Chiang, B.L., Chen, W.J. & Hu, Y.C. (2010). Enterovirus 71 virus-like particle vaccine: improved production conditions for enhanced yield. *Vaccine,* 28(43), pp. 6951-6957.

Chung, Y.C., Huang, J.H., Lai, C.W., Sheng, H.C., Shih, S.R., Ho, M.S. & Hu, Y.C. (2006). Expression, purification and characterization of enterovirus-71 virus-like particles. *World Journal of Gastroenterology,* 12(6), pp. 921-927.

Cohen, B.J. & Richmond, J.E. (1982). Electron microscopy of hepatitis B core antigen synthesized in E. coli. *Nature,* 296(5858), pp. 677-679.

Cooper, C. & Mackie, D. (2011). Hepatitis B surface antigen-1018 ISS adjuvant-containing vaccine: a review of HEPLISAV safety and efficacy. *Expert Review of Vaccines,* 10(4), pp. 417-427.

Cooper, J.B., Pratt, W.R., English, B.K. & Shearer, W.T. (1983). Coxsackievirus B3 producing fatal meningoencephalitis in a patient with X-linked agammaglobulinemia. *American Journal of Diseases of Children (1960),* 137(1), pp. 82-83.

Cornuz, J., Zwahlen, S., Jungi, W.F., Osterwalder, J., Klingler, K., van Melle, G., Bangala, Y., Guessous, I., Müller, P., Willers, J., Maurer, P., Bachmann, M.F. & Cerny, T. (2008). A vaccine against nicotine for smoking cessation: a randomized controlled trial. *PLOS ONE,* 3(6), pp. e2547.

Cunningham, M.W., Antone, S.M., Gulizia, J.M., McManus, B.M., Fischetti, V.A. & Gauntt, C.J. (1992). Cytotoxic and viral neutralizing antibodies crossreact with streptococcal M protein, enteroviruses, and human cardiac myosin. *Proceedings of the National Academy of Sciences of the United States of America,* 89(4), pp. 1320-1324.

Curry, S., Fry, E., Blakemore, W., Abu-Ghazaleh, R., Jackson, T., King, A., Lea, S., Newman, J. & Stuart, D. (1997). Dissecting the roles of VP0 cleavage and RNA packaging in picornavirus capsid stabilization: the structure of empty capsids of foot-and-mouth disease virus. *Journal of Virology,* 71(12), pp. 9743-9752.

Dan, M. & Chantler, J.K. (2005). A genetically engineered attenuated coxsackievirus B3 strain protects mice against lethal infection. *Journal of Virology,* 79(14), pp. 9285-9295.

Daughenbaugh, K.F., Fraser, C.S., Hershey, J.W. & Hardy, M.E. (2003). The genome-linked protein VPg of the Norwalk virus binds eIF3, suggesting its role in translation initiation complex recruitment. *The EMBO Journal,* 22(11), pp. 2852-2859.

de Martel, C., Ferlay, J., Franceschi, S., Vignat, J., Bray, F., Forman, D. & Plummer, M. (2012). Global burden of cancers attributable to infections in 2008: a review and synthetic analysis. *The Lancet Oncology,* 13(6), pp. 607-615.

De Pourcq, K., Vervecken, W., Dewerte, I., Valevska, A., Van Hecke, A. & Callewaert, N. (2012). Engineering the yeast Yarrowia lipolytica for the production of therapeutic proteins homogeneously glycosylated with $Man_8GlcNAc_2$ and $Man_5GlcNAc_2$. *Microbial Cell Factories,* 11, pp. 53-2859-11-53.

De Vuyst, H., Clifford, G.M., Nascimento, M.C., Madeleine, M.M. & Franceschi, S. (2009). Prevalence and type distribution of human papillomavirus in carcinoma and intraepithelial neoplasia of the vulva, vagina and anus: a meta-analysis. *International Journal of Cancer,* 124(7), pp. 1626-1636.

Debbink, K., Lindesmith, L.C. & Baric, R.S. (2014). The state of norovirus vaccines. *Clinical Infectious Diseases,* 58(12), pp. 1746-1752.

Debbink, K., Lindesmith, L.C., Donaldson, E.F. & Baric, R.S. (2012). Norovirus immunity and the great escape. *PLOS Pathogens,* 8(10), pp. e1002921.

Delchambre, M., Gheysen, D., Thines, D., Thiriart, C., Jacobs, E., Verdin, E., Horth, M., Burny, A. & Bex, F. (1989). The GAG precursor of simian immunodeficiency virus assembles into virus-like particles. *The EMBO Journal,* 8(9), pp. 2653-2660.

Desmet, C.J. & Ishii, K.J. (2012). Nucleic acid sensing at the interface between innate and adaptive immunity in vaccination. *Nature Reviews Immunology,* 12(7), pp. 479-491.

Ding, F.X., Wang, F., Lu, Y.M., Li, K., Wang, K.H., He, X.W. & Sun, S.H. (2009). Multiepitope peptide-loaded virus-like particles as a vaccine against hepatitis B virus-related hepatocellular carcinoma. *Hepatology,* 49(5), pp. 1492-1502.

Donaldson, E.F., Lindesmith, L.C., Lobue, A.D. & Baric, R.S. (2010). Viral shape-shifting: norovirus evasion of the human immune system. *Nature Reviews. Microbiology,* 8(3), pp. 231-241.

Dorn, D.C., Lawatscheck, R., Zvirbliene, A., Aleksaite, E., Pecher, G., Sasnauskas, K., Ozel, M., Raftery, M., Schönrich, G., Ulrich, R.G. & Gedvilaite, A. (2008). Cellular and humoral immunogenicity of hamster polyomavirus-derived virus-like particles harboring a mucin 1 cytotoxic T-cell epitope. *Viral Immunology,* 21(1), pp. 12-27.

Dotzauer, A. & Kraemer, L. (2012). Innate and adaptive immune responses against picornaviruses and their counteractions: An overview. *World Journal of Virology,* 1(3), pp. 91-107.

Dunn, J.J., Bradrick, S.S., Chapman, N.M., Tracy, S.M. & Romero, J.R. (2003). The stem loop II within the 5' nontranslated region of clinical coxsackievirus B3 genomes determines cardiovirulence phenotype in a murine model. *The Journal of Infectious Diseases,* 187(10), pp. 1552-1561.

El-Kamary, S.S., Pasetti, M.F., Mendelman, P.M., Frey, S.E., Bernstein, D.I., Treanor, J.J., Ferreira, J., Chen, W.H., Sublett, R., Richardson, C., Bargatze, R.F., Sztein, M.B. & Tacket, C.O. (2010). Adjuvanted intranasal Norwalk virus-like particle vaccine elicits antibodies and antibody-secreting cells that express homing receptors for mucosal and peripheral lymphoid tissues. *The Journal of Infectious Diseases,* 202(11), pp. 1649-1658.

Eriksson, F., Tötterman, T., Maltais, A., Pisa, P. & Yachnin, J. (2013). DNA vaccine coding for the rhesus prostate specific antigen delivered by intradermal electroporation in patients with relapsed prostate cancer. *Vaccine,* 31(37), pp. 3843-3848.

Esfandiarei, M. & McManus, B.M. (2008). Molecular biology and pathogenesis of viral myocarditis. *Annual Review of Pathology,* 3, pp. 127-155.

Estes, M.K. (2004). Virus like particle (VLP) vaccines. *In New Generation Vaccines.* Levine, M.M. (Ed.), pp. 283-294. Academic Press, NY, USA.

European Medicines Agency, EMA. (2012). Guideline on the requirements for quality documentation concerning biological investigational medicinal products in clinical trials. EMA/CHMP/BWP/534898/2008. Available at: www.ema.europa.eu/ema/pages/includes/document/open_document.jsp?webContentId=WC500127370 (accessed 2015, 2/18).

Ezure, T., Suzuki, T., Shikata, M., Ito, M. & Ando, E. (2010). A cell-free protein synthesis system from insect cells. *Methods in Molecular Biology,* 607, pp. 31-42.

Fankhauser, R.L., Monroe, S.S., Noel, J.S., Humphrey, C.D., Bresee, J.S., Parashar, U.D., Ando, T. & Glass, R.I. (2002). Epidemiologic and molecular trends of "Norwalk-like viruses" associated with outbreaks of gastroenteritis in the United States. *The Journal of Infectious Diseases,* 186(1), pp. 1-7.

Ferraro, B., Morrow, M.P., Hutnick, N.A., Shin, T.H., Lucke, C.E. & Weiner, D.B. (2011). Clinical applications of DNA vaccines: current progress. *Clinical Infectious Diseases,* 53(3), pp. 296-302.

Feuer, R., Mena, I., Pagarigan, R.R., Harkins, S., Hassett, D.E. & Whitton, J.L. (2003). Coxsackievirus B3 and the neonatal CNS: the roles of stem cells, developing neurons, and apoptosis in infection, viral dissemination, and disease. *The American Journal of Pathology,* 163(4), pp. 1379-1393.

Fiers, W., De Filette, M., El Bakkouri, K., Schepens, B., Roose, K., Schotsaert, M., Birkett, A. & Saelens, X. (2009). M2e-based universal influenza A vaccine. *Vaccine,* 27(45), pp. 6280-6283.

Fifis, T., Gamvrellis, A., Crimeen-Irwin, B., Pietersz, G.A., Li, J., Mottram, P.L., McKenzie, I.F. & Plebanski, M. (2004). Size-dependent immunogenicity: therapeutic and protective properties of nano-vaccines against tumors. *Journal of Immunology,* 173(5), pp. 3148-3154.

Fohlman, J., Ilback, N.G., Friman, G. & Morein, B. (1990). Vaccination of Balb/c mice against enteroviral mediated myocarditis. *Vaccine,* 8(4), pp. 381-384.

Gaaloul, I., Riabi, S., Harrath, R., Hunter, T., Hamda, K.B., Ghzala, A.B., Huber, S. & Aouni, M. (2014). Coxsackievirus B detection in cases of myocarditis, myopericarditis, pericarditis and dilated cardiomyopathy in hospitalized patients. *Molecular Medicine Reports,* 10(6), pp. 2811-2818.

Garcea, R.L. & Gissmann, L. (2004). Virus-like particles as vaccines and vessels for the delivery of small molecules. *Current Opinion in Biotechnology,* 15(6), pp. 513-517.

Gastañaduy, P.A., Hall, A.J., Curns, A.T., Parashar, U.D. & Lopman, B.A. (2013). Burden of norovirus gastroenteritis in the ambulatory setting - United States, 2001-2009. *The Journal of Infectious Diseases,* 207(7), pp. 1058-1065.

Glass, R.I., Parashar, U.D. & Estes, M.K. (2009). Norovirus gastroenteritis. *The New England Journal of Medicine,* 361(18), pp. 1776-1785.

Godon, O., Fontaine, H., Kahi, S., Meritet, J., Scott-Algara, D., Pol, S., Michel, M. & Bourgine, M. (2014). Immunological and antiviral responses after therapeutic DNA immunization in chronic hepatitis B patients efficiently treated by analogues. *Molecular Therapy,* 22(3), pp. 675-684.

Goldman, M. & Lambert, P.H. (2004). Immunological safety of vaccines: facts hypothesis and allegations. *In Novel Vaccination Strategies.* Kaufmann, S.H.E. (Ed.), pp. 595-611. Wiley-VCH, Weinheim, Germany.

Goodridge, L., Goodridge, C., Wu, J., Griffiths, M. & Pawliszyn, J. (2004). Isoelectric point determination of norovirus virus-like particles by capillary isoelectric focusing with whole column imaging detection. *Analytical Chemistry,* 76(1), pp. 48-52.

Green, K.Y., Ando, T., Balayan, M.S., Berke, T., Clarke, I.N., Estes, M.K., Matson, D.O., Nakata, S., Neill, J.D., Studdert, M.J. & Thiel, H.J. (2000). Taxonomy of the caliciviruses. *The Journal of Infectious Diseases,* 181 Suppl 2, pp. S322-30.

Green, K.Y., Lew, J.F., Jiang, X., Kapikian, A.Z. & Estes, M.K. (1993). Comparison of the reactivities of baculovirus-expressed recombinant Norwalk virus capsid antigen with those of the native Norwalk virus antigen in serologic assays and some epidemiologic observations. *Journal of Clinical Microbiology,* 31(8), pp. 2185-2191.

Grgacic, E.V. & Anderson, D.A. (2006). Virus-like particles: passport to immune recognition. *Methods,* 40(1), pp. 60-65.

Grist, N.R. & Reid, D. (1997). Organisms in myocarditis/endocarditis viruses. *The Journal of Infection,* 34(2), pp. 155.

Gröner, A. (1986). Specificity and safety of baculoviruses. *In The Biology of Baculoviruses Vol. I: Practical Application for Insect Control.* Granados, R.R. & Federici, B.A. (Eds), pp. 177-202. CRC Press, Boca Raton, FL, USA.

Guerrero-Rodríguez, J., Manuel-Cabrera, C.A., Palomino-Hermosillo, Y.A., Delgado-Guzmán, P.G., Escoto-Delgadillo, M., Silva-Rosales, L., Herrera-Rodríguez, S.E., Sánchez-Hernández, C. & Gutiérrez-Ortega, A. (2014). Virus-like particles from escherichia coli-derived untagged papaya ringspot virus capsid protein purified by immobilized metal affinity chromatography enhance the antibody response against a soluble antigen. *Molecular Biotechnology,* 56(12), pp. 1110-1120.

Gurramkonda, C., Zahid, M., Nemani, S.K., Adnan, A., Gudi, S.K., Khanna, N., Ebensen, T., Lünsdorf, H., Guzmán, C.A. & Rinas, U. (2013). Purification of hepatitis B surface antigen virus-like particles from recombinant Pichia pastoris and in vivo analysis of their immunogenic properties. *Journal of Chromatography.B, Analytical Technologies in the Biomedical and Life Sciences,* 940, pp. 104-111.

Haarmann, C.M., Schwimmbeck, P.L., Mertens, T., Schultheiss, H.P. & Strauer, B.E. (1994). Identification of serotype-specific and nonserotype-specific B-cell epitopes of coxsackie B virus using synthetic peptides. *Virology,* 200(2), pp. 381-389.

Hamilton, S.R. & Gerngross, T.U. (2007). Glycosylation engineering in yeast: the advent of fully humanized yeast. *Current Opinion in Biotechnology,* 18(5), pp. 387-392.

Harper, D.M., Franco, E.L., Wheeler, C.M., Moscicki, A.B., Romanowski, B., Roteli-Martins, C.M., Jenkins, D., Schuind, A., Costa Clemens, S.A., Dubin, G. & HPV Vaccine Study group. (2006). Sustained efficacy up to 4.5 years of a bivalent L1 virus-like particle vaccine against human papillomavirus types 16 and 18: follow-up from a randomised control trial. *Lancet,* 367(9518), pp. 1247-1255.

Harrington, P.R., Lindesmith, L., Yount, B., Moe, C.L. & Baric, R.S. (2002). Binding of Norwalk virus-like particles to ABH histo-blood group antigens is blocked by antisera from infected human volunteers or experimentally vaccinated mice. *Journal of Virology,* 76(23), pp. 12335-12343.

Harrington, P.R., Vinjé, J., Moe, C.L. & Baric, R.S. (2004). Norovirus Capture with Histo-Blood Group Antigens Reveals Novel Virus-Ligand Interactions. *Journal of Virology,* 78(6), pp. 3035-3045.

Haynes, J.R., Cunningham, J., von Seefried, A., Lennick, M., Garvin, R.T. & Shen, S. (1986). Development of a Genetically-Engineered, Candidate Polio Vaccine Employing the Self-Assembling Properties of the Tobacco Mosaic Virus Coat Protein. *Nature Biotechnology,* 4(7), pp. 637-641.

Hellen, C.U. & Wimmer, E. (1992). Maturation of poliovirus capsid proteins. *Virology,* 187(2), pp. 391-397.

Henke, A., Wagner, E., Whitton, J.L., Zell, R. & Stelzner, A. (1998). Protection of mice against lethal coxsackievirus B3 infection by using DNA immunization. *Journal of Virology,* 72(10), pp. 8327-8331.

Herbst-Kralovetz, M., Mason, H.S. & Chen, Q. (2010). Norwalk virus-like particles as vaccines. *Expert Review of Vaccines,* 9(3), pp. 299-307.

Hertel, N.T., Pedersen, F.K. & Heilmann, C. (1989). Coxsackie B3 virus encephalitis in a patient with agammaglobulinaemia. *European Journal of Pediatrics,* 148(7), pp. 642-643.

Hinton, H.J., Jegerlehner, A. & Bachmann, M.F. (2008). Pattern recognition by B cells: the role of antigen repetitiveness versus Toll-like receptors. *Current Topics in Microbiology and Immunology,* 319, pp. 1-15.

Hochuli, E., Bannwarth, W., Döbeli, H., Gentz, R. & Stüber, D. (1988). Genetic Approach to Facilitate Purification of Recombinant Proteins with a Novel Metal Chelate Adsorbent. *Nature Biotechnology,* 6(11), pp. 1321-1325.

Hochuli, E., Döbeli, H. & Schacher, A. (1987). New metal chelate adsorbent selective for proteins and peptides containing neighbouring histidine residues. *Journal of Chromatography,* 411, pp. 177-184.

Huber, S. (2008). Host immune responses to coxsackievirus B3. *Current Topics in Microbiology and Immunology,* 323, pp. 199-221.

Huber, S., Polgar, J., Moraska, A., Cunningham, M., Schwimmbeck, P. & Schultheiss, P. (1993). T lymphocyte responses in CVB3-induced murine myocarditis. *Scandinavian Journal of Infectious Diseases.Supplementum,* 88, pp. 67-78.

Huhti, L., Blazevic, V., Nurminen, K., Koho, T., Hytönen, V.P. & Vesikari, T. (2010). A comparison of methods for purification and concentration of norovirus GII-4 capsid virus-like particles. *Archives of Virology,* 155(11), pp. 1855-1858.

Hutson, A.M., Atmar, R.L. & Estes, M.K. (2004). Norovirus disease: changing epidemiology and host susceptibility factors. *Trends in Microbiology,* 12(6), pp. 279-287.

International Committee on Taxonomy of Viruses, ICTV. (2013). Virus Taxonomy: 2013 Release, EC 45, Edinburgh. Available at: http://ictvonline.org/virusTaxonomy.asp (accessed 2015, 2/17).

Jackson, R.J. & Hunt, T. (1983). Preparation and use of nuclease-treated rabbit reticulocyte lysates for the translation of eukaryotic messenger RNA. *Methods in Enzymology,* 96, pp. 50-74.

Jarvis, D.L. (2003). Developing baculovirus-insect cell expression systems for humanized recombinant glycoprotein production. *Virology,* 310(1), pp. 1-7.

Jenner, E. (1798). An inquiry into the causes and effects of the variolae vaccinae: a disease discovered in some of the western counties of England, particularly Gloucestershire, and known by the name of the cow pox. *Published by the author. Printed for the author by Sampson Low,* London, UK.

Jennings, G.T. & Bachmann, M.F. (2009). Immunodrugs: therapeutic VLP-based vaccines for chronic diseases. *Annual Review of Pharmacology and Toxicology,* 49, pp. 303-326.

Jennings, G.T. & Bachmann, M.F. (2008). The coming of age of virus-like particle vaccines. *Biological Chemistry,* 389(5), pp. 521-536.

Jiang, X., Wang, M., Graham, D.Y. & Estes, M.K. (1992). Expression, self-assembly, and antigenicity of the Norwalk virus capsid protein. *Journal of Virology,* 66(11), pp. 6527-6532.

Jiang, X., Wang, M., Wang, K. & Estes, M.K. (1993). Sequence and genomic organization of Norwalk virus. *Virology,* 195(1), pp. 51-61.

Jones, S., Evans, K., McElwaine-Johnn, H., Sharpe, M., Oxford, J., Lambkin-Williams, R., Mant, T., Nolan, A., Zambon, M., Ellis, J., Beadle, J. & Loudon, P.T. (2009). DNA vaccination protects against an influenza challenge in a double-blind randomised placebo-controlled phase 1b clinical trial. *Vaccine,* 27(18), pp. 2506-2512.

Josefsberg, J.O. & Buckland, B. (2012). Vaccine process technology. *Biotechnology and Bioengineering,* 109(6), pp. 1443-1460.

Kalams, S.A., Parker, S.D., Elizaga, M., Metch, B., Edupuganti, S., Hural, J., De Rosa, S., Carter, D.K., Rybczyk, K., Frank, I., Fuchs, J., Koblin, B., Kim, D.H., Joseph, P., Keefer, M.C., Baden, L.R., Eldridge, J., Boyer, J., Sherwat, A., Cardinali, M., Allen, M., Pensiero, M., Butler, C., Khan, A.S., Yan, J., Sardesai, N.Y., Kublin, J.G., Weiner, D.B. & NIAID HIV Vaccine Trials Network. (2013). Safety and comparative

immunogenicity of an HIV-1 DNA vaccine in combination with plasmid interleukin 12 and impact of intramuscular electroporation for delivery. *The Journal of Infectious Diseases,* 208(5), pp. 818-829.

Kaltgrad, E., O'Reilly, M.K., Liao, L., Han, S., Paulson, J.C. & Finn, M.G. (2008). On-virus construction of polyvalent glycan ligands for cell-surface receptors. *Journal of the American Chemical Society,* 130(14), pp. 4578-4579.

Kapikian, A.Z., Wyatt, R.G., Dolin, R., Thornhill, T.S., Kalica, A.R. & Chanock, R.M. (1972). Visualization by immune electron microscopy of a 27-nm particle associated with acute infectious nonbacterial gastroenteritis. *Journal of Virology,* 10(5), pp. 1075-1081.

Kärkkäinen, H.R., Lesch, H.P., Määttä, A.I., Toivanen, P.I., Mähönen, A.J., Roschier, M.M., Airenne, K.J., Laitinen, O.H. & Ylä-Herttuala, S. (2009). A 96-well format for a high-throughput baculovirus generation, fast titering and recombinant protein production in insect and mammalian cells. *BMC Research Notes,* 2, pp. 63-0500-2-63.

Kemball, C.C., Alirezaei, M. & Whitton, J.L. (2010). Type B coxsackieviruses and their interactions with the innate and adaptive immune systems. *Future Microbiology,* 5(9), pp. 1329-1347.

Kemball, C.C., Harkins, S. & Whitton, J.L. (2008). Enumeration and functional evaluation of virus-specific CD4+ and CD8+ T cells in lymphoid and peripheral sites of coxsackievirus B3 infection. *Journal of Virology,* 82(9), pp. 4331-4342.

Kim, D.S. & Nam, J.H. (2011). Application of attenuated coxsackievirus B3 as a viral vector system for vaccines and gene therapy. *Human Vaccines,* 7(4), pp. 410-416.

Kim, J.Y., Jeon, E.S., Lim, B.K., Kim, S.M., Chung, S.K., Kim, J.M., Park, S.I., Jo, I. & Nam, J.H. (2005). Immunogenicity of a DNA vaccine for coxsackievirus B3 in mice: protective effects of capsid proteins against viral challenge. *Vaccine,* 23(14), pp. 1672-1679.

Klenerman, P., Cerundolo, V. & Dunbar, P.R. (2002). Tracking T cells with tetramers: new tales from new tools. *Nature Reviews.Immunology,* 2(4), pp. 263-272.

Klump, W.M., Bergmann, I., Muller, B.C., Ameis, D. & Kandolf, R. (1990). Complete nucleotide sequence of infectious Coxsackievirus B3 cDNA: two initial 5' uridine residues are regained during plus-strand RNA synthesis. *Journal of Virology,* 64(4), pp. 1573-1583.

Knowlton, K.U., Jeon, E.S., Berkley, N., Wessely, R. & Huber, S. (1996). A mutation in the puff region of VP2 attenuates the myocarditic phenotype of an infectious cDNA of the Woodruff variant of coxsackievirus B3. *Journal of Virology,* 70(11), pp. 7811-7818.

Kochetkov, S.N., Rusakova, E.E. & Tunitskaya, V.L. (1998). Recent studies of T7 RNA polymerase mechanism. *FEBS Letters,* 440(3), pp. 264-267.

Kong, Q., Richter, L., Yang, Y.F., Arntzen, C.J., Mason, H.S. & Thanavala, Y. (2001). Oral immunization with hepatitis B surface antigen expressed in transgenic plants. *Proceedings of the National Academy of Sciences of the United States of America,* 98(20), pp. 11539-11544.

Kost, T.A., Condreay, J.P. & Jarvis, D.L. (2005). Baculovirus as versatile vectors for protein expression in insect and mammalian cells. *Nature Biotechnology,* 23(5), pp. 567-575.

Kratz, P.A., Böttcher, B. & Nassal, M. (1999). Native display of complete foreign protein domains on the surface of hepatitis B virus capsids. *Proceedings of the National Academy of Sciences of the United States of America,* 96(5), pp. 1915-1920.

Kushnir, N., Streatfield, S.J. & Yusibov, V. (2012). Virus-like particles as a highly efficient vaccine platform: diversity of targets and production systems and advances in clinical development. *Vaccine,* 31(1), pp. 58-83.

Lacey, C.J., Lowndes, C.M. & Shah, K.V. (2006). Chapter 4: Burden and management of non-cancerous HPV-related conditions: HPV-6/11 disease. *Vaccine,* 24 Suppl 3, pp. S3/35-41.

Lapointe, R., Thumbi, D. & Lucarotti, C.J. (2012). Recent Advances in Our Knowledge of Baculovirus Molecular Biology and Its Relevance for the Registration of Baculovirus-Based Products for Insect Pest Population Control. *In Integrated Pest Management and Pest Control - Current and Future Tactics.* Soloneski, S. (Ed.), pp. 481-522. InTech, Europe.

Lata, S., Reichel, A., Brock, R., Tampé, R. & Piehler, J. (2005). High-affinity adaptors for switchable recognition of histidine-tagged proteins. *Journal of the American Chemical Society,* 127(29), pp. 10205-10215.

Latham, T. & Galarza, J.M. (2001). Formation of wild-type and chimeric influenza virus-like particles following simultaneous expression of only four structural proteins. *Journal of Virology,* 75(13), pp. 6154-6165.

Ledgerwood, J.E., Hu, Z., Gordon, I.J., Yamshchikov, G., Enama, M.E., Plummer, S., Bailer, R., Pearce, M.B., Tumpey, T.M., Koup, R.A., Mascola, J.R., Nabel, G.J., Graham, B.S. & VRC 304 and VRC 305 Study Teams. (2012). Influenza virus h5 DNA vaccination is immunogenic by intramuscular and intradermal routes in humans. *Clinical and Vaccine Immunology,* 19(11), pp. 1792-1797.

Lee, L.A., Niu, Z. & Wang, Q. (2009). Viruses and virus-like protein assemblies - Chemically programmable nanoscale building blocks. *Nano Research,* 2(5), pp. 349-364.

Liang, T.J. (2013). Current progress in development of hepatitis C virus vaccines. *Nature Medicine,* 19(7), pp. 869-878.

Liang, Z.L., Mao, Q.Y., Wang, Y.P., Zhu, F.C., Li, J.X., Yao, X., Gao, F., Wu, X., Xu, M. & Wang, J.Z. (2013). Progress on the research and development of inactivated EV71 whole-virus vaccines. *Human Vaccines & Immunotherapeutics,* 9(8), pp. 1701-1705.

Lin, J.Y., Chen, T.C., Weng, K.F., Chang, S.C., Chen, L.L. & Shih, S.R. (2009). Viral and host proteins involved in picornavirus life cycle. *Journal of Biomedical Science,* 16, pp. 103-117.

Lin, Y.L., Yu, C.I., Hu, Y.C., Tsai, T.J., Kuo, Y.C., Chi, W.K., Lin, A.N. & Chiang, B.L. (2012). Enterovirus type 71 neutralizing antibodies in the serum of macaque monkeys immunized with EV71 virus-like particles. *Vaccine,* 30(7), pp. 1305-1312.

Lindesmith, L., Moe, C., Marionneau, S., Ruvoen, N., Jiang, X., Lindblad, L., Stewart, P., LePendu, J. & Baric, R. (2003). Human susceptibility and resistance to Norwalk virus infection. *Nature Medicine,* 9(5), pp. 548-553.

Lindesmith, L.C., Donaldson, E.F., Lobue, A.D., Cannon, J.L., Zheng, D.P., Vinjé, J. & Baric, R.S. (2008). Mechanisms of GII.4 norovirus persistence in human populations. *PLOS Medicine,* 5(2), pp. e31.

Liu, F., Wu, X., Li, L., Liu, Z. & Wang, Z. (2013a). Use of baculovirus expression system for generation of virus-like particles: Successes and challenges. *Protein Expression and Purification,* 90(2), pp. 104-116.

Liu, Q., Huang, X., Ku, Z., Wang, T., Liu, F., Cai, Y., Li, D., Leng, Q. & Huang, Z. (2013b). Characterization of enterovirus 71 capsids using subunit protein-specific polyclonal antibodies. *Journal of Virological Methods,* 187(1), pp. 127-131.

Liu, Q., Yan, K., Feng, Y., Huang, X., Ku, Z., Cai, Y., Liu, F., Shi, J. & Huang, Z. (2012a). A virus-like particle vaccine for coxsackievirus A16 potently elicits neutralizing antibodies that protect mice against lethal challenge. *Vaccine,* 30(47), pp. 6642-6648.

Liu, W. & Chen, Y.H. (2005). High epitope density in a single protein molecule significantly enhances antigenicity as well as immunogenicity: a novel strategy for modern vaccine development and a preliminary investigation about B cell discrimination of monomeric proteins. *European Journal of Immunology,* 35(2), pp. 505-514.

Liu, Y., Wang, C., Mueller, S., Paul, A.V., Wimmer, E. & Jiang, P. (2010). Direct interaction between two viral proteins, the nonstructural protein 2C and the capsid protein VP3, is required for enterovirus morphogenesis. *PLOS Pathogens,* 6(8), pp. e1001066.

Liu, Z., Qiao, J., Niu, Z. & Wang, Q. (2012b). Natural supramolecular building blocks: from virus coat proteins to viral nanoparticles. *Chemical Society Reviews,* 41(18), pp. 6178-6194.

Lua, L.H.L., Connors, N.K., Sainsbury, F., Chuan, Y.P., Wibowo, N. & Middelberg, A.P.J. (2014). Bioengineering virus-like particles as vaccines. *Biotechnology and Bioengineering,* 111(3), pp. 425-440.

Ma, Y., Nolte, R.J. & Cornelissen, J.J. (2012). Virus-based nanocarriers for drug delivery. *Advanced Drug Delivery Reviews,* 64(9), pp. 811-825.

Maier, R., Krebs, P. & Ludewig, B. (2004). Immunopathological basis of virus-induced myocarditis. *Clinical & Developmental Immunology,* 11(1), pp. 1-5.

Makidon, P.E., Bielinska, A.U., Nigavekar, S.S., Janczak, K.W., Knowlton, J., Scott, A.J., Mank, N., Cao, Z., Rathinavelu, S., Beer, M.R., Wilkinson, J.E., Blanco, L.P., Landers, J.J. & Baker, J.R.,Jr. (2008). Pre-clinical evaluation of a novel nanoemulsion-based hepatitis B mucosal vaccine. *PLOS ONE,* 3(8), pp. e2954.

Malm, M., Uusi-Kerttula, H., Vesikari, T. & Blazevic, V. (2014). High serum levels of norovirus genotype-specific blocking antibodies correlate with protection from infection in children. *The Journal of Infectious Diseases,* 210(11), pp. 1755-1762.

Malvern Instruments. (2011). *Inform White Paper.*

Mao, C., Solis, D.J., Reiss, B.D., Kottmann, S.T., Sweeney, R.Y., Hayhurst, A., Georgiou, G., Iverson, B. & Belcher, A.M. (2004). Virus-based toolkit for the directed synthesis of magnetic and semiconducting nanowires. *Science,* 303(5655), pp. 213-217.

Mason, H.S., Ball, J.M., Shi, J.J., Jiang, X., Estes, M.K. & Arntzen, C.J. (1996). Expression of Norwalk virus capsid protein in transgenic tobacco and potato and its oral immunogenicity in mice. *Proceedings of the National Academy of Sciences of the United States of America,* 93(11), pp. 5335-5340.

McCallus, D.E., Pachuk, C.J., Lee, S. & Satishchandran, C. (2001). DNA Vaccines. *In New Vaccine Technologies.* Ellis, R.W. (Ed.), pp. 240-262. Eurekah.com/ Landes Bioscience, USA.

McLean, H.Q., Fiebelkorn, A.P., Temte, J.L., Wallace, G.S. & Centers for Disease Control and Prevention. (2013). Prevention of measles, rubella, congenital rubella syndrome, and mumps, 2013: summary recommendations of the Advisory Committee on Immunization Practices (ACIP). *Morbidity and Mortality Weekly Report. Recommendations and Reports / Centers for Disease Control,* 62(RR-04), pp. 1-34.

McMinn, P.C. (2012). Recent advances in the molecular epidemiology and control of human enterovirus 71 infection. *Current Opinion in Virology,* 2(2), pp. 199-205.

Melnick, J.L. (1996). Enteroviruses: polioviruses, coxsackieviruses, echoviruses and newer enteroviruses. *In Fields Virology.* Fields, B.N., Knipe, D.M., Howley, P.M., Channock,

R.M., Melnick, J.L., Monath, T.P., Roizman, B. & Straus, S.E. (Eds), 3rd edition, pp. 655–712. Lippincott-Raven Publishers, Philadelphia, PA, USA.

Mena, I., Fischer, C., Gebhard, J.R., Perry, C.M., Harkins, S. & Whitton, J.L. (2000). Coxsackievirus infection of the pancreas: evaluation of receptor expression, pathogenesis, and immunopathology. *Virology,* 271(2), pp. 276-288.

Mena, I., Perry, C.M., Harkins, S., Rodriguez, F., Gebhard, J. & Whitton, J.L. (1999). The role of B lymphocytes in coxsackievirus B3 infection. *The American Journal of Pathology,* 155(4), pp. 1205-1215.

Meyer, R.G., Meyer-Ficca, M.L., Kaiser, H., Selinka, H.C., Kandolf, R. & Küpper, J.H. (2004). Plasmid-based generation of recombinant coxsackievirus B3 particles carrying capsid gene replacement replicons. *Virus Research,* 104(1), pp. 17-26.

Misbah, S.A., Spickett, G.P., Ryba, P.C., Hockaday, J.M., Kroll, J.S., Sherwood, C., Kurtz, J.B., Moxon, E.R. & Chapel, H.M. (1992). Chronic enteroviral meningoencephalitis in agammaglobulinemia: case report and literature review. *Journal of Clinical Immunology,* 12(4), pp. 266-270.

Morenweiser, R. (2005). Downstream processing of viral vectors and vaccines. *Gene Therapy,* 12(Suppl 1), pp. S103-10.

Muckelbauer, J.K., Kremer, M., Minor, I., Diana, G., Dutko, F.J., Groarke, J., Pevear, D.C. & Rossmann, M.G. (1995). The structure of coxsackievirus B3 at 3.5 A resolution. *Structure,* 3(7), pp. 653-667.

Mulligan, M.J., Russell, N.D., Celum, C., Kahn, J., Noonan, E., Montefiori, D.C., Ferrari, G., Weinhold, K.J., Smith, J.M., Amara, R.R., Robinson, H.L. & NIH/NIAID/DAIDS HIV Vaccine Trials Network. (2006). Excellent safety and tolerability of the human immunodeficiency virus type 1 pGA2/JS2 plasmid DNA priming vector vaccine in HIV type 1 uninfected adults. *AIDS Research and Human Retroviruses,* 22(7), pp. 678-683.

Murphy, T.V., Gargiullo, P.M., Massoudi, M.S., Nelson, D.B., Jumaan, A.O., Okoro, C.A., Zanardi, L.R., Setia, S., Fair, E., LeBaron, C.W., Wharton, M., Livengood, J.R. & Rotavirus Intussusception Investigation Team. (2001). Intussusception among infants given an oral rotavirus vaccine. *The New England Journal of Medicine,* 344(8), pp. 564-572.

Newman, M., Chua, P.K., Tang, F.M., Su, P.Y. & Shih, C. (2009). Testing an electrostatic interaction hypothesis of hepatitis B virus capsid stability by using an in vitro capsid disassembly/reassembly system. *Journal of Virology,* 83(20), pp. 10616-10626.

Ng, B.C., Chan, S.T., Lin, J. & Tolbert, S.H. (2011). Using Polymer Conformation to Control Architecture in Semiconducting Polymer/Viral Capsid Assemblies. *ACS Nano,* 5(10), pp. 7730-7738.

Noad, R. & Roy, P. (2003). Virus-like particles as immunogens. *Trends in Microbiology,* 11(9), pp. 438-444.

Noel, J.S., Fankhauser, R.L., Ando, T., Monroe, S.S. & Glass, R.I. (1999). Identification of a distinct common strain of "Norwalk-like viruses" having a global distribution. *The Journal of Infectious Diseases,* 179(6), pp. 1334-1344.

Ou, X., Guo, L., Wu, J., Mi, K., Yin, N., Zhang, G., Li, H. & Sun, M. (2013). Construction, expression and immunogenicity of a novel anti-hypertension angiotensin II vaccine based on hepatitis A virus-like particle. *Human Vaccines & Immunotherapeutics,* 9(6), pp. 1191-1199.

Pallansch, M.A. & Roos, R.P. (2001). Enteroviruses: polioviruses, coxsackieviruses, echoviruses and newer enteroviruses. *In Fields Virology.* Knipe, D.M., Howley, P.M.,

Griffin, D.E., Lamb, R.A., Martin, M.A., Roizman, B. & Straus, S.E. (Eds), 4th edition, pp. 723–775. Lippincot Williams & Wilkins, Philadelphia.

Park, J.H., Kim, D.S., Cho, Y.J., Kim, Y.J., Jeong, S.Y., Lee, S.M., Cho, S.J., Yun, C.W., Jo, I. & Nam, J.H. (2009). Attenuation of coxsackievirus B3 by VP2 mutation and its application as a vaccine against virus-induced myocarditis and pancreatitis. *Vaccine,* 27(13), pp. 1974-1983.

Park, M.A., Kim, H.J. & Kim, H.J. (2008). Optimum conditions for production and purification of human papillomavirus type 16 L1 protein from Saccharomyces cerevisiae. *Protein Expression and Purification,* 59(1), pp. 175-181.

Parra, G.I., Bok, K., Taylor, R., Haynes, J.R., Sosnovtsev, S.V., Richardson, C. & Green, K.Y. (2012). Immunogenicity and specificity of norovirus Consensus GII.4 virus-like particles in monovalent and bivalent vaccine formulations. *Vaccine,* 30(24), pp. 3580-3586.

Patel, M.M., Hall, A.J., Vinjé, J. & Parashar, U.D. (2009). Noroviruses: a comprehensive review. *Journal of Clinical Virology,* 44(1), pp. 1-8.

Pattenden, L.K., Middelberg, A.P., Niebert, M. & Lipin, D.I. (2005). Towards the preparative and large-scale precision manufacture of virus-like particles. *Trends in Biotechnology,* 23(10), pp. 523-529.

Paumier, G., Ronan, P., NIH, Fijałkowski, A. J., Walker, J., Jones, M. D., Heal, T., Ruiz, M., Science Primer (National Center for Biotechnology Information), Liquid_2003, Nordmann, A. & The Tango! Desktop Project. (2009). Available at: http://en.wikipedia.org/wiki/File:Biological_and_technological_scales_compared-en.svg (accessed 2015, 3/4).

Pejawar-Gaddy, S., Rajawat, Y., Hilioti, Z., Xue, J., Gaddy, D.F., Finn, O.J., Viscidi, R.P. & Bossis, I. (2010). Generation of a tumor vaccine candidate based on conjugation of a MUC1 peptide to polyionic papillomavirus virus-like particles. *Cancer Immunology, Immunotherapy,* 59(11), pp. 1685-1696.

Pizza, M., Scarlato, V., Masignani, V., Giuliani, M.M., Aricò, B., Comanducci, M., Jennings, G.T., Baldi, L., Bartolini, E., Capecchi, B., Galeotti, C.L., Luzzi, E., Manetti, R., Marchetti, E., Mora, M., Nuti, S., Ratti, G., Santini, L., Savino, S., Scarselli, M., Storni, E., Zuo, P., Broeker, M., Hundt, E., Knapp, B., Blair, E., Mason, T., Tettelin, H., Hood, D.W., Jeffries, A.C., Saunders, N.J., Granoff, D.M., Venter, J.C., Moxon, E.R., Grandi, G. & Rappuoli, R. (2000). Identification of vaccine candidates against serogroup B meningococcus by whole-genome sequencing. *Science,* 287(5459), pp. 1816-1820.

Plotkin, S.A. (2005). Vaccines: past, present and future. *Nature Medicine,* Apr;11(4 Suppl), pp. S5-11.

Pniewski, T., Kapusta, J., Bociąg, P., Wojciechowicz, J., Kostrzak, A., Gdula, M., Fedorowicz-Strońska, O., Wójcik, P., Otta, H., Samardakiewicz, S., Wolko, B. & Płucienniczak, A. (2011). Low-dose oral immunization with lyophilized tissue of herbicide-resistant lettuce expressing hepatitis B surface antigen for prototype plant-derived vaccine tablet formulation. *Journal of Applied Genetics,* 52(2), pp. 125-136.

Porter, D.C., Ansardi, D.C. & Morrow, C.D. (1995). Encapsidation of poliovirus replicons encoding the complete human immunodeficiency virus type 1 gag gene by using a complementation system which provides the P1 capsid protein in trans. *Journal of Virology,* 69(3), pp. 1548-1555.

Porter, D.C., Ansardi, D.C., Wang, J., McPherson, S., Moldoveanu, Z. & Morrow, C.D. (1998). Demonstration of the specificity of poliovirus encapsidation using a novel

replicon which encodes enzymatically active firefly luciferase. *Virology,* 243(1), pp. 1-11.

Prasad, B.V., Hardy, M.E., Dokland, T., Bella, J., Rossmann, M.G. & Estes, M.K. (1999). X-ray crystallographic structure of the Norwalk virus capsid. *Science,* 286(5438), pp. 287-290.

Prasad, B.V., Hardy, M.E. & Estes, M.K. (2000). Structural studies of recombinant Norwalk capsids. *The Journal of Infectious Diseases,* 181 Suppl 2, pp. S317-21.

Prasad, B.V., Rothnagel, R., Jiang, X. & Estes, M.K. (1994). Three-dimensional structure of baculovirus-expressed Norwalk virus capsids. *Journal of Virology,* 68(8), pp. 5117-5125.

Pushko, P., Pumpens, P. & Grens, E. (2013). Development of virus-like particle technology from small highly symmetric to large complex virus-like particle structures. *Intervirology,* 56(3), pp. 141-165.

Pushko, P., Tumpey, T.M., Bu, F., Knell, J., Robinson, R. & Smith, G. (2005). Influenza virus-like particles comprised of the HA, NA, and M1 proteins of H9N2 influenza virus induce protective immune responses in BALB/c mice. *Vaccine,* 23(50), pp. 5751-5759.

Racaniello, V.R. (2007). *Picornaviridae*: the viruses and their replication. *In Fields virology.* Knipe, D.M., Howley, P.M., Griffin, D.E., Lamb, R.A., Martin, M.A., Roizman, B. & Straus, S.E. (Eds), 5th edition, pp. 795-838. Lippincott Williams & Wilkins, Philadelphia, PA.

Ramirez, K., Wahid, R., Richardson, C., Bargatze, R.F., El-Kamary, S.S., Sztein, M.B. & Pasetti, M.F. (2012). Intranasal vaccination with an adjuvanted Norwalk virus-like particle vaccine elicits antigen-specific B memory responses in human adult volunteers. *Clinical Immunology,* 144(2), pp. 98-108.

Rappuoli, R. (2000). Reverse vaccinology. *Current Opinion in Microbiology,* 3(5), pp. 445-450.

Rappuoli, R. (2009). Foreword. *In Vaccines for Biodefense and Emerging and Neglected Diseases.* Barrett, A.D.T. & Stanberry, L.R. (Eds), pp. xix-xxi. Academic Press, London, UK.

Rerks-Ngarm, S., Pitisuttithum, P., Nitayaphan, S., Kaewkungwal, J., Chiu, J., Paris, R., Premsri, N., Namwat, C., de Souza, M., Adams, E., Benenson, M., Gurunathan, S., Tartaglia, J., McNeil, J.G., Francis, D.P., Stablein, D., Birx, D.L., Chunsuttiwat, S., Khamboonruang, C., Thongcharoen, P., Robb, M.L., Michael, N.L., Kunasol, P., Kim, J.H. & MOPH-TAVEG Investigators. (2009). Vaccination with ALVAC and AIDSVAX to prevent HIV-1 infection in Thailand. *The New England Journal of Medicine,* 361(23), pp. 2209-2220.

Roche, S., Rey, F.A., Gaudin, Y. & Bressanelli, S. (2007). Structure of the prefusion form of the vesicular stomatitis virus glycoprotein G. *Science,* 315(5813), pp. 843-848.

Rockx, B., Baric, R.S., de Grijs, I., Duizer, E. & Koopmans, M.P. (2005). Characterization of the homo- and heterotypic immune responses after natural norovirus infection. *Journal of Medical Virology,* 77(3), pp. 439-446.

Rodríguez-Limas, W.A., Sekar, K. & Tyo, K.E. (2013). Virus-like particles: the future of microbial factories and cell-free systems as platforms for vaccine development. *Current Opinion in Biotechnology,* 24(6), pp. 1089-1093.

Roivainen, M., Knip, M., Hyöty, H., Kulmala, P., Hiltunen, M., Vähäsalo, P., Hovi, T. & Åkerblom, H.K. (1998). Several different enterovirus serotypes can be associated with prediabetic autoimmune episodes and onset of overt IDDM. Childhood Diabetes in Finland (DiMe) Study Group. *Journal of Medical Virology,* 56(1), pp. 74-78.

Roldão, A., Mellado, M.C., Castilho, L.R., Carrondo, M.J. & Alves, P.M. (2010). Virus-like particles in vaccine development. *Expert Review of Vaccines,* 9(10), pp. 1149-1176.

Rolland, D., Gauthier, M., Dugua, J.M., Fournier, C., Delpech, L., Watelet, B., Letourneur, O., Arnaud, M. & Jolivet, M. (2001). Purification of recombinant HBc antigen expressed in Escherichia coli and Pichia pastoris: comparison of size-exclusion chromatography and ultracentrifugation. *Journal of Chromatography.B, Biomedical Sciences and Applications,* 753(1), pp. 51-65.

Roy, P. & Noad, R. (2008). Virus-like particles as a vaccine delivery system: myths and facts. *Human Vaccines,* 4(1), pp. 5-12.

RTS-S Clinical Trials Partnership. (2014). Efficacy and safety of the RTS,S/AS01 malaria vaccine during 18 months after vaccination: a phase 3 randomized, controlled trial in children and young infants at 11 African sites. *PLOS Medicine,* 11(7), pp. e1001685.

Rueda, P., Hurtado, A., del Barrio, M., Martínez-Torrecuadrada, J.L., Kamstrup, S., Leclerc, C. & Casal, J.I. (1999). Minor displacements in the insertion site provoke major differences in the induction of antibody responses by chimeric parvovirus-like particles. *Virology,* 263(1), pp. 89-99.

Russell, B.J., Velez, J.O., Laven, J.J., Johnson, A.J., Chang, G.J. & Johnson, B.W. (2007). A comparison of concentration methods applied to non-infectious flavivirus recombinant antigens for use in diagnostic serological assays. *Journal of Virological Methods,* 145(1), pp. 62-70.

Santi, L., Batchelor, L., Huang, Z., Hjelm, B., Kilbourne, J., Arntzen, C.J., Chen, Q. & Mason, H.S. (2008). An efficient plant viral expression system generating orally immunogenic Norwalk virus-like particles. *Vaccine,* 26(15), pp. 1846-1854.

Schiller, J.T., Castellsagué, X., Villa, L.L. & Hildesheim, A. (2008). An update of prophylactic human papillomavirus L1 virus-like particle vaccine clinical trial results. *Vaccine,* 26 Suppl 10, pp. K53-61.

Scott, M.D. & Murad, K.L. (1998). Cellular camouflage: fooling the immune system with polymers. *Current Pharmaceutical Design,* 4(6), pp. 423-438.

See, D.M. & Tilles, J.G. (1994). Efficacy of a polyvalent inactivated-virus vaccine in protecting mice from infection with clinical strains of group B coxsackieviruses. *Scandinavian Journal of Infectious Diseases,* 26(6), pp. 739-747.

Selinka, H.C., Wolde, A., Sauter, M., Kandolf, R. & Klingel, K. (2004). Virus-receptor interactions of coxsackie B viruses and their putative influence on cardiotropism. *Medical Microbiology and Immunology,* 193(2-3), pp. 127-131.

Semler, B. & Wimmer, E. (Eds). (2002). Molecular biology of picornaviruses. ASM Press, Washington D.C., USA.

Shevchenko, A., Wilm, M., Vorm, O. & Mann, M. (1996). Mass spectrometric sequencing of proteins silver-stained polyacrylamide gels. *Analytical Chemistry,* 68(5), pp. 850-858.

Siebenga, J.J., Vennema, H., Renckens, B., de Bruin, E., van der Veer, B., Siezen, R.J. & Koopmans, M. (2007). Epochal evolution of GGII.4 norovirus capsid proteins from 1995 to 2006. *Journal of Virology,* 81(18), pp. 9932-9941.

Siebenga, J.J., Vennema, H., Zheng, D.P., Vinjé, J., Lee, B.E., Pang, X.L., Ho, E.C., Lim, W., Choudekar, A., Broor, S., Halperin, T., Rasool, N.B., Hewitt, J., Greening, G.E., Jin, M., Duan, Z.J., Lucero, Y., O'Ryan, M., Hoehne, M., Schreier, E., Ratcliff, R.M., White, P.A., Iritani, N., Reuter, G. & Koopmans, M. (2009). Norovirus illness is a global problem: emergence and spread of norovirus GII.4 variants, 2001-2007. *The Journal of Infectious Diseases,* 200(5), pp. 802-812.

Slifka, M.K., Pagarigan, R., Mena, I., Feuer, R. & Whitton, J.L. (2001). Using recombinant coxsackievirus B3 to evaluate the induction and protective efficacy of CD8+ T cells during picornavirus infection. *Journal of Virology,* 75(5), pp. 2377-2387.

Smith, G.E., Fraser, M.J. & Summers, M.D. (1983). Molecular Engineering of the Autographa californica Nuclear Polyhedrosis Virus Genome: Deletion Mutations Within the Polyhedrin Gene. *Journal of Virology,* 46(2), pp. 584-593.

Smith, M.T., Varner, C.T., Bush, D.B. & Bundy, B.C. (2012). The incorporation of the A2 protein to produce novel Qbeta virus-like particles using cell-free protein synthesis. *Biotechnology Progress,* 28(2), pp. 549-555.

Sokolenko, S., George, S., Wagner, A., Tuladhar, A., Andrich, J.M. & Aucoin, M.G. (2012). Co-expression vs. co-infection using baculovirus expression vectors in insect cell culture: Benefits and drawbacks. *Biotechnology Advances,* 30(3), pp. 766-781.

Solomon, T., Lewthwaite, P., Perera, D., Cardosa, M.J., McMinn, P. & Ooi, M.H. (2010). Virology, epidemiology, pathogenesis, and control of enterovirus 71. *The Lancet Infectious Diseases,* 10(11), pp. 778-790.

Spohn, G., Keller, I., Beck, M., Grest, P., Jennings, G.T. & Bachmann, M.F. (2008). Active immunization with IL-1 displayed on virus-like particles protects from autoimmune arthritis. *European Journal of Immunology,* 38(3), pp. 877-887.

Sprent, J. (1997). Immunological memory. *Current Opinion in Immunology,* 9(3), pp. 371-379.

Stadnick, E., Dan, M., Sadeghi, A. & Chantler, J.K. (2004). Attenuating mutations in coxsackievirus B3 map to a conformational epitope that comprises the puff region of VP2 and the knob of VP3. *Journal of Virology,* 78(24), pp. 13987-14002.

Storni, T., Ruedl, C., Schwarz, K., Schwendener, R.A., Renner, W.A. & Bachmann, M.F. (2004). Nonmethylated CG motifs packaged into virus-like particles induce protective cytotoxic T cell responses in the absence of systemic side effects. *Journal of Immunology,* 172(3), pp. 1777-1785.

Strable, E. & Finn, M.G. (2009). Chemical modification of viruses and virus-like particles. *Current Topics in Microbiology and Immunology,* 327, pp. 1-21.

Takahashi, H., Pool, V., Tsai, T.F. & Chen, R.T. (2000). Adverse events after Japanese encephalitis vaccination: review of post-marketing surveillance data from Japan and the United States. *Vaccine,* 18(26), pp. 2963-2969.

Takai, K., Sawasaki, T. & Endo, Y. (2008). Development of Key Technologies for High-Throughput Cell-Free Protein Production with the Extract from Wheat Embryos. *Advances in Protein Chemistry and Structural Biology,* 75, pp. 53-84.

Tamminen, K., Huhti, L., Koho, T., Lappalainen, S., Hytönen, V.P., Vesikari, T. & Blazevic, V. (2012). A comparison of immunogenicity of norovirus GII-4 virus-like particles and P-particles. *Immunology,* 135(1), pp. 89-99.

Tamminen, K., Lappalainen, S., Huhti, L., Vesikari, T. & Blazevic, V. (2013). Trivalent combination vaccine induces broad heterologous immune responses to norovirus and rotavirus in mice. *PLOS ONE,* 8(7), pp. e70409.

Tan, M., Fang, P., Chachiyo, T., Xia, M., Huang, P., Fang, Z., Jiang, W. & Jiang, X. (2008). Noroviral P particle: structure, function and applications in virus-host interaction. *Virology,* 382(1), pp. 115-123.

Tan, M. & Jiang, X. (2012a). Norovirus P particle: a subviral nanoparticle for vaccine development against norovirus, rotavirus and influenza virus. *Nanomedicine,* 7(6), pp. 889-897.

Tan, M. & Jiang, X. (2005a). Norovirus and its histo-blood group antigen receptors: an answer to a historical puzzle. *Trends in Microbiology,* 13(6), pp. 285-293.

Tan, M. & Jiang, X. (2005b). The p domain of norovirus capsid protein forms a subviral particle that binds to histo-blood group antigen receptors. *Journal of Virology,* 79(22), pp. 14017-14030.

Tan, M., Zhong, W., Song, D., Thornton, S. & Jiang, X. (2004). E. coli-expressed recombinant norovirus capsid proteins maintain authentic antigenicity and receptor binding capability. *Journal of Medical Virology,* 74(4), pp. 641-649.

Tan, M. & Jiang, X. (2012b). The formation of P particle increased immunogenicity of norovirus P protein. *Immunology,* 136(1), pp. 28-29.

Tan, M., Xia, M., Huang, P., Wang, L., Zhong, W., McNeal, M., Wei, C. & Jiang, X. (2011). Norovirus P Particle as a Platform for Antigen Presentation. *Procedia in Vaccinology,* 4(0), pp. 19-26.

Tatman, J.D., Preston, V.G., Nicholson, P., Elliott, R.M. & Rixon, F.J. (1994). Assembly of herpes simplex virus type 1 capsids using a panel of recombinant baculoviruses. *The Journal of General Virology,* 75(Pt 5), pp. 1101-1113.

Taube, S., Kurth, A. & Schreier, E. (2005). Generation of recombinant norovirus-like particles (VLP) in the human endothelial kidney cell line 293T. *Archives of Virology,* 150(7), pp. 1425-1431.

Thara, E., Dorff, T.B., Pinski, J.K. & Quinn, D.I. (2011). Vaccine therapy with sipuleucel-T (Provenge) for prostate cancer. *Maturitas,* 69(4), pp. 296-303.

Tiriveedhi, V., Fleming, T.P., Goedegebuure, P.S., Naughton, M., Ma, C., Lockhart, C., Gao, F., Gillanders, W.E. & Mohanakumar, T. (2013). Mammaglobin-A cDNA vaccination of breast cancer patients induces antigen-specific cytotoxic CD4+ICOShi T cells. *Breast Cancer Research and Treatment,* 138(1), pp. 109-118.

Tissot, A.C., Maurer, P., Nussberger, J., Sabat, R., Pfister, T., Ignatenko, S., Volk, H., Stocker, H., Müller, P., Jennings, G.T., Wagner, F. & Bachmann, M.F. (2008). Effect of immunisation against angiotensin II with CYT006-AngQb on ambulatory blood pressure: a double-blind, randomised, placebo-controlled phase IIa study. *The Lancet,* 371(9615), pp. 821-827.

Treanor, J.J., Atmar, R.L., Frey, S.E., Gormley, R., Chen, W.H., Ferreira, J., Goodwin, R., Borkowski, A., Clemens, R. & Mendelman, P.M. (2014). A novel intramuscular bivalent norovirus virus-like particle vaccine candidate--reactogenicity, safety, and immunogenicity in a phase 1 trial in healthy adults. *The Journal of Infectious Diseases,* 210(11), pp. 1763-1771.

Trilisky, E.I., Koku, H., Czymmek, K.J. & Lenhoff, A.M. (2009). Relation of structure to performance characteristics of monolithic and perfusive stationary phases. *Journal of Chromatography.A,* 1216(36), pp. 6365-6376.

Trilisky, E.I. & Lenhoff, A.M. (2009). Flow-dependent entrapment of large bioparticles in porous process media. *Biotechnology and Bioengineering,* 104(1), pp. 127-133.

Tsoka, S., Ciniawskyj, O.C., Thomas, O.R., Titchener-Hooker, N.J. & Hoare, M. (2000). Selective flocculation and precipitation for the improvement of virus-like particle recovery from yeast homogenate. *Biotechnology Progress,* 16(4), pp. 661-667.

Tu, E.T., Bull, R.A., Greening, G.E., Hewitt, J., Lyon, M.J., Marshall, J.A., McIver, C.J., Rawlinson, W.D. & White, P.A. (2008). Epidemics of gastroenteritis during 2006 were associated with the spread of norovirus GII.4 variants 2006a and 2006b. *Clinical Infectious Diseases,* 46(3), pp. 413-420.

Tu, Z., Chapman, N.M., Hufnagel, G., Tracy, S., Romero, J.R., Barry, W.H., Zhao, L., Currey, K. & Shapiro, B. (1995). The cardiovirulent phenotype of coxsackievirus B3 is determined at a single site in the genomic 5' nontranslated region. *Journal of Virology,* 69(8), pp. 4607-4618.

U.S. Food and Drug Administration, FDA. (2014). Approval Letter. Gardasil 9. Available at: http://www.fda.gov/BiologicsBloodVaccines/Vaccines/ApprovedProducts/ucm

426520.htm (accessed 2015, 4/13).
U.S. Food and Drug Administration, FDA. (2010). Guidelines for Industry. Characterization and qualification of cell substrate and other biological materials used in the production of viral vaccines for infectious disease indications. Available at: http://www.fda.gov/downloads/biologicsbloodvaccines/guidancecomplianceregulatoryinformation/guidances/vaccines/ucm202439.pdf (accessed 2015, 2/18).
U.S. Food and Drug Administration, FDA. (2001). Approval Letter. Twinrix. Available at: http://www.fda.gov/BiologicsBloodVaccines/Vaccines/ApprovedProducts/ucm110085.htm (accessed 2015, 2/17).
U.S. National Cancer Institute, NCI. (2011). Cancer Vaccines. Fact Sheet. Available at: http://www.cancer.gov/cancertopics/factsheet/Therapy/cancer-vaccines (accessed 2015, 2/16).
U.S. National Institutes of Health, NIH. (2014). ClinicalTrials.gov. Safety and Immunogenicity of Plant-Derived Pfs25 VLP-FhCMB Malaria Transmission Blocking Vaccine in Healthy Adults. Available at: https://clinicaltrials.gov/show/NCT02013687 (accessed 2015, 2/17).
Uusi-Kerttula, H., Tamminen, K., Malm, M., Vesikari, T. & Blazevic, V. (2014). Comparison of human saliva and synthetic histo-blood group antigens usage as ligands in norovirus-like particle binding and blocking assays. *Microbes and Infection,* 16(6), pp. 472-480.
Valenzuela, P., Medina, A., Rutter, W.J., Ammerer, G. & Hall, B.D. (1982). Synthesis and assembly of hepatitis B virus surface antigen particles in yeast. *Nature,* 298(5872), pp. 347-350.
van Oers, M.M., Pijlman, G.P. & Vlak, J.M. (2015). Thirty years of baculovirus-insect cell protein expression: from dark horse to mainstream technology. *The Journal of General Virology,* 96(Pt 1), pp. 6-23.
Vasan, S., Hurley, A., Schlesinger, S.J., Hannaman, D., Gardiner, D.F., Dugin, D.P., Boente-Carrera, M., Vittorino, R., Caskey, M., Andersen, J., Huang, Y., Cox, J.H., Tarragona-Fiol, T., Gill, D.K., Cheeseman, H., Clark, L., Dally, L., Smith, C., Schmidt, C., Park, H.H., Kopycinski, J.T., Gilmour, J., Fast, P., Bernard, R. & Ho, D.D. (2011). In vivo electroporation enhances the immunogenicity of an HIV-1 DNA vaccine candidate in healthy volunteers. *PLOS ONE,* 6(5), pp. e19252.
Vicente, T., Roldão, A., Peixoto, C., Carrondo, M.J. & Alves, P.M. (2011). Large-scale production and purification of VLP-based vaccines. *Journal of Invertebrate Pathology,* 107 Suppl, pp. S42-8.
Voigt, A., Jäkel, S., Textoris-Taube, K., Keller, C., Drung, I., Szalay, G., Klingel, K., Henklein, P., Stangl, K., Kloetzel, P.M. & Kuckelkorn, U. (2010). Generation of in silico predicted coxsackievirus B3-derived MHC class I epitopes by proteasomes. *Amino Acids,* 39(1), pp. 243-255.
Wang, Q., Lin, T., Tang, L., Johnson, J.E. & Finn, M.G. (2002). Icosahedral virus particles as addressable nanoscale building blocks. *Angewandte Chemie (International Ed.in English),* 41(3), pp. 459-462.
Wang, X., Liu, J., Zheng, Y., Li, J., Wang, H., Zhou, Y., Qi, M., Yu, H., Tang, W. & Zhao, W.M. (2008). An optimized yeast cell-free system: sufficient for translation of human papillomavirus 58 L1 mRNA and assembly of virus-like particles. *Journal of Bioscience and Bioengineering,* 106(1), pp. 8-15.
Weinzierl, A.O., Rudolf, D., Maurer, D., Wernet, D., Rammensee, H.G., Stevanović, S. & Klingel, K. (2008). Identification of HLA-A*01- and HLA-A*02-restricted CD8+ T-

cell epitopes shared among group B enteroviruses. *The Journal of General Virology,* 89(Pt 9), pp. 2090-2097.

White, L.J., Hardy, M.E. & Estes, M.K. (1997). Biochemical characterization of a smaller form of recombinant Norwalk virus capsids assembled in insect cells. *Journal of Virology,* 71(10), pp. 8066-8072.

Wiessner, C., Wiederhold, K.H., Tissot, A.C., Frey, P., Danner, S., Jacobson, L.H., Jennings, G.T., Lüönd, R., Ortmann, R., Reichwald, J., Zurini, M., Mir, A., Bachmann, M.F. & Staufenbiel, M. (2011). The second-generation active Abeta immunotherapy CAD106 reduces amyloid accumulation in APP transgenic mice while minimizing potential side effects. *The Journal of Neuroscience,* 31(25), pp. 9323-9331.

Winblad, B., Andreasen, N., Minthon, L., Floesser, A., Imbert, G., Dumortier, T., Maguire, R.P., Blennow, K., Lundmark, J., Staufenbiel, M., Orgogozo, J.M. & Graf, A. (2012). Safety, tolerability, and antibody response of active Abeta immunotherapy with CAD106 in patients with Alzheimer's disease: randomised, double-blind, placebo-controlled, first-in-human study. *The Lancet Neurology,* 11(7), pp. 597-604.

Wong, A.H., Lau, C.S., Cheng, P.K., Ng, A.Y. & Lim, W.W. (2011). Coxsackievirus B3-associated aseptic meningitis: an emerging infection in Hong Kong. *Journal of Medical Virology,* 83(3), pp. 483-489.

Wringe, A., Fine, P.E., Sutter, R.W. & Kew, O.M. (2008). Estimating the extent of vaccine-derived poliovirus infection. *PLOS ONE,* 3(10), pp. e3433.

Xia, M., Farkas, T. & Jiang, X. (2007). Norovirus capsid protein expressed in yeast forms virus-like particles and stimulates systemic and mucosal immunity in mice following an oral administration of raw yeast extracts. *Journal of Medical Virology,* 79(1), pp. 74-83.

Xiang, S.D., Scalzo-Inguanti, K., Minigo, G., Park, A., Hardy, C.L. & Plebanski, M. (2008). Promising particle-based vaccines in cancer therapy. *Expert Review of Vaccines,* 7(7), pp. 1103-1119.

Xu, W., Shen, Y., Jiang, Z., Wang, Y., Chu, Y. & Xiong, S. (2004). Intranasal delivery of chitosan-DNA vaccine generates mucosal SIgA and anti-CVB3 protection. *Vaccine,* 22(27-28), pp. 3603-3612.

Yang, F.Q., Yu, Y.Y., Wang, G.Q., Chen, J., Li, J.H., Li, Y.Q., Rao, G.R., Mo, G.Y., Luo, X.R. & Chen, G.M. (2012). A pilot randomized controlled trial of dual-plasmid HBV DNA vaccine mediated by in vivo electroporation in chronic hepatitis B patients under lamivudine chemotherapy. *Journal of Viral Hepatitis,* 19(8), pp. 581-593.

Yuan, J., Ku, G.Y., Adamow, M., Mu, Z., Tandon, S., Hannaman, D., Chapman, P., Schwartz, G., Carvajal, R., Panageas, K.S., Houghton, A.N. & Wolchok, J.D. (2013). Immunologic responses to xenogeneic tyrosinase DNA vaccine administered by electroporation in patients with malignant melanoma. *Journal for Immunotherapy of Cancer,* 1, pp. 20-20.

Zamora, E., Handisurya, A., Shafti-Keramat, S., Borchelt, D., Rudow, G., Conant, K., Cox, C., Troncoso, J.C. & Kirnbauer, R. (2006). Papillomavirus-Like Particles Are an Effective Platform for Amyloid-β Immunization in Rabbits and Transgenic Mice. *Journal of Immunology,* 177(4), pp. 2662-2670.

Zeltins, A. (2013). Construction and characterization of virus-like particles: a review. *Molecular Biotechnology,* 53(1), pp. 92-107.

Zhang, H., Morgan-Capner, P., Latif, N., Pandolfino, Y.A., Fan, W., Dunn, M.J. & Archard, L.C. (1997). Coxsackievirus B3-induced myocarditis. Characterization of stable attenuated variants that protect against infection with the cardiovirulent wild-type strain. *The American Journal of Pathology,* 150(6), pp. 2197-2207.

Zhang, L., Parham, N.J., Zhang, F., Aasa-Chapman, M., Gould, E.A. & Zhang, H. (2012). Vaccination with coxsackievirus B3 virus-like particles elicits humoral immune response and protects mice against myocarditis. *Vaccine,* 30(13), pp. 2301-2308.

Zheng, D., Ando, T., Fankhauser, R.L., Beard, R., Glass, R.I. & Monroe, S.S. (2006). Norovirus classification and proposed strain nomenclature. *Virology,* 346(2), pp. 312 - 323.

ORIGINAL COMMUNICATIONS

Journal of Virological Methods 179 (2012) 1–7

Contents lists available at ScienceDirect

Journal of Virological Methods

journal homepage: www.elsevier.com/locate/jviromet

Production and characterization of virus-like particles and the P domain protein of GII.4 norovirus

Tiia Koho[a], Leena Huhti[b], Vesna Blazevic[b], Kirsi Nurminen[b], Sarah J. Butcher[c], Pasi Laurinmäki[c], Nisse Kalkkinen[c], Gunilla Rönnholm[c], Timo Vesikari[b], Vesa P. Hytönen[a], Markku S. Kulomaa[a,*]

[a] Institute of Biomedical Technology and BioMediTech, University of Tampere and Tampere University Hospital, Biokatu 6, FI-33014 University of Tampere, Finland
[b] Vaccine Research Center, Biokatu 10, FI-33014 University of Tampere, Finland
[c] Institute of Biotechnology, Viikinkaari 9 (P.O. Box 56), FI-00014 University of Helsinki, Finland

Article history:
Received 3 August 2010
Received in revised form 21 April 2011
Accepted 4 May 2011
Available online 12 May 2011

Keywords:
Virus-like particle
VLP
Norovirus
P domain protein
Diagnostics

A B S T R A C T

Noroviruses are an important cause of epidemic acute gastroenteritis in humans. In this study the production and characterization of GII.4 norovirus virus-like particles (VLPs) in insect cells is reported. Furthermore, the expression of corresponding norovirus polyhistidine-tagged P domain protein in *Escherichia coli* is described. The protruding P domain of the norovirus capsid is known to contain determinants for antibody and receptor binding. Therefore, P domain proteins were studied as an alternative diagnostic tool for evaluating norovirus infection. Analyses by dynamic light scattering and cryo-electron microscopy revealed the presence of intact VLPs with an average diameter of about 40 nm. Immunostaining and ELISA assays using norovirus-specific human sera revealed that VLPs and the P domain are recognized by norovirus-specific antibodies and by their putative receptor. The VLPs and P domain protein are potentially useful in the development of diagnostic and vaccination tools for noroviruses.

1. Introduction

Noroviruses (NoVs), formerly known as Norwalk-like viruses, belong to the family *Caliciviridae*. World-wide, NoVs are a major causative agent of nonbacterial acute gastroenteritis in all age groups. Noroviruses possess a high level of genetic and antigenic diversity. Based on the amino acid sequence of the capsid protein, norovirus genotypes can be classified into five genogroups (GI–GV), of which virus strains from GI, GII, and GIV are known to infect humans. In spite of the genetic diversity, only a few strains, primarily those of genogroup II genotype 4 (GII.4), are responsible for a majority of the gastroenteritis outbreaks in humans (Fankhauser et al., 2002; Glass et al., 2009; Zheng et al., 2006).

Noroviruses are small, round viruses of approximately 38 nm in diameter and possess a single-stranded, positive-sense, polyadenylated RNA genome of about 7.7 kb. The genome contains three open reading frames (ORFs). The first ORF encodes a polyprotein precursor, which is further processed into non-structural proteins. ORF2 encodes the 58-kDa capsid protein VP1, and ORF3 encodes the minor structural protein, VP2 (Scipioni et al., 2008). Following their discovery in the early 1970s (Adler and Zickl, 1969; Kapikian et al., 1972), the biological characterization of human noroviruses has been hampered by the lack of an appropriate cell culture system and small animal model for propagation of the viruses. However, when expressed in a baculovirus or other eukaryotic expression system (Santi et al., 2008; Taube et al., 2005; Xia et al., 2007), the recombinant VP1 capsid proteins self-assemble into empty non-infectious virus-like particles (VLPs) that are antigenically and morphologically similar to the native virions (Green et al., 1993). Norovirus VLPs have been used extensively to study virus structure and stability, host-cell interactions, and as a tool in diagnostic serological assays (Ausar et al., 2006; Patel et al., 2009; Prasad et al., 1999).

The X-ray crystallographic structure of the recombinant norovirus capsid, determined at a resolution of 3.4 Å, shows that the capsid exhibits a $T = 3$ icosahedral symmetry with 180 molecules of the capsid protein organized into 90 dimeric capsomers (Prasad et al., 1999). The capsid protein consists of two domains linked by a short hinge region, the shell (S) domain and the protruding (P) domain. The P domain dimers project out from the icosahedral shell. The P domain can be divided further into two subdomains, P1 and P2. Of the two, the highly variable P2 subdomain is predicted to contain the antigenic determinants of host immunological response (Choi et al., 2008; Prasad et al., 1999).

Norovirus research relies on the use of VLPs that are typically generated using eukaryotic expression systems. The use of such systems is time consuming and expensive. For vaccine development, and especially for diagnostic purposes, a simpler and less time-consuming bacterial production system would be beneficial. As the P domains are believed to contain the receptor-binding sites

* Corresponding author at: Institute of Biomedical Technology, Biokatu 6, FI-33520 Tampere, Finland. Tel.: +358 500 599904; fax: +358 3 3551 7710.
E-mail address: markku.kulomaa@uta.fi (M.S. Kulomaa).

0166-0934/$ – see front matter © 2011 Elsevier B.V. All rights reserved.
doi:10.1016/j.jviromet.2011.05.009

and the antigenic determinants of host immunological response, the production of the P domain in an *Escherichia coli* system was examined in this study. The purpose of this study was to produce and characterize recombinant insect cell-expressed norovirus VLPs representing the common GII.4 strain for diagnostic and vaccination purposes and to describe a more efficient, cost-effective method for the production of the P domain in bacterial cells to be used as a potential alternative diagnostic tool for the detection of noroviruses.

2. Materials and methods

2.1. Preparation and purification of recombinant virus-like particles

Norovirus genotype GII.4 (GenBank sequence database accession number AF080551) was isolated from patient stool collected in 1999 in Finland. RNA from the stool was extracted with an RNA isolation kit (Qiagen, Hilden, Germany). A 1.6 kb DNA fragment containing the complete VP1 capsid gene (ORF2) was amplified by reverse transcriptase polymerase chain reaction (RT-PCR) with the following primers: JV24 forward (5′-GTGAATGAAGATGGCGTCGA-3′) (Buesa et al., 2002) and reverse (5′-TTATAATGCACGTCTACGCCC-3′). The full-length cDNA copy of VP1 capsid gene was amplified by PCR with the primers shown in Table 1 using the PTC-200 DNA Engine (MJ Research, Waltham, MA). The amplified fragment was first cloned into a pCR2.1-TOPO vector (Invitrogen, Carlsbad, CA) and then subcloned into a baculovirus pFastBac1 donor plasmid. After transformation into TOP10 Chemically Competent *E. coli* cells, the VP1 sequence was verified by DNA sequencing (ABI PRISM 3130XL Genetic Analyzer, Applied Biosystems, Carlsbad, CA).

The recombinant norovirus VP1 monomers were expressed in a baculovirus-infected *Spodoptera frugiperda* ovarian cell line Sf9 using the Bac-to-Bac® Baculovirus expression system (Invitrogen) according to the manufacturer's instructions. Insect cell lysate from cells and lysate infected with baculoviruses created from an empty donor plasmid were used as negative controls. An MOI of 2 was used for the infections. The insect cells were grown in HyQ SFX-insect serum-free medium (HyClone Laboratories, Logan, UT) at 27 °C without antibiotics.

After five days, the infected cell culture was clarified by centrifugation at 1000 × *g* at 4 °C for 10 min at 4 °C. The VLPs in the supernatant were concentrated by precipitation with 7% (w/v) polyethylene glycol 6000 and 380 mM NaCl in agitation for 2–4 h at 4 °C, after which the suspension was pelleted at 9500 × *g* at 4 °C for 30 min. The pellet was resuspended in PBS buffer and loaded onto the discontinuous sucrose gradient (60–10%, w/v). After ultracentrifugation at 24 000 rpm in a Beckman Js24.38 rotor at 4 °C for 4 h, the gradient was fractionated by bottom puncture. The peak fractions were pooled and stored at 4 °C until further use. The isolated capsid proteins were analyzed by SDS-PAGE, and the particle size and particle size distribution were assayed by dynamic light scattering technique. An aliquot of the VLP sample was concentrated further by ultracentrifugation at 53 000 rpm (TLA100.3 rotor) at 4 °C for 1.5 h. The resulting pellet was resuspended in PBS and stored at 4 °C until used. The concentrated VLP specimen was examined by cryo-electron microscopy to examine the integrity of the particles. Protein concentrations were measured by the Bradford method using bovine serum albumin as a standard.

2.2. Preparation and purification of recombinant P domain protein

The pET101 directional TOPO vector (Invitrogen) was used to express the P domain of the capsid. The PCR-amplified fragment with a C-terminal polyhistidine-tag was generated using the primer pairs shown in Table 1. The pFastBac1 plasmid containing the complete VP1 capsid sequence of norovirus GII.4 was used as a template DNA. The generated PCR fragment was cloned into the pET101 directional TOPO vector and transformed into TOP10 Chemically Competent *E. coli* cells (Invitrogen). Positive transformants were confirmed by DNA sequencing using an ABI PRISM 3130XL Genetic Analyzer (Applied Biosystems).

E. coli BL21 star cells (Invitrogen) were used for the production of the P domain protein, and the protein was isolated by Ni–NTA affinity chromatography. The details of the purification protocol are shown in the Supplementary Data. The quality of the purified protein was assessed by SDS-PAGE followed by Coomassie staining. The functional and antigenic properties of P domain samples were analyzed as described above for the VLPs in Section 2.1.

2.3. Dynamic light scattering (DLS)

Sucrose gradient fractions containing VLP particles were measured by DLS using pre-specified solvent profile containing 40% sucrose. Viscosity and refractive index values of 5.7717 cP and 1.45 (material)/1.4 (dispersant) were used in particle size calculations. Measurements were recorded at 22 °C by a dynamic light scattering instrument (Zetasizer Nano ZS, Malvern Instruments) equipped with a HeNe gas laser (λ = 633 nm) using a non-invasive back scatter (NIBS®) technology at a scattering angle of 173°. The hydrodynamic diameter was calculated from the diffusion coefficient by the Stokes–Einstein equation using the method of cumulants (Brown et al., 1975). For each sample, six consequent measurements, each containing 17 readings over 10-s intervals, were recorded and plotted as the mean hydrodynamic diameter of particle population with accompanying standard error.

2.4. Cryo-electron microscopy

The vitrified samples of the purified VLP solution were loaded onto Quantifoil grids with 2 μm holes as described previously (Baker et al., 1999). A Gatan 626 cryoholder was used to observe the sample in an FEI Tecnai F20 field emission gun transmission electron microscope at 200 kV under low-dose conditions (~20 e/A^2) at −180 °C. The images were recorded using a Gatan Ultrascan 4000 CCD camera at nominal magnification of 68 000× resulting in the final sampling of the images at 0.22 nm/pixel.

2.5. Peptide mass fingerprinting, mass spectrometric analysis, and N-terminal sequencing

For peptide mass fingerprinting (PMF), proteins were separated by SDS-PAGE followed by silver staining. Protein bands were isolated from the polyacrylamide gel and "in-gel" digested essentially as described previously (Shevchenko et al., 1996). Proteins were reduced with dithiothreitol and alkylated with iodoacetamide before digestion with trypsin (Sequencing Grade modified Trypsin, #V5111, Promega, Madison, WI). The recovered peptides were, after desalting with a Millipore C_{18} ZipTip, subjected to MALDI-TOF mass spectrometric analysis using an Ultraflex TOF/TOF instrument (Bruker-Daltonik GmbH, Bremen, Germany). Protein identification with the generated data was performed using Mascot Peptide Mass Fingerprint program (http://www.matrixscience.com).

For molecular weight determination and Edman degradation, the proteins were first subjected to reversed phase chromatography in a 1 mm × 20 mm C1 column (TSK gel TMS-250, 10 μm, 250 Å, TOSOH Corporation, Japan) using a linear gradient of acetonitrile (0–100% in 60 min) in 0.1% trifluoroacetic acid. Collected proteins were subjected to molecular mass determination by MALDI-TOF mass spectrometry on the Bruker Ultraflex TOF/TOF

Table 1
Names, sequences, and nucleotide positions on ORF2 of primers used in the present study.

Primer	Sequence (5′–3′)	Position[a] (nt)	Underlined
GII-4-for	CACAGGATCC*ATG*AAGATGGCGTCGAATGAC	1–21	BamHI
GII-4-rev	CTCTGAATTC*TTA*TAATGCACGTCTACGCCCCGCTCCA	1593–1620	EcoRI
GII-4-P-for	CACC*ATG*AAACCATTCACCGTCCCAATCTTAACTG	673–700	
GII-4-P-rev	*TTA*ATGATGGTGATGGTGGTGTAATGCACGTCTACGCCCCGCTCCA	1593–1617	Histidine-tag

[a] NoV GenBank accession no. AF080551. The enzyme recognition or polyhistidine-tag sites are underlined. The start or stop codons are in italics.

instrument. Edman degradation was conducted on a Procise 494A-HT Sequencer (PerkinElmer, Applied Biosystems Division). The theoretical protein masses were calculated using ExPASy ProtParam tool (http://au.expasy.org/tools/protparam.html).

2.6. Western blot analysis

Proteins separated by SDS-PAGE were transferred onto a nitrocellulose membrane. After blocking overnight at 4 °C with 5% skimmed milk in TBS containing 0.05% Tween 20 (TBS-T), the membrane was incubated at 22 °C for 1 h with norovirus-positive or negative human serum at a dilution of 1:500 in TBS-T containing 1% skimmed milk. The positive serum was a convalescent serum that was shown in ELISA to seroconvert and had a high concentration of NoV GII.4 IgG and IgA (Nurminen et al., 2011). The serum was obtained from a patient who had had NoV GII.4 infection confirmed by RT-PCR of RNA isolated from stool. The negative control serum was GII.4 IgG and IgA negative in ELISA. The donor was a 9-month-old infant. After incubation with a horseradish peroxidase-conjugated secondary antibody (goat anti-human IgG, #62-8420, Invitrogen) at a dilution of 1:10 000, the bound antibodies were detected by utilizing Opti-4CN substrate (Bio-Rad Laboratories, Hercules, CA).

2.7. Antigen ELISA

Briefly, 96-well microwell plates (Nunc Immuno Maxisorp, Thermo Fisher Scientific, Waltham, MA) were coated with 50 ng/well of the recombinant VLPs or P domain proteins (overnight, 4 °C) followed by blocking with 5% (w/v) skimmed milk in PBS at 22 °C for 1 h. The wells were then washed and incubated (1 h, 37 °C) with 12 norovirus-positive sera that were diluted serially in 1% skimmed milk in PBS-T (100 μl/well). The sera were obtained from patients hospitalized for acute gastroenteritis in Tampere and Kuopio University Hospitals during the years 2006–2008, and they were stored at −20 °C until used. After washing, the wells were incubated with 100 μl of horseradish peroxidase-conjugated goat anti-human IgG (#62-8420, Invitrogen) diluted 1:4000 in 1% skimmed milk in PBS-T. Phenylenediamine dihydrochloride substrate (FAST OPD Tablet Set, Sigma–Aldrich, St. Louis, MO) was used for detection of antibodies, and the reaction was stopped with 50 μl of 2 M sulfuric acid after a 30-min incubation at 22 °C. Absorbance at a wavelength of 490 nm was measured in an ELISA plate reader (Victor^2 1420 Multilabel counter, Perkin Elmer, Waltham, MA).

Norovirus-positive and negative sera (described above in Section 2.6) were included on all plates as internal controls. Previous testing of negative control wells, coated with an equivalent concentration of wild-type baculovirus-infected Sf9 cell lysate with norovirus-positive serum, showed no difference to the dilution buffer. Therefore, wells with only dilution buffer were used as blanks. OD_{490} value of the blank wells was subtracted from the sample values, and the sample was considered positive when the OD_{490} value for the sample exceeded the set cut off (mean OD_{490} value of 1:100 dilutions of the norovirus-negative serum plus three times the standard deviation of 1:100 dilutions of the negative serum).

2.8. Assay of protein binding to carbohydrates

The binding capabilities of the recombinant VLPs and P domain proteins to their putative receptor among ABH and Lewis histo-blood group antigens were determined as previously described by Rockx et al. (2005). Briefly, purified VLPs or P domain proteins (200 ng/well) were added to 96-well microwell plates (Nunc Maxisorp). The plates were incubated at 22 °C for 4 h, washed five times with PBS-T, and blocked overnight with 5% (w/v) skimmed milk in PBS at 4 °C. After washing, synthetic biotinylated H type 3 and Lewis b (Leb) histo-blood group carbohydrates (#0059-BP and #0041-BP, respectively, Lectinity, Moscow, Russia) were diluted to 40–2.5 μg/ml in 1% skimmed milk in PBS-T, added (100 μl/well), and incubated at 37 °C for 4 h. After washing, AP-conjugated streptavidin (1 mg/ml, #S2890, Sigma–Aldrich) diluted 1:250 in 1% skimmed milk in PBS-T was added and incubated at 37 °C for 1 h. After the final washes, 100 μl of 1 mg/ml p-nitrophenyl phosphate substrate (FAST-pNPP tablets, Sigma–Aldrich) was added, and the reaction was stopped with 50 μl of 3 M NaOH after 1-h incubation at 22 °C. Optical density at 405 nm was determined with an ELISA plate reader (Victor^2 1420 Multilabel counter, Perkin Elmer). The OD_{405} value of the wells incubated with dilution buffer instead of carbohydrates was subtracted from the OD_{405} values of the sample wells.

3. Results

3.1. GII.4 VLPs can efficiently be produced in insect cells and P domain proteins in E. coli

The expression of the GII.4 capsid proteins in Sf9 insect cells resulted in a high yield of over 100 mg/l culture. The SDS-PAGE analysis showed the presence of a protein approximately 58 kDa with a doublet band pattern (Fig. 1A, second lane). An intensity-based analysis by dynamic light scattering (DLS) revealed the presence of uniform population of particles with an average hydrodynamic diameter of 36.8 ± 0.5 nm (Fig. 2). The mean polydispersity index (PdI) between measurements was 0.560 and the intercept value was 0.939. Examination of the pooled and concentrated VLP sample under a cryo-electron microscopy confirmed the presence of intact and fairly uniform particles (Fig. 3).

The polyhistidine-tagged P domain proteins of genotype GII.4 norovirus were produced in *E. coli* and purified using a Ni–NTA column at a yield of 6 mg/l culture. The P domain proteins showed a single major protein band of about 35 kDa (P protein monomer) in SDS-10% PAGE gel (Fig. 1A, third lane). The endotoxin contents of the VLPs (0.16 EU/10 μg protein) and P domain samples (100 EU/10 μg protein) were measured by Limulus Amebocyte Lysate (LAL) assay (Lonza, Walkersville, MD).

3.2. Recombinant VLP proteins show partial N-terminal cleavage in peptide mass fingerprinting, mass spectrometric analysis, and N-terminal sequencing

The purified VLP sample was visible as two bands in SDS-PAGE with apparent molecular weights of about 56 kDa (major

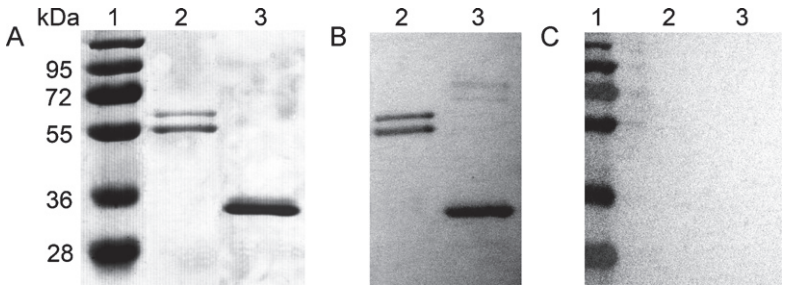

Fig. 1. Expression and western blot analysis of norovirus GII.4 VLPs and P domain protein. (A) SDS-PAGE analysis of the purified VLPs expressed in insect cells and P domain protein expressed in *E. coli*. (B) Western blot analysis was performed using norovirus-positive human serum. (C) Proteins were not detected by norovirus-negative human serum. Lane 1, molecular weight marker; lane 2, ~1 μg of rNoV VLP; lane 3, ~1 μg of P domain protein.

band) and 61 kDa (minor band). Both bands resulted in similar peptide mass fingerprints and were both identified as GII.4 norovirus capsid protein with probability-based Mowse scores of 78 and 85 (56 kDa band and 61 kDa band, respectively). Reversed phase chromatography of the purified VLPs resulted in only one peak containing both protein forms. MALDI-TOF mass spectrometric analysis of this collected fraction resulted in masses of 55.3 and 58.8 kDa corresponding to the two bands in SDS-PAGE. N-terminal sequence analysis of the reversed phase chromatography fraction with the both protein forms showed in Edman degradation only one sequence beginning with the sequence: AAIAAPVAGQ, which can be found from the amino acid 35 onwards in the primary structure of the GII.4 capsid protein. For an unknown reason, the N-terminal sequence of the putative full-length protein could not be determined. It is possible that the N-terminal methionine, if blocked, could have prevented the sequencing reaction (Rose et al., 1987).

The theoretical average masses, calculated without disulfide bridges, of the smaller product starting with the amino acid sequence of AAIAAPV and the full-length protein starting with MKMASND are 55 400.51 and 58 884.41 Da, respectively. The amino acid sequence of produced NoV GII.4 strain differs from the Uniprot/TrEMBL reference sequence Q77VT1 by one point mutation L333 M. Taken together, the results suggest that the band of about 61 kDa observed in the SDS-PAGE analysis corresponds to the full-length capsid protein, and the 56 kDa band represents a product that has been truncated by 34 amino acids from its N-terminal end. Analysis of the amino acid sequence by program PeptideCutter (http://ca.expasy.org/tools/peptidecutter/) revealed a potential cleavage site only for broad-spectrum proteases proteinase K and thermolysin in this position.

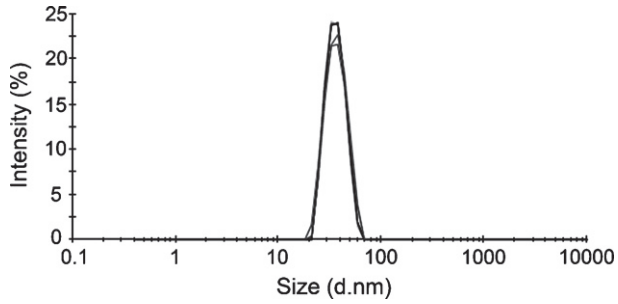

Fig. 2. Dynamic light scattering analysis of particle sizes of norovirus GII.4 VLPs. Six measurements of a representative sample are shown. The mean diameter of VLP measurements was 36.8 ± 0.5 nm with the polydispersity index value of 0.560.

3.3. Recombinant VLPs and P domain are recognized by norovirus-specific antibodies

To compare the antigenic properties of the recombinant VLPs and the P domain proteins, equal amounts of the proteins were loaded on a SDS-PAGE gel for a western blot analysis. Immunostaining using norovirus-specific human serum revealed signal intensities similar to each other (Fig. 1B) suggesting similar antigenic properties. No binding of norovirus-positive serum to the negative controls was detected, nor any binding of norovirus-negative serum to any of the proteins (data not shown). To further assess the antigenic activity of the recombinant VLPs and the P domain proteins, they were used as coating antigens in an ELISA assay and examined using norovirus-positive sera. The results suggested that the IgGs of norovirus-positive sera had better recognition for VLPs than for the P domain protein (Fig. 4). In fact, when the geometric mean of the end-point positive titer was determined, the VLPs were recognized about five-fold more strongly compared to the P domain protein by both moderately and strongly positive sera ($p = 0.065$, Student's *t*-test).

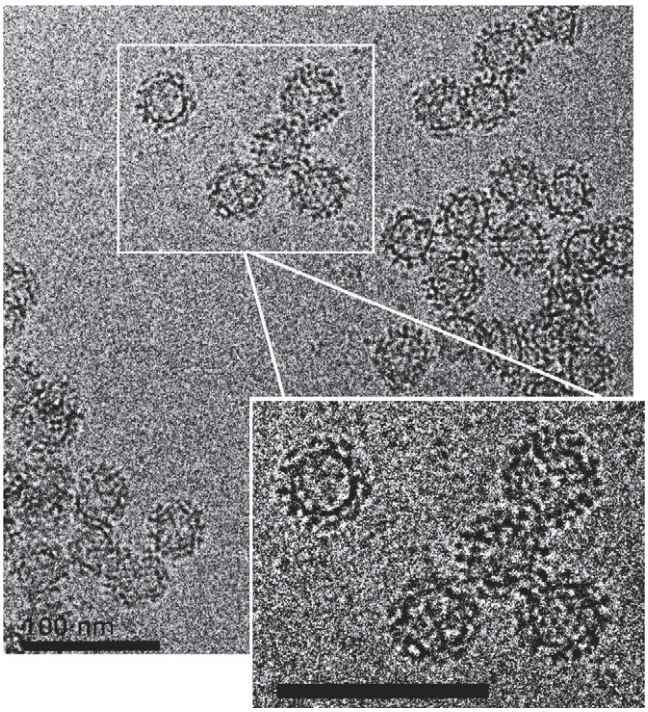

Fig. 3. Cryo-EM image of norovirus GII.4 VLPs. Bar, 100 nm.

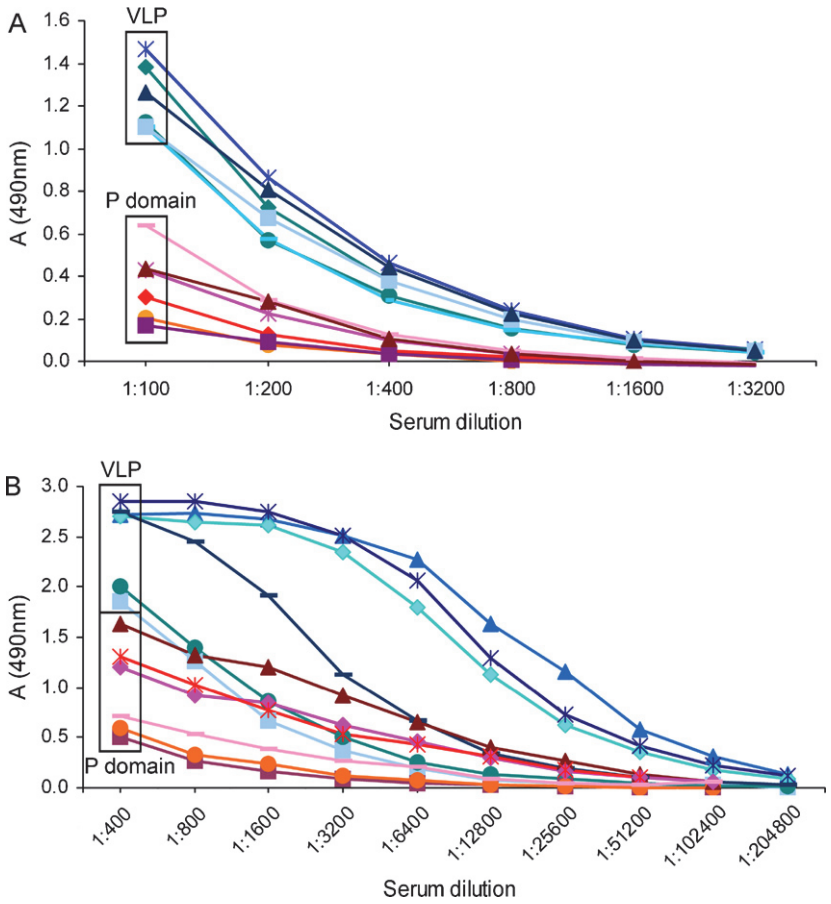

Fig. 4. Immunoreactivity of norovirus GII.4 VLPs and P domain protein analyzed by ELISA assay. (A) Moderately norovirus-positive sera and (B) strongly norovirus-positive sera were used for binding to the proteins. Red-toned lines (boxed) represent the sera dilutions using P domain protein as an antigen. Blue-toned lines (boxed) represent the sera dilutions using VLP as an antigen. (For interpretation of the references to color in this figure legend, the reader is referred to the web version of the article.)

3.4. Recombinant VLPs and P domain proteins bind to their putative histo-blood group antigen receptor

Several previous observations suggest noroviruses recognize carbohydrates linked to the human histo-blood group antigens as receptors and host-susceptibility factors. Such evidence has been obtained from outbreak investigations, volunteer challenge studies, sequence comparison with other NoVs, and structure-function analyses of norovirus capsids and P domain (Cao et al., 2007; Choi et al., 2008). Noroviruses recognize human histo-blood group antigen receptors in a strain specific manner. At least eight distinct binding patterns have been described, and all three major histo-blood group antigen families, the ABO, Lewis, and secretor families, have been shown to be involved in norovirus recognition (Tan and Jiang, 2005a).

The functionality of the VLPs and P domain proteins were demonstrated by comparing their putative receptor-binding activities to synthetic oligosaccharides representing two, H type 3 and Lewis b (Leb) histo-blood group antigens (Fig. 5). Both VLP and P domain protein bound moderately and with a similar binding pattern to H type 3, which is one of the putative receptors of GII.4 noroviruses (Rockx et al., 2005). However, it was noted that the binding affinity of P domain to H type 3 was weaker than that of VLP. Binding of VLPs or P domain proteins to Lewis b antigen was not detected. These findings are in good agreement with the previous results reported before for other GII.4 genotype noroviruses (Huang et al., 2005; LoBue et al., 2006; Rockx et al., 2005).

4. Discussion

In this study, baculovirus-mediated production and characterization of the recombinant GII.4 norovirus capsid protein, and the expression of polyhistidine-tagged P domain protein of the corresponding genotype in *E. coli* is reported. The antigenic properties of both proteins were compared. The production of the capsid protein in insect cells resulted in formation of VLPs that were similar morphologically to the native viruses. The studied genotype is interesting, as the viruses of the GII.4 genotype have been predominant during the past decade in the United States, Europe, and Oceania, causing 70–80% of all NoV outbreaks (Siebenga et

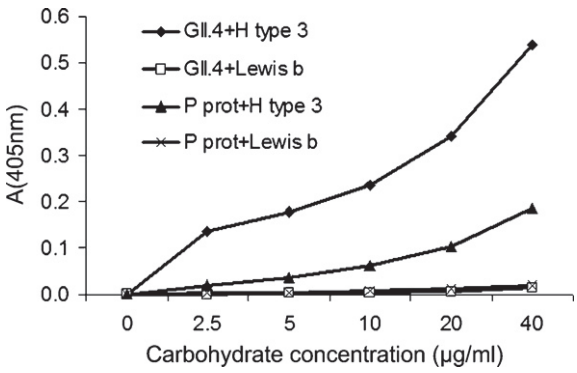

Fig. 5. Binding of synthetic ABH histo-blood group antigens to norovirus GII.4 VLPs and P domain protein.

al., 2009). In this study, GII.4 genotype diversity was evaluated by comparing five strains of GII.4. The strains were found to be 94.4–95.9% identical to each other in terms of the primary amino acid sequence. However, a significant amount of sequence variability was observed in the P2 subdomain of the VP1 capsid. The sequence comparison is presented in the Supplementary material. Examination of the purified VLPs under the cryo-electron microscope revealed the presence of capsids with an average diameter of 40 nm and spike-like structures on their surface.

The results obtained from the peptide mass fingerprinting followed by mass spectrometric analysis and N-terminal sequencing of the intact VLPs suggested that the doublet pattern seen in the SDS-PAGE analysis constituted the full-length form of the recombinant GII.4 NoV capsid protein of about 61 kDa in size and its N-terminally truncated product with molecular weight of about 56 kDa. The ratio between the two bands remained unchanged with and without protease inhibitors and showed hardly any noticeable change following 12 months of storage at 4 °C. The doublet patterning of recombinant NoV VLPs was also seen in other studies (Bertolotti-Ciarlet et al., 2003; Jiang et al., 1992; Tan et al., 2004b). Our results are in good agreement with the findings of White et al. (1997). They reported production of Norwalk virus (classified now as genotype GI-1 virus, Vinje et al., 2004) VLPs with a diameter of 38 nm that showed the same protein composition pattern, represented by a doublet at about 58 kDa and 56 kDa. This finding was often seen in the purified preparations of VLPs, even when protease inhibitors were present during the purification. They also observed only a modest change upon storage and hypothesized that the smaller protein was likely an early cleavage product of the capsid protein within Sf9 cells that do not affect VLP assembly. This hypothesis is supported by the fact that the N-terminus is located on the interior side of the particles (Prasad et al., 1999) and is therefore presumably protected from protease activity once the particle has formed. Furthermore, in the present study, no special protease cleavage site was found at the position in question, between the amino acid residues G34 and A35. Taken together, the results presented above suggest that the N-terminally truncated capsid proteins are embedded in the VLPs. Interestingly, it was demonstrated previously that producing a recombinant virus capsid mutant with N-terminal deletion of 34 amino acids (NT34) resulted in no particles being detectable by EM (Bertolotti-Ciarlet et al., 2002). However, due to the low expression levels of the mutant, it was difficult to assess the involvement of the deletion in the assembly of the VLPs.

Although expression of foreign proteins by baculovirus expression systems has been proven to be excellent technique for producing large quantities of recombinant proteins, and it often enables production of biologically active proteins, it is also time-consuming and expensive. For vaccine development, and especially for diagnostic purposes, a simpler and less time-consuming system for production and purification of an antigen would be valuable. Because the P domains of noroviruses are believed to contain the receptor-binding sites and the antigenic determinants of the immunological response of the host, a cost-effective and simple method for production of the P domain in an *E. coli* system was examined.

To assess the antigenic activity of the recombinant capsid proteins and the P domain proteins, both proteins were analyzed by western blot and ELISA analyses. Although both VLPs and P domain proteins were virtually equally effective antigens for norovirus-positive serum in the western blot analysis, IgGs of both moderately and strongly norovirus-positive sera showed somewhat higher binding to VLP in the ELISA assay as compared to P domain. Similarly, although both the VLPs and P domain proteins bound moderately and with a similar binding pattern to their putative receptor H type 3, the binding affinity of the P domain proteins to H type 3 appeared weaker than that of the VLPs. The difference in antibody binding to VLPs and P domain protein could be associated with changes in the conformation of the proteins. Antibodies in the ELISA assay may bind to additional conformational epitopes present in the VLPs that are lacking in the P domain structure. The linear epitopes may account for the similar recognition of the proteins in western blot (Fig. 1B), as the proteins are mainly in their denaturated state. Therefore, the results presented above may suggest that the linear epitopes are mainly located in the P domain region, whereas VLP may display unique structural epitopes, which are associated with the assembly of proteins. The structural nature of the epitopes was not, however, evaluated throughout in this study.

In addition, a previous study showed that the norovirus (strain VA387) P domain lacking the hinge region between P and S domains spontaneously formed a small (about 5 nm in diameter) $T = 1$ icosahedral particles (Tan and Jiang, 2005b). These particles, named the P particles, showed VLP-like or even higher receptor-binding activity. In the presence of the hinge, the P domain formed predominantly dimers and bound to HGBAs with a lower affinity (Tan et al., 2004a). Furthermore, it was demonstrated that the P particle formation could be enhanced by addition of cysteine residues at the C-terminal end of the P domain, and as a result even hinge-containing P domain could form a stable P particle (Tan and Jiang, 2005b; Tan et al., 2008). Although signs of dimer formation in SDS-PAGE analyses (data not shown) and in the Western blot (Fig. 1B, lane 3) were noted in the current study, the observed lower receptor-binding activity suggests that the P domains expressed in *E. coli* did not form P particles. This finding could account for the decreased affinity of both norovirus-specific antibodies and putative receptor to P domains. Therefore, the question arises whether the six histidine residues at the C-terminal end of our recombinant P domain pose a steric hindrance that results in unfavorable inter-P dimer interactions and subsequent dynamic P particle formation. On the other hand, the C-terminal histidine-tag enables the use of affinity matrices for orienting the protein or immobilizing the P domain on the surface of microparticles and other appropriate surfaces.

In conclusion, the production and characterization of GII.4 VLPs in insect cells and the expression of the corresponding P domain protein in *E. coli* was demonstrated in this study. Both products were detectable using norovirus-raised antibodies from patient sera, though VLPs showed somewhat superior binding to P domain proteins in ELISA assays. The structural and physicochemical properties of the VLPs were thoroughly characterized. The products will be used for the development of norovirus diagnostic methods and as preliminary tools for vaccine development.

Acknowledgements

The authors thank Dr. Olli Laitinen for many helpful suggestions and discussions as well as Ulla Kiiskinen for technical assistance with insect cell cultures and reagents. The work was supported by grants from the Academy of Finland (1115976), Pirkanmaa Hospital District (EVO grants), and from the National Graduate School in Informational and Structural Biology (ISB), Finland.

Appendix A. Supplementary data

Supplementary data associated with this article can be found, in the online version, at doi:10.1016/j.jviromet.2011.05.009.

References

Adler, J.L., Zickl, R., 1969. Winter vomiting disease. J. Infect. Dis. 119, 668–673.

Ausar, S.F., Foubert, T.R., Hudson, M.H., Vedvick, T.S., Middaugh, C.R., 2006. Conformational stability and disassembly of Norwalk virus-like particles. Effect of pH and temperature. J. Biol. Chem. 281, 19478–19488.

Baker, T.S., Olson, N.H., Fuller, S.D., 1999. Adding the third dimension to virus life cycles: three-dimensional reconstruction of icosahedral viruses from cryo-electron micrographs. Microbiol. Mol. Biol. Rev. 63, 862–922.

Bertolotti-Ciarlet, A., Crawford, S.E., Hutson, A.M., Estes, M.K., 2003. The 3′ end of Norwalk virus mRNA contains determinants that regulate the expression and stability of the viral capsid protein VP1: a novel function for the VP2 protein. J. Virol. 77, 11603–11615.

Bertolotti-Ciarlet, A., White, L.J., Chen, R., Prasad, B.V., Estes, M.K., 2002. Structural requirements for the assembly of Norwalk virus-like particles. J. Virol. 76, 4044–4055.

Brown, J.C., Pusey, P.N., Dietz, R., 1975. Photon correlation study of polydisperse samples of polystyrene in cyclohexane. J. Chem. Phys. 62, 1136–1145.

Buesa, J., Collado, B., López-Andújar, P., Abu-Mallouh, R., Rodríguez Díaz, J., García Díaz, A., Prat, J., Guix, S., Llovet, T., Prats, G., Bosch, A., 2002. Molecular epidemiology of caliciviruses causing outbreaks and sporadic cases of acute gastroenteritis in Spain. J. Clin. Microbiol. 40, 2854–2859.

Cao, S., Lou, Z., Tan, M., Chen, Y., Liu, Y., Zhang, Z., Zhang, X.C., Jiang, X., Li, X., Rao, Z., 2007. Structural basis for the recognition of blood group trisaccharides by norovirus. J. Virol. 81, 5949–5957.

Choi, J.M., Hutson, A.M., Estes, M.K., Prasad, B.V., 2008. Atomic resolution structural characterization of recognition of histo-blood group antigens by Norwalk virus. Proc. Natl. Acad. Sci. U.S.A. 105, 9175–9180.

Fankhauser, R.L., Monroe, S.S., Noel, J.S., Humphrey, C.D., Bresee, J.S., Parashar, U.D., Ando, T., Glass, R.I., 2002. Epidemiologic and molecular trends of "Norwalk-like viruses" associated with outbreaks of gastroenteritis in the United States. J. Infect. Dis. 186, 1–7.

Glass, R.I., Parashar, U.D., Estes, M.K., 2009. Norovirus gastroenteritis. N. Engl. J. Med. 361, 1776–1785.

Green, K.Y., Lew, J.F., Jiang, X., Kapikian, A.Z., Estes, M.K., 1993. Comparison of the reactivities of baculovirus-expressed recombinant Norwalk virus capsid antigen with those of the native Norwalk virus antigen in serologic assays and some epidemiologic observations. J. Clin. Microbiol. 31, 2185–2191.

Huang, P., Farkas, T., Zhong, W., Tan, M., Thornton, S., Morrow, A.L., Jiang, X., 2005. Norovirus and histo-blood group antigens: demonstration of a wide spectrum of strain specificities and classification of two major binding groups among multiple binding patterns. J. Virol. 79, 6714–6722.

Jiang, X., Wang, M., Graham, D.Y., Estes, M.K., 1992. Expression, self-assembly, and antigenicity of the Norwalk virus capsid protein. J. Virol. 66, 6527–6532.

Kapikian, A.Z., Wyatt, R.G., Dolin, R., Thornhill, T.S., Kalica, A.R., Chanock, R.M., 1972. Visualization by immune electron microscopy of a 27-nm particle associated with acute infectious nonbacterial gastroenteritis. J. Virol. 10, 1075–1081.

LoBue, A.D., Lindesmith, L., Yount, B., Harrington, P.R., Thompson, J.M., Johnston, R.E., Moe, C.L., Baric, R.S., 2006. Multivalent norovirus vaccines induce strong mucosal and systemic blocking antibodies against multiple strains. Vaccine 24, 5220–5234.

Nurminen, K., Huhti, L., Räsänen, S., Koho, T., Hytönen, V.P., Vesikari, T., Blazevic, V., 2011. Prevalence of norovirus GII-4 antibodies in Finnish children. J. Med. Virol. 53, 525–531.

Patel, M.M., Hall, A.J., Vinje, J., Parashar, U.D., 2009. Noroviruses: a comprehensive review. J. Clin. Virol. 44, 1–8.

Prasad, B.V., Hardy, M.E., Dokland, T., Bella, J., Rossmann, M.G., Estes, M.K., 1999. X-ray crystallographic structure of the Norwalk virus capsid. Science 286, 287–290.

Rockx, B., Baric, R.S., de Grijs, I., Duizer, E., Koopmans, M.P., 2005. Characterization of the homo- and heterotypic immune responses after natural norovirus infection. J. Med. Virol. 77, 439–446.

Rose, K., Savoy, L.A., Simona, M.G., Offord, R.E., Wingfield, P.T., Mattaliano, R.J., Thatcher, D.R., 1987. The state of the N-terminus of recombinant proteins: determination of N-terminal methionine (formylated, acetylated, or free). Anal. Biochem. 165, 59–69.

Santi, L., Batchelor, L., Huang, Z., Hjelm, B., Kilbourne, J., Arntzen, C.J., Chen, Q., Mason, H.S., 2008. An efficient plant viral expression system generating orally immunogenic Norwalk virus-like particles. Vaccine 26, 1846–1854.

Scipioni, A., Mauroy, A., Vinje, J., Thiry, E., 2008. Animal noroviruses. Vet. J. 178, 32–45.

Shevchenko, A., Wilm, M., Vorm, O., Mann, M., 1996. Mass spectrometric sequencing of proteins silver-stained polyacrylamide gels. Anal. Chem. 68, 850–858.

Siebenga, J.J., Vennema, H., Zheng, D.P., Vinjé, J., Lee, B.E., Pang, X.L., Ho, E.C., Lim, W., Choudekar, A., Broor, S., Halperin, T., Rasool, N.B., Hewitt, J., Greening, G.E., Jin, M., Duan, Z.J., Lucero, Y., O'Ryan, M., Hoehne, M., Schreier, E., Ratcliff, R.M., White, P.A., Iritani, N., Reuter, G., Koopmans, M., 2009. Norovirus illness is a global problem: emergence and spread of norovirus GII.4 variants, 2001–2007. J. Infect. Dis. 200, 802–812.

Tan, M., Fang, P., Chachiyo, T., Xia, M., Huang, P., Fang, Z., Jiang, W., Jiang, X., 2008. Noroviral P particle: structure, function and applications in virus–host interaction. Virology 382, 115–123.

Tan, M., Hegde, R.S., Jiang, X., 2004a. The P domain of norovirus capsid protein forms dimer and binds to histo-blood group antigen receptors. J. Virol. 78, 6233–6242.

Tan, M., Zhong, W., Song, D., Thornton, S., Jiang, X., 2004b. E. coli-expressed recombinant norovirus capsid proteins maintain authentic antigenicity and receptor binding capability. J. Med. Virol. 74, 641–649.

Tan, M., Jiang, X., 2005a. Norovirus and its histo-blood group antigen receptors: an answer to a historical puzzle. Trends Microbiol. 13, 285–293.

Tan, M., Jiang, X., 2005b. The p domain of norovirus capsid protein forms a subviral particle that binds to histo-blood group antigen receptors. J. Virol. 79, 14017–14030.

Taube, S., Kurth, A., Schreier, E., 2005. Generation of recombinant norovirus-like particles (VLP) in the human endothelial kidney cell line 293T. Arch. Virol. 150, 1425–1431.

Vinje, J., Hamidjaja, R.A., Sobsey, M.D., 2004. Development and application of a capsid VP1 (region D) based reverse transcription PCR assay for genotyping of genogroup I and II noroviruses. J. Virol. Methods 116, 109–117.

White, L.J., Hardy, M.E., Estes, M.K., 1997. Biochemical characterization of a smaller form of recombinant Norwalk virus capsids assembled in insect cells. J. Virol. 71, 8066–8072.

Xia, M., Farkas, T., Jiang, X., 2007. Norovirus capsid protein expressed in yeast forms virus-like particles and stimulates systemic and mucosal immunity in mice following an oral administration of raw yeast extracts. J. Med. Virol. 79, 74–83.

Zheng, D., Ando, T., Fankhauser, R.L., Beard, R., Glass, R.I., Monroe, S.S., 2006. Norovirus classification and proposed strain nomenclature. Virology 346, 312–323.

Supplementary Data

Production and characterization of virus-like particles and the P domain protein of GII.4 norovirus

Tiia Koho[a], Leena Huhti[b], Vesna Blazevic[b], Kirsi Nurminen[b], Sarah J. Butcher[c], Pasi Laurinmäki[c], Nisse Kalkkinen[c], Gunilla Rönnholm[c], Timo Vesikari[b], Vesa P. Hytönen[a], Markku S. Kulomaa[a,*]

[a] Institute of Biomedical Technology and BioMediTech, University of Tampere and Tampere University Hospital, Biokatu 6, FI-33014 University of Tampere, Finland
[b] Vaccine Research Center, Biokatu 10, FI-33014 University of Tampere, Finland
[c] Institute of Biotechnology, Viikinkaari 9 (P.O. Box 56), FI-00014 University of Helsinki, Finland

Production and purification of recombinant P domain protein by Ni-NTA affinity chromatography

BL21 Star *E. coli* cells (Invitrogen) were used for the production of the P domain protein. A total of 100 ml of LB medium, supplemented with 50 μg/ml ampicillin and 0.1% glucose (w/v), was inoculated 1:25 with an overnight culture of the plasmid-containing BL21 Star bacteria and incubated with shaking at 200 rpm at 37 °C. Once an optical density (OD600 nm) of about 0.3 was reached, bacteria were further incubated with shaking at 150 rpm at 26 °C for 30 min before adding 0.5 mM IPTG (final concentration) to induce the protein expression. After 16–18 h of incubation at 150 rpm at 26 °C, the bacteria were harvested by centrifugation for 5 min at 5,000 × *g* at 4°C. The supernatant was removed, and the cell pellet was suspended in 30 ml of lysis/binding buffer (50 mM NaH_2PO_4, 600 mM NaCl, 10 mM imidazole, pH 8.0). Lysozyme was added to concentration of 0.2 mg/ml, and the suspension was incubated on ice for 30 min. Bacteria were lysed by sonication for 2 min (1 s on, 1 s off) with amplitude of 40%.

Lysate was clarified by centrifugation at 10,000 × *g* for 30 min at 4°C, after which the protein-containing supernatant was mixed with 2 ml of binding buffer equilibrated nickel-charged resin (Qiagen Ni-NTA Superflow) on a roller mixer at 4°C for 1 h. The resulting slurry was applied to a column and washed with 40 ml of buffer containing 50 mM NaH_2PO_4, 600 mM NaCl, and 20 mM imidazole at pH 8.0. The same buffer with increasing imidazole concentration was used to elute the P domain protein. Protein was eluted in 1 ml fractions as follows: the first four fractions were eluted with buffer containing 40 mM imidazole, the next four fractions with 100 mM imidazole, and the last four with 500 mM imidazole.

Aliquots from the collected fractions were analyzed in SDS-PAGE followed by staining with Coomassie blue. The fractions containing P domain protein were pooled and dialyzed against 100 mM NaH_2PO_4 buffer (pH 6.0) for 2 h at room temperature and after buffer change at 4°C overnight. The protein concentration was quantified by Bradford method using Bio-Rad Model 680 XR microplate reader at 595 nm, and bovine serum albumin as a standard. Endotoxin content of the VLPs (0.16 EU/10 µg protein) and P domain samples (100 EU/10 µg protein) were measured by Limulus Amebocyte Lysate (LAL) assay (Lonza, Walkersville, MD). The protein was stored at 4°C until further use. The purified P domain proteins were further examined for purity by SDS-PAGE followed by Coomassie blue staining. Functionality and antigenic property evaluation was conducted by western blot, ELISA, and histo-blood group antigen binding analyses.

Mass spectrometric analysis

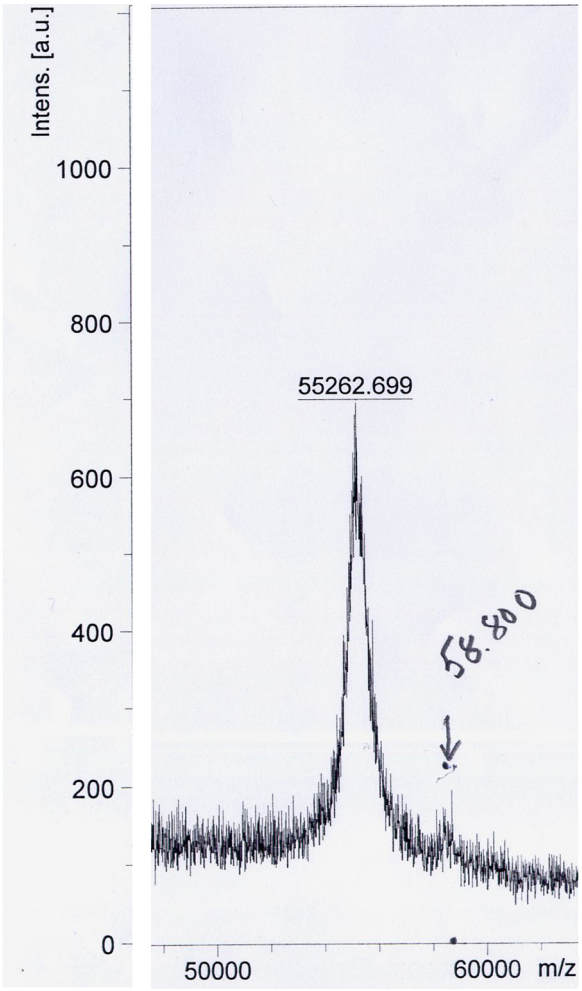

Figure S1. Mass spectrometric analysis of norovirus GII.4 VLPs resulted in masses of 55.3 and 58.8 kDa.

Similarity alignment

Similarity alignment, homology percent matrix, and distance matrix of VP1 monomer sequences (GenBank sequence database accession numbers are given in parentheses). Sequences are named after the virus cluster they belong to. Clusters are from Lindesmith et al., 2008. Grimsby represents the GII.4 strain used in this study, and other sequences represent more recent strains of GII.4 noroviruses.

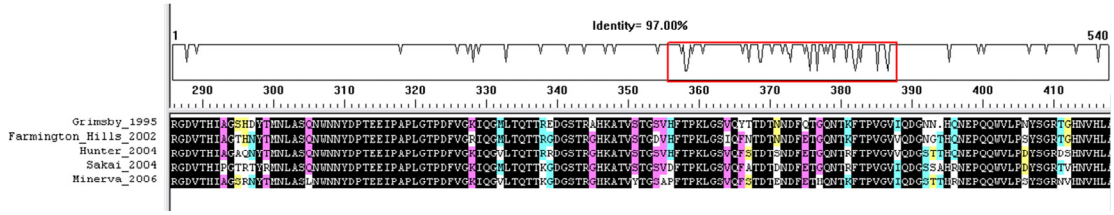

Figure S2. An aa alignment of VP1 capsid monomer sequences. The sequences are shown covering only the most variable region.

	1.	2.	3.	4.	5.
1. Grimsby_1995_(AF080551)	100%				
2. Farmington_Hills_2002_(AY502023)	95.9%	100%			
3. Hunter_2004_(DQ078794)	94.4%	95.0%	100%		
4. Sakai_2004_(AB220922)	95.0%	94.8%	94.6%	100%	
5. Minerva_2006_(EU078417)	94.6%	95.4%	94.6%	95.7%	100%

Table S1. Homology matrix of 5 norovirus sequences.

	1.	2.	3.	4.	5.
1. Grimsby_1995_(AF080551)	0				
2. Farmington_Hills_2002_(AY502023)	0.041	0			
3. Hunter_2004_(DQ078794)	0.056	0.050	0		
4. Sakai_2004_(AB220922)	0.050	0.052	0.054	0	
5. Minerva_2006_(EU078417)	0.054	0.046	0.054	0.043	0

Table S2. Estimates of evolutionary divergence between norovirus sequences. The number of amino acid substitutions per site from between sequences are shown. Analyses were conducted using the Poisson correction model (Zuckerkandl & Pauling, 1965). The analysis involved 5 amino acid sequences. All positions containing gaps and missing data were eliminated. There were a total of 539 positions in the final dataset. Evolutionary analyses were conducted by using program DNAMAN (Lynnon Corporation).

	1.	2.	3.	4.	5.
1. Grimsby_1995_(AF080551)	100%				
2. Farmington_Hills_2002_(AY502023)	93.6%	100%			
3. Hunter_2004_(DQ078794)	91.6%	93.6%	100%		
4. Sakai_2004_(AB220922)	90.9%	92.2%	92.2%	100%	
5. Minerva_2006_(EU078417)	90.9%	92.6%	93.2%	93.6%	100%

Table S4. Homology matrix of 5 P domain sequences.

	1.	2.	3.	4.	5.
1. Grimsby_1995_(AF080551)	0				
2. Farmington_Hills_2002_(AY502023)	0.064	0			
3. Hunter_2004_(DQ078794)	0.084	0.064	0		
4. Sakai_2004_(AB220922)	0.091	0.078	0.078	0	
5. Minerva_2006_(EU078417)	0.091	0.074	0.068	0.064	0

Table S5. Estimates of evolutionary divergence between P domain sequences. The number of amino acid substitutions per site from between sequences are shown. Analyses were conducted using the Poisson correction model (Zuckerkandl & Pauling, 1965). The analysis involved 5 amino acid sequences. All positions containing gaps and missing data were eliminated. There were a total of 295 positions in the final dataset. Evolutionary analyses were conducted by using program DNAMAN (Lynnon Corporation).

References

Zuckerkandl E. and Pauling L. Evolutionary divergence and convergence in proteins. Edited in Evolving Genes and Proteins by V. Bryson and H.J. Vogel. Academic Press, NY 1965 pp. 97-166.

Lindesmith LC, Donaldson EF, Lobue AD, Cannon JL, Zheng DP, Vinje J, Baric RS. Mechanisms of GII.4 norovirus persistence in human populations. PLoS Med. 2008 Feb;5(2):e31.

Journal of Virological Methods 181 (2012) 6–11

Contents lists available at SciVerse ScienceDirect

Journal of Virological Methods

journal homepage: www.elsevier.com/locate/jviromet

Purification of norovirus-like particles (VLPs) by ion exchange chromatography

Tiia Koho[a,e,1], Tuomas Mäntylä[a,1], Pasi Laurinmäki[b], Leena Huhti[c], Sarah J. Butcher[b], Timo Vesikari[c,d], Markku S. Kulomaa[a,e], Vesa P. Hytönen[a,e,*]

[a] Institute of Biomedical Technology, Biokatu 6, FI-33014 University of Tampere and Tampere University Hospital, Finland
[b] Institute of Biotechnology, Viikinkaari 1 (P. O. Box 65), FI-00014 University of Helsinki, Finland
[c] Vaccine Research Center, University of Tampere, Biokatu 10, FI-33520 Tampere, Finland
[d] Department of Pediatrics, Tampere University Hospital, Teiskontie 35, FI-33520 Tampere, Finland
[e] BioMediTech, Tampere, Finland

Article history:
Received 23 August 2011
Received in revised form 3 January 2012
Accepted 5 January 2012
Available online 14 January 2012

Keywords:
Norovirus
Virus-like particle
Ion exchange chromatography
Vaccines

A B S T R A C T

Recombinant expression of the norovirus capsid protein VP1 leads to self-assembly of non-infectious virus-like particles (VLPs), which are recognized as promising vaccine candidates against norovirus infections. To overcome the scalability issues connected to the ultracentrifugation-based purification strategies used in previous studies, an anion exchange-based purification method for norovirus VLPs was developed in this study. The method consists of precipitation by polyethylene glycol (PEG) and a single anion exchange chromatography step for purifying baculovirus-expressed GII.4 norovirus VLPs, which can be performed within one day. High product purity was obtained using chromatography. The purified material also contained fully assembled monodispersed VLPs, which were recognized by human sera containing polyclonal antibodies against norovirus GII.4.

1. Introduction

Noroviruses (formerly Norwalk-like viruses) infect people of all ages and are a major cause of acute nonbacterial gastroenteritis worldwide. Symptoms appear 12–48 h after viral infection and are characterized by acute onset of nausea, vomiting, abdominal cramps and diarrhea. Although norovirus gastroenteritis is generally mild and short (lasting normally 2–3 days), severe illness and complications can occur in the elderly, in children and in immunocompromised individuals (Glass et al., 2009; Patel et al., 2009). The virus is spread by food and water and *via* person-to-person contact.

Noroviruses are genetically diverse: currently over 30 different norovirus genotypes and numerous subgroups are known. These are classified into five different genogroups (GI–V). Human strains cluster into genogroups GI, GII and GIV and contain at least 25 genotypes. Despite the genetic diversity, only a few strains cause most of the cases of norovirus gastroenteritis, primarily those of genogroup II, genotype 4 (GII.4) (Glass et al., 2009; Patel et al., 2009). The genome of norovirus consists of single-stranded, positive-sense RNA that is approximately 7.6 kilobases in length and contains three open reading frames (ORFs). Structural studies have shown that the viral capsid is composed almost entirely of the 58 kDa VP1 protein encoded by ORF2 (Choi et al., 2008; Prasad et al., 1999).

Several different expression systems, including baculovirus-insect cell and transgenic plant expression systems, have been developed for the production of norovirus-like particles (Jiang et al., 1992; Mason et al., 1996; Santi et al., 2008). The recombinant expression of VP1 major capsid protein results in self-assembly of empty, non-infectious virus-like particles (VLPs) that are morphologically similar to the virion (Jiang et al., 1992).

For the development of vaccines against norovirus, an efficient purification method is essential. Methods used to purify norovirus VLPs include cesium chloride (CsCl) (Ausar et al., 2006) or sucrose (Mason et al., 1996) gradient ultracentrifugation, and combinations of the two (Jiang et al., 1992). However, the drawback of ultracentrifugation-based purification methods is the poor scalability and long process times required. Ultracentrifugation is also a demanding process, with significant batch-to-batch variation.

Recombinant norovirus VLPs could be used in immunization against norovirus and as a carrier to deliver other vaccine agents (Herbst-Kralovetz et al., 2010). However, to produce an adequate amount for vaccination purposes, a scalable and robust purification method is required. In this study, the development of a scalable and fast two-step purification method for norovirus VLPs is reported.

Abbreviations: VLP, virus-like particle; EM, electron microscopy; AEX, anion exchange; DLS, dynamic light scattering.

* Corresponding author at: Institute of Biomedical Technology, Biokatu 6, FI-33014 University of Tampere, Finland. Tel.: +358 40 1901517; fax: +358 33 5517710.
E-mail address: Vesa.Hytonen@uta.fi (V.P. Hytönen).

[1] These authors contributed equally to this work.

0166-0934/$ – see front matter © 2012 Elsevier B.V. All rights reserved.
doi:10.1016/j.jviromet.2012.01.003

The method consists of polyethylene glycol (PEG) precipitation followed by anion exchange (AEX) chromatography.

2. Materials and methods

2.1. Production and PEG precipitation of norovirus VLPs

The recombinant VP1 capsid monomers of GII.4 norovirus (GenBank accession number AF080551) were expressed in baculovirus-transformed *Spodoptera frugiperda* insect ovarian cells (Sf9; Invitrogen, Carlsbad, CA) cultured in HyQ SFX insect medium (HyClone; Thermo Fisher Scientific, Logan, UT) at 28 °C without antibiotics as described previously (Koho et al., 2012). The infected cells and cell culture medium were harvested 5 days post infection and stored at −20 °C until further use.

Norovirus VLPs were isolated from the cell culture supernatant. The supernatant was clarified by centrifugation at 5000 × *g* at 4 °C for 10 min. This step was followed by precipitation of VLPs from the clarified supernatant by the addition of PEG 6000 and sodium chloride to final concentrations of 7% (w/v) and 2% (w/v), respectively. The supernatant was then agitated at 4 °C for 4 h and centrifuged at 9500 × *g* at 4 °C for 30 min. This step can be performed at the liter-scale using standard centrifuges, such as a Sorvall RC5 or a Sorvall ST 40. Next, the supernatant was carefully removed, and the VLP-containing pellet was resuspended into 4–5 ml of 50 mM sodium phosphate buffer (pH 7.0) or PBS. The resuspended pellets were stored at −20 °C until further use. Total protein concentrations were analyzed using the Bradford method with bovine serum albumin as a standard.

2.2. Purification of norovirus VLP precipitate by anion exchange chromatography

The chromatographic purification of the VLPs was performed using a column packed with Q Sepharose XL anion exchange resin (5 ml HiTrap Q XL; GE Healthcare, Uppsala, Sweden). A flow rate of 150 cm/h was used throughout the chromatographic purification. The column was equilibrated with running buffer consisting of 50 mM sodium phosphate (pH 7.0). An aliquot from the thawed PEG-precipitated VLP suspension was diluted 1:5 in running buffer, mixed and centrifuged at 3500 × *g* at room temperature (20–23 °C) for 5 min before loading onto the chromatography column. Unbound proteins were washed out from the column with running buffer. Column-bound proteins were then eluted using a step gradient generated with elution buffer (1 M NaCl, 50 mM sodium phosphate, pH 7.0), and each of the steps (10%, 20% and 40% of elution buffer) lasted for 5 column volumes (CVs). Finally, the column was washed with 10 CVs of elution buffer and equilibrated with running buffer until a constant UV (280 nm) and conductivity baseline were observed. The VLP-containing chromatography fractions were pooled and stored at 4 °C until further use.

2.3. Purification of norovirus VLPs by cesium chloride ultracentrifugation

The thawed PEG-precipitated VLP suspension was diluted 1:5 in PBS, and 300 μl of this dilution was mixed with 4.6 ml of 2.5 M CsCl in PBS. This step was followed by ultracentrifugation at 115 878 × *g* at 15 °C for 24 h. The fractions containing norovirus VLPs were collected by bottom puncture, dialyzed against PBS, and then stored at 4 °C until further use.

2.4. SDS-PAGE and immunoblotting

The purity was confirmed by running 0.23 μg of protein (equal sample load/well) or equal sample volume (15 μl/well) in a 10% SDS-PAGE gel. The protein bands were visualized by staining the gel with silver stain (Page Silver; Fermentas, Burlington, Canada) or with Coomassie brilliant blue stain.

For immunoblotting, 0.45 μg of protein was loaded and resolved using a 12% SDS-PAGE gel (Ready Gel Tris–HCl Gel; Bio-Rad, Hercules, CA). Next, the protein bands were transferred onto a nitrocellulose membrane (Trans-Blot transfer membranes; Bio-Rad). The membrane was blocked overnight at 4 °C with 5% non-fat milk in Tris-buffered saline containing 0.05% Tween 20 (TBS-T). This step was followed by probing with 1:500 dilution of human antiserum against norovirus GII.4 in TBS-T containing 1% non-fat milk. This convalescent serum was from a patient that was shown to seroconvert (in ELISA) and had very high levels of NoV IgG and IgA. The patient (14 years old) had GII-4 infection (confirmed by PCR analysis from stool). HRP-conjugated anti-human IgG produced in goat (Invitrogen) was used as a secondary antibody at a dilution of 1:10 000 in TBS-T containing 1% non-fat milk. The membrane was washed 4 × 5 min with TBS-T after both of the incubations in primary and secondary antibody dilutions. The bands were detected using an Opti-4CN detection kit (Bio-Rad).

For the detection of baculovirus in the samples, equal sample volumes (15 μl/well) were loaded and resolved in a 10% SDS-PAGE gel. A baculovirus positive control was loaded in a volume of 3 μl. The immunoblotting was performed as above with the exceptions that mouse anti-baculovirus gp64 (Santa Cruz Biotechnology, Santa Cruz, CA) was used as the primary antibody at a dilution of 1:1000 and alkaline phosphatase-conjugated anti-mouse antibody (Sigma, St. Louis, MO) generated in goat was used as the secondary antibody at a dilution of 1:20 000. The bands were detected using a BCIP/NBT-solution as a substrate for alkaline phosphatase.

2.5. Particle size analysis and cryo-electron microscopy

The purified norovirus VLP samples were analyzed for particle size using dynamic light scattering (DLS) and cryo-electron microscopy (cryo-EM) to assess their hydrodynamic radius and homogeneity. The hydrodynamic diameters of particles were analyzed using a Zetasizer Nano ZS DLS device (Malvern Instruments, Malvern, UK). The results were calculated as averages of six consecutive measurements recorded at 20 °C. Pre-determined viscosity and refractive index values were used in particle size calculations.

For the cryo-EM analysis, the vitrified samples of the purified VLP solution were prepared on Quantifoil grids with 2 μm holes as previously described (Baker et al., 1999). Three microliter of sample was applied onto Quantifoil holey carbon film grids (Quantifoil Micro Tools, Jena, Germany). The grids were vitrified by rapid plunging into liquid-nitrogen cooled ethane. A Gatan 626 cryoholder was used to observe the sample in an FEI Tecnai F20 field emission gun transmission electron microscope at 200 kV under low-dose conditions (~20 e/A^2) at −180 °C. The images were recorded using a Gatan Ultrascan 4000 CCD camera at nominal magnification of 68 000× resulting in a final sampling of the images at 0.22 nm/pixel.

3. Results

3.1. Expression and purification of VP1

Recombinant protein was recovered from clarified cell culture supernatant by PEG precipitation. An aliquot of precipitate was then diluted and subjected to further purification with either anion exchange chromatography or CsCl gradient equilibrium ultracentrifugation. In the chromatographic purification, column-bound VLPs were eluted using a step gradient. The VLPs eluted from the column at a NaCl concentration between 0.1 and 0.2 M

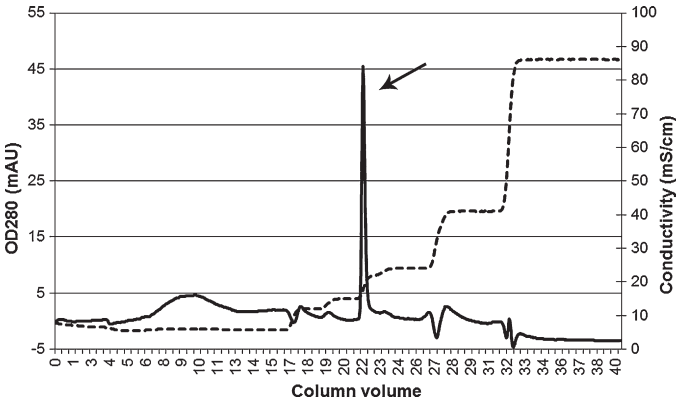

Fig. 1. Chromatographic purification of PEG-precipitated norovirus VLPs. PEG-precipitated VLPs were diluted into running buffer (50 mM sodium phosphate, pH 7.0) and loaded onto an anion exchange column packed with Q Sepharose XL resin. The column bound VLPs were eluted by step gradient created using 1 M NaCl, 50 mM sodium phosphate (pH 7.0) as elution buffer. (—), OD280; (- -), conductivity; the elution of VLPs is indicated by an arrow.

(conductivity 14.5–21 mS/cm) (Fig. 1). Fractions containing the VP1 protein were pooled. The purification of the VP1 proteins by AEX chromatography or CsCl gradient ultracentrifugation resulted in a yield of approximately 10 mg/l culture and 35 mg/l culture, respectively.

3.2. AEX chromatography-purified VLPs are recognized by norovirus-specific antibodies, and show high purity in SDS-PAGE

The purity and antigenic properties of norovirus VLPs were evaluated by SDS-PAGE and immunoblotting. As shown in Fig. 2A and B (lanes 2–4), the VP1 protein was efficiently precipitated from the clarified cell harvest, whereas many of the host cell protein contaminants remained in the supernatant. Due to relatively low concentration, no clear signal of VP1 protein was detected in the starting material analyzed using SDS-PAGE and detected using either Coomassie staining or immunoblotting (Fig. 2, lane 5). However, after purification, clear norovirus-specific bands were detected indicating that the VP1 protein was significantly concentrated compared to the contaminating impurities.

Similar double bands were observed in SDS-PAGE analysis performed on samples taken from batches purified with either AEX chromatography or CsCl ultracentrifugation (Fig. 2). All of the samples contained two distinct bands with approximate molecular weights of 58 kDa and 55 kDa. Both of these bands have previously been confirmed to consist of norovirus VP1 protein (Koho et al., 2012). There were no additional visible bands observed on any of the samples analyzed. The purity of the purified material was estimated to be >95% (Fig. 3, lane 3). Immunoblot analysis confirmed that VP1 protein could be recognized and detected from purified norovirus VLP samples using human serum containing polyclonal antibodies against norovirus GII.4 (Fig. 2). No residual baculovirus-related impurities were detected in the purified material (Fig. 4).

3.3. Cryo-EM and DLS confirm the correct structure and homogeneity of the purified VLPs

The cryo-EM and particle size analysis using DLS technique confirmed the assembly of VP1 protein into monodisperse viral-like particles (Figs. 5 and 6). Although slight clustering of VLPs was observed in cryo-EM analysis, no deformation of the VLPs was detected. The particle size analysis performed on diluted PEG-precipitated norovirus VLPs (the starting material for AEX chromatography) indicated the presence of more than one size

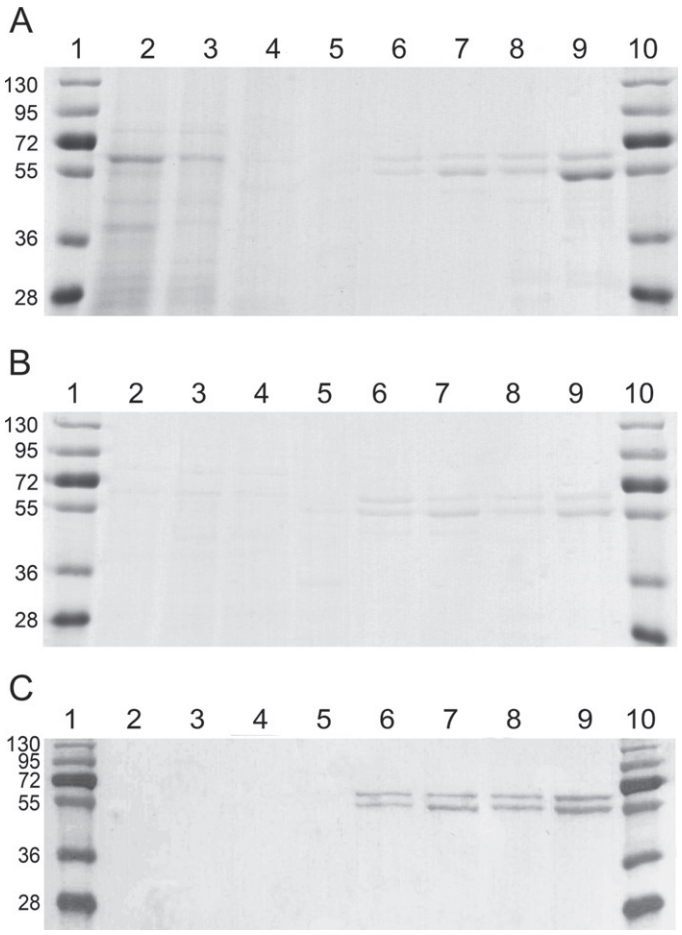

Fig. 2. SDS-PAGE and immunoblot analyses of samples collected during purification of different VLP batches. Samples of 15 μl (A) or equal amount (B) of protein (0.23 μg of protein/well) were analyzed by SDS-PAGE. For the immunoblot analysis equal amounts of protein (0.45 μg of protein/well) were loaded into each well (C). The analysis was performed using norovirus-positive human serum. Lanes 1 and 10: molecular weight marker; lane 2: total cell lysate; lane 3: cell lysate after clarification by centrifugation; lane 4: supernatant from PEG precipitation; lane 5: starting material for chromatography; lanes 6 and 7: VLP-containing fractions from AEX chromatography; lanes 8 and 9: VLP-containing fractions from CsCl ultracentrifugation.

particle population (Fig. 6). However, after the chromatographic purification, a single narrow peak in particle size distribution (by intensity) was observed. An average particle size (hydrodynamic diameter) of approximately 50 nm was measured for VLPs purified by anion exchange chromatography (Table 1). Polydispersity index (PDI) describes how much the data measured by DLS deviates from single-exponential-fitted autocorrelation function. Thereby, it is a measure of deviation from perfectly monodisperse particle solution. PDI value was calculated by the DLS instrument software. The description for the calculation of PDI is described in International Standard on DLS: ISO 13321:1996. For VLPs purified by anion exchange chromatography, PDI was below 0.1. This result suggests that samples contained monodisperse and pure VLPs after chromatographic purification.

An intensity-based analysis of CsCl-purified VLPs by DLS revealed the presence of particles with an average hydrodynamic diameter of approximately 45 nm (Table 1). The mean polydispersity index was below 0.3. There was more batch-to-batch variation observed after CsCl purification when compared to that observed after AEX chromatography.

The stability of the AEX chromatography-purified VLPs during long-term storage was also determined. The particle size of

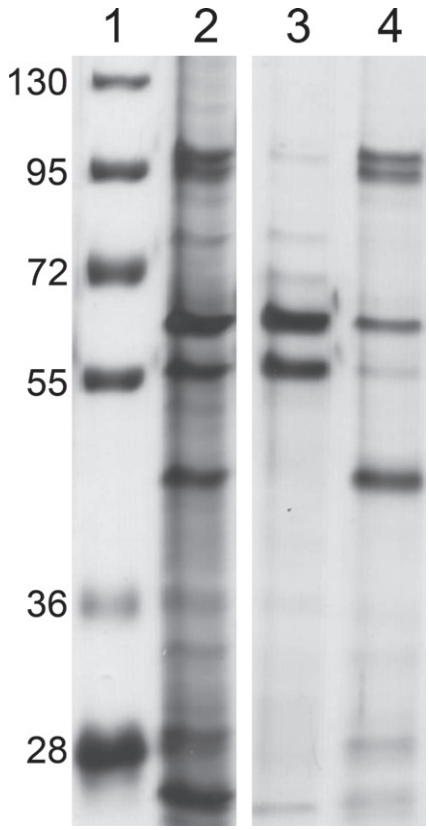

Fig. 3. Analysis of AEX chromatography-purified VLPs using SDS-PAGE. Maximal sample volumes were loaded into each well. The gel was silver-stained to maximize the detection sensitivity. Lane 1: molecular weight marker; lane 2: starting material for chromatography; lane 3: VLP-containing fraction from chromatography; lane 4: high salt wash fraction from chromatography.

the material purified by anion exchange chromatography was re-analyzed by DLS technique after 4 months of storage at 4 °C, in the absence of preservative agents. No change in the average particle size or polydispersity index of the VLP sample that had a higher initial particle concentration was detected (Table 1; batch 1). However, in the case of the second batch purified by anion exchange chromatography, a slight increase in both of these values was observed. This result indicates that the material might have started to slightly aggregate during storage. To prevent this aggregation, detergents or alternative buffer components could be useful (Shi et al., 2005).

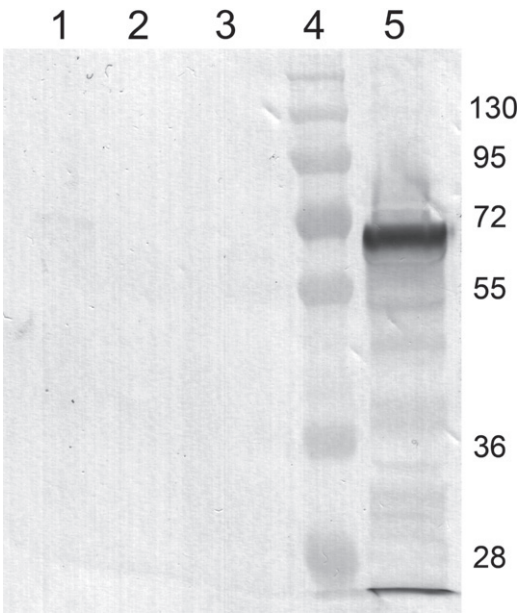

Fig. 4. Immunoblot analysis using anti-baculovirus antibody. Equal volumes (15 μl) of each protein sample were loaded into each well for SDS-PAGE analysis. Lanes 1 and 2: VLP-containing fractions from AEX chromatography; lane 3: VLP fraction from CsCl ultracentrifugation; lane 4: molecular weight marker; lane 5: baculovirus-positive control (3 μl/well). Analyzed AEX chromatography fractions were collected from purification of two different VLP batches.

4. Discussion

Despite the diverse methods for VLP extraction and purification available, in general, norovirus VLPs have been produced based on only a few variations of centrifugation and precipitation methods (Herbst-Kralovetz et al., 2010). PEG precipitation has been used in several previous studies, and it appears to be an efficient method for the precipitation of norovirus VLPs. PEG precipitation alone, however, is not sufficient for the separation of VLPs from various source material substances. The use of VLPs in vaccines would require highly pure material, and therefore, additional purification steps are necessary. Furthermore, PEG-precipitated VLP samples contained larger particles (see Fig. 6), and PEG itself may be a harmful contaminant in some applications. High concentration of PEG can potentially lead to VLP instability (Huhti et al., 2010) and can interfere the downstream VLP applications (Russell et al., 2007). However, in the current study, we found ion-exchange chromatography suitable for efficient removal of PEG and

Table 1
Particle size analysis of norovirus VLP samples purified by different purification methods. Hydrodynamic diameters were calculated as averages of six consequent measurements.

Sample	Measurement time point	*Z*-average (diameter in nm)[a]	PDI[b]	Size (diameter in nm)[c]	
PEG precipitate	Before AEX/CsCl	81.7	0.584	Peak 1	44.8 (76.3%)
				Peak 2	1593 (22.7%)
				Peak 3	4968 (0.9%)
AEX – 1st batch	After purification	50.1	0.046	Peak 1	45.0 (100%)
	4 months at 4 °C	49.9	0.068	Peak 1	44.6 (100%)
AEX – 2nd batch	After purification	49.5	0.042	Peak 1	44.7 (100%)
	4 months at 4 °C	52.1	0.167	Peak 1	43.9 (99.7%)
				Peak 2	5052 (0.3%)
CsCl – 1st batch	After purification	40.6	0.102	Peak 1	34.5 (100%)
CsCl – 2nd batch	After purification	50.4	0.270	Peak 1	30.8 (98.5%)
				Peak 2	692 (0.4%)
				Peak 3	2744 (1.0%)

[a] The mean hydrodynamic diameter of particles calculated from the signal intensity distribution.
[b] Polydispersity index.
[c] The mean hydrodynamic diameter of particles calculated from volume distribution. Percentages of peak distributions by volume are given in parenthesis.

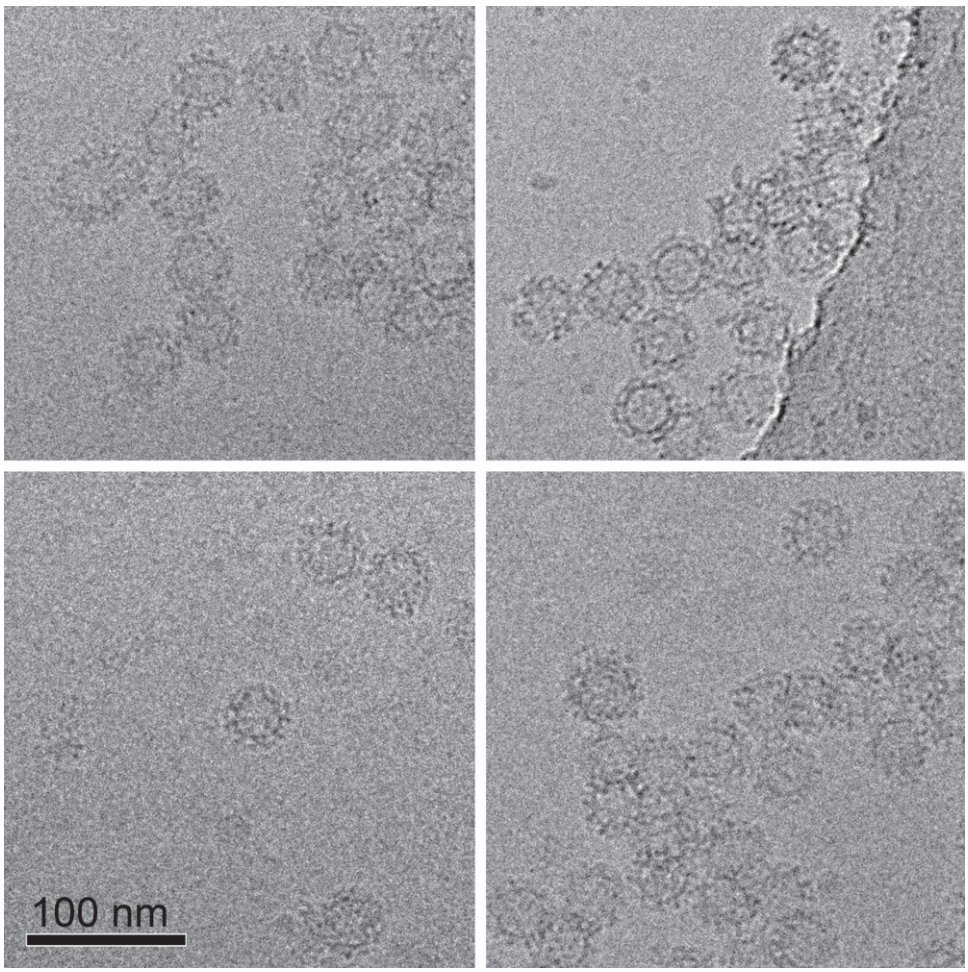

Fig. 5. Cryo-electron micrograph of norovirus VLPs. Scale bar: 100 nm.

the produced particles were monodisperse (Fig. 6). The benefit of PEG precipitation is that it efficiently decreases the sample volume before loading into the chromatography column. VLPs, like native viruses, are typically purified based on their size and density using ultracentrifugation techniques, with sucrose and CsCl being the most commonly used reagents for gradient generation. However, these methods are not practical for large-scale vaccine manufacturing because they are time-consuming, difficult to scale up, and produce poor yields (Herbst-Kralovetz et al., 2010). To circumvent the limitations of traditional VLP purification methods, an alternative downstream purification process is highly desirable. In this study, a purification method for norovirus VLPs was developed. The two-step purification method is based on PEG precipitation and a subsequent anion exchange chromatography step. The purification procedure results in fully assembled VLPs with high purity (>95%), and the purification protocol can easily be performed within one working day.

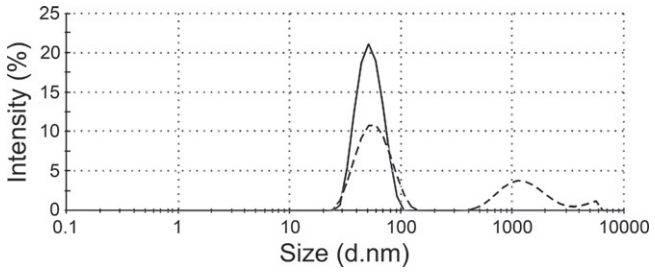

Fig. 6. Particle size distribution of PEG-precipitated VLPs (dashed line) and VLP-containing pool fraction after chromatographic purification (solid line). Samples were measured by dynamic light scattering at 20 °C. Results were calculated as an average of six consecutive measurements using the Stokes–Einstein equation. Pre-determined viscosity and refractive index values were used in particle size calculations.

Despite the vast number of studies focusing on noroviruses and norovirus VLPs, there are only two previous studies where a chromatographic purification method has been applied for norovirus VLPs. Kissmann et al. (2008) reported a purification protocol consisting of ammonium sulfate precipitation and a chromatographic purification process that involved three different chromatography columns. However, their main objective was not to develop a chromatographic purification method, but rather to determine the effect of different stabilizers on norovirus VLP stability. In the same year, Chen (2008) reported a scalable purification process for plant-expressed norovirus VLPs that was based on low pH precipitation and chromatographic steps.

Both Kovac et al. (2009) and Schultz et al. (2010) reported the employment of anion exchange chromatography coupled with a novel Convective Interaction Media® (CIM) monolithic matrix (BIA Separations, Slovenia) to concentrate noroviruses from bottled water. Additionally, other novel chromatographic matrices and strategies are being developed that aim to improve the recovery and binding capacities of viruses and VLPs (reviewed in Herbst-Kralovetz et al., 2010; Pattenden et al., 2005). Because the physicochemical properties of native VLPs and genetically modified VLPs vary significantly, it is unlikely that the same

chromatographic purification method could be applied in all cases. However, chromatographic methods offer several advantages over centrifugation-based methods, and it remains to be seen if some of these novel chromatography technologies show clear advantages over others in large-scale experimentation.

Two bands were detected during the analysis of purified norovirus VLP samples with SDS-PAGE and immunoblotting. A similar banding pattern has also been detected and reported in other studies (Bertolotti-Ciarlet et al., 2003; Jiang et al., 1992; Tan et al., 2004). We reported previously that both 55 kDa and 58 kDa bands consisted of norovirus GII.4 capsid protein (VP1) as confirmed by fingerprinting mass spectrometry analysis (Koho et al., 2012). The reason for the presence of two different protein forms in norovirus VLP is currently unknown. However, the smaller form is known to represent the VP1 protein missing the 34 N-terminal amino acid residues, while the larger band represents the full-length VP1 (Koho et al., 2012). Interestingly though, the high salt wash fraction from chromatography (Fig. 3, lane 4) contained some remaining VP1 protein with different ratio of full-length to shorter form, the vast majority of protein being in the full-length form. The phenomenon could indicate that VLPs assembled of the full-length VP1s bind to the column with higher affinity and, thus, higher salt concentration is needed for their elution. In favor of this hypothesis, the evaluation of the characteristics of VP1 forms with Protparam tool (http://web.expasy.org/protparam/) reveals a pI of 5.59 for the full-length form, whereas N-terminally truncated protein has a pI of 5.95.

The norovirus particles had a diameter of approximately 39 nm by cryoEM as reported previously (Prasad et al., 1999). The difference between the particle sizes reported by cryoEM and DLS are explained by the different methods used. In the DLS method, a water layer is included around the particle and calculated into the hydrodynamic radius, typically leading to an apparent diameter increase of approximately 5 nm when compared to other methods (Malvern Instruments Ldt., 2009). Importantly, the purified material was shown to contain monodispersed particles; furthermore, the samples were stable and monodisperse even after 4-month storage in a refrigerator.

This study demonstrates that a total yield of approximately 10 mg of VP1 protein could be obtained using anion exchange chromatography from 1 l of insect cell culture transfected with recombinant baculovirus. The yield can, however, be improved by process optimization. Higher VLP concentrations were obtained using the CsCl gradient ultracentrifugation method as compared to anion exchange chromatography (Fig. 2A). Although gradient ultracentrifugation-based methods are useful tools for effectively isolating small-scale quantities of VLPs for research purposes, they are not practical for large-scale vaccine manufacturing mainly due to the difficulties in method scale-up. Before material purified with either of these two methods can be used for example in experiments *in vivo*, a formulation step is required. This step is especially important in the case of CsCl purified material due to the high concentration of salt. Tangential flow filtration (TFF) is a technique that could be utilized for this purpose. In addition to buffer exchange, TFF could be used to concentrate the product to the required particle concentration.

5. Conclusions

The purification of GII.4 norovirus VLPs by anion exchange chromatography provides a fast and scalable alternative to more time consuming and non-scalable ultracentrifugation-based purification methods. High particle purity was obtained, and the purified VLPs were stable for over 4 months in storage without further treatments or preservatives.

Acknowledgements

The authors thank Ulla Kiiskinen and Soili Hiltunen for assistance with insect cell cultures and preparation of reagents and buffers. The authors also thank The Biocenter Finland National Cryo-Electron Microscopy Unit, Institute of Biotechnology, Helsinki University for providing facilities. The work was supported by grants from the Academy of Finland (115976), Sigrid Jusélius Foundation, Competitive Research Funding of the Tampere University Hospital [Grants 9K063, 9J046, 9M019 and 9M042], and from The National Doctoral Programme in Informational and Structural Biology (ISB).

References

Ausar, S.F., Foubert, T.R., Hudson, M.H., Vedvick, T.S., Middaugh, C.R., 2006. Conformational stability and disassembly of Norwalk virus-like particles. Effect of pH and temperature. J. Biol. Chem. 281, 19478–19488.

Baker, T.S., Olson, N.H., Fuller, S.D., 1999. Adding the third dimension to virus life cycles: three-dimensional reconstruction of icosahedral viruses from cryo-electron micrographs. Microbiol. Mol. Biol. Rev. 63, 862–922.

Bertolotti-Ciarlet, A., Crawford, S.E., Hutson, A.M., Estes, M.K., 2003. The 3′ end of Norwalk virus mRNA contains determinants that regulate the expression and stability of the viral capsid protein VP1: a novel function for the VP2 protein. J. Virol. 77, 11603–11615.

Chen, Q., 2008. Expression and purification of pharmaceutical proteins in plants. Biol. Eng. 1, 291–321.

Choi, J.M., Hutson, A.M., Estes, M.K., Prasad, B.V., 2008. Atomic resolution structural characterization of recognition of histo-blood group antigens by Norwalk virus. Proc. Natl. Acad. Sci. U.S.A. 105, 9175–9180.

Glass, R.I., Parashar, U.D., Estes, M.K., 2009. Norovirus gastroenteritis. N. Engl. J. Med. 361, 1776–1785.

Herbst-Kralovetz, M., Mason, H.S., Chen, Q., 2010. Norwalk virus-like particles as vaccines. Expert Rev. Vaccines 9, 299–307.

Huhti, L., Blazevic, V., Nurminen, K., Koho, T., Hytönen, V.P., Vesikari, T., 2010. A comparison of methods for purification and concentration of norovirus GII-4 capsid virus-like particles. Arch. Virol. 155, 1855–1858.

Jiang, X., Wang, M., Graham, D.Y., Estes, M.K., 1992. Expression, self-assembly, and antigenicity of the Norwalk virus capsid protein. J. Virol. 66, 6527–6532.

Kissmann, J., Ausar, S.F., Foubert, T.R., Brock, J., Switzer, M.H., Detzi, E.J., Vedvick, T.S., Middaugh, C.R., 2008. Physical stabilization of Norwalk virus-like particles. J. Pharm. Sci. 97, 4208–4218.

Koho, T., Huhti, L., Blazevic, V., Nurminen, K., Butcher, S., Laurinmäki, P., Kalkkinen, N., Rönnholm, G., Vesikari, T., Hytönen, V.P., Kulomaa, M.S., 2012. Production and characterization of virus-like particles and the P domain protein of GII.4 norovirus. J. Virol. Methods 179, 1–7.

Kovac, K., Gutierrez-Aguirre, I., Banjac, M., Peterka, M., Poljsak-Prijatelj, M., Ravnikar, M., Mijovski, J.Z., Schultz, A.C., Raspor, P., 2009. A novel method for concentrating hepatitis A virus and caliciviruses from bottled water. J. Virol. Methods 162, 272–275.

Malvern Instruments Ldt., 2009. Zetasizer Nano Series User Manual. MAN0317-4.0.

Mason, H.S., Ball, J.M., Shi, J.J., Jiang, X., Estes, M.K., Arntzen, C.J., 1996. Expression of Norwalk virus capsid protein in transgenic tobacco and potato and its oral immunogenicity in mice. Proc. Natl. Acad. Sci. U. S. A. 93, 5335–5340.

Patel, M.M., Hall, A.J., Vinje, J., Parashar, U.D., 2009. Noroviruses: a comprehensive review. J. Clin. Virol. 44, 1–8.

Pattenden, L.K., Middelberg, A.P., Niebert, M., Lipin, D.I., 2005. Towards the preparative and large-scale precision manufacture of virus-like particles. Trends Biotechnol. 23, 523–529.

Prasad, B.V., Hardy, M.E., Dokland, T., Bella, J., Rossmann, M.G., Estes, M.K., 1999. X-ray crystallographic structure of the Norwalk virus capsid. Science 286, 287–290.

Russell, B.J., Velez, J.O., Laven, J.J., Johnson, A.J., Chang, G.J., Johnson, B.W., 2007. A comparison of concentration methods applied to non-infectious flavivirus recombinant antigens for use in diagnostic serological assays. J. Virol. Methods 145, 62–70.

Santi, L., Batchelor, L., Huang, Z., Hjelm, B., Kilbourne, J., Arntzen, C.J., Chen, Q., Mason, H.S., 2008. An efficient plant viral expression system generating orally immunogenic Norwalk virus-like particles. Vaccine 26, 1846–1854.

Schultz, A.C., Perelle, S., Di Pasquale, S., Kovac, K., De Medici, D., Fach, P., Sommer, H.M., Hoorfar, J., 2010. Collaborative validation of a rapid method for efficient virus concentration in bottled water. Int. J. Food Microbiol.

Shi, L., Sanyal, G., Ni, A., Luo, Z., Doshna, S., Wang, B., Graham, T.L., Wang, N., Volkin, D.B., 2005. Stabilization of human papillomavirus virus-like particles by non-ionic surfactants. J. Pharm. Sci. 94, 1538–1551.

Tan, M., Zhong, W., Song, D., Thornton, S., Jiang, X., 2004. *E. coli*-expressed recombinant norovirus capsid proteins maintain authentic antigenicity and receptor binding capability. J. Med. Virol. 74, 641–649.

Antiviral Research 104 (2014) 93–101

Contents lists available at ScienceDirect

Antiviral Research

journal homepage: www.elsevier.com/locate/antiviral

Coxsackievirus B3 VLPs purified by ion exchange chromatography elicit strong immune responses in mice

Tiia Koho [a], Minni R.L. Koivunen [b], Sami Oikarinen [c], Laura Kummola [d,f], Selina Mäkinen [a], Anssi J. Mähönen [a], Amirbabak Sioofy-Khojine [c], Varpu Marjomäki [e], Artur Kazmertsuk [e], Ilkka Junttila [d,f], Markku S. Kulomaa [a], Heikki Hyöty [c,d,f], Vesa P. Hytönen [a,f], Olli H. Laitinen [b,g,*]

[a] BioMediTech, University of Tampere and Tampere University Hospital, Biokatu 6, FI-33014 University of Tampere, Finland
[b] Vactech Ltd, Biokatu 8, FI-33520 Tampere, Finland
[c] Department of Virology, School of Medicine, Biokatu 10, FI-33014 University of Tampere, Finland
[d] School of Medicine, FI-33014 University of Tampere, Finland
[e] Department of Biological and Environmental Science/Nanoscience Center, University of Jyväskylä, P.O. Box 35, FI-40014 University of Jyväskylä, Finland
[f] Fimlab Laboratories, Pirkanmaa Hospital District, Biokatu 4, FI-33520 Tampere, Finland
[g] The Center for Infectious Medicine, Department of Medicine HS, Karolinska Institutet, Karolinska University Hospital Huddinge F59, SE-141 86 Stockholm, Sweden

ARTICLE INFO

Article history:
Received 14 October 2013
Revised 20 December 2013
Accepted 20 January 2014
Available online 28 January 2014

Keywords:
VLP
CVB3
Ion exchange chromatography

ABSTRACT

Coxsackievirus B3 (CVB3) is an important cause of acute and chronic viral myocarditis, and dilated cardiomyopathy (DCM). Although vaccination against CVB3 could significantly reduce the incidence of serious or fatal viral myocarditis and various other diseases associated with CVB3 infection, there is currently no vaccine or therapeutic reagent in clinical use. In this study, we contributed towards the development of a CVB3 vaccine by establishing an efficient and scalable ion exchange chromatography-based purification method for CVB3 virus and baculovirus-insect cell-expressed CVB3 virus-like particles (VLPs). This purification system is especially relevant for vaccine development and production on an industrial scale. The produced VLPs were characterized using a number of biophysical methods and exhibited excellent quality and high purity. Immunization of mice with VLPs elicited a strong immune response, demonstrating the excellent vaccine potential of these VLPs.

1. Introduction

Coxsackievirus B3 (CVB3) is an important human pathogen that frequently causes mild infections (Melnick, 1996) but can also lead to serious diseases affecting the heart, pancreas, or central nervous system. CVB3 is among the most common causes of acute and chronic viral myocarditis, which can lead to dilated cardiomyopathy (DCM), often requiring heart transplantation (Selinka et al., 2004; Maier et al., 2004). In addition, CVB3 is associated with meningitis (Wong et al., 2011) and inflammatory diseases of the pancreas (Mena et al., 2000), and it is known to infect stem cells in the neonatal central nervous system (Feuer et al., 2003).

CVB3 is a non-enveloped virus within the genus *Enterovirus* in the *Picornaviridae* family. The 7.4-kb, single-stranded positive-sense RNA genome consists of a single open reading frame (ORF) that is translated into a single long polypeptide containing the P1–P3 regions. The P1 region is further processed by a viral protease to produce the four capsid proteins, VP0 (further cleaved to give VP4 and VP2 during viral maturation), VP3, and VP1. The P2 and P3 regions are processed into seven nonstructural proteins that have roles in polyprotein cleavage and RNA replication (Krausslich et al., 1988; Klump et al., 1990). The single ORF is flanked by a 5′ non-coding region (5′NCR) and a polyadenylated 3′NCR.

Sixty copies of VP1–VP4 form the ~30 nm capsid, which contains canyon-like structures that allow viral attachment through interactions with the host-cell proteins coxsackievirus and adenovirus receptor (CAR) and decay-accelerating factor (DAF) (Park et al., 2009; Bergelson et al., 1994, 1997). Although the VP1 protein contains the main antigenic determinants (Haarmann et al., 1994), changes in the 5′NCR of the genome (Tu et al., 1995; Dunn et al., 2003), as well as in the VP2 and VP3 regions of the capsid, have been found to attenuate the virulence of CVB3 (Knowlton et al., 1996; Stadnick et al., 2004; Park et al., 2009). Potential

Abbreviations: CVB3, Coxsackievirus B3; VLP, virus like particle; DCM, dilated cardiomyopathy; ORF, open reading frame; IEX, ion exchange chromatography.

* Corresponding author at: The Center for Infectious Medicine, Department of Medicine HS, Karolinska Institutet, Karolinska University Hospital Huddinge F59, SE-141 86 Stockholm, Sweden. Tel.: +358 503427273.
E-mail address: olli.laitinen@ki.se (O.H. Laitinen).

http://dx.doi.org/10.1016/j.antiviral.2014.01.013
0166-3542/

CVB-specific T cell epitopes have been mapped to both VP1 and VP2 regions (Huber et al., 1993; Voigt et al., 2010).

Although vaccination against CVB3 could significantly reduce the incidence of serious or fatal viral myocarditis and various other diseases associated with CVB3 infection, there is currently no vaccine or therapeutic reagent in clinical use. In the first attempt to develop a CVB3-specific vaccine, a temperature-sensitive mutant virus was found to elicit serum-neutralizing anti-CVB3 antibodies in mice after vaccination (Godney et al., 1987). Since then, several approaches have been used to demonstrate the potential usefulness of vaccination against CVB3, including a subunit vaccine (Fohlman et al., 1990), several DNA vaccines (Henke et al., 1998; Kim et al., 2005; Xu et al., 2004), and attenuated or inactivated virus vaccines (See and Tilles, 1994; Zhang et al., 1997; Dan and Chantler, 2005; Park et al., 2009; Kim and Nam, 2011). However, these vaccines may have safety issues, or they might not stimulate an ideal immune response (Goldman and Lambert, 2004). Virus-like particles (VLPs) represent a new promising vaccine technology that can overcome these disadvantages, as they offer equally efficient but safer protection than inactivated or live-attenuated viral vaccines.

VLPs are formed by the self-assembly of recombinant viral structural proteins. VLPs are structurally and antigenically similar to the parental infectious virus, but lack viral nucleic acid and are therefore noninfectious. Consequently, they do not carry the risk of reversion to a virulent form. In addition, VLPs lack the safety concerns related to inactivation failures, which may occur when inactivated virus-based vaccines are used. VLPs are highly immunogenic because they present viral epitopes in an authentic conformation and because their receptor binding properties are similar to those of the infective virus (Grgacic and Anderson, 2006; Roy and Noad, 2008). Importantly, the size of VLPs allows uptake by dendritic cells (Fifis et al., 2004). Therefore, VLP vaccines are able to stimulate both humoral and cellular immune responses, overcoming a common major drawback encountered with traditional subunit vaccines (Grgacic and Anderson, 2006). VLPs have emerged as a safe and effective strategy for vaccine development targeting viral diseases (reviewed in Grgacic and Anderson (2006) and Jennings and Bachmann (2008)). Since the first VLP-based vaccines were licensed for clinical use against human papillomavirus (Gardasil, Cervarix) and hepatitis B virus (Recombivax HB, Engerix), VLP vaccine candidates have been developed for many different types of viruses, including enteroviruses (Zhang et al., 2012; Liu et al., 2012; Chung et al., 2008; Rombaut and Jore, 1997). In this study, a scalable and efficient chromatographic production method was developed for CVB3 VLPs. The potential of the resulting high-quality particles to serve as a vaccine was studied by immunizing mice, which resulted in strong immune responses and high titers of neutralizing antibodies.

2. Materials and methods

2.1. Design and construction of the CVB3 VLP transfer vector and generation of the VLP-producing recombinant baculovirus

Baculoviral transfer vector pFastBac™ Dual (Invitrogen, Carlsbad, CA) containing the desired inserts was ordered from GENEART AG (Regensburg, Germany). The fully sequenced CVB3 strain (GenBank accession number M33854.1) was chosen as a template. The construct contained two separate cassettes (Fig. 1). The first cassette contained the P1 region of the CVB3 strain M33854.1 and the second cassette contained the whole CVB3 genome with the exception of the P1 region, which was replaced with a mCherry coding sequence followed by an artificial recognition site for the enteroviral 3A protease.

The recombinant baculovirus was generated according to the instructions given with the Bac-to-Bac® Baculovirus Expression System (Invitrogen) with the exception that the cassettes were transferred into the F-bacmid baculovirus genome (Karkkainen et al., 2009). An empty pFastBac™ Dual baculoviral transfer vector was used for the generation of empty baculoviruses.

2.2. Production and purification of the CVB3 VLPs

The CVB3 VLPs were expressed in baculovirus-transformed *Spodoptera frugiperda* insect cells (Sf9; Invitrogen) and harvested 5–6 days post-infection. After clarification by centrifugation (10,409×*g* at 4 °C for 20 min), CVB3 VLPs were concentrated from the clarified cell culture supernatant by polyethylene glycol (PEG) precipitation and detergent-treated as previously described (Abraham and Colonno, 1984). The precipitated VLPs were then recovered by centrifugation (10,409×*g* at 4 °C for 5 min) and diluted 1:10 with 20 mM Tris–HCl (pH 7.5) prior to loading onto the chromatography column.

Chromatographic ion exchange purification (IEX) of the pretreated VLPs was performed using monolithic columns (6.7 mM ID × 4.2 mM, V: 1 ml) based on CIM Convective Interaction Media® technology from BIA Separations (Ljubljana, Slovenia) with either quaternary amine (QA) or sulfate (SO3) chemical functionalization. The details of the purification protocol are described in the Supplementary data.

Sf9 insect cells infected with the empty baculovirus were subjected to the same purification process, and the product served as the negative control antigen in the mouse immunization studies.

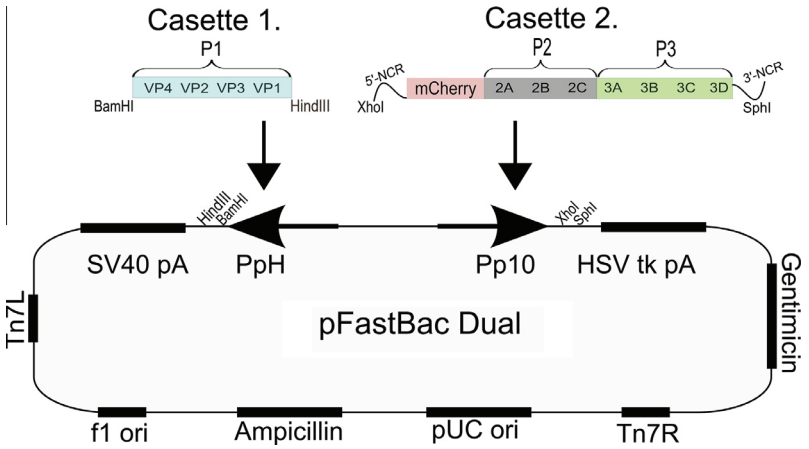

Fig. 1. Cloning of the CVB3 VLP cassettes into the pFastBac™ Dual baculoviral transfer vector.

2.3. Culturing and purification of the CVB3 virus

The CVB3 virus (a Moldova strain variant, GenBank: AY896763.1), was propagated in green monkey kidney cells (GMK) cultured at 37 °C with 5% CO_2 in HyClone SFM4MegaVir protein-free medium (Thermo Fisher Scientific) containing 2 mM L-glutamine and 0.1% penicillin–streptomycin. A MOI of 0.5 plaque-forming units (PFU)/cell was used for the infections. After 2 days of incubation, the viruses were harvested by repeated freeze–thaw cycles and centrifugation (9605×*g* at 4 °C for 20 min). The viruses were precipitated with PEG and detergent-treated as described in Section 2.2. The precipitated viruses were further purified by ultracentrifugation with a 20–5% (w/v) discontinuous sucrose gradient (103,864×*g* at 4 °C for 4 h). The virus-containing fractions were pooled, pelleted, and resuspended in 200–300 μl of Dulbecco's PBS (DPBS) containing Ca/Mg.

The chromatographic purification of the precipitated viruses was performed using a monolithic column (6.7 mM ID × 4.2 mM, V: 1 ml) based on CIM Convective Interaction Media® technology from BIA Separations with the quaternary amine (QA) chemistry. Details of the purification protocol are described in the Supplementary data. The virus titers were determined based on the cytopathic effect (CPE) in infected GMK cells.

2.4. Characterization of the CVB3 VLPs and virus

VLPs and virus samples were run on 12% SDS–PAGE gels and analyzed by Western blotting using either the mouse anti-enterovirus clone 5-D8/1 (DAKO, Glostrup, Denmark) or the mouse anti-baculovirus gp64 clone AcV5 (Santa Cruz Biotechnology Inc., Heidelberg, Germany) at a dilution of 1:3000 and 1:1000, respectively, followed by incubation with an HRP-labeled horse antibody against mouse immunoglobulins (Vector Laboratories Inc., Burlingame, CA) diluted 1:20,000. The samples were visualized using the ECL detection substrate (Thermo Scientific). For assessment of the total protein content, the samples were run on 12% SDS–PAGE gels and subsequently visualized by silver staining (Pierce Silver Stain Kit, Thermo Scientific). The total protein concentrations of the fractions were analyzed using the Pierce BCA Protein Assay kit (Thermo Scientific). The total DNA concentrations of the VLP fractions were analyzed using Quant-iT™ dsDNA Broad-Range Assay Kit (Invitrogen), and the number of baculovirus genomes in the fractions was determined using a qRT-PCR kit (BacPAK™ qPCR titration kit, Clontech Laboratories, Mountain View, CA).

Dynamic light scattering (DLS) analysis was performed with a Zetasizer Nano ZS instrument (Malvern Instruments Ltd., Worcestershire, UK). The hydrodynamic diameter was determined using three 10 × 10-second datasets at 25 °C in 20 mM Tris, 20 mM NaCl, and 5 mM $MgCl_2$ (pH 7.5). The samples were further subjected to stepwise heating. Starting at 25 °C, each sample was heated in 5 °C increments and equilibrated for 5 min at each temperature before analysis. The samples were heated to a final temperature of 90 °C, after which they were cooled back to 25 °C.

For the transmission electron microscopy (TEM) analysis, a small aliquot of CVB3 VLPs or infective virus was briefly bound to formvar-coated copper grids that had been glow-discharged just before use. The excess liquid was blotted away, after which a drop of 1% phosphotungstic acid (prepared in water, pH 7) or 2% uranyl acetate was applied to the grid for 1 min and blotted away. The grid was air-dried before visualization with a JEM-1400 (JEOL, Tokyo, Japan) or a Tecnai 10 (FEI, Hillsboro, OR) transmission electron microscope. The scanning electron microscopy (SEM) analysis is presented in the Supplementary data.

To determine if the VLPs contained the modified genome, a 20-μl aliquot was digested with 25 U of RNase If enzyme (New England Biolabs) in 1× NE buffer at 37 °C for 2 h. Then the enzyme was inactivated at 70 °C for 20 min. Another 40-μl aliquot of VLPs was digested at RT for 20 min with 2.7 Kunitz units of DNase I (Qiagen) in 1× RDD buffer. Both digestions were followed by nucleic acid extraction (Qiagen Viral RNA Kit), and samples were analyzed by enterovirus- and mCherry-specific PCR with and without a preceding reverse transcriptase reaction. The PCR run was performed using the primers and probes shown in Table 1 according to the instructions provided with the Quantitect Probe kit (Qiagen) using Taqman chemistry.

2.5. Vaccination and sampling of the mice

The vaccination trial was performed according to the guidelines of the Tampere University Animal Welfare program under the approval number ESAVI/4588/04.10.03/2012 from the Regional State Administrative Agency. Twelve female Balb/c mice, 6–8 weeks old were randomly divided into two groups of six. The first group was administered 5 μg of CVB3 VLPs, and the second group was given an identical volume of negative control vaccine (see Section 2.2). In addition, positive control experiment was performed by administering formalin-inactivated CVB3 virus to a group of six mice. All vaccine preparations were mixed with an equal volume of either complete (primary vaccination) or incomplete (booster vaccinations) Freund's adjuvant (Sigma–Aldrich) immediately before administration.

The primary vaccination was given in a volume of 100 μl s.c. and the two booster vaccinations (at day 21 and day 42) were given in volumes of 200 μl i.p. Blood samples were collected before vaccination, at days 21 and 42, and by heart puncture at day 63 when the mice were sacrificed. Spleens were collected, disrupted mechanically, and used to prepare into single-cell suspensions as follows: cells were washed with PBS, and red blood cells were lysed by incubating them for 1 min in ACK lysing buffer (Lonza). Splenocytes were suspended in 50 ml of 2% FBS, 0.5% penicillin–streptomycin, and 1% L-glutamine supplemented RPMI-1640 medium (Lonza).

2.6. ELISA and neutralization assays

For the ELISA assay, 96-well plates were coated with 150 ng/well of either purified CVB3 VLPs or virus. The wells were blocked at room temperature for 30 min using PBST supplemented with 0.1% (w/v) BSA, followed by incubation at 37 °C for 1 h with day 63 mouse antisera serially diluted in PBST containing 1% BSA (50 μl/well). HRP-conjugated horse anti-mouse IgG (Vector) diluted 1:2300 in 1% BSA in PBST (50 μl/well) was used as a secondary antibody, and the antibodies were detected using *O*-phenylenediamine dihydrochloride (Sigma–Aldrich) as a substrate. The reaction was stopped with 0.5 M sulfuric acid after a 30-min incubation at 37 °C, and the OD values were measured at 490 nm using an ELISA plate reader (Victor^2 1420 Multilabel counter, Perkin Elmer, Waltham, MA). The values were reported as the mean OD values for each dilution of the antisera. Statistical significance was determined by the unpaired two-tailed *t*-test using GraphPad Prism version 6.

Table 1
Primers and probes used in the study.

Primer/probe	Sequence (5′–3′)
5′NCR-for	CGG CCC CTG AAT GCG GCT AA
5′NCR-rev	GAA ACA CGG ACA CCC AAA GTA
5′NCR-probe	FAM-TCT GCA GCG GAA CCG ACT A-TAMRA
mCherry-for	CAC TAC GAC GCT GAG GTC AA
mCherry-rev	TAG TCC TCG TTG TGG GAG GT
mCherry-probe	VIC®-TGT GGG AGG TGA TGT C-MGB

The presence of neutralizing antibodies in mice against the ATCC reference strain Nancy (ATCC number VR-30) was analyzed using a plaque seroneutralization assay (Roivainen et al., 1998). The details of the neutralizing assay are described in the Supplementary data.

2.7. Immunological assays

To analyze immune cells using flow cytometry, mouse spleens were disrupted mechanically. Single-cell splenocyte suspensions (2 ml of per mouse) in RPMI medium were analyzed. The cells were washed with 0.1% BSA in PBS and stained for 20 min at +4 °C with the following antibodies (dilution, 1:400): CD3-APC (a pan-T cell marker), CD4-PerCP/Cy5.5 (a $CD4^+$ T cell marker), CD8-FITC (a $CD8^+$ T cell marker), CD44-APC/eFluor780 (a differentiated T cell marker), CD62L-PE (a naïve T cell marker), and B220-PE/Cy7 (a B cell marker). All antibodies were from eBioscience (San Diego, CA, USA). The cells were then filtered with cell strainer cap FACS tubes (BD, Franklin Lakes, NJ, USA) and washed with 0.1% BSA in PBS. The FACS analysis was performed using a FACSCanto™II flow cytometer (BD). Flow cytometric data was analyzed using FlowJo (Tree Star, Ashland, OR, USA). A total of 50,000 cells was analyzed for each sample. Live cells were gated, and the number of live cells was confirmed to be similar in each of the sample groups. Among the live cells, the $CD3^+/CD4^+$ and $CD3^+/CD8^+$ T cell populations were gated by plotting CD3-positive cells vs. CD4- or CD8-positive cells. The effector-memory (EM) T cell populations in these two populations were examined by plotting CD62L vs. CD44.

3. Results

3.1. Ion exchange purification resulted in highly purified CVB3 VLPs and CVB3 virus that were recognized by enterovirus-specific antibodies

Recombinant CVB3 VLPs were recovered from clarified insect cell culture supernatants by PEG precipitation and then subjected to further purification with either anion or cation exchange chromatography. The VLPs eluted from the QA anion exchange column at a NaCl concentration of 100 mM and from the SO3 cation exchange column between 410 and 550 mM NaCl (Fig. 2A). The yield was approximately 0.5 mg of VLPs per liter of insect cell culture.

Isolation of CVB3 virus by PEG precipitation and purification by sucrose gradient ultracentrifugation resulted in approximately 1.4 mg CVB3 virus per liter of cell culture with an infectivity of 2.8×10^{10} PFU. The PEG-precipitated virus that was further purified by anion exchange chromatography and eluted from the QA column at 60 mM NaCl (Fig. 3A) resulted in a yield of approximately 2 mg of viruses per liter of cell culture with an infectivity of 5.6×10^{10} PFU.

SDS–PAGE analysis and subsequent silver staining of CVB3 virus samples showed the presence of four proteins of approximately 34 kDa, 30 kDa, 26 kDa, and 8 kDa in size (Fig. 3B, lanes 4 and 5). These molecular weights correspond well with the estimated molecular weights of the four CVB3 capsid proteins, VP1, VP2, VP3, and VP4, respectively (Cunningham et al., 1992). The purified VLP sample contained three protein bands in the silver-stained SDS–PAGE gel (Fig. 2B, lane 4) that correlated with the molecular weights of the capsid proteins VP0, VP1, and VP3. VP0 appears not to undergo cleavage to yield the VP4 and VP2 proteins in insect cells. The purity confirmed by silver staining was very high for all the purified material (Fig. 2B, lane 4; Fig. 3B, lanes 4 and 5) and was estimated to be >95% for both CVB3 VLPs and CVB3 virus. No residual protein impurities were detected in any of the purified materials. The total DNA content of the purified VLPs was very low (0.82 ± 0.38 ng/µl), measured from three independent purifications. The baculovirus genome content of the samples was 0.02 ± 0.02 ng/µl, measured from three independent purifications. Both the virus and the VLPs were recognized by an antibody against enterovirus VP1 (Figs. 2C and 3C). None of the proteins were recognized by an antibody against baculovirus (Supplementary Fig. S5).

3.2. The assembly and homogeneity of the IEX-purified CVB3 VLPs and viruses were confirmed by dynamic light scattering and electron microscopy

DLS analysis showed that a majority (98.2%) of the particles in the VLP sample purified using SO3-based ion exchange chromatography had an average diameter of 30.7 nm, and the sample was relatively monodisperse (polydispersity index, PdI = 0.316) (Fig. 4A).

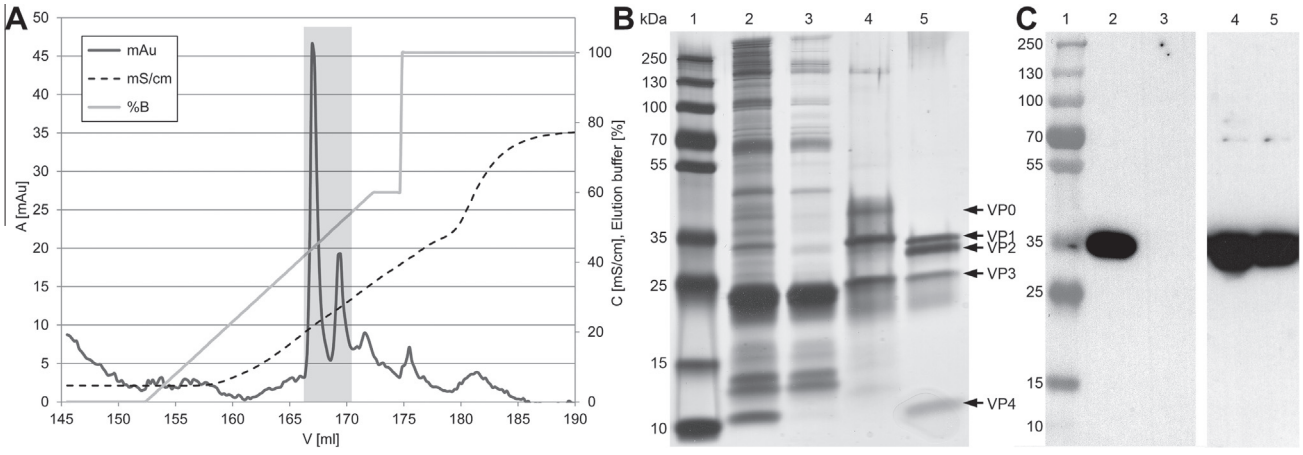

Fig. 2. Characterization of the chromatography-purified CVB3 VLPs. (A) PEG-precipitated VLPs were loaded onto a cation exchange column and were eluted from the column with a linear gradient using 1 M NaCl, 20 mM Tris–HCl, and 5 mM $MgCl_2$ (pH 7.4) as the elution buffer. A flow rate of 1 ml/min was used. The peak fractions (indicated by shading) eluted from the column between 410 and 550 mM NaCl. A: absorbance at 280 nm, V: volume, C: conductivity. (B) Analysis of the silver-stained SDS–PAGE gel showed that the VLPs were efficiently purified and concentrated during the chromatography purification process. Lane 1: molecular weight marker; lane 2: chromatography input sample; lane 3: flow-through sample; lane 4: VLP-containing elution sample; lane 5: ultracentrifugation-purified CVB3 virus control sample. (C) Western blot analysis of chromatography-purified CVB3 VLPs revealed that the VLPs were recognized by an anti-enterovirus VP1 antibody. Lane 1: molecular weight marker; lane 2: chromatography input sample; lane 3: flow-through sample; lanes 4 and 5: VLP-containing elution samples.

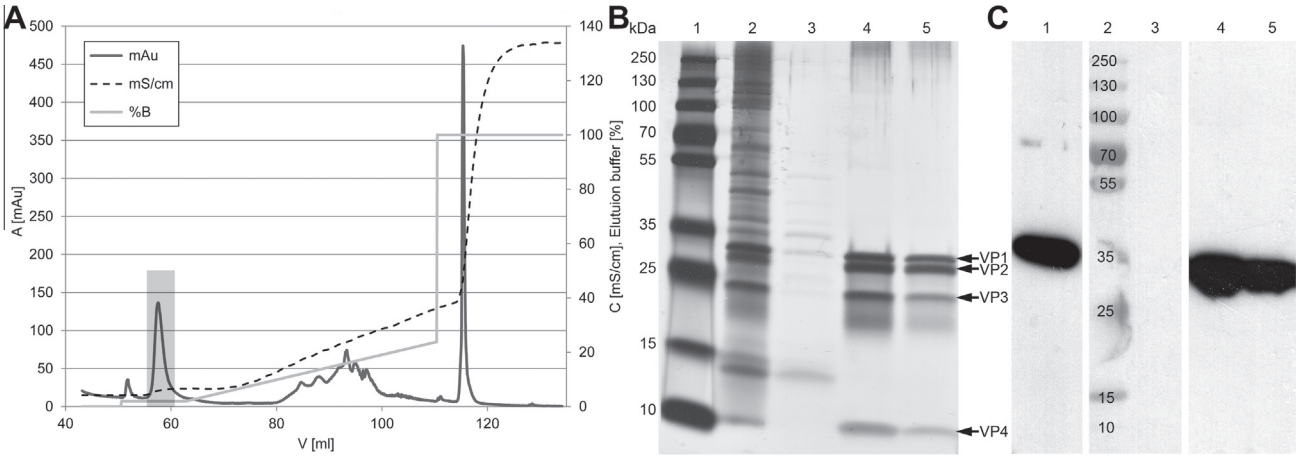

Fig. 3. Chromatographic purification of the CVB3 virus and comparison of the purified virus with the ultracentrifugation-purified virus. (A) PEG-precipitated viruses were loaded onto an anion exchange column and were eluted from the column using a combination of stepwise and linear gradients as shown in the figure. A flow rate of 1 ml/min was used, and the elution buffer contained 2 M NaCl, 20 mM Tris–HCl, and 5 mM $MgCl_2$ (pH 7.4). The peak fractions (indicated by shading) eluted from the column at a NaCl concentration of 60 mM. A: absorbance at 280 nm, V: volume, C: conductivity. (B) Analysis of silver-stained SDS–PAGE gels showed that the viruses were efficiently purified by both chromatography and ultracentrifugation. Lane 1: molecular weight marker; lane 2: chromatography input sample; lane 3: flow-through sample; lane 4: virus-containing elution sample; lane 5: ultracentrifugation-purified CVB3 virus sample. (C) Western blot analysis of chromatography-purified CVB3 viruses revealed that the viruses were recognized by an anti-enterovirus VP1 antibody. Lane 1: chromatography input sample; lane 2: molecular weight marker; lane 3: flow-through sample; lanes 4 and 5: virus-containing elution samples.

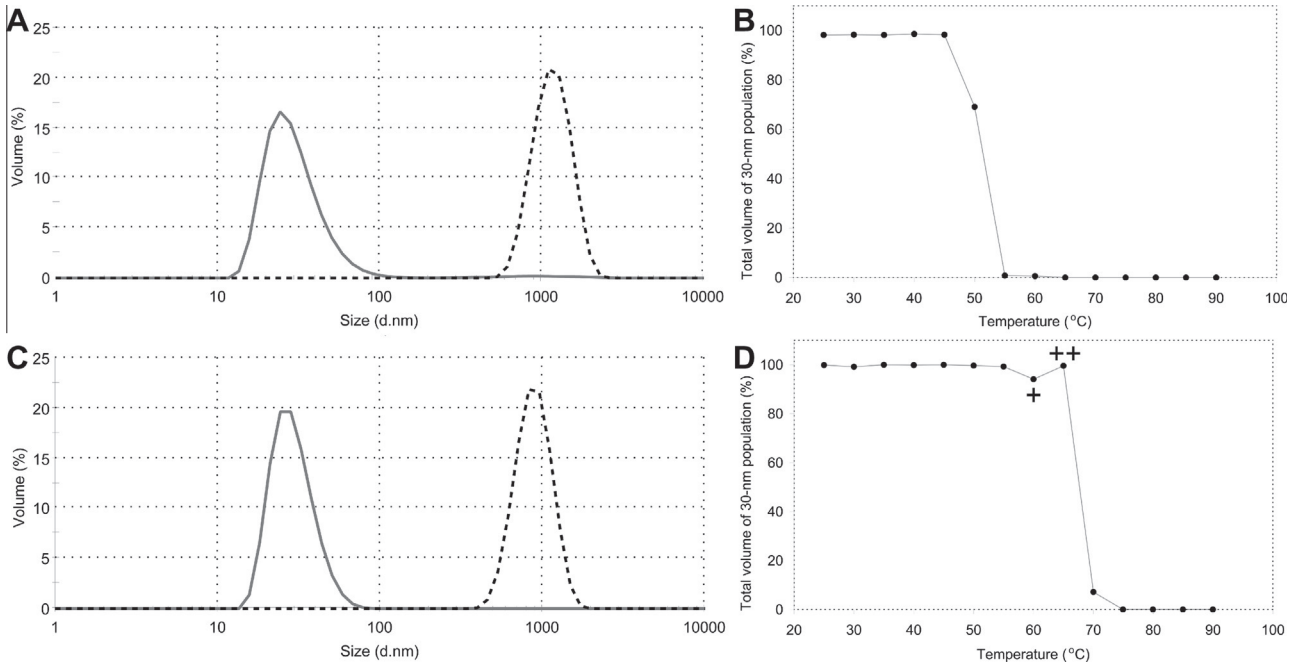

Fig. 4. Dynamic light scattering (DLS) analysis of the CVB3 VLPs and viruses. (A) Chromatography-purified VLP sample contained 98.2% particles (determined by particle volume) with a hydrodynamic diameter of 30.7 nm (solid gray line). After gradual heating of the sample to 90 °C, followed by cooling of the sample to 25 °C, the particles were aggregated with an average particle size of 1191 nm (dotted line). (B) Volume-% of the 30-nm particle population in the VLP sample over the temperature range analyzed (25–90 °C). (C) DLS analysis of the CVB3 virus as described in (A). The virus sample contained 100% particles with an average hydrodynamic diameter of 29.8 nm. (D) Heating of the virus sample indicated the onset of thermal denaturation at 60 °C, and an increase in the average particle diameter (40.8 nm) was observed (+). Further heating to 65 °C led to an increase in the average size to 82.0 nm (++), after which larger aggregates were formed (200–500 nm). When the sample was cooled to 25 °C, 898.7 nm particles were observed (C, dotted line).

A sample of chromatography-purified CVB3 virus contained mainly (99.9%) particles with an average diameter of 28.2 nm (Fig. 4C). The sample was homogenous, with a PdI of 0.173.

The heating of both the VLPs and the virus from 25 °C to 95 °C led to aggregation of the sample, resulting in particles of 600–1000 nm in diameter (Supplementary Figs. S6 and S7). After cooling to 25 °C, a further increase in the particle size was observed, indicating irreversible thermal unfolding. A difference between the VLPs and the virus was observed in the temperature at which they aggregated. The VLPs showed signs of thermally induced aggregation at 50 °C and were completely aggregated at 55 °C (Fig. 4B), whereas the virus sample showed the first signs of aggregation at 60 °C and was completely aggregated at 75 °C (Fig. 4D). Therefore, the thermally induced events occurred over much

broader temperature range in case of CVB3 virus and the midpoint of the thermal aggregation was 10–15 °C higher than in the case of the VLPs.

Examination of the CVB3 VLP and virus samples by both transmission and scanning electron microscopy showed the presence of intact and uniform particles with the correct size (approximately 30 nm in diameter) and morphology (Figs. 5 and 6), although in the SEM images, the VLPs appeared somewhat smaller in size than the virus particles.

To determine whether modified viral RNA or baculoviral DNA was packaged into the VLPs, RNase If or DNase I digestions for the supernatant aliquots were performed. Nucleases will digest RNA or DNA in the supernatant, but not inside the VLP. Digestion was followed by nucleic acid extraction and PCR amplification with and without reverse transcriptase (RT-) step to control whether PCR signal originates from RNA or DNA. The supernatant DNase I-digested samples were negative indicating that the supernatant was free of viral RNA, and that the VLP particles did not contain RNA or DNA, both of which would have given signals in the RT-PCR and/or in the PCR if positive. Therefore, the DNA in the supernatant was digested. The VLP supernatants digested with RNase If were positive with and without the RT-step, which demonstrated that the samples contained traces of baculovirus-derived DNA outside the particle.

3.3. CVB3 VLP vaccination generated a strong antibody-mediated immune response in mice

The antibodies generated in immunized mice were quantified using an ELISA (Fig. 7). The negative control vaccine did not elicit any reactivity against either inactivated CVB3 (ATTC, Nancy strain) or the VLP proteins. In contrast, the sera of the VLP-vaccinated mice reacted strongly to both antigens, and high IgG titers were generated in all but one mouse (mouse no. 11, Supplementary Fig. S8). The mean titers were slightly higher when the VLPs were used as an antigen rather than when intact CVB3 particles were used.

Sera from mice immunized with CVB3 VLPs and the negative control vaccine were further evaluated for their ability to neutralize infective CVB3 *in vitro*. The end-point neutralizing titers (up to 1:4096) were determined for sera collected on day 0 and day 63. The negative control vaccine failed to elicit any neutralization at 1:4, whereas high neutralizing antibody titers were induced in mice immunized with CVB3 VLPs (Table 2). The mean neutralizing titer in the VLP-vaccinated group at day 63 was over 1:1100, but considerable variations were observed between individual mice. One mouse (mouse no. 7) generated neutralizing antibodies only after the second booster dose; however the final end-point antibody titer was higher than those seen in other mice. Additionally, one mouse (mouse no. 11) failed to generate neutralizing antibodies after vaccination. The mean neutralizing titer of the mice infected with purified formaldehyde-inactivated CVB3 virus, which was used as a positive control was 1:2200 at day 63 ($n = 6$).

3.4. CVB3 VLPs induced cell-mediated immunity in mice

The spleen cells of CVB3 VLP- and negative control-vaccinated mice were analyzed for markers of immune activation (Supplementary Table 1). Initially, when the numbers of B cells, $CD4^+$ T cells, and $CD8^+$ T cells were determined, there was no statistically significant expansion of effector B or T cells, nor differences between the study groups. When activated by virus infection, EM-T cells expanded in number and modulated their expression of cell surface molecules such as CD62L and CD44. Upon EM-generation, T cells down-regulate CD62L and up-regulate CD44 (Sprent, 1997). Thus, the numbers and proportions of the memory cell populations of CD3 and CD4/CD8 double-positive cells were measured based on the expression of CD44 and CD62L. We found that 9 weeks after the initial VLP immunization, the numbers of $CD62L^{low}$ $CD44^{high}$ cells in both the CD4 and CD8 cell populations

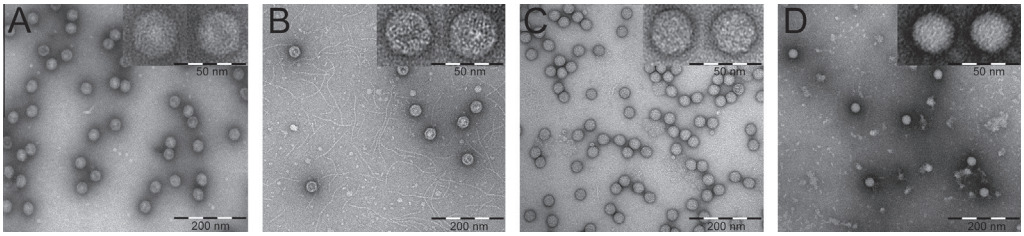

Fig. 5. Transmission electron micrographs of (A) S03 chromatography-purified VLPs, (B) QA chromatography-purified VLPs, (C) ultracentrifugation-purified viruses, and (D) QA chromatography-purified viruses. Scale bars, 200 nm and 50 nm (close-up).

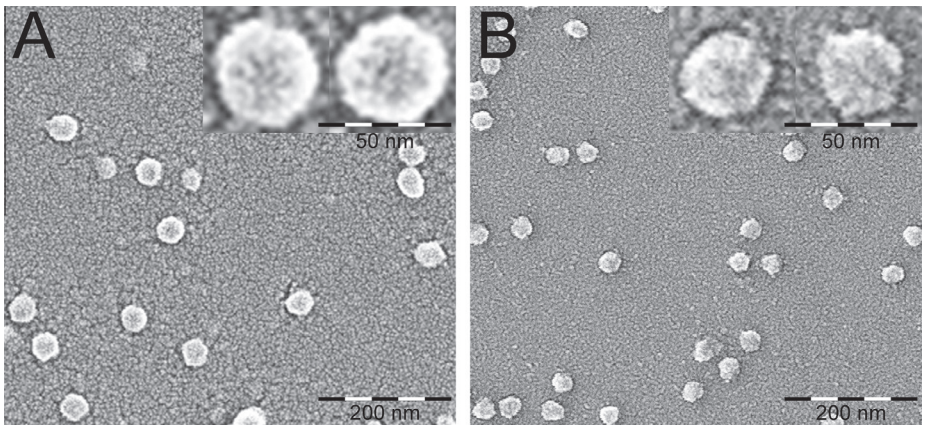

Fig. 6. Scanning electron micrographs of (A) the S03 chromatography-purified viruses and (B) VLPs. Scale bars, 200 nm and 50 nm (close-up).

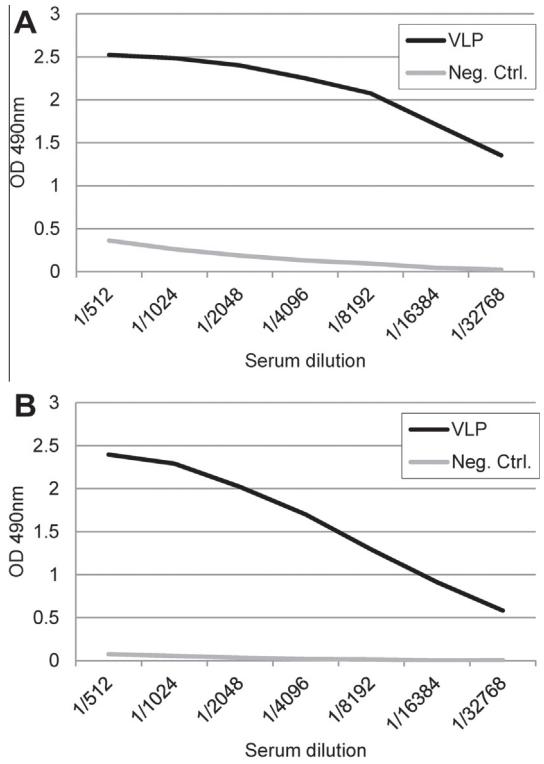

Fig. 7. Mean antibody responses elicited in mice by CVB3 VLP immunization. Two groups of mice were injected on days 0, 21, and 42 with 5 μg of CVB3 VLPs or an equivalent amount of negative control vaccine. The immunized mice were sacrificed on day 63, and serum samples were collected. The results represent the mean of three replicate experiments. (A) The binding activity of the antisera to a CVB3 VLP antigen. (B) Binding activity of the antisera to a CVB3 virus.

Table 2
Neutralizing titers analyzed by seroneutralization assay.

Vaccination group	Neutralizing titer[a]			
	Day 0	Day 21[b]	Day 42[b]	Day 63
Negative control				
Mouse 1	–	–	–	–
Mouse 2	–	–	–	–
Mouse 3	–	–	–	–
Mouse 4	–	–	–	–
Mouse 5	–	–	–	–
Mouse 6	–	–	–	–
CVB3 VLP				
Mouse 7	–	–	1:16	1:4096
Mouse 8	–	1:16	1:16	1:256
Mouse 9	–	1:16	1:16	1:1024
Mouse 10	–	1:16	1:16	1:1024
Mouse 11	–	–	–	–
Mouse 12	–	1:16	1:16	1:256

[a] Titers were determined against ATCC reference strain Nancy (ATCC number VR-30). –, no detectable neutralizing antibodies (titer <1:4).
[b] Neutralizing titers were analyzed only at dilutions of 1:4 and 1:16.

were consistently higher than in control mice. For CD4 cells, the induction was from ~500 to 700 cells, and for CD8 cells, the induction was from ~30 to 45 cells. No significant differences in the total number of $CD4^+$ or $CD8^+$ T cells were observed between the study groups.

4. Discussion

In this article, we describe a technology that allows the production of high-quality enterovirus VLPs for different applications. We have shown herein that the produced VLPs were stable and highly purified. The preparations were determined to be free of contaminating proteins by silver stain, which has a detection limit of 0.25 ng for proteins, thus verifying purity >95%. In addition, the VLP samples were virtually free of contaminating DNA (0.82 ± 0.38 ng/μl). The VLPs were indistinguishable from the native virus in size, composition, and appearance, as determined by SDS–PAGE, Western blotting, and transmission electron microscopy. Moreover, the VLPs were also almost as stable as native viruses when exposed to elevated temperatures, and they also withstood a year-long storage at −20 °C without declining (data not shown). Most importantly, VLPs were highly immunogenic, as shown by the vaccination experiments in mice.

Since the launch of polio vaccines in 1950s, no other enterovirus vaccines have been developed and registered for human use. One reason for the lack of enterovirus vaccines is due to the large number of different enterovirus serotypes (over 100), which circulate around the world and are rapidly and continuously recombining and evolving. It has not, therefore, been easy to identify causal serotype-disease relationships. There are, however, certain virus-disease associations that are currently well established which make the development of novel vaccines worthy of consideration. Among such enteroviruses are EV71 and CVB3, both of which commonly cause severe infections that can be fatal (McMinn, 2012; Maier et al., 2004). The recent progress in the development of an EV71 vaccine has been encouraging. Several vaccine formulae have been studied in animal models, and human clinical trials have yielded promising results (Liang et al., 2013). However, to date, such breakthroughs in the development of a CVB3 vaccine have not been made.

In research settings, enteroviruses are routinely purified by sucrose gradient ultracentrifugation. Although meticulously performed ultracentrifugation generates high-quality virus material, the procedure is cumbersome, and the yields are modest considering the laborious nature of the method. On the industrial scale, other methods such as tangential flow filtration, ultrafiltration, and chromatography-based purification are more feasible (Morenweiser, 2005). In response to this demand, we developed an easily scalable ion exchange chromatography-based purification system for the CVB3 VLP vaccine. We also developed an analogous ion exchange chromatography-based purification method for the CVB3 virus. The single-step chromatography procedure yielded highly pure and stable CVB3 VLP and virus preparations, and the developed methodology is therefore an easily scalable purification system for industrial-scale vaccine production.

Most importantly, the anti-VLP sera raised by CVB3 VLP vaccination exhibited a strong neutralizing capacity against the homologous CVB3 strain. In addition, we showed by ELISA that mice immunized with CVB3 VLPs had a strong serum IgG antibody response and that the generated antibodies reacted with both VLP and virus antigens within the same genogroup. There are several previous studies showing the efficacy of enteroviral VLPs as immunogens (Zhang et al., 2012; Liu et al., 2012; Lin et al., 2012). All of these studies measured immune responses by ELISA and/or seroneutralization as part of their main analyses, and our results are very similar. Closely analogous to our study is the work performed by Zhang et al. (2012), who obtained neutralizing titers against their CVB3 VLPs of up to 1:320. In comparison, our titers had an average over 1:1100. Zhang et al. used a similar vaccination regime and similar adjuvants as to those used in the present study, but in contrast to the 5 μg dose used in the present study, they used one of 20 μg. We therefore were able to generate comparable or even higher neutralizing titers with smaller doses, thus highlighting the purity and high immunogenicity of the chromatography-purified VLPs. The efficacy of the VLP vaccine was also found comparable to the positive control, formaldehyde-inactivated virus. The

small difference in the efficacy of these two formulations may be due to the formaldehyde used to inactivate the virus or the lack of VP0 maturation cleavage in VLP. One mouse vaccinated with VLP did not generate measurable amounts of neutralizing antibodies, and may represent somehow immunocompromised animal.

Our analysis of the B cell, $CD8^+$, and $CD4^+$ T cell responses induced by CVB3 VLPs revealed a limited degree of activation. However, the effector-memory T cell populations were consistently increased by CVB3 VLPs indicating that an immunological response to the VLP was obtained. These findings are consistent with similar studies carried out with CVB3 virus (Slifka et al., 2001; Kemball et al., 2008). When comparing the increase in the size of the EM-T cell pool with the efficacy of neutralizing antibody production, the degrees of the responses appear to be consistent. A future challenge will be to construct a tetramer that could indicate that $CD8^+$ and $CD4^+$ memory T cells have been induced specifically by CVB3 VLPs.

In conclusion, we present the construction, production, and purification of an immunologically efficient and safe vaccine candidate for CVB3-related diseases in the form of VLPs. The introduced purification system in particular is highly relevant for industrial-scale vaccine production, which enables a smooth shift from pre-clinical studies to human clinical trials. The produced VLP vaccine was able to induce a strong immune response in mice, as determined by seroneutralization and ELISA assays and also by immune cell assay. In addition, we developed an efficient and scalable purification method for the CVB3 virus, which will facilitate its further characterization and provides the possibility of using the virus as the basis of a conventional attenuated or killed vaccine.

Acknowledgments

The authors thank Tanja Rämö, Laura Kananen, Ulla Kiiskinen, Outi Väätäinen, Tuula Koivuharju, Jussi Lehtonen, Niila Saarinen, Juha Määttä, and Outi Tolonen for their valuable technical assistance. Anni Laitinen and Pär Larsson are acknowledged for their help with the mouse experiments and Sanna Hämäläinen for the assistance with the flow cytometry experiments. Mari Leinonen, Tommi Isoniemi, Lars Haag, and Josefina Nilsson are acknowledged for their support with the electron microscopy. The authors thank Raimo Harju for many helpful suggestions during the study. The work was supported by grants from the Academy of Finland (136288, 140978, 273192, 257125), TEKES (FiDiPro project "NOVAC", Novel methods for vaccination and virus detection), Competitive Research Funding of the Tampere University Hospital District, the National Doctoral Programme in Informational and Structural Biology (ISB), the European Commission, PEVNET (FP-7 Programme, contract No. 261441), and Vactech Ltd.

Appendix A. Supplementary data

Supplementary data associated with this article can be found, in the online version, at http://dx.doi.org/10.1016/j.antiviral.2014.01.013.

References

Abraham, G., Colonno, R.J., 1984. Many rhinovirus serotypes share the same cellular receptor. J. Virol. 51, 340–345.
Bergelson, J.M., Chan, M., Solomon, K.R., St John, N.F., Lin, H., Finberg, R.W., 1994. Decay-accelerating factor (CD55), a glycosylphosphatidylinositol-anchored complement regulatory protein, is a receptor for several echoviruses. Proc. Natl. Acad. Sci. USA 91, 6245–6248.
Bergelson, J.M., Cunningham, J.A., Droguett, G., Kurt-Jones, E.A., Krithivas, A., Hong, J.S., Horwitz, M.S., Crowell, R.L., Finberg, R.W., 1997. Isolation of a common receptor for Coxsackie B viruses and adenoviruses 2 and 5. Science 275, 1320–1323.
Chung, Y., Ho, M., Wu, J., Chen, W., Huang, J., Chou, S., Hu, Y., 2008. Immunization with virus-like particles of enterovirus 71 elicits potent immune responses and protects mice against lethal challenge. Vaccine 26, 1855–1862.
Cunningham, M.W., Antone, S.M., Gulizia, J.M., McManus, B.M., Fischetti, V.A., Gauntt, C.J., 1992. Cytotoxic and viral neutralizing antibodies crossreact with streptococcal M protein, enteroviruses, and human cardiac myosin. Proc. Natl. Acad. Sci. USA 89, 1320–1324.
Dan, M., Chantler, J.K., 2005. A genetically engineered attenuated coxsackievirus B3 strain protects mice against lethal infection. J. Virol. 79, 9285–9295.
Dunn, J.J., Bradrick, S.S., Chapman, N.M., Tracy, S.M., Romero, J.R., 2003. The stem loop II within the 5′ nontranslated region of clinical coxsackievirus B3 genomes determines cardiovirulence phenotype in a murine model. J. Infect. Dis. 187, 1552–1561.
Feuer, R., Mena, I., Pagarigan, R.R., Harkins, S., Hassett, D.E., Whitton, J.L., 2003. Coxsackievirus B3 and the neonatal CNS: the roles of stem cells, developing neurons, and apoptosis in infection, viral dissemination, and disease. Am. J. Pathol. 163, 1379–1393.
Fifis, T., Gamvrellis, A., Crimeen-Irwin, B., Pietersz, G.A., Li, J., Mottram, P.L., McKenzie, I.F., Plebanski, M., 2004. Size-dependent immunogenicity: therapeutic and protective properties of nano-vaccines against tumors. J. Immunol. 173, 3148–3154.
Fohlman, J., Ilback, N.G., Friman, G., Morein, B., 1990. Vaccination of Balb/c mice against enteroviral mediated myocarditis. Vaccine 8, 381–384.
Godney, E.K., Arizpe, H.M., Gaunti, C.J., 1987. Characterization of the antibody response in vaccinated mice protected against Coxsackievirus B3-induced myocarditis. Viral Immunol. 1, 305–314.
Goldman, M., Lambert, P.H., 2004. Immunological safety of vaccines: facts hypothesis and allegations. In: Kaufmann, S.H.E. (Ed.), Novel Vaccination Strategies. Wiley-VCH, Weinheim, Germany, pp. 595–611.
Grgacic, E.V., Anderson, D.A., 2006. Virus-like particles: passport to immune recognition. Methods 40, 60–65.
Haarmann, C.M., Schwimmbeck, P.L., Mertens, T., Schultheiss, H.P., Strauer, B.E., 1994. Identification of serotype-specific and nonserotype-specific B-cell epitopes of coxsackie B virus using synthetic peptides. Virology 200, 381–389.
Henke, A., Wagner, E., Whitton, J.L., Zell, R., Stelzner, A., 1998. Protection of mice against lethal Coxsackievirus B3 infection by using DNA immunization. J. Virol. 72, 8327–8331.
Huber, S., Polgar, J., Moraska, A., Cunningham, M., Schwimmbeck, P., Schultheiss, P., 1993. T lymphocyte responses in CVB3-induced murine myocarditis. Scand. J. Infect. Dis. Suppl. 88, 67–78.
Jennings, G.T., Bachmann, M.F., 2008. The coming of age of virus-like particle vaccines. Biol. Chem. 389, 521–536.
Karkkainen, H.R., Lesch, H.P., Maatta, A.I., Toivanen, P.I., Mahonen, A.J., Roschier, M.M., Airenne, K.J., Laitinen, O.H., Yla-Herttuala, S., 2009. A 96-well format for a high-throughput baculovirus generation, fast titering and recombinant protein production in insect and mammalian cells. BMC Res. Notes 2, 63. http://dx.doi.org/10.1186/1756-0500-2-63.
Kemball, C.C., Harkins, S., Whitton, J.L., 2008. Enumeration and functional evaluation of virus-specific CD4+ and CD8+ T cells in lymphoid and peripheral sites of Coxsackievirus B3 infection. J. Virol. 82, 4331–4342.
Kim, D.S., Nam, J.H., 2011. Application of attenuated Coxsackievirus B3 as a viral vector system for vaccines and gene therapy. Hum. Vaccine 7, 410–416.
Kim, J.Y., Jeon, E.S., Lim, B.K., Kim, S.M., Chung, S.K., Kim, J.M., Park, S.I., Jo, I., Nam, J.H., 2005. Immunogenicity of a DNA vaccine for Coxsackievirus B3 in mice: protective effects of capsid proteins against viral challenge. Vaccine 23, 1672–1679.
Klump, W.M., Bergmann, I., Muller, B.C., Ameis, D., Kandolf, R., 1990. Complete nucleotide sequence of infectious Coxsackievirus B3 cDNA: two initial 5′ uridine residues are regained during plus-strand RNA synthesis. J. Virol. 64, 1573–1583.
Knowlton, K.U., Jeon, E.S., Berkley, N., Wessely, R., Huber, S., 1996. A mutation in the puff region of VP2 attenuates the myocarditic phenotype of an infectious cDNA of the Woodruff variant of Coxsackievirus B3. J. Virol. 70, 7811–7818.
Krausslich, H.G., Nicklin, M.J., Lee, C.K., Wimmer, E., 1988. Polyprotein processing in picornavirus replication. Biochimie 70, 119–130.
Liang, Z.L., Mao, Q.Y., Wang, Y.P., Zhu, F.C., Li, J.X., Yao, X., Gao, F., Wu, X., Xu, M., Wang, J.Z., 2013. Progress on the research and development of inactivated EV71 whole-virus vaccines. Hum. Vaccine Immunother. 9, 6.
Lin, Y.L., Yu, C.I., Hu, Y.C., Tsai, T.J., Kuo, Y.C., Chi, W.K., Lin, A.N., Chiang, B.L., 2012. Enterovirus type 71 neutralizing antibodies in the serum of macaque monkeys immunized with EV71 virus-like particles. Vaccine 30, 1305–1312.
Liu, Q., Yan, K., Feng, Y., Huang, X., Ku, Z., Cai, Y., Liu, F., Shi, J., Huang, Z., 2012. A virus-like particle vaccine for Coxsackievirus A16 potently elicits neutralizing antibodies that protect mice against lethal challenge. Vaccine 30, 6642–6648.
Maier, R., Krebs, P., Ludewig, B., 2004. Immunopathological basis of virus-induced myocarditis. Clin. Dev. Immunol. 11, 1–5.
McMinn, P.C., 2012. Recent advances in the molecular epidemiology and control of human enterovirus 71 infection. Curr. Opin. Virol. 2, 199–205.
Melnick, J.L., 1996. Enteroviruses: polioviruses, Coxsackieviruses, echoviruses and newer enteroviruses. In: Fields, B.N., Knipe, D.M., Howley, P.M., Channock, R.M., Melnick, J.L., Monath, T.P., Roizman, B., Straus, S.E. (Eds.), Fields Virology, third ed. Lippincott-Raven Publishers, Philadelphia, PA, pp. 655–712.
Mena, I., Fischer, C., Gebhard, J.R., Perry, C.M., Harkins, S., Whitton, J.L., 2000. Coxsackievirus infection of the pancreas: evaluation of receptor expression, pathogenesis, and immunopathology. Virology 271, 276–288.
Morenweiser, R., 2005. Downstream processing of viral vectors and vaccines. Gene Ther. 12 (Suppl. 1), S103–S110.

Park, J.H., Kim, D.S., Cho, Y.J., Kim, Y.J., Jeong, S.Y., Lee, S.M., Cho, S.J., Yun, C.W., Jo, I., Nam, J.H., 2009. Attenuation of Coxsackievirus B3 by VP2 mutation and its application as a vaccine against virus-induced myocarditis and pancreatitis. Vaccine 27, 1974–1983.

Roivainen, M., Knip, M., Hyoty, H., Kulmala, P., Hiltunen, M., Vahasalo, P., Hovi, T., Akerblom, H.K., 1998. Several different enterovirus serotypes can be associated with prediabetic autoimmune episodes and onset of overt IDDM. Childhood diabetes in Finland (DiMe) study group. J. Med. Virol. 56, 74–78.

Rombaut, B., Jore, J.P., 1997. Immunogenic, non-infectious polio subviral particles synthesized in *Saccharomyces cerevisiae*. J. Gen. Virol. 78 (Pt 8), 1829–1832.

Roy, P., Noad, R., 2008. Virus-like particles as a vaccine delivery system: myths and facts. Hum. Vaccine 4, 5–12.

See, D.M., Tilles, J.G., 1994. Efficacy of a polyvalent inactivated-virus vaccine in protecting mice from infection with clinical strains of group B Coxsackieviruses. Scand. J. Infect. Dis. 26, 739–747.

Selinka, H.C., Wolde, A., Sauter, M., Kandolf, R., Klingel, K., 2004. Virus-receptor interactions of Coxsackie B viruses and their putative influence on cardiotropism. Med. Microbiol. Immunol. 193, 127–131.

Slifka, M.K., Pagarigan, R., Mena, I., Feuer, R., Whitton, J.L., 2001. Using recombinant Coxsackievirus B3 to evaluate the induction and protective efficacy of CD8+ T cells during picornavirus infection. J. Virol. 75, 2377–2387.

Sprent, J., 1997. Immunological memory. Curr. Opin. Immunol. 9, 371–379.

Stadnick, E., Dan, M., Sadeghi, A., Chantler, J.K., 2004. Attenuating mutations in Coxsackievirus B3 map to a conformational epitope that comprises the puff region of VP2 and the knob of VP3. J. Virol. 78, 13987–14002.

Tu, Z., Chapman, N.M., Hufnagel, G., Tracy, S., Romero, J.R., Barry, W.H., Zhao, L., Currey, K., Shapiro, B., 1995. The cardiovirulent phenotype of coxsackievirus B3 is determined at a single site in the genomic 5′ nontranslated region. J. Virol. 69, 4607–4618.

Voigt, A., Jakel, S., Textoris-Taube, K., Keller, C., Drung, I., Szalay, G., Klingel, K., Henklein, P., Stangl, K., Kloetzel, P.M., Kuckelkorn, U., 2010. Generation of in silico predicted Coxsackievirus B3-derived MHC class I epitopes by proteasomes. Amino Acids 39, 243–255.

Wong, A.H., Lau, C.S., Cheng, P.K., Ng, A.Y., Lim, W.W., 2011. Coxsackievirus B3-associated aseptic meningitis: an emerging infection in Hong Kong. J. Med. Virol. 83, 483–489.

Xu, W., Shen, Y., Jiang, Z., Wang, Y., Chu, Y., Xiong, S., 2004. Intranasal delivery of chitosan-DNA vaccine generates mucosal SIgA and anti-CVB3 protection. Vaccine 22, 3603–3612.

Zhang, H., Morgan-Capner, P., Latif, N., Pandolfino, Y.A., Fan, W., Dunn, M.J., Archard, L.C., 1997. Coxsackievirus B3-induced myocarditis. Characterization of stable attenuated variants that protect against infection with the cardiovirulent wild-type strain. Am. J. Pathol. 150, 2197–2207.

Zhang, L., Parham, N.J., Zhang, F., Aasa-Chapman, M., Gould, E.A., Zhang, H., 2012. Vaccination with Coxsackievirus B3 virus-like particles elicits humoral immune response and protects mice against myocarditis. Vaccine 30, 2301–2308.

Supplementary data

Coxsackievirus B3 VLPs purified by ion exchange chromatography elicit strong immune responses in mice

Tiia Koho[a], Minni R.L. Koivunen[b], Sami Oikarinen[c], Laura Kummola[d,f], Selina Mäkinen[a], Anssi J. Mähönen[a], Amirbabak Sioofy-Khojine[c], Varpu Marjomäki[e], Artur Kazmertsuk[e], Ilkka Junttila[d,f], Markku S. Kulomaa[a], Heikki Hyöty[c,d,f], Vesa P. Hytönen[a,f], Olli H. Laitinen[b,g,*]

[a] BioMediTech, University of Tampere and Tampere University Hospital, Biokatu 6, FI-33014 University of Tampere, Finland
[b] Vactech Ltd, Biokatu 8, FI-33520 Tampere, Finland
[c] Department of Virology, School of Medicine, Biokatu 10, FI-33014 University of Tampere, Finland
[d] School of Medicine, FI-33014 University of Tampere, Finland
[e] Department of Biological and Environmental Science/Nanoscience Center, University of Jyväskylä, P.O. Box 35, FI-40014 University of Jyväskylä, Finland
[f] Fimlab Laboratories, Pirkanmaa Hospital District, Biokatu 4, FI-33520 Tampere, Finland
[g] The Center for Infectious Medicine, Department of Medicine HS, Karolinska Institutet, Karolinska University Hospital Huddinge F59, SE-141 86 Stockholm, Sweden

Chromatographic purification of the CVB3 VLPs

The chromatographic ion exchange purification (IEX) of the pre-treated VLPs was performed using monolithic columns (6.7 mm ID × 4.2 mm, V: 1 ml) based on CIM Convective Interaction Media® technology from BIA Separations (Ljubljana, Slovenia) with either quaternary amine (QA) or sulfate (SO3) chemical functionalization. The details of the purification protocol are described in the Supplementary data. A buffer containing 20 mM Tris (pH 7.5), 20 mM NaCl and 5 mM $MgCl_2$ was used as the running buffer, and running buffer containing 2 M (QA) or 1 M (SO3) NaCl was used as the elution buffer. After sample loading, unbound proteins were washed out from the column with running buffer. Column-bound VLPs were then eluted using either a stepwise gradient (for the QA column), with each step (1.5%, 4%, and 24% elution buffer) lasting for 12 column volumes (CVs), or a linear gradient (for the SO3 column) as depicted in Figure 2A. A flow rate of 2 ml/min was used throughout the chromatographic purification process except for elution from the SO3 column, for which a flow rate of 1 ml/min was used.

Chromatographic purification of the CVB3 viruses

The chromatographic purification of the pre-treated viruses was performed using a monolithic column (6.7 mm ID × 4.2 mm, V: 1 ml) based on CIM Convective Interaction Media® technology from BIA Separations with the quaternary amine (QA) chemistry. A buffer containing 20 mM Tris (pH 7.5), 20 mM NaCl, and 5 mM $MgCl_2$ was used as the running buffer, and running buffer containing 2 M NaCl was used as the elution buffer. Prior to being loaded onto the chromatography

column, the virus-containing supernatant was diluted 1:10 with 20 mM Tris-HCl (pH7.5) and filtered through a 0.2 µm filter. Column-bound viruses were eluted using a combination of stepwise and linear gradients as depicted in Figure 3A. A flow rate of 2 ml/min was used throughout the chromatographic purification process except during elution, when a flow rate of 1 ml/min was used.

Scanning electron microscopy

For scanning electron microscopy (SEM) analysis, the CVB3 VLP and virus samples were fixed and subsequently coated. Highly doped monocrystalline silicon substrates were treated with oxygen plasma in a reactive-ion etcher (Oxford Plasmalab 80 Plus) to increase the hydrophilicity by adding hydroxyl groups to the surface (Suni et al., 2002). To fix the samples, 6 µl of the sample was deposited onto the silica surface and allowed to dry for 10 minutes, followed by glutaraldehyde (2.5%) treatment for 3 minutes (20°C). The samples were then dried step-wise with methanol, t-butyl alcohol, and silazane for 2 minutes per step (20°C). Lastly, the samples were coated with a 5 nm palladium (Pd) layer using an ultra-high vacuum electron beam evaporator. For SEM imaging, a Raith eLiNE 50 system (Raith Inc., Dortmund, Germany) was used at an acceleration voltage of 20 kV.

Neutralization assay

The presence of neutralizing antibodies in mice against the ATCC reference strain Nancy (ATCC number VR-30) was analyzed using a plaque seroneutralization assay (Roivainen et al., 1998). Monolayers of GMK cells were prepared in 12-well tissue culture plates at 95% confluency. 3 µl of the final dilutions of sera (1:4, 1:16, 1:64, 1:256, 1:1024, or 1:4096) were incubated at room temperature for 1.5 h with equal volumes of virus solution containing approximately 100 PFU of infectious particles. The volume of the neutralization reaction was brought up to 100 µl using HBSS supplemented with 20 mM HEPES (HBSS-HEPES) before the cells were infected. After incubation at 37°C for 30 minutes, the neutralized virus suspension was removed, and each well was overlaid with plaque assay medium containing MEM, 1% (v/v) inactivated FCS, 4 IU/ml PS, 20 mM HEPES, 0.23% (w/v) glucose, 1% L-glutamine, 15 mM $MgCl_2$, and 0.5% (w/v) carboxymethyl cellulose. HBSS-HEPES and positive serum were used as controls. Infected cells were incubated at 37°C with 5% CO_2 for 2 days, after which the cells were fixed and stained with a 0.8% (v/v) formalin suspension in PBS containing 0.25% (w/v) crystal violet for 10 minutes. The number of viral plaques was identified, and the last dilution of the serum able to reduce the virus infectivity by

80% was reported as the final titer. The end-point titers were determined only for the day 0 and the day 63 sera. The sera from days 21 and 42 were analyzed only at dilutions of 1:4 and 1:16.

References

Roivainen, M., Knip, M., Hyöty, H., Kulmala, P., Hiltunen, M., Vähäsalo, P., Hovi, T., Åkerblom, H.K., 1998. Several different enterovirus serotypes can be associated with prediabetic autoimmune episodes and onset of overt IDDM. Childhood Diabetes in Finland (DiMe) Study Group. J. Med. Virol. 56, 74-78.

Suni, T., Henttinen, K., Suni, I., Mäkinen, J., 2002. Effects of Plasma Activation on Hydrophilic Bonding of Si and SiO[sub 2]. J. Electrochem. Soc. 149, G348. doi: 10.1149/1.1477209.

Supplementary figures and tables

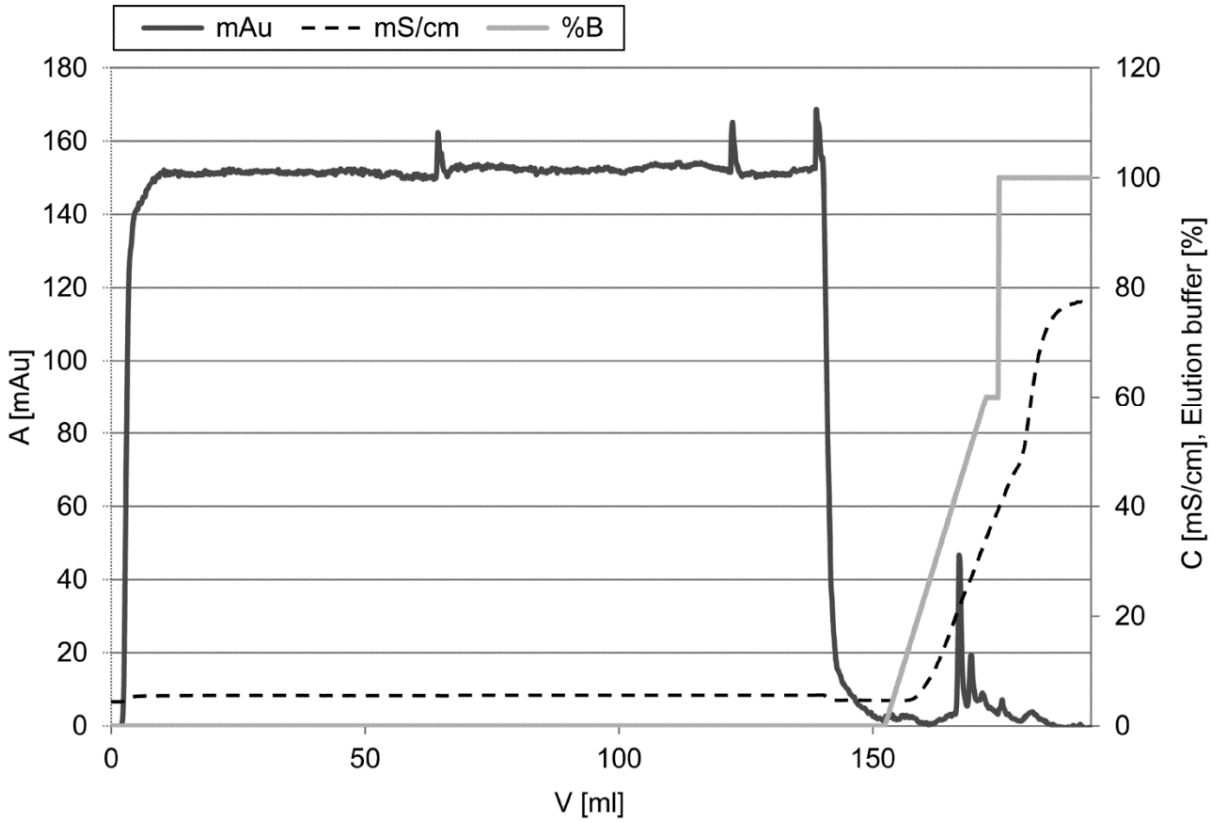

Figure S1. Complete chromatogram of the cation exchange chromatography run of CVB3 VLPs. PEG-precipitated VLPs were eluted from the column by linear gradient (target: 60% elution buffer, gradient length: 20 ml) created using 1 M NaCl, 20 mM Tris-HCl, 5 mM $MgCl_2$ (pH 7.4) as elution buffer. Flow rate of 1 ml/min was used. The peak fractions eluted from the column between 410-550 mM of NaCl. A: absorbance at 280 nm, V: volume, C: conductivity.

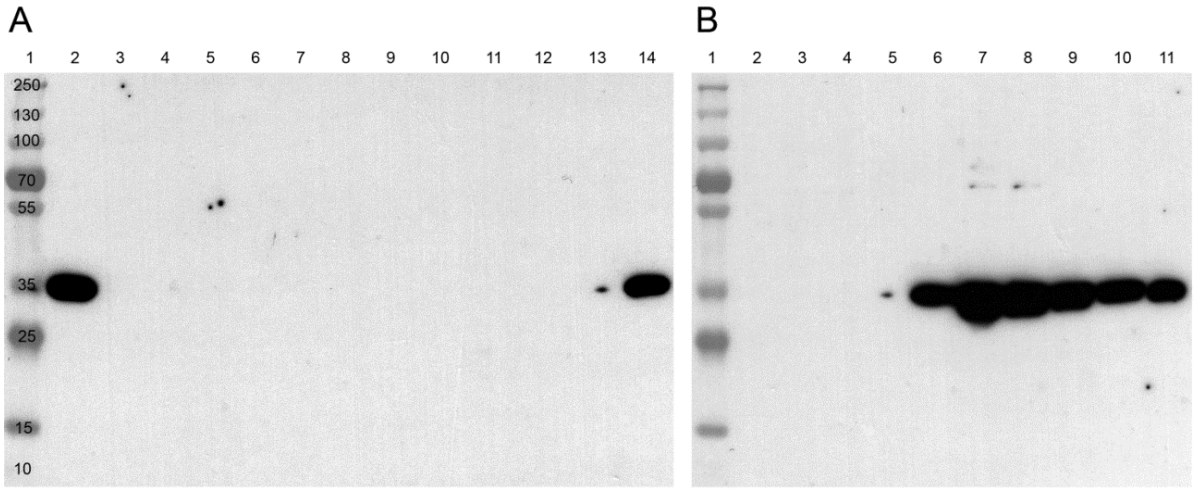

Figure S2. Western blot analysis of chromatography-purified CVB3 VLPs detected by anti-enterovirus VP1. (A) Lane 1: molecular weight marker; lane 2: chromatography input sample; lane 3-13: flow-through samples; lane 14: CVB3 positive control. (B) Lane 1: molecular weight marker; lanes 2-5: elution samples 4-7; lanes 6-10: VLP-containing elution samples; lane 11: CVB3 positive control.

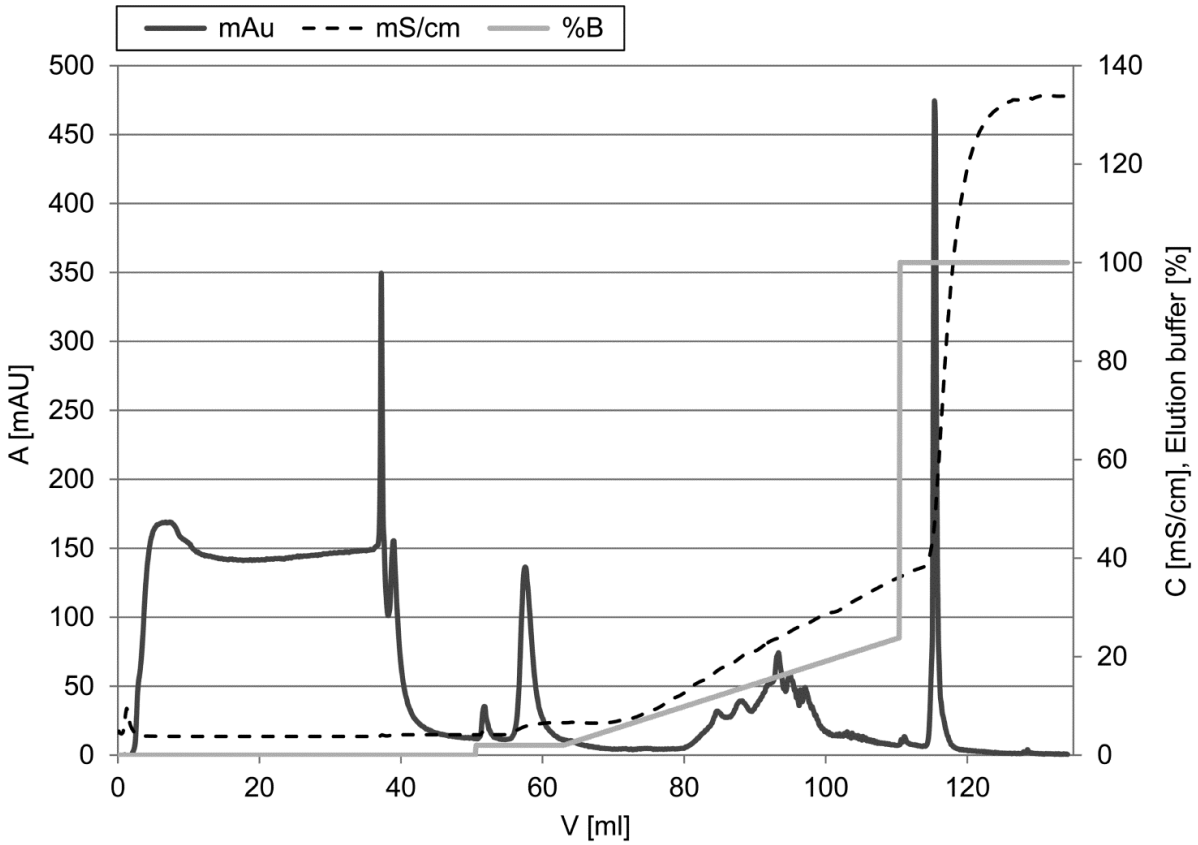

Figure S3. Complete chromatogram of the anion exchange chromatography run of CVB3 virus. PEG-precipitated viruses were eluted from the column by using a combination of stepwise and linear gradients as shown in the figure (step: 2% elution buffer, length: 15 ml; linear target: 25% elution buffer, length: 50 ml). A flow rate of 1 ml/min was used, and the elution buffer contained 2 M NaCl, 20 mM Tris-HCl, and 5 mM $MgCl_2$ (pH 7.4). The peak fractions eluted from the column at a NaCl concentration of 60 mM. A: absorbance at 280 nm, V: volume, C: conductivity.

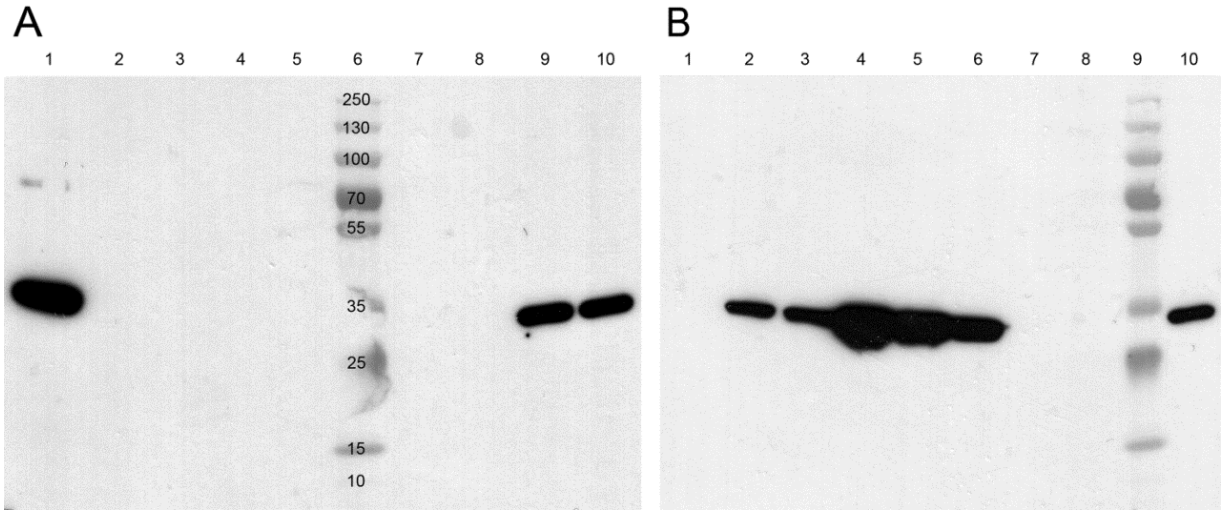

Figure S4. Western blot analysis of chromatography-purified CVB3 viruses detected by anti-enterovirus VP1. (A) Lane 1: chromatography input sample; lanes 2-5: flow-through samples; lane 6: molecular weight marker; lane 7-8: flow-through samples; lane 9: virus-containing elution sample; lane 10: CVB3 positive control. (B) Lane 1: wash sample; lanes 2 - 6: virus-containing elution samples; lanes 7-8: elution samples; lane 9: molecular weight marker; lane 10: CVB3 positive control.

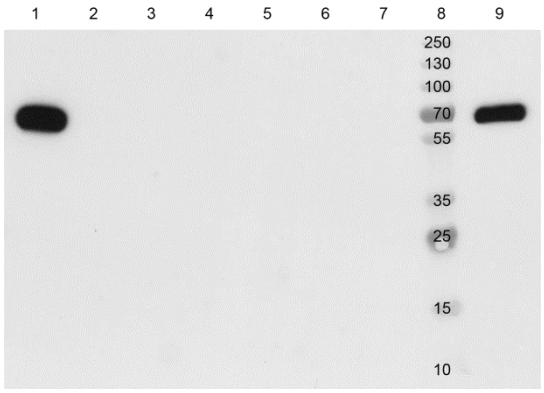

Figure S5. Western blot analysis of chromatography-purified CVB3 VLPs detected by anti-baculovirus gp64. Lane 1: chromatography input sample; lanes 2-7: elution samples; lane 8: molecular weight marker; lane 9: baculovirus positive control.

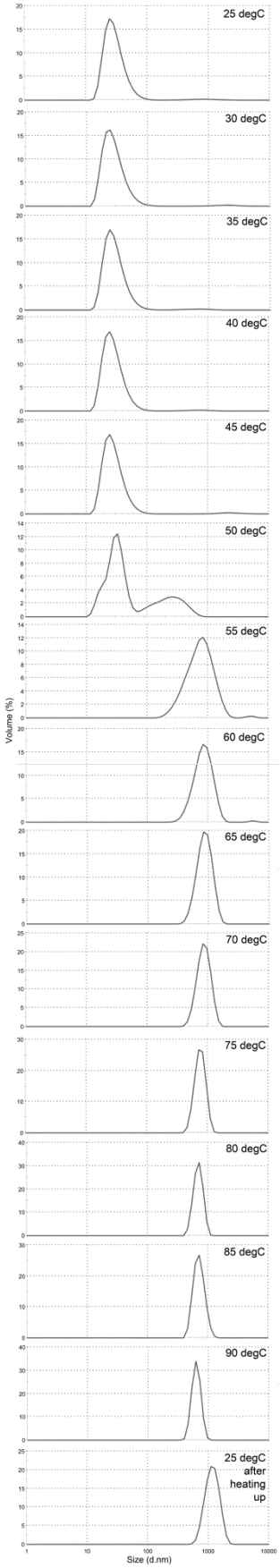

Figure S6. Particle size distribution measured for the CVB3 VLP sample over a range of temperatures. Each curve represents an average of three 10x10 sec measurements. Before

measurement, the sample was equilibrated for 5 minutes at the target temperature. The last measurement was done after cooling the sample to 25°C.

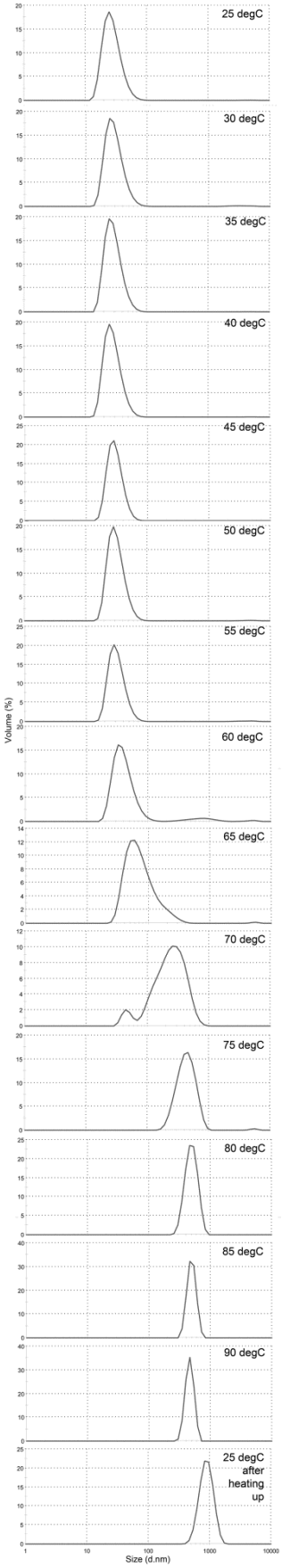

Figure S7. Particle size distribution measured for the CVB3 virus sample over a range of temperatures. Each curve represents an average of three 10x10 sec measurements. Before

measurement, the sample was equilibrated for 5 minutes at the target temperature. The last measurement was done after cooling the sample to 25°C.

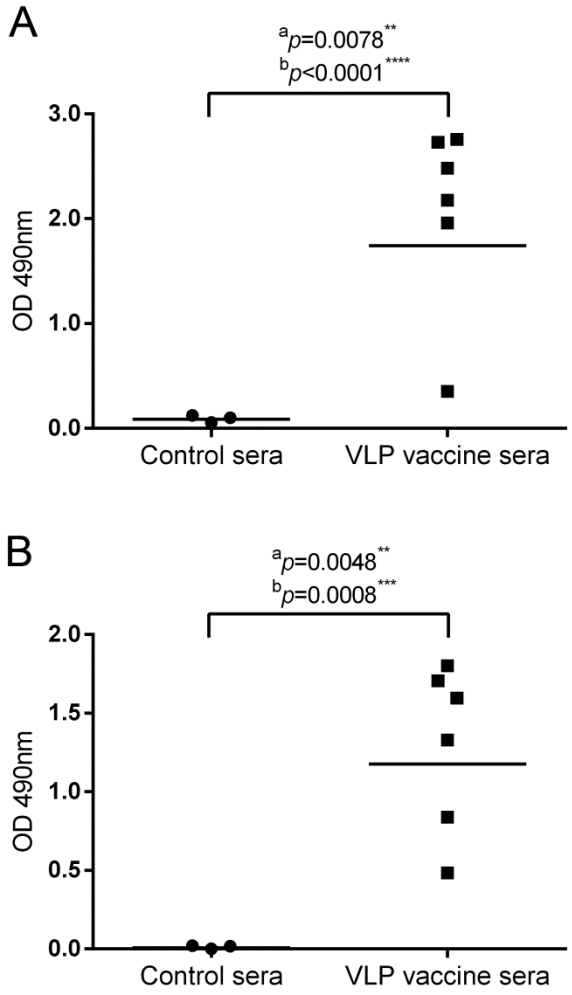

Figure S8. Antibody responses elicited in mice by CVB3 VLP immunization. Two groups of mice were injected at days 0, 21, and 42 with 5 μg of CVB3 VLP or equivalent amount of negative control vaccine. Immunized mice were sacrificed at day 63, and the serum samples were collected. The sera were diluted 1:8192, and the results represent the mean of three replicate experiments. Each symbol represents a mouse, and the line indicates a geometric mean of the group (n=3 in control group, n=6 in VLP group). **, $p \leq 0.01$; ***, $p \leq 0.001$; ****, $p \leq 0.0001$; [a] the one non-responsive mouse included in the calculation; [b] the one non-responsive mouse omitted from the calculation. (A) Binding activity of antisera to a CVB3 VLP antigen. (B) Binding activity of antisera to a CVB3 virus.

Supplementary Table 1. The numbers of immune cells of VLP and negative control vaccination groups at day 63.

Vaccination group	Number of B cells	Number of CD4 T cells	Number of CD4 memory T cells	Number of CD8 T cells	Number of CD8 memory T cells	Total number of cells
Negative control						
Mouse 1	9144	5647	475	2704	28	24426
Mouse 2	8601	5399	535	2286	33	22973
Mouse 3	11751	6037	598	3131	34	26705
Mouse 4	7463	4222	563	1533	25	23493
Mouse 5	6464	7079	256	2582	18	22468
Mouse 6	10636	6180	478	2861	24	24704
Average	9010	5761	484	2516	27	24128
CVB3 VLP						
Mouse 7	10198	7172	768	2596	39	27605
Mouse 8	8614	6065	657	2572	51	26065
Mouse 9	8842	5733	711	2227	43	24841
Mouse 10	7327	8412	1055	3262	84	27384
Mouse 11	8986	6474	327	2531	23	26231
Mouse 12	9220	5990	711	2456	32	29421
Average	8865	6641	705	2607	45	26925